Biophysical Mechanisms of Lymphocyte Adhesion to Activated Vascular Endothelium

by

Gerald C. Koenig

B.S. Mechanical Engineering
GMI Engineering and Management Institute
(1991)

Submitted to the
Harvard-M.I.T. Division of Health Sciences and Technology
in partial fulfillment of the requirements for the degree of

Doctor of Philosophy in Medical Engineering

at the

MASSACHUSETTS INSTITUTE OF TECHNOLOGY

September 1998

Signature of Author: _____
Harvard-M.I.T. Division of Health Sciences and Technology
July 31, 1998

Certified by: _ _____
Rakesh K. Jain
Andrew Werk Cook/Professor of Tumor Biology, Harvard Medical School
Thesis Supervisor

Certified by: _____ _____
Robert J. Melder
Assistant Professor of Radiation Oncology, Harvard Medical School
Thesis Supervisor

Accepted by: _____
C. Forbes Dewey, Jr.
Professor, Massachusetts Institute of Technology
Chairman, Thesis Committee

Accepted by: _____
Martha L. Gray
Co-Director, Harvard-M.I.T. Division of Health Sciences and Technology

1

Biophysical Mechanisms of Lymphocyte Adhesion to Activated Vascular Endothelium

by

Gerald C. Koenig

Abstract

The recruitment of lymphocytes to areas of inflammation and angiogenesis involves specific receptor-ligand interactions between cell surface adhesion molecules (CAMs) on lymphocytes and the vascular endothelium. The adhesion process follows a multi-step cascade which has been shown both *in vitro* and *in vivo* to involve intercellular adhesion molecule-1 (ICAM-1), vascular cell adhesion molecule-1 (VCAM-1), and endothelial leukocyte adhesion molecule-1 (E-selectin) expressed on endothelial cells. The expression of these CAMs on endothelial cells is modulated by the local concentration of cytokines and growth factors released by resident tissue cells, infiltrating leukocytes, and/or cancer cells. The regulatory mechanisms of adhesion molecule expression by angiogenic factors in tumor and the resulting leukocyte-endothelial interaction are poorly understood.

The objectives of this thesis were to determine: a) the binding kinetics of each non-activated and IL-2 activated lymphocyte subpopulation (CD4+, CD8+, and CD56+ cells), to human umbilical vein endothelial cells (HUVECs) through the use of a parallel-plate flow chamber; b) the expression levels of various cell adhesion molecules on intact HUVEC monolayers treated with tumor interstitial fluid (TIF) and various angiogenic factors, such as VEGF, bFGF, TNFα, and TGFβ, using targeted sampling fluorometry (TSF) and flow cytometry; c) the molecular mechanisms used by bFGF in regulating TNFα-mediated cell adhesion molecule (CAM) expression and function; and d) integration of the mechanisms into a framework for lymphocyte-endothelial interaction in disease and health.

These studies demonstrated that both IL-2 activated and non-activated lymphocytes vary in their ability to adhere to activated vascular endothelial cells over a wide-range of physiological flow rates. Also, activated lymphocytes are able to bind with increased levels of efficiency over the non-activated populations, and that variability in lymphocyte subset binding kinetics is dependent on the level of counter-ligand expression and the state of activation. Additional studies demonstrated that IL-2 activated natural killer cells (CD56+) principally utilize an integrin-dependent (β_1 and β_2), selectin-independent adhesion process in binding to activated vascular endothelium.

The expression studies revealed that fluid extracted from the tumor interstitium upregulates specific CAMs on endothelial cells *in vitro*, which promotes lymphocyte binding. These results correlated with *in vivo* findings and validated the use of the tumor fluid as a model for the tumor microenvironment. Analysis of the individual angiogenic factors showed that TNFα and VEGF are able to upregulate specific cell surface CAMs in a dose-dependent manner with similar temporal kinetics. In contrast, bFGF produced a biphasic effect on ICAM-1 regulation, and failed to exhibit an observable effect on the

expression of other CAMs. TGFβ demonstrated no significant differences in CAM expression. Treatment regimens combining bFGF with TNFα or VEGF showed a reduction in the levels of induced CAM expression in a time-dependent process, independent of prior exposure to activating cytokines. This inhibitory effect of bFGF was the result of transcriptional regulation of the inducible CAM genes. Additionally, the early signaling events mediating bFGF action involve the regulation of its receptor tyrosine kinase activity, followed by activation of phospholipase C-γ, phospholipase D, and protein kinase C.

The findings from these studies suggest that cytokines and growth factors differentially effect lymphocyte subset binding to activated vascular endothelium by altering cell adhesion molecule expression. Thus, valuable insight is provided into the accumulation of lymphocytes in normal and pathological conditions, such as in tumor and inflammation, and the role of angiogenic factors in regulating the host responsiveness at these sites.

Thesis Supervisor: Rakesh K. Jain
Title: Andrew Werk Cook Professor of Tumor Biology

Thesis Supervisor: Robert J. Melder
Title: Assistant Professor of Radiation Oncology

Thesis Chairman: C. Forbes Dewey, Jr., Ph.D.
Title: Professor of Mechanical Engineering

Thesis Reader: Michael A. Gimbrone, Jr., M.D.
Title: Elsie T. Friedman Professor of Pathology

Acknowledgments

I would first like to take this opportunity to thank my two thesis advisors, Rakesh Jain and Robert Melder. Their unwavering support and guidance have made this dissertation a reality and a success. I greatly admire them both for their tremendous expertise, enthusiasm, and genuine interest in me, both as a student and as an individual. I could always count on them for much needed advice and encouragement.

I would also like to thank my other two committee members, C. Forbes Dewey, Jr. and Michael A. Gimbrone, Jr. Professor Dewey, who served as my committee chairman, provided beneficial engineering guidance to my thesis and many helpful suggestions and comments. Dr. Gimbrone was an invaluable source of support and provided tremendously insightful advice and comments.

An additional thanks also goes to Roger Mark, former co-director of HST, from whom I received a great deal of inspiration and direction. Dr. Mark was instrumental in my decision to join HST and served as a compassionate and thought-provoking mentor.

Other faculty members in the Steele Laboratory also contributed to this research. Lance Munn introduced me to many of the lab culture and experimental techniques, and continued to provide endless support and expertise throughout my studies. Fan Yuan, Larry Baxter, and Yves Boucher provided encouragement and advice which significantly enhanced my experience.

The Steele Laboratory technicians, Yi Chen and Sylvie Roberge, also provided valuable assistance. Yi contributed significant time and expertise to facilitate the molecular biology experiments, and Sylvie dedicated time and energy to implanting tumors and extracting the fluid for experimental analysis.

My other colleagues and associates in the lab have been a constant source of encouragement, assistance, and friendship. Hera Lichtenbeld, Gabriel Helmlinger, and Paolo Netti were especially so with their genuine good-nature and expertise. Yong, Jin, Nils, Sybill, Dai, Claus, and Christian deserve special mention for their added helpfulness and viewpoints. My fellow HST classmates also provided a stimulating and enriching environment, out of which came many endearing friendships.

The administrative staff also made graduate life a little more enjoyable and easier to handle. From the Steele Laboratory, Carol Lyons and Phyllis McNally were extremely helpful and provided a warm and pleasant environment to work. I especially thank Carol for all her extra support and compassion. From the HST organization, Patty Cunningham, Keiko Oh, Ron Smith, and Carol Campbell all provided significant contributions.

Despite all which the aforementioned have provided, I especially thank my parents, Roland and Gerlinde Koenig, and my sister, Michaela, for their tremendous love and support in all my pursuits in life. Their hard work, dedication, and unending encouragement have instilled in me a passion for life and exploring the unknown. Also, thanks to my loving friends and relatives, for their fresh viewpoints and good-natured spirit.

Finally, I would like to thank my wife Marie, who provided me with unconditional support, understanding, and patience throughout my graduate studies. I am truly blessed to have her as my soul mate for life, and for giving me the joy of a son, Alexander. With an endless love, I cherish thee both.

To Marie, Alexander, and my parents

May God bless us all in our pursuits of truth and happiness

Table of Contents

9

List of Figures

11

13

14

List of Tables

Chapter 1

Introduction

1.1 Motivation and Background

Each year in the United States, over 1.2 million individuals are diagnosed with cancer for the first time. According to the American Cancer Society, cancer took the lives of over 560,000 Americans in 1997, representing 23% of all mortality and the second leading cause of death, as defined by 1994 statistics [Vital Statistics of the United States, 1994]. More than 85% of these cancers are solid tumors, and approximately one-half of the patients with these tumors die of their disease. A most sobering and troublesome reality.

Solid tumors, derived from normal host cells which have gone awry, have a fundamental characteristic in being dependent on blood supply for oxygen, nutrients and waste removal beyond a size of 1-2 mm in diameter [Folkman, 1990]. The development of new blood vessels from pre-existing vessels is termed angiogenesis, and occurs in a range of pathologies in addition to cancer (tumor angiogenesis), including atherosclerosis (hyperproliferation of the *vasa vasorum* within atherosclerotic plaques), endometriosis, and diabetic retinopathy.

Cancer cells, as well as surrounding and infiltrating host cells, produce multiple polypeptide cytokines that are essential for promoting the process of angiogenesis, and are appropriately termed angiogenic growth factors. Among the most well-documented are vascular endothelial growth factor (VEGF), basic fibroblast growth factor (bFGF), transforming growth factor-β (TGFβ), and tumor necrosis factor-α (TNFα). These factors, in addition to other cellular products produced by the neoplastic and non-neoplastic

cells, influence the tumor microenvironment by establishing temporal and spatial heterogeneities in blood flow, altering expression of cell adhesion molecules on parenchymal, stromal, and vascular cells, and modifying physiological and metabolic properties. The changes in the microenvironment produce effective barriers against the delivery of cells and molecular therapeutics to tumors.

The mounting and delivery of an effective immunogenic response to tumors by the host immune system involves a progressive sequence of steps, each of which is potentially modified by the tumor microenvironment. The steps include: a) entering the tumor vasculature from host sites, b) interacting with the vascular compartment and forming stable cell:cell adhesion to the vessel wall, c) transporting across the microvascular wall into the interstitium, d) transporting through the interstitial compartment to reach the cancer cells, and then e) actively attacking or supporting the killing of the cancer cells.

The mechanisms of lymphocyte interaction with the vascular endothelial cells serves as a particular point of interest for its importance in the initial steps of the immune response and potentially subserving specific cell populations. The capture and adhesive interactions are influenced by the local hemodynamic forces, determined by the vessel diameter, viscosity, and fluid velocity, and by the adhesive forces, determined by the spatial arrangement and level, affinity, and kinetics of bond formation between receptor-ligand pairs. A working hypothesis is that the specific microenvironment present in regions of angiogenesis, specifically the biological influence of growth factors on the vascular endothelium, is necessary for the interactive process.

The same or closely related adhesion molecules used in angiogenesis to promote cell migration and proliferation also mediate immune cell adhesion to the vasculature. This seemingly paradoxical influence is further complicated by the fact that immune cells themselves are able to produce significant levels of angiogenic factors to either facilitate additional immune cell infiltration or promote tumor vessel formation. An increased understanding of the temporal regulation of the adhesion molecules and angiogenic factors expressed in tumors, as well as the particular molecular mechanisms used by lymphocyte subpopulations, is needed to further elucidate this interactive process.

The influence of angiogenesis and the growth factors and cytokines involved in the interaction of blood leukocytes with the vascular endothelium extends beyond the pathophysiology of tumors. Other diseases with fundamentally similar angiogenic processes involved include atherosclerosis, vasculitis, allograft rejection, graft vs. host disease, and chronic inflammation. It is also vital to several normal physiological processes as well, such as acute inflammation, tissue repair, and embryogenesis.

1.2 Hypotheses and Specific Aims

In formulating the thesis, a set of hypotheses were initially postulated which provided a framework on which the specific objectives were derived. The original hypotheses were as follows:

Tumor interstitial fluid and purified angiogenic factors can modulate cell adhesion molecules (CAMs) on the endothelium.

Diversity among angiogenic factors can result in the differential regulation of CAMs.

Endothelial CAMs induced by angiogenic factors can be recognized differentially by lymphocyte sub-populations, namely T lymphocytes and natural killer cells.

Differences in the intracellular signaling pathways used by the angiogenic factors can result in differential CAM modulation.

The specific goals of this thesis were to test these hypotheses by performing the following experimental studies:

Measure the binding kinetics of each specific non-activated and IL-2 activated lymphocyte subpopulation, namely CD4+, CD8+, and natural killer cells (CD56+), through the use of parallel-plate flow chamber studies.

Quantify the expression of various cell adhesion molecules on intact HUVEC monolayers treated with tumor interstitial fluid and various angiogenic factors, such as VEGF, bFGF, TNFα, and TGFβ, using targeted sampling fluorometry (TSF) and flow cytometry.

Determine the molecular mechanisms used by bFGF in regulating TNFα-mediated cell adhesion molecule (CAM) expression and function.

Integrate the mechanisms into a framework for lymphocyte-endothelial interaction in disease and health

1.3 Significance

Current therapies, which include chemotherapy, radiation, and surgery, can cure about half of the diagnosed cancers. While encouraging, it still leaves a large population of individuals that cannot be treated successfully. New therapies are continuously being explored, including combined treatment protocols. Of particular interest are gene-based therapy [Goldspiel, et al., 1993], and adoptive immunotherapy, whereby TIL (tumor-infiltrating lymphocyte) or LAK (lymphokine-activated killer) cells are delivered to cancer patients in the hope that the body's natural immune cells will resolve the tumor [Rosenberg, 1990]. However, both have had only obtained limited success, but have helped raise questions about the fundamental mechanisms by which the immune system acts.

The studies proposed in this thesis can provide increased understanding to several physiological and pathophysiological processes. The binding kinetics and molecular mechanisms used by the individual lymphocyte subpopulations in interacting with the vasculature, both in tumor, inflammation, and wound healing, are essential for determining mechanisms used by the immune system in localizing to areas requiring active immunological response. In addition, improvements can be made to current modeling schemes which attempt to predict the biodistribution of effector cell populations in the human.

The effects of angiogenic factors on cell adhesion can provide necessary insight into the regulatory and protective mechanisms potentially found in tumors, as well as in inflammation and wound healing. It may also contribute to a better understanding of metastasis and the role of cytokines and growth factors in the process.

Finally, defining the signaling mechanisms used by specific growth factors, may contribute to a better understanding of the molecular mechanisms used by the growth factors to modify cell adhesion molecule expression, and its relation to the other physiological functions which it produces. Also, it gives insight into the angiogenic process and the kinetic responses elicited by specific growth factors in the microenvironment.

Clearly, a better understanding of these processes may provide new insights into the mechanisms of tumor evasion, immune response and neovascular growth, which may be used for developing alternative or modified modalities of therapies against cancer and other diseases.

1.4 Organization of Thesis

The thesis is organized into the following chapters, and is outlined in Figure 1-1:

Chapter 1 gives the motivation and significance of the work, as well as the hypotheses and specific aims addressed in the thesis.

Chapter 2 provides a summary of the background essential for the studies conducted in this investigation on lymphocyte-endothelial interactions and cell signaling.

Chapter 3 discusses the materials and methods used in this research. Included is a description of the lymphocyte and endothelial preparations, as well as the protein, mRNA, and functional adhesion assays performed.

Chapter 4 provides results and discussion on the experiments performed examining the lymphocyte binding kinetics for both non-activated and activated lymphocyte subpopulations.

Chapter 5 presents results and discussion on the analysis of cell surface adhesion molecule expression induced by the angiogenic factors TNFα, VEGF, bFGF, and TGFβ, as well as the tumor interstitial fluid.

Chapter 6 describes the results and provides discussion on the studies performed analyzing the molecular mechanisms used by bFGF in modulating CAM expression.

Chapter 7 provides a summary of the studies conducted in the thesis, and discusses future directions for the research, along with its clinical significance.

The work presented in this thesis has at least partially contributed to four published manuscripts [Munn, et al., 1995; Melder, et al., 1996; Melder, et al., 1996; Jain, et al., 1996], and two in preparation involving the findings presented in Chapters 4 and 6. In addition, a patent is pending with the U.S. Patent Office, based on the inhibitory mechanisms of basic fibroblast growth factor (bFGF) and includes as co-inventors: R.K. Jain, R.J. Melder, and L.L. Munn.
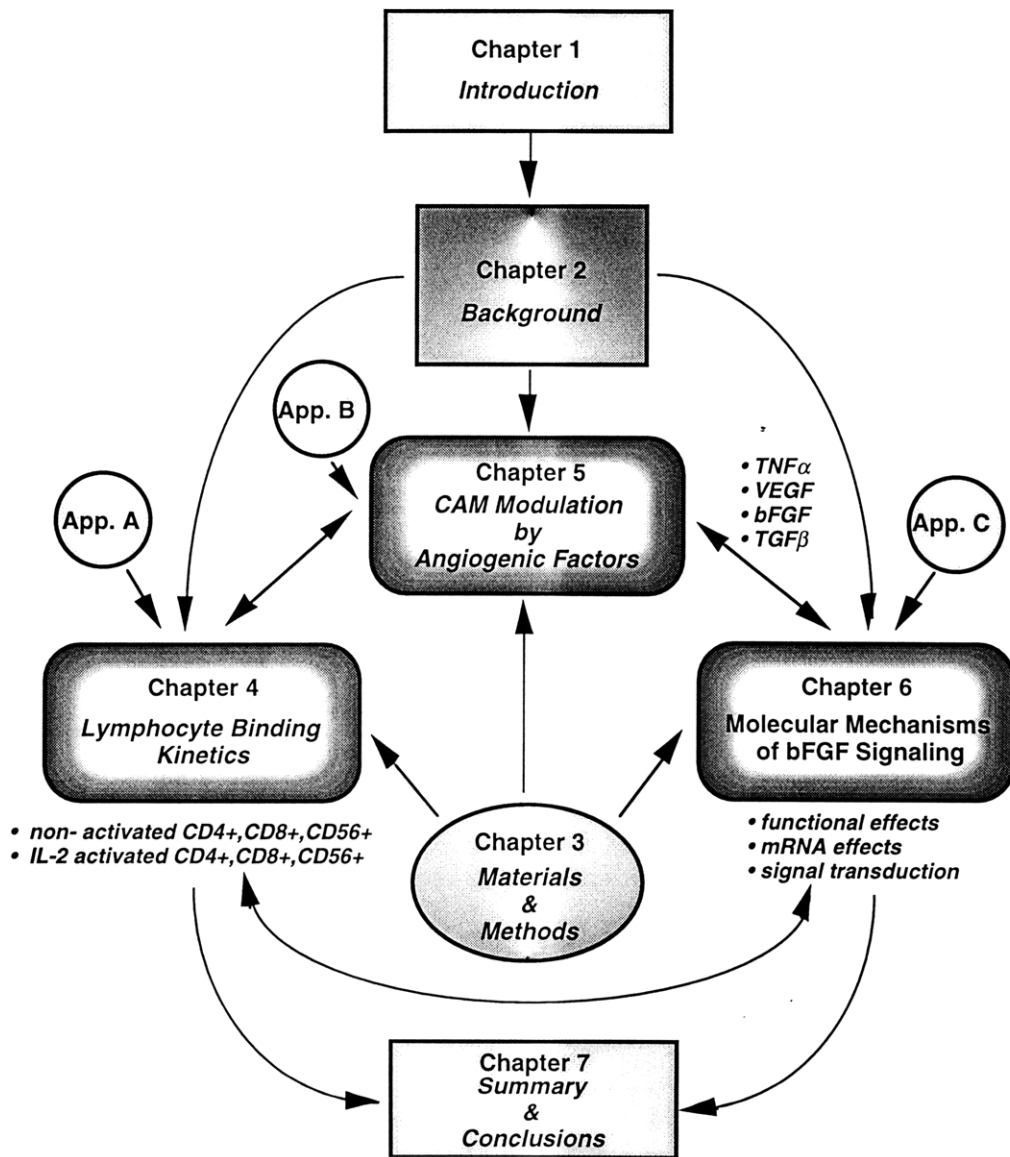
Figure 1-1. Schematic outline of the thesis.

Chapter 2

Background

2.1 Introduction

The active recruitment of circulating lymphocytes to sites of inflammation, wound repair, and tumor is an integral event in mounting an effective immune response. Adhesive forces resulting from the spatial arrangement, quantity, affinity and kinetics of bond formation between receptor-ligand pairs of cell adhesion molecules (CAMs) must overcome the hemodynamic forces present in the blood vessels. The expression of these CAMs on the endothelium is modulated by the local concentration of inflammatory cytokines and angiogenic factors, see Table 2-1 [Osborn, 1990; Jain, et al., 1996]. The majority of studies involving the growth factors have focused on the specific angiogenic responses. Only recently has there been increased interest in defining the role of these factors in cell adhesion molecule induction and modulation. Growing interest has been placed on the specific signaling transduction pathways used by these cytokines and growth factors in regulating cellular responses in the hopes of developing new therapies for several pathological conditions, such as cancer and heart diseases.

This chapter is designed to serve as a basic reference of the literature related to the understanding of lymphocyte capture mechanisms, the function and signaling pathways used by several cytokine and growth factors, and the fluid mechanics of the *in vitro* vessel model used in this thesis. With this background, it is hoped that the reader will have a better fundamental understanding of the studies conducted in this thesis, and be able to follow the general findings and appreciate the significance of this work.

Table 2-1. Regulation of adhesion molecules by cytokines and angiogenic factors. Adapted from [Jain, et al., 1996].

Cytokine	Cell Type	ICAM-1	VCAM-1	E-Selectin	P-Selectin
bFGF	HUVEC	↔, ↓	↔, ↓	↔	↔
	HDMEC	↓	↔	↔	NM
IFNγ	HUVEC	↑	↔	↔	NM
	HDMEC	NM	↔	NM	NM
	MME	↑	↑	NM	NM
	RME	NM	↑	NM	NM
IL-1	HUVEC	↑	↑	↑	NM
	HDMEC	↑	↔	↑	NM
	MME	↑	↑	NM	NM
IL-4	HUVEC	↓, ↔	↑	↔, ↓	NM
	HDMEC	NM	↔	NM	NM
	MME	NM	↔	NM	NM
	BDEC	↔	↑	↔	NM
TGFβ	HUVEC	↔	↔	↓	NM
	MME	↔	↔	NM	NM
TNFα	HUVEC	↑	↑	↑	↑
	HDMEC	NM	↑	NM	NM
	MME	↑, ↔	↑	NM	NM
	BDEC	↑	↑	↑	NM
	BCE	NM	NM	↑	NM
VEGF	HUVEC	↑	↑	↑	↔
IL-1 + IL-4	HUVEC	↓	↑↑	↓	NM
IL-1 + bFGF	HUVEC	↓	↓	↔	NM
IL-1 + IFNγ	HUVEC	↑	NM	↑	NM
IL-1 + TGFβ	HUVEC	NM	NM	↓	NM
TNFα + IL-4	HUVEC	↓	↑↑	↓	NM
	HDMEC	NM	↔	NM	NM
	BDEC	↔	↔	↔	NM
TNFα + IFNγ	HUVEC	↑↑	NM	↑	NM
TNFα + bFGF	HUVEC	↓	↓	↓	NM
TNFα + TGFβ	HUVEC	↔	↔	↓	NM
TGFβ + IL-8	HUVEC	↔	NM	NM	NM
bFGF + VEGF	HUVEC	↔	NM	NM	NM
IFNγ + IL-4	HUVEC	↓	↔	NM	NM
IL-4 + TGFβ	HUVEC	NM	NM	↓	NM

↑ = upregulation, ↔ = no effect, ↓ = downregulation, NM = not measured. Effect of combined treatments are relative to the individual treatments, whereby: ↑↑ = synergistic upregulation, ↑ = additive effect, ↔ = no difference from responsive individual treatment, ↓ = negative combined effect. HUVEC = Human Umbilical Vein Endothelial Cell (EC), HDMEC = Human Dermal Microvascular EC, MME = Murine Microvascular Endothelium, RME = Rat Microvascular Endothelium, BDEC = Baboon Dermal EC (in vivo), BCE = Bovine Capillary EC.

2.2 Cell Adhesion Molecules

There are basically two families of CAMs involved in producing the adhesive forces between leukocytes and endothelial cells: 1) the selectins (e.g. E-, L-, and P-selectin) and 2) the immunoglobulin (Ig) superfamily members (ICAM-1 and VCAM-1) on endothelial cells and the corresponding integrin receptors on the leukocytes (β_2 and β_1) [Springer, 1995; Collins, 1995].

2.1.1 Selectins

Selectins consist of an N-terminal lectin domain, one epidermal growth factor-like module, and from two to nine short consensus repeats [Lawrence and Springer, 1991]. To date, they have only been shown to exist on circulating cells and the endothelium, unlike integrins and Ig superfamily members. The three members of this group of CAMs are: a) E-selectin (ELAM-1, CD62E), b) P-selectin (PADGEM, CD62P), and c) L-selectin (LECAM-1, CD62L). E-selectin is synthesized by endothelial cells in response to inflammatory agents and promotes attachment of monocytes, neutrophils, and certain lymphocytes by combining with the ligand sialyl-Lewis X [Bevilacqua, et al., 1989]. P-selectin is expressed in Weibel-Palade bodies of endothelial cells and in α granules of platelets, becoming mobilized to the cell membrane upon inflammatory activation and promoting adhesion to monocytes and neutrophils [Larsen, et al., 1989]. L-selectin is expressed on leukocytes, promoting lymphocyte adhesion in peripheral lymph nodes and in neutrophils, monocytes, and lymphocyte emigration at inflammatory locales [Spertini, et al., 1991]. The structure of the selectins and their corresponding carbohydrate ligands allow for a high on-rate to complex formation resulting in efficient interactions of rapidly flowing cells with the endothelium, and along with a high off-rate, permit active rolling to occur. Thereby, the selectins are considered to primarily mediate leukocyte capture and rolling.

2.1.2 Integrins and Immunoglobulin Superfamily

Integrins consist of a $\alpha\beta$ heterodimer, with the α subunits (120-180 kD) covalently associated with a β subunit (90-110 kD) [Hynes, 1992]. Most integrins are expressed on a wide variety of cells and are major receptors for cell attachment to extracellular matrices and in mediating cell-cell adhesion events. There consists a large, yet restrictive, diversity of integrins with currently 8 known β units and 15 known α subunits (see Table 2-2) [Hynes, 1992; Rouslahti, 1991]. The α and β subunit combination determines the ligand specificity. While the majority of these integrins are recognized by extracellular matrix

proteins involved in cell-substratum adhesion, there are some which recognize integral membrane proteins of the immunoglobulin superfamily and mediate direct firm cell-cell adhesion.

The Ig superfamily consists of a group of proteins with one or more Ig domains, regions of 70 to 110 amino residues homologous to either Ig variable (V) or constant (C) domains. Most members of this superfamily are integral plasma membrane proteins with Ig domains in the extracellular portions, transmembrane domains composed of hydrophobic amino acids, and widely divergent cytoplasmic tails with no homology to one another. The most common of these which are associated with leukocyte adhesion to vascular endothelium are ICAM-1 (intercellular adhesion molecule-1), ICAM-2, and VCAM-1 (vascular cell adhesion molecule-1) [Rothlein, et al., 1986; Stauton, et al., 1989; Osborn, et al., 1989]. ICAM-1 (CD54) and ICAM-2 (CD102), a constitutively expressed adhesion molecule, on the endothelium bind to LFA-1 (β_2 integrin) on the leukocytes, and VCAM-1 (CD106) on the endothelium binds to VLA-4 (β_1 integrin) on the leukocytes [Marlin and Springer, 1987; Elices, et al., 1990; Hemler, 1990].

Table 2-2. Known $\alpha\beta$ integrin complexes.

β_1 [CD29]	$\rightarrow$	α_1 (CD49a), α_2 (CD49b), α_3 (CD49c), α_4 (CD49d), α_5 (CD49e), α_6 (CD49f), α_7, α_8, α_9, α_v (CD51)
β_2 [CD18]	$\rightarrow$	α_L (CD11a), α_M (CD11b), α_X (CD11c)
β_3 [CD61]	$\rightarrow$	α_{IIb} , α_v
β_4 [CD104]	$\rightarrow$	α_6
β_5	$\rightarrow$	α_v
β_6	$\rightarrow$	α_v
β_7	$\rightarrow$	α_4 , α_{IEL}
β_8	$\rightarrow$	α_v

2.3 Leukocyte-Endothelial Interaction

As for functional studies involving cell adhesion, many investigators have analyzed leukocyte adhesion to cytokine activated endothelial cell monolayers *in vitro* [Bevilacqua, et al., 1985; Schleimer and Rutledge, 1987; Cavender, et al., 1987; Cotran and Pober, 1990]. Early studies were performed using static conditions and showed that basal adhesion of blood monocytes was significantly greater than that of neutrophils and lymphocytes [Bevilacqua, et al., 1985; Luscinskas and Lawler, 1994]. On activated endothelium, i.e. TNFα, IL-1, or LPS treatment, increases of 2- to 5-fold were seen in monocyte and lymphocyte adhesion and a 10- to 15-fold increase in neutrophil adhesion [Bevilacqua, et

al., 1985; Lo, et al., 1989; Pober, et al., 1987]. Multiple adhesion molecules and leukocyte chemoattractants, e.g. ICAM-1, VCAM-1, E-selectin, P-selectin, L-selectin, MCP-1 and PAF, were proven to be essential in the process and were suggestive of redundant or overlapping function [Springer, 1994]. More recent studies using defined laminar flow conditions have revealed a more complex process in which sequential and overlapping functions exist for the multiple receptor-ligand pairs [Lawrence and Springer, 1991; Springer, 1994; Luscinskas, et al., 1994; Butcher, 1991]. The general model commonly accepted now involves a multi-step cascade consisting of four events (phases 1-4): (i) leukocyte capture and rolling mediated by L-selectin, E-selectin, and P-selectin, (ii) leukocyte arrest dependent on β_1 integrins/VCAM-1 with (iii) leukocyte firm adhesion and spreading mediated by β_2 integrins/ICAM-1, and (iv) in conjunction with CD31, β_2 mediated leukocyte diapedesis, with some overlap in the functions of the adhesion molecules.

Studies have been carried out defining the specific adhesive interactions between T lymphocytes and vascular endothelium. Previous *in vitro* studies have demonstrated the roles of LFA-1/ICAM-1, VLA-4/VCAM-1, and sialyl-Lewis X/E-selectin in resting CD4+ cell adhesion to activated endothelial cells under static conditions [Shimizu, et al., 1991; Dustin and Springer, 1988; Bierer and Burakoff, 1988]. More recent *in vitro* studies have determined the cellular processes and molecular events involved in resting CD4+ and CD3+ T cells to TNFα-activated HUVEC monolayers and murine-transfected cell lines [Luscinskas, et al., 1995; Melder, et al., 1995]. Results using resting CD4+ T cells showed that a) P-selectin, but not E- or L-selectin, mediated the initial capture and rolling, b) VLA-4 (β_1 integrin) participated in rolling and was predominant in stable arrest, and c) LFA-1 (β_2 integrin) contributed to stable arrest and predominated cell spreading and transmigration [Luscinskas, et al., 1995]. Resting CD3+ T cells displayed similar characteristics in terms of VLA-4/VCAM-1 and LFA-1/ICAM-1 contributions to rolling, stable arrest, and cell spreading [Melder, et al., 1995]. Interestingly, the contributions of E- and L-selectin were shown to be essential in mediating the initial interaction process, being limited to the range of 1-3 dyn/cm^2 [Melder, et al., 1995; Yago, et al., 1995]. It has also been observed that the number of rolling CD45RA$^-$ T cells on E-selectin-transfected cells was much higher than those of CD45RA$^+$ T cells, emphasizing a potential molecular difference between naive and memory T cells [Yago, et al., 1995].

When compared to other leukocytes, T cells exhibit some inherent differences in their adhesive characteristics. Rolling velocities for CD4+ T cells were reported to be approximately half that of neutrophils under similar flow conditions [Abassi, et al., 1993], preferential cell attachment downstream of adhered cells was shown to be characteristic of

monocytes and not of CD4+ T cells, and that P-selectin mediated a significant role in CD4+ T cell initial contact and not L-selectin, as was observed in monocyte adhesion [Luscinskas, et al., 1994].

Recent studies have shown the localization of lymphocytes in the microvasculature of growing tumors [Sasaki, et al., 1991; Melder, et al., 1995], as well as along the invasive margin [Suzuki, et al., 1995]. Evidence suggests that the localization of these lymphocytes is due primarily to the adhesive characteristics of the endothelium [Butcher, 1991; Basse, et al., 1991], whereby a variable set of cell adhesion molecules are expressed [Luscinskas and Lawler, 1994], and the effective level of receptor expression and affinity for the particular expressed ligand. The alteration in endothelial cell phenotype is likely a result of the tumor microenvironment, particularly the angiogenic factors present [Folkman, 1995]. The effects of the individual factors alone, or in combination with each other, in terms of CAM modulation have only been explored to a limited extent, and are summarized in Table 2-1 [Melder, et al., 1996; Kitayama, et al., 1994; Gamble and Khew-Goodall, 1993].

2.4 Cell Signaling

The ability of the cell to sense and respond to its environment is essential for its survival and proper function. Extracellular molecules, such as cytokines, polypeptide hormones, neurotransmitters, and antigens bind to cell surface receptors and generate intracellular signals that are transmitted to different systems of the cell. These signaling systems involve interactions between various components of a single pathway, as well as complex interactions between mediators of other pathways and common factors involved in different processes.

A growing interest has accumulated towards determining the specific signal transduction pathways used by the various cytokines and growth factors in elucidating the mechanisms of cell proliferation and differentiation, angiogenesis, apoptosis, cell adhesion molecule regulation, as well as to enhance the use of novel chemotherapy, immunotherapy, and gene therapy [Levitzki, 1994].

Several pathways are shared among the different cytokines and growth factors, and provide a means of cross-talk between different signaling pathways. Among the intracellular signaling molecules commonly utilized are the second messengers cyclic adenosine monophosphate (cAMP), inositol-1,4,5-triphosphate (Ins1,4,5P3), and calcium ions (Ca^{2+}). Elevated levels of these compounds can directly activate some metabolic pathways, as well as stimulate the activity of certain protein kinases. The protein kinases

can consequently activate other enzymes, eventually leading to the modulation of gene expression.

Receptors for several activating agents are linked to the enzyme, adenylyl cyclase, through a G-protein. Activation of adenylyl cyclase results in the conversion of adenosine trisphosphate (ATP) into adenosine 3',5'-monophosphate, or cyclic AMP. A variety of enzymes within the cell, including a number of protein kinases (PKA), interact with cAMP to modulate specific metabolic pathways.

Another set of specific receptors on endothelial cells regulates the second-messenger system involving the stimulation of phosphoinositide hydrolysis. Often through a G-protein, but not always the case, the receptors stimulate the activity of a phospholipase C (PLC) that specifically hydrolyzes phosphatidylinositol-4,5-bisphosphate (PIP$_2$) and phosphatidylcholine, two of four major phospholipids found in the plasma membrane. PtdInsP$_2$ activates two second messengers, diacylglycerol (DAG) and inositol-1,4,5-trisphosphate (IP$_3$),which lead to further downstream release of cytoplasmic Ca^{2+} stores and the activation of protein kinase C (PKC), which has multiple functions within cells.

The receptors for most of the growth factors are transmembrane tyrosine-specific protein kinases (PTK) [Carpenter, 1987]. PTK can be classified as (a) receptor tyrosine kinases (RTK), which directly receive signals through the growth factor-bound extracellular domain, and (b) cellular tyrosine kinases (CTK), which are signal transducers. The family of receptor tyrosine kinases can be divided into a number of structural subfamilies, in which all signal cells through tyrosine phosphorylation reactions. The signaling begins with the dimerization of the receptor upon ligand binding and the subsequent *trans*-autophosphorylation, or cross-phosphorylation of the dimer [Yu, et al., 1985; Sternberg and Gullick, 1990; Ullrich and Schlessinger, 1990]. The activated receptor then phosphorylates exogenous substrates and recruits adapter molecules and enzymes through its autophosphorylated domains via SH2 domains [Sierke and Koland, 1993]. These events lead to the signal propagating through a number of pathways within the cytoplasm, with the specific pathway dependent on the given cell type. Ultimately, the signals lead to nuclear activation of gene regulatory proteins and stimulation of specific gene transcription (early- and delayed-response).

RTK signaling can be inhibited for study by blocking ligand binding, receptor dimerization, RTK activity or recruitment of signaling molecules. Inhibition of growth factor ligand binding has been performed using growth factor antagonists (i.e., suramin), growth factor toxins (i.e., chimeras between the growth factors and a bacterial or plant toxin), antibodies and antibody-toxin chimeras. Inhibition of the tyrosine-kinase activity has been carried out using: (a) tyrphostins, a family of synthetic benzyldiaminonitrile

compounds, and (b) genistein, methyl 2,5-dihydroxycinnamate, lavendustin A, and 2,5-dihydroxybenzyl-aminobenzoic acid [Levitzki, 1992; Hawker and Granger, 1994]. The inhibition of PLC-γ and phospholipase D (PLD) has been done using 1-O-octadecyl-2-O-methyl-lac-glycerol-3-phosphocholine or 2-nitro-4-carboxyphenyl N,N-diphenylcarbamate (NCDC), and propranolol, respectively. The blocking of signaling transducers further downstream has involved inhibition of RAS activation by interrupting the Sos exchanger, Raf-1 Ser/Thr kinase, and post-translational modification by farnesylation. Blocking of Ca^{2+} activity has been demonstrated using carboxamide amino-imidazole (CAI), which had no effect on cAMP production or inositol phosphate. Lastly, high doses of phorbol esters and moderate doses of bisindolylmaleimide, calphostin C, and sphingosine have been used to inhibit the protein kinase C isozymes [Levitzki, 1994].

The protein kinase C family has been a particular source of interest for its diverse physicochemical and regulatory properties in mammalian cells, as well as its differential tissue expression with specific intracellular localization. Ten isoforms or subspecies of PKC have been identified which are all dependent on phosphatidylserine, but exhibit different requirements of phospholipid metabolites and Ca^{2+} [Nishizuka, 1992; Asaoka, et al., 1992]. The isozymes may be tentatively divided into three groups based on their dependent processes: cPKC $(\alpha,\beta_I/\beta_{II},\gamma)$, nPKC $(\delta,\varepsilon,\eta,\theta)$, and aPKC (ζ,λ). Those PKC isozymes which have been shown to be specific for human endothelial cells are: cPKC-α,β, nPKC-δ,η,θ, and aPKC-ζ, with nPKC-ε being specifically absent [Kent, et al., 1995]. Differences have also been found in the cellular distribution of PKC-α,ε with the number of endothelial cell passages (1 vs. 3) [Haller, et al., 1996].

Most of the individual signaling pathways which have been elucidated are derived from studies involving epidermal growth factor (EGF) and platelet-derived growth factor (PDGF) [Cadena and Gill, 1992; Jaye, et al., 1992]. A limited number of studies have defined the pathways explicitly relevant to bFGF, VEGF, TNFα, and TGFβ [Hawker and Granger, 1994; Jaye, et al., 1992]. While the receptors for bFGF and VEGF have been proven to be protein tyrosine kinases [Jaye, et al., 1992; DeVries, et al., 1992], the receptors for the TGFβ superfamily have been identified as serine/threonine protein kinases [Segarini, 1993]. TNFα has been shown to influence the behavior of vascular endothelial cells by inducing granulocyte-macrophage colony-stimulating factor [Broudy, et al., 1986], with its receptor being a protein tyrosine kinase, transient expression of surface antigen correlated with enhanced leukocyte binding to the endothelium [Pober, et al., 1986], and increasing the sensitivity of cells to undergo apoptosis through the sphingomyelin signal transduction pathway [Kolesnick, et al., 1994].

Transcription of cell adhesion molecules and the role of individual cytokines and angiogenic growth factors in the process have provided a direct linkage to the integration of angiogenesis, adhesion, and metastasis, three areas previously considered to be distinct [Jain, et al., 1996; Friesel and Maciag, 1995]. Positive regulatory domains required for cytokine induction (TNFα, IL-1β) have been determined in the promoter regions of E-selectin, ICAM-1, and VCAM-1 [Collins, et al., 1995]. The endothelial cell NF-κB/IκB system and a limited set of other transcriptional activators (e.g. ATF-2, IRF, and HMG I(Y)) are essential in the assembly of unique transcriptional factor complexes that activate multiple endothelial genes.

The following section provides a more detailed description of the signaling pathways used by bFGF, VEGF, TNFα, and TGFβ, and, where possible, emphasis on signaling within endothelial cells and the regulation of cell adhesion molecule expression by these factors.

2.4.1 Basic FGF Signaling

Basic fibroblast growth factor (bFGF or FGF-2) is the prototypical member of the FGF gene family, which is comprised of a total of seventeen members (FGF-1 to 17) which share a partial amino acid sequence homology [Friesel and Maciag, 1995; Hoshikawa, et al., 1998]. FGFs are potent mitogens for mesenchymal and neuroectoderm-derived cells, including vascular endothelial cells, and elicit diverse biological activities on a large number of different cell types. Basic FGF, along with the other FGFs, have been implicated in several physiological and pathological processes, including embryonic development, angiogenesis, wound healing, tissue repair, differentiation, neuronal outgrowth and function, migration, and cell survival [Christofori, 1997]. Additionally, bFGF is known to be the only cytokine that can trigger all the phenomena associated with angiogenesis, including EC proliferation, migration, increase plasminogen activities, collagenase production, and decrease plasminogen activator inhibitors [Kumar, et al., 1998].

The biological effects of bFGF on endothelial cells, as well as numerous other tissues and cell types, are mediated through four high-affinity, transmembrane tyrosine kinase receptors: FGFR-1 (flg, cek 1), FGFR-2 (bek, cek 3), FGFR-3 (cek 2), and FGFR-4. These receptors belong to the superfamily of RTKs and possess high diversity with variable ligand specificity and affinity. Basic FGF also binds to heparan sulfate polysaccharides (low-affinity receptors) and heparin, which act to form a ternary complex

with bFGF and its high-affinity receptor to potentially increase signaling efficiency and bioactivity [Jaye, et al., 1992; Yayon, et al., 1991].

Binding of bFGF induces conformational changes to its high-affinity receptors, followed by dimerization and transphosphorylation of its tyrosine residues [Ullrich and Schlessinger, 1990]. The autophosphorylated intracellular tyrosine kinase domains become targets for SH2, SH3, and phosphotyrosine-binding domain-containing molecules. Intracellular mediators interacting via such a process are phospholipase C-γ1 (PLC-γ1) [Roth, 1994], cortactin [Zhan, et al., 1994], Shc [Spivak-Kroizman, et al., 1994] and phosphatidyl-inositol 3' kinase [Varticovski, et al., 1994]. Activated PLC-γ1 catalyzes the breakdown of the membrane phospholipid, phosphatidylinositol bisphosphate, to generate inositol 1,4,5-triphosphate and diacylglycerol [Ullrich and Schlessinger, 1990]. Inostitol triphosphate subsequently mobilizes Ca^{2+} from intracellular stores, which combines with DAG to activate protein kinase C. PKC can, in turn, activate phospholipase D to catalyze the hydrolysis of phosphatidylcholine (PC) to form phosphatidic acid (PA), a precursor of DAG [Billah and Anthes, 1990; Exton, 1990]. PC-PLD may also be activated via an independent pathway from PKC activation, and thus may serve as a regulator of long-term activation of PKC [Ahmed, et al., 1994]. The secondary messengers generated in this cascade may activate Raf kinase, mitogen-activated protein (MAP) kinase, extracellular signal-regulated kinase (ERK), and NF-κB, and have been implicated in controlling many of the physiological responses produced by bFGF, namely cell proliferation, differentiation, migration and angiogenesis [Friesel and Maciag, 1995]. However, the specific role of each messenger in mediating the cellular functions of bFGF are strongly cell-type and function-dependent [Jaye, et al., 1992; Peters, et al., 1992; Mohammadi, et al., 1992]. A schematic of the bFGF-mediated signaling pathways is shown in Figure 2-4-1 for reference.

Studies involving the elucidation of the second messengers activated by bFGF using several of the aforementioned inhibitors have been controversial. In fibroblast cell lines, it has been shown that bFGF activates the enzyme phospholipase Cγ1, yet it has not been shown to correlate with increased FGF mitogenicity [Peters, et al., 1992; Coughlin, et al., 1988]. Additionally, neither Ca^{2+} nor phosphotidylinositol hydrolysis appears to play a role in FGF mitogenic activity [Peters, et al., 1992; Mohammadi, et al., 1992]. In endothelial cells, there have also been conflicting results with emphasis on the role of PKC in the mitogenic signaling mechanism. PKC has been shown to inhibit bFGF-dependent DNA synthesis in capillary endothelial cells [Doctrow and Folkman, 1987], yet be essential for bFGF mitogenic activity in normal and transformed fetal bovine aortic endothelial cells [Presta, et al., 1989]. Additionally, studies have demonstrated increased bFGF-activated

PKC-α, δ, ϵ, θ, η, and ζ immunoreactivity in human umbilical vein endothelial cells [Kent, et al., 1995; Haller, et al., 1996], and that endothelial proliferation may be mediated by a Ca^{2+}-independent PKC isozyme activated by bFGF [Kent, et al., 1995].
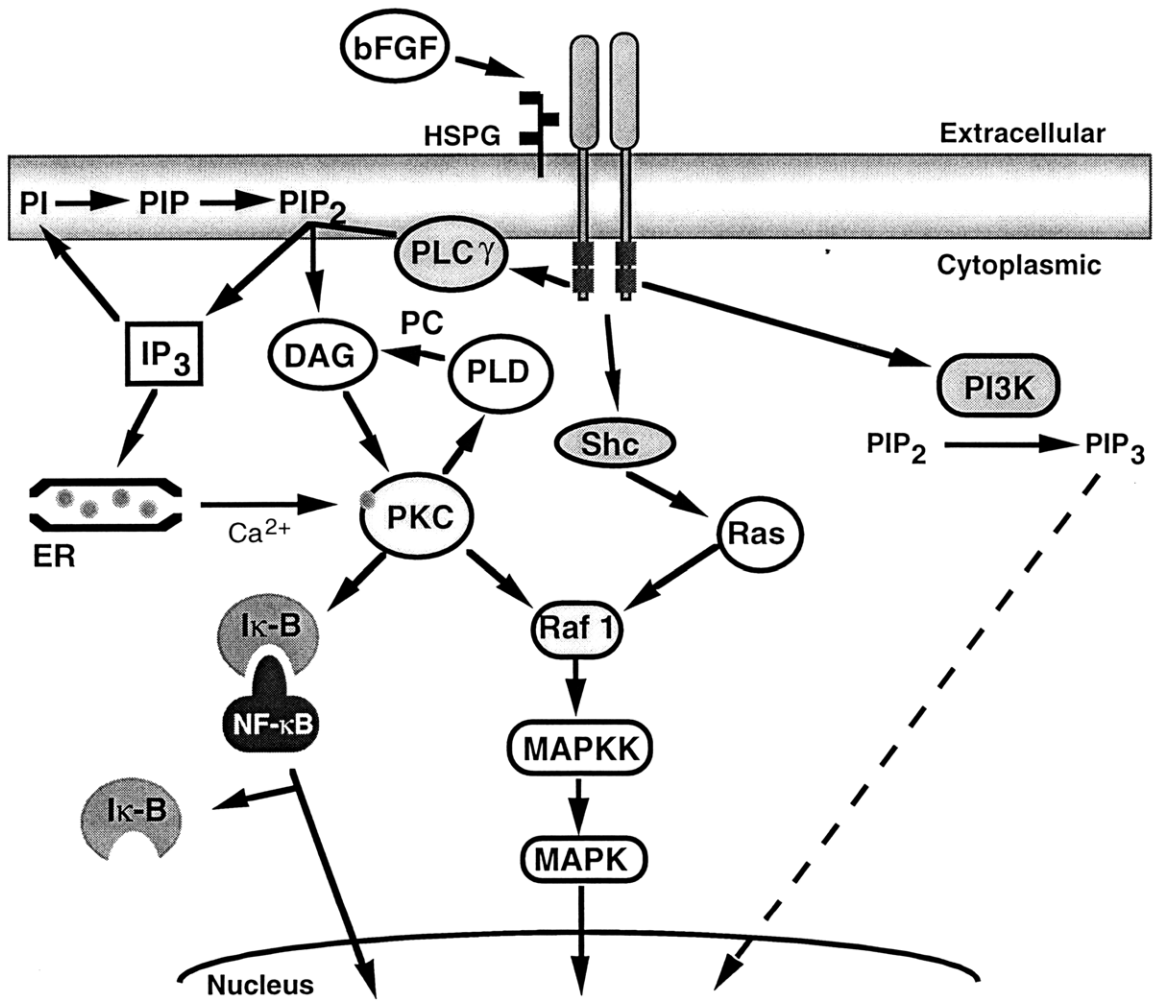
Figure 2-4-1. Schematic of the potential signaling pathways used by bFGF.

2.4.2 VEGF Signaling

Vascular endothelial growth factor (VEGF), also known as vascular permeability factor (VPF), is a homodimeric, heparin-binding glycoprotein with potent angiogenic, mitogenic, chemotactic, and vascular permeability-promoting activities specific for endothelial cells. The VEGF gene encodes four different proteins ($VEGF_{121}$, $VEGF_{165}$, $VEGF_{189}$, and $VEGF_{206}$) as a result of alternative splicing [Tisher, et al., 1991]. $VEGF_{121}$ and $VEGF_{165}$ are diffusible proteins that are readily secreted, while $VEGF_{189}$ and $VEGF_{206}$ have high affinity for heparin and principally remain bound to heparin-containing proteoglycans in the extracellular matrix [Ferrara, et al., 1992]. VEGF has been implicated in inflammation and in normal and pathological angiogenesis associated with wound healing, embryonic development, growth and metastasis of solid tumors.

The biological effects of VEGF on endothelial cells are mediated through two receptor tyrosine kinases, Flt-1 (*fms*-like tyrosine kinase-1) and KDR (kinase-insert-domain-containing receptor; or the mouse homologue, Flk-1, fetal liver kinase-1). Binding of VEGF induces conformational changes in KDR and Flt-1, followed by dimerization and autophosphorylation on tyrosine residues [Heldin, 1995]. Activation of the low-affinity, high-capacity KDR mediates actin reorganization, membrane ruffling, chemotaxis, and mitogenicity [Waltenberger, et al., 1994]. The functions and mechanisms of action of the high-affinity, low-capacity Flt-1 are less clearly understood, but appear to mediate chemotactic activity in monocytes and stimulate tissue factor expression in monocytes and endothelial cells [Clauss, et al., 1996].

In molecular terms, VEGF is able to act through KDR and at least partly through Flt-1 to increase the tyrosine phosphorylation of phospholipase Cγ, phosphatidylinositol 3-kinase, and GTPase-activating protein in endothelial cells [Waltenberger, et al., 1994; Guo, et al., 1995]. The activation of these early signal transduction events by VEGF, as for bFGF, leads to the phosphorylation of protein kinase C via phospholipase Cγ and the hydrolysis of phosphatidylinositol-4,5 bisphosphate, and MAP kinases via the Ras pathway. PKC isoforms α and β_{II} have been found to be translocated in VEGF-stimulated endothelial cells, while PKC-δ and -ϵ are not, and that the stimulated cell growth is largely mediated by the PKC-β isoform [Xia, et al., 1996]. Additionally, VEGF-activated PKC has been shown to stimulate PLD in HUVECs, which is unlikely to be directly involved in the control of DNA synthesis, but rather in regulating cytoskeleton-dependent effects such as cell migration [Seymour, et al., 1996]. A schematic of VEGF cell signaling is shown in Figure 2-4-2.
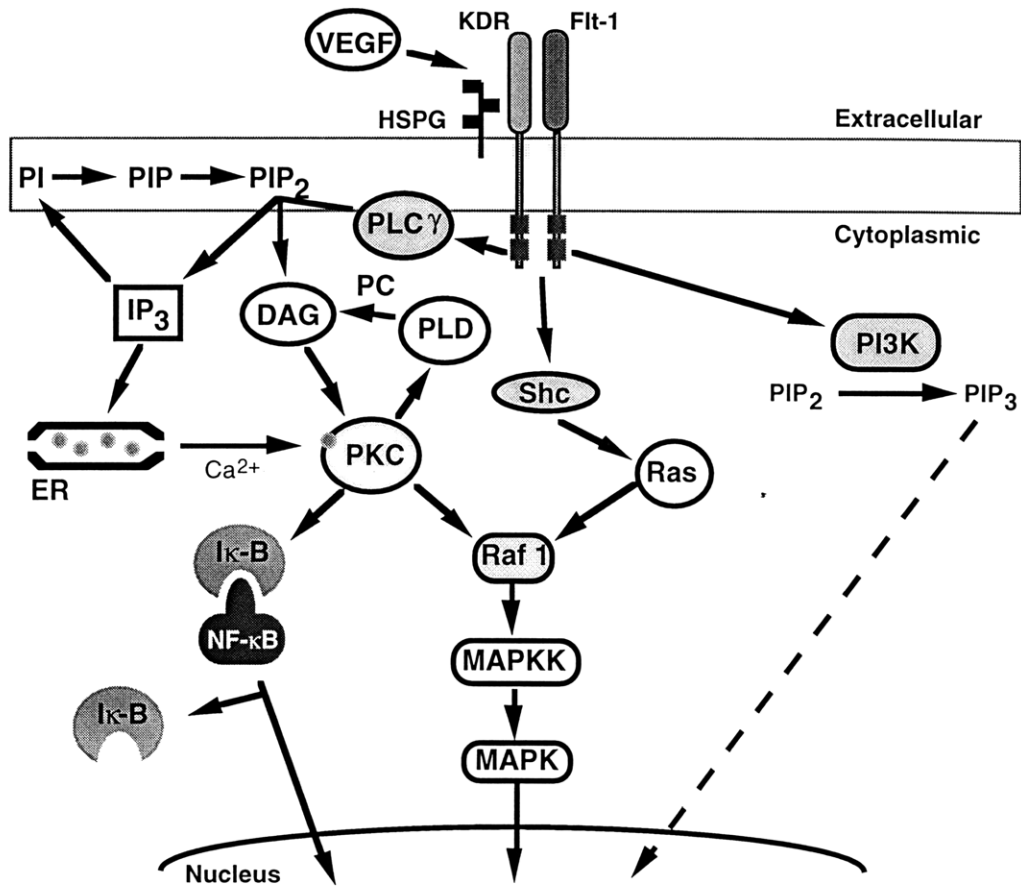
Figure 2-4-2. Schematic of the signaling pathways used by VEGF.

2.4.3 TNFα Signaling

Tumor necrosis factor-α (TNFα), or cachectin, is a pleiotropic polypeptide that is member of a broader, TNF ligand superfamily consisting of nine different proteins. It is capable of producing a wide variety of effects on a large number of cells by activating multiple signal transduction pathways, inducing or suppressing a vast number of genes, and using ubiquitous receptors. As a consequence of this diversity, TNFα has been recognized in many physiological and pathological processes, including normal host resistance to infection, angiogenesis, cachexia, septic shock, autoimmune disorders, and meningococcal septicemia.

With respect to endothelial cells, TNFα has been shown to induce the expression of adhesion molecules, thromboplastin, tissue-type plasminogen activator, plasminogen activator inhibitor type 1, prostacyclin, neutral metalloproteinases, class I MHC, NF-kB, and IL-6, IL-8 and basic fibroblast growth factor [Fajardo L.-G. and Allison, 1997]. It is also able to induce cell growth in cultured endothelial cells in a biphasic, dose-dependent manner.

TNFα exerts its biological effect by interacting with two distinct cell surface receptors, TR55 (TNFR-I) and TR75 (TNFR-II), which are expressed in most cell lines, but in different densities [Hohmann, et al., 1989]. Both receptors are transmembrane glycoproteins with molecular weights of 55 kDa and 75 kDa, respectively. The intracellular domains of the two receptors are apparently unrelated and distinct immunologically, suggesting they employ different signal transduction pathways. Moreover, while TR55 has been shown to be an essential component for TNFα signal transduction [Schütze, et al., 1992; Wiegmann, et al., 1992], TR75 has been shown to function as a TNFα antagonist by neutralizing TNFα, as well as a TNFα agonist by facilitating TNFα:TR55 complex formation [Peschon, et al., 1998; Pinckard, et al., 1997].

Two major and independent pathways for TNFα signaling have been identified and found to occur in endothelial cells. One involves TNF-mediated phospholipase A_2 (PLA_2) activation, resulting in the production of arachidonic acid [Clark, et al., 1988]. The second major pathway involves specific C-type phospholipases and protein kinases. The TNFα:TR55 complex triggers intracellular signaling of a specific phospholipase C that hydrolyzes phosphatidylcholine to produce the second messenger diacylglycerol [Schütze, et al., 1991]. DAG then activates two enzymes, protein kinase C (PKC) and an acidic sphingomyelinase (SMase) that hydrolyzes sphingomyelin (SM) to produce ceramide [Schütze, et al., 1992]. While PKC can induce the pleiotropic transcription factor, NF-κB, it has been demonstrated that PKC is not required for NF-κB activation by TNFα. However, the TNFα-responsive PC-PLC system, acting through the second messenger-like molecule ceramide, is able to induce NF-κB and permit the expression of a variety of genes, including E-selectin, VCAM-1, and ICAM-1. Interestingly, the induction of VCAM-1 expression on endothelial cells by TNFα appears to be highly PKC-dependent, as well requiring NF-κB-like binding activity for transcription [Deisher, et al., 1993; Read, et al., 1996]. A schematic of TNFα cell signaling is included for reference and is shown in Figure 2-4-3.
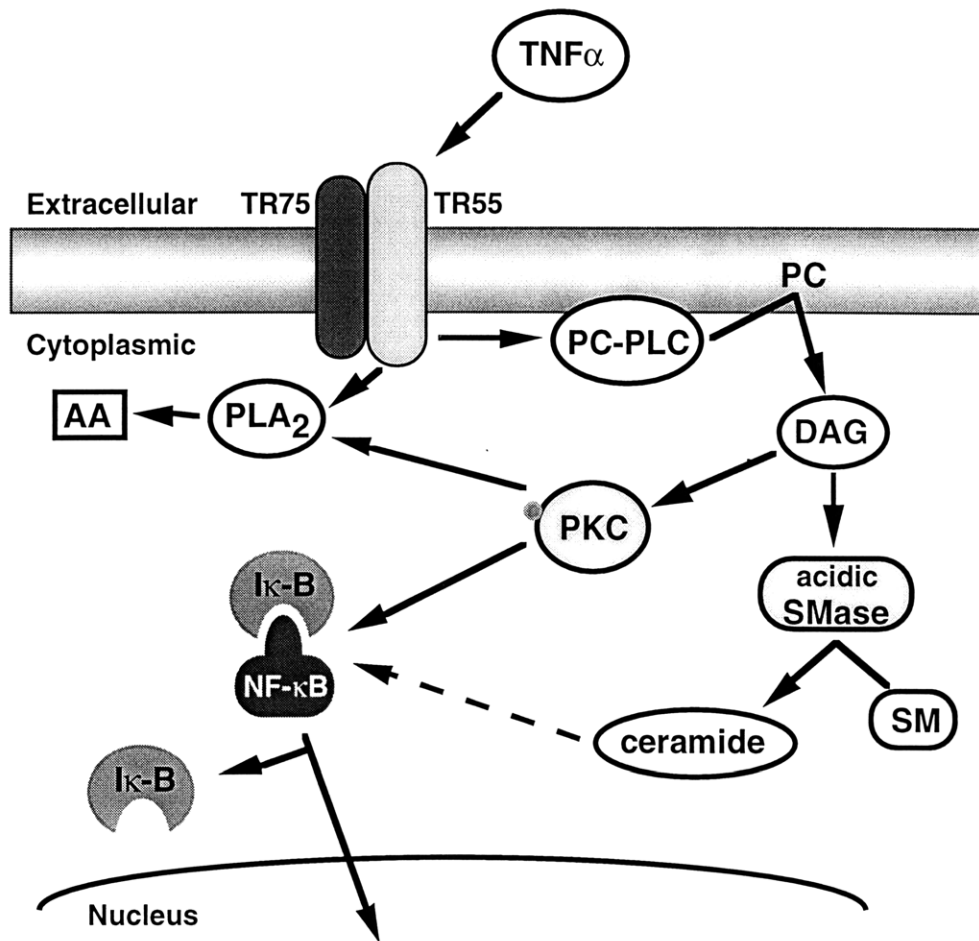
Figure 2-4-3. Schematic of the signaling pathways used by TNFα.

2.4.4 TGFβ Signaling

Transforming growth factor-β (TGFβ) is a pleiotrophic polypeptide and the prototype for a superfamily (TGFβ superfamily) of growth-regulatory polypeptides that also include activins, inhibins, bone morphogenetic proteins (BMPs), and decapentaplegic (Dpp). One subset of this superfamily is the TGFβ family, which includes three mammalian isoforms, TGFβ$_{1,2,3}$ [Hartsough and Mulder, 1997]. Members of the TGFβ family exert wide ranging effects on several different cell types. Among the most common

biological effects are regulation of cell growth, apoptosis, differentiation, adhesion and extracellular matrix production [Heldin, et al., 1997]. With such a plethora of effects on cells, it is not suprising that TGFβ has been implicated in many physiological processes, including embryogenesis, inflammation, wound repair, and immunosuppression.

TGFβ elicits its cellular action by initially binding to a specific set of receptors, classified as TGFβ receptor Type I (R_I), Type II (R_{II}), Type III (R_{III}), and endoglin [Segarini, 1993; Yamashita, et al., 1994]. Each member of the TGFβ superfamily binds to a characteristic combination of receptor Type I and Type II, both of which are needed for proper signaling and have intrinsic serine/threonine kinase activity. TGFβ₁ initially binds to the type II receptor (TβR-II), which then sequentially recruits the type I receptor (TβR-I) and forms a complex. TβR-II phosphorylates TβR-I, which consequently determines the specificity of the intracellular signals [Carcamo, et al., 1994].

Currently, six distinct types of signaling components have been described for the cytoplasmic signal transduction cascade of TGFβ. These include protein kinase C, phopholipase C, protein phosphatase 1, Ras, mothers against decapentaplegic (MAD) superfamily members, and several mitogen-activated protein kinase superfamily members, such as TAK-1 and stress-activated protein kinase/Jun-N-terminal kinase (JNK). A schematic of the potential TGFβ-mediated signaling pathways is shown in Figure 2-4-4.

TGFβ R_I receptor interaction with the α-subunit of farnesyl-protein transferase (αFTP) may be the upstream mechanism for the activation of Ras, and the subsequent activation of the MAPK cascade and cell cycle components downstream. This particular pathway may mediate TGFβ production, AP-1 or ATF-dependent gene transcription, growth inhibition, control of extracellular matrix production, and/or apoptosis.

TGFβ R_I receptor activation may also stimulate the phosphorylation, nuclear translocation and transcriptional activation of several SMAD proteins (vertebrate homologues of MAD). This may also lead to gene transcription, growth inhibition, and control of ECM.

The functions of TGFβ-activated PKC and PLC have been implicated in the prevention of c-jun-dependent transcription and augmentation of fibronectin and plasminogen activator inhibitor-1 (PAI-1) mRNA expression [Halstead, et al., 1995]. Protein phosphatase 1 activation by TGFβ was associated with growth-arrest in keratinocytes, and it is unknown if the activity is cell-type specific or a general consequence of TGFβ treatment [Gruppuso, et al., 1991].

38
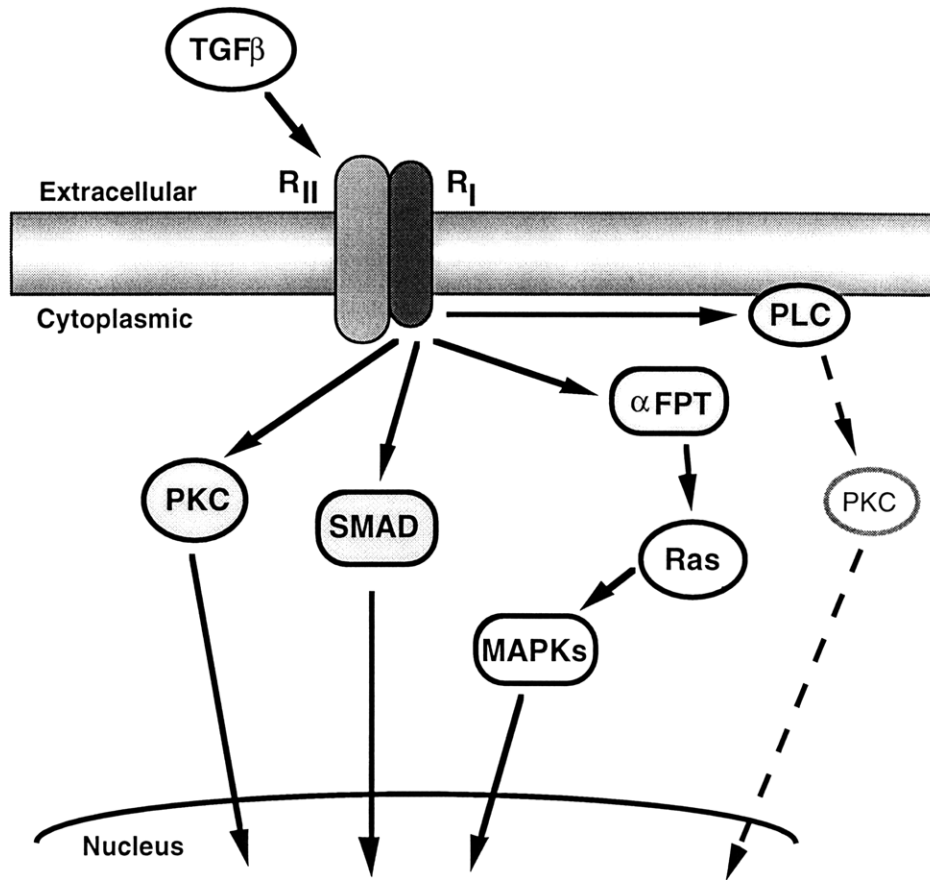
Figure 2-4-4. Schematic of the potential signaling pathways used by TGFβ.

2.5 Fluid Dynamics

The dynamic flow experiments performed by the various studies mentioned above, which provide *in vitro* simulation of the *in vivo* biomechanical environment, have been carried out using one of two basic systems: 1) a parallel-plate flow chamber [van Kooten, et al., 1992], or 2) a modified cone-plate viscometer [Bussolari, et al., 1982]. The latter involves the generation of fluid shear stresses between a stationary base plate and a rotating cone. The system used in this thesis is the parallel-plate flow chamber. It consists of a polycarbonate block, a silastic gasket and a transparent microscope slide, on which a confluent endothelial monolayer presides, all of which is held together by a vacuum pump (see Figure 3-3). A syringe pump is able to generate a well-defined, unidirectional laminar flow across the chamber, and the wall shear stress can be calculated using the Navier-

Stokes equations for fluid mechanics. Beginning with the equations of continuity and conservation of momentum:

$$\frac{\partial \rho}{\partial t} + \nabla \rho \vec{V} = 0 \tag{1}$$

$$\rho \frac{\partial \vec{V}}{\partial t} = -\nabla P + \mu \nabla^2 \vec{V} \tag{2}$$

where ρ is the fluid density, t is the time variable, V is the local fluid velocity, P is the pressure, and μ is the dynamic viscosity of the fluid.

Assuming a parallel, fully-developed flow of an incompressible Newtonian fluid of constant viscosity in a rectangular duct of uniform cross-section, equations (1) and (2) can be simplified and the axial fluid velocity u resolved to the following:

$$\frac{\partial u}{\partial z} = 0 \tag{3}$$

$$\rho \frac{\partial u}{\partial t} = -\frac{\partial P}{\partial z} + \mu \left(\frac{\partial^2 u}{\partial x^2} + \frac{\partial^2 u}{\partial y^2} \right) \tag{4}$$

where u is the axial fluid velocity, and x, y, z are the Cartesian space coordinates of the flow chamber, with z being the axial coordinate.

The momentum equation (4) can further be simplified by assuming steady-state flow conditions, and the following boundary conditions:

$$u|_{\pm a, y} = 0 \quad \text{and} \quad u|_{x, \pm b} = 0 \tag{5}$$

where a and b represent the distance from the center of the flow chamber to the corresponding sides. Integrating equations (3) and (4) with the set boundary conditions (5) and performing some algebraic re-arrangement, an analytical solution can found for the steady-state condition [Savino and Siegel, 1964]:

$$(X,Y) = \frac{-\dfrac{\gamma}{8} + \dfrac{\gamma X^2}{8} - \dfrac{4\gamma}{\pi^3} \sum_{n=1,3,5...}^{\infty} \dfrac{(-1)^{(n+1)/2}}{n^3 \cosh(\frac{n\pi\gamma}{2})} \cosh\left(\dfrac{n\pi\gamma Y}{2}\right) \cos\left(\dfrac{n\pi X}{2}\right)}{-\dfrac{\gamma}{12} + \dfrac{16}{\pi^5} \sum_{n=1,3,5...}^{\infty} \dfrac{1}{n^5} \tanh\left(\dfrac{n\pi\gamma}{2}\right)} \tag{6}$$

40

where the dimensionless coordinates $X=x/a$ and $Y=y/b$ and the dimensionless axial fluid velocity $U=u/u_m$ have been introduced, and u_m represents the mean fluid velocity defined as $u_m=Q/4ab$, where Q is the volumetric flow rate.

The wall shear stress τ_w acting on the cell monolayer can be determined with respect to the velocity profile in the chamber by the following equation:

$$\tau_w = \mu \frac{\partial u}{\partial y}\bigg|_{y=-b} = \mu \frac{u_m}{b} \frac{\partial U}{\partial Y}\bigg|_{Y=-1} \tag{7}$$

Using the dimensionless velocity profile derived in equation (6), the wall shear stress can be equated from equation (7) to form:

$$\tau_w(X,Q,\gamma) = \frac{Q\mu\gamma^2}{\pi^2 ab^2} \frac{\sum_{n=1,3,5...}^{\infty} \frac{(-1)^{(n+1)/2}}{n^2} \tanh\left(\frac{n\pi Y}{2}\right)\cos\left(\frac{n\pi X}{2}\right)}{-\frac{\gamma}{6} + \frac{32}{\pi^5}\sum_{n=1,3,5...}^{\infty} \frac{1}{n^5}\tanh\left(\frac{n\pi\gamma}{2}\right)} \tag{8}$$

The resulting equation for the wall shear stress τ_w is plotted in Figure 2-5-1 as a function of the dimensionless width of the channel X for a volume flow rate of 0.085 ml/min, a commonly used flow rate to simulate physiological flow conditions. Additionally, the values of the viscosity $\mu = 0.015$ poise, chamber height $a = 40$ μm, and chamber width $b = 0.625$ cm are utilized.

Due to the significantly small aspect ratio of the chamber, $\gamma = 0.006 \ll 1$, and the relatively uniform wall shear stress distribution across the channel over which the measurements are to be taken, it can be assumed that the chamber represents channel flow and $u = u(y)$ only. Using equations (4) and (7), with the boundary conditions specified in equation (5), an exact solution for the wall shear stress can be derived in the form:

$$\tau_w = \frac{3\mu Q}{4a^2 b} \tag{9}$$

This equations demonstrates a linear relationship between the wall shear stress and the volumetric flow rate and is valid to within a 2% error for a wide range of flow rates. Consequently, equation (9) was used to calculate τ_w in the functional adhesion studies performed in the thesis.
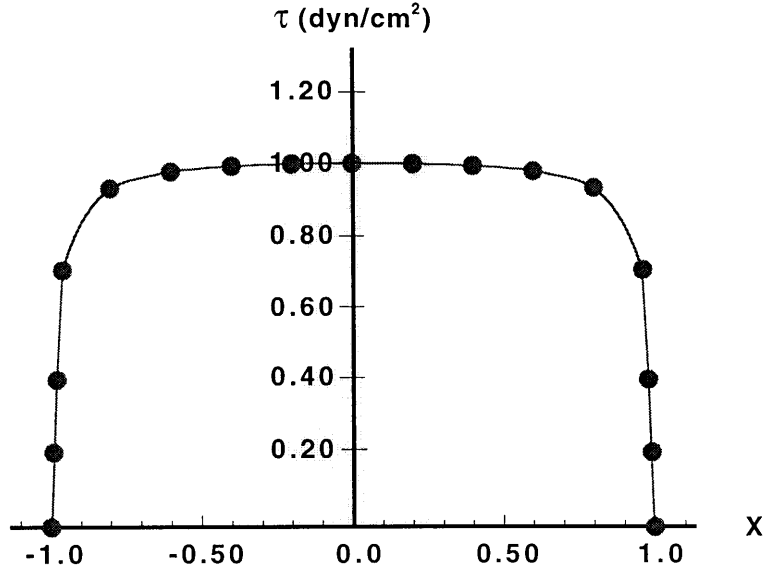
Figure 2-5-1. Wall shear stress as a function of the transverse coordinate in the parallel-plate flow chamber for a volumetric flow rate of Q=0.085 ml/min. The shaded region designates the range over which all measurements were taken in the functional experiments.

The calculated wall shear stresses induced by multiple flow rates can be incorporated with a normalization routine which provides a more accurate method for interpreting binding data for cell capture and efficiency using the parallel-plate flow chamber [Munn, et al., 1994]. The routine provides an estimate of the cell flux near the surface based on the sedimentation rate and velocity profile in the chamber. Thus, a more detailed analysis on the interactions and kinetics of receptor-ligand binding can be performed.

For the functional analysis experiments using a multiple series of flow rates, the time to reach steady state for each flow rate is defined by equalizing the total number of cells, G_i, passing at each step change in flow rate and is governed by the following equation:

$$G_i = \frac{Cx}{2}\left(\frac{u_{i-1}}{u_i} + \frac{2vx}{u_i h} + 1\right) + Cu_i\left(1 + \frac{vx}{u_i h}\right)\left(t_{wi} - \frac{x}{u_i}\right) \qquad (10)$$

where G_i = total number of cells passing at each flow rate, i = flow rate index, C = bulk concentration, u_i = average flow velocity at flow index i, v = settling velocity, h = 13 μm layer of fluid at the bottom of the flow chamber, t_{wi} = time period at given flow rate i (including sampling time), and x = direction of axial flow.

Having this normalization of cell flux allows for the efficiency of cell capture to be calculated, which is a function of the detachment force generated by flow-induced shear stress. Efficiency, E, is specifically defined as the number of cells that bind, N_b, at a given shear stress divided by the total number of cells, N_t, that pass over the surface. Cumulative cell binding curves can then be fitted to the equation [Melder, et al., 1995]:

$$E = \frac{N_b}{N_t} = E_o' e^{-\kappa S} \tag{11}$$

where S is the shear stress, and E_o' and κ are fitted parameters. The efficiency at zero shear stress, E_o, provides a measure of the stability of the adhesion complex following initial capture and can be derived from equation (11) to be of the form:

$$E_o = E_o'\left(1 - e^{-\kappa \Delta S}\right) \tag{12}$$

where ΔS is the difference in shear stress between successive flow rates. The capture coefficient, k, also provides a useful measure by reflecting the relative sensitivity of the cells to initial capture leading potentially to rolling and firm adhesion.

The receptor-ligand mediated adhesion of cells in a fluid stream to specific cell surfaces is a complex process. A number of physical mechanisms have been shown to be involved in the process, which include: the kinetics of receptor-ligand binding, receptor-ligand affinities, forces and torques acting on the cell, and the delivery rate of cells to the surface. Additional complexities are apparent when one considers that more than one receptor-ligand pair mediates cell adhesion and that each system has its own distinctive kinetics. The routines described above provide a useful means for giving further insight into these processes and comparing the relative net adhesive forces between different cell populations and receptor-ligand interactions.

Chapter 3

Materials and Methods

3.1 Introduction

One of the goals of this thesis was to characterize the *in vitro* molecular and cellular interactions between resting and IL-2-activated human CD4+, CD8+, and CD56+ (NK) lymphocyte populations and vascular endothelial cells activated by various angiogenic factors. This involved quantifying the individual contributions of the cell adhesion molecule receptors on the lymphocytes essential for capture and stable adhesion, and correlating the adhesive characteristics of the cells with the levels of receptor and ligand expression and binding kinetics.

The level of CAM expression on HUVEC monolayers treated with tumor interstitial fluid and various angiogenic growth factors, namely TNFα, VEGF, bFGF, TGFβ, was also determined to further characterize the endothelial response and correlating with specific ligand-receptor interactions involved in cell adhesion to the endothelium.

Additionally, the essential signal transduction pathways used by bFGF in modulating the CAM expression was determined in providing a framework for the molecular mechanisms of adhesion regulation.

To obtain this information, several techniques were utilized: a) parallel-plate flow chamber for the functional studies involving lymphocyte binding kinetics, efficiencies, and receptor-ligand pairings, b) targeted sampling fluorometry, flow cytometry, and a fluorescence immunoassay for the expression studies involving endothelial cell monolayers, and c) Northern blot for the transcriptional studies.

44

3.2 Lymphocyte Preparation

3.2.1 Lymphocyte Isolation

Human lymphocyte populations were isolated from Leukopack preparations (Massachusetts General Hospital Blood Bank) or from peripheral blood donors and diluted 1:1 with RPMI-1640 + 10% FCS (Gibco, Grand Island, NY) and centrifuged over a Ficoll-Hypaque gradient (Lymphoprep; Nycomel, Oslo, Norway). The lymphocyte layer collected from the interface of the gradient was washed twice with DPBS and depleted of monocytes by the plastic adherence method for 45 min and, in the case of Leukopack preparations, was then incubation with L-phenylalanine methyl ester (PME; Fluka Chemical, Buchs, Switzerland) for approximately 15 min in a Hanks' Balanced Salt Solution (HBSS, with Ca^{2+} + Mg^{2+}) [Leung, 1989]. The cells were subsequently centrifuged and resuspended in RPMI-1640 + 10% FCS.

The resting lymphocyte subpopulations, namely unactivated CD4+, CD8+, and CD56+, were isolated using a magnet bead separation technique (MACS; Miltenyi Biotech, GmbH, Gladbach, Germany) in conjunction with targeted antibodies [Miltenyi, et al., 1990]. The technique involved using a two-step, indirect staining process. The cells were first washed with a solution of DPBS + Ca^{2+} + Mg^{2+} + 1% BSA + 5 mM EDTA + 0.01% sodium azide (DPBS*) and incubated with an excess of primary antibody, 10 µg antibody/15 x 10^6 cells, in 0.1 ml of DPBS* at 4°C for 30 min. The cells were washed three times with DPBS* and 10 µg of goat-anti-mouse IgG MicroBeads (Miltenyi Biotech) was applied to a 0.1 ml cell suspension for 30 min at 4°C. The cells were then washed three times, resuspend in 0.5 ml of DPBS*, and loaded on to magnetic separation columns for selection following the manufacturer's instructions.

For use in the adhesion assays, the cells were positively selected for their respective antigens, namely anti-CD4, anti-CD8 and anti-CD56 mAb were used as the primary antibody. For flow cytometric analysis, the cells were negatively selected to prevent cross-reactive binding of the antibodies to the fluorescein isothiocyanate (FITC) conjugate. Therefore, CD4+ cells were obtained by positively selecting for CD8 (specific T cell antigen), CD15 (monocyte antigen), CD19 (B cell antigen), and CD56 (NK cell antigen); CD8+ cells by selecting for CD4 (specific T cell antigen), CD15 (monocyte antigen), CD19 (B cell antigen), and CD56 (NK cell antigen); and CD56+ cells by selecting for CD4 (specific T cell antigen), CD8 (specific T cell antigen), CD15 (monocyte antigen), and CD19 (B cell antigen). Extracted cell populations were shown to be greater than 90% selective for their respective populations, as determined by flow cytometric analysis. The

isolated non-activated lymphocytes were then maintained in RPMI + 10% FCS + 0.1% sodium azide at 4°C, reversibly limiting respiration and energy production, prior to experimentation.

The activated lymphocyte subpopulations were prepared by initially incubating the peripheral blood lymphocytes at a concentration of 2 x 10^6 cells/ml in a tissue culture medium consisting of RPMI-1640 supplemented with 2 mM L-glutamine, 10% FCS, 5% human serum, 100 U/ml penicillin, 100 μg/ml streptomycin, and 1000 U/ml of recombinant interleukin-2 (rIL-2) (Cetus/Chiron, Emeryville, CA), and placed in 25 cm^2 plastic culture flasks (Corning, Corning, NY) for 24 hr in a 37°C humidified incubator containing 5% CO_2. The non-adherent cells were removed, centrifuged to a pellet, resuspended in tissue culture medium, placed in new, vertically aligned 25 cm^2 plastic flasks and cultured for 1.5 to 4 weeks. Fresh tissue culture medium with 1000 U/ml of rIL-2 was added regularly to maintain cell concentrations below 2 x 10^6 cells/ml. This produced cultures of activated-lymphocytes with relatively significant populations of CD8+ (~25%) and CD4+ (~20%) cells, as determined by MACS technique and hemocytometer counting. The activated lymphocyte subpopulations, namely CD4+ and CD8+ were isolated using the magnet bead separation technique in conjunction with targeted antibodies, as per the protocol previously described.

The plastic-adherent cells from the original 24 hr incubation were gently washed four times with RPMI + 10% FCS. The supernatant from the non-adherent cells was added the adherent cells and cultured for 1-4 weeks in 25 cm^2 plastic flasks aligned horizontally to produce cultures of activated-natural killer cells, as described previously [Pober and Cotran, 1990]. Fresh tissue culture medium with 1000 U/ml of rIL-2 was added regularly to maintain cell concentrations below 2 x 10^6 cells/ml. Expanded cell populations were shown to be 90-98% CD56+/CD3- and <5% CD3+ cells by flow cytometric analysis.

3.2.2 Lymphocyte Labeling

The lymphocytes were labeled with a cytosolic fluorescent dye, calcein-AM (calcein acetoxymethyl ester, Molecular Probes, Eugene, OR), for better visualization of the flowing, rolling, and adhered cells against the endothelial cell monolayer. The dye causes no distinguishable physical changes to the adhesion receptors or other related properties of the cell [Weston and Parish, 1990]. The cells were prepared using a calcein-AM concentration of 0.01 mM in PBS and applied for 15 min at room temperature, washed and resuspended in HBSS to a concentration of 1 x 10^6 cells/ml prior to the flow experiments.

3.2.3 Lymphocyte CAM Receptors

IL-2 activated and non-activated CD4+, CD8+, and CD56+ cells were labeled with antibody to the following receptors: CD18, VLA-4, L-selectin, or sLeX, with IgG_1 and IgG_{2a} isotype antibodies as controls. Using a two-step, indirect staining process, the cells were first washed with a solution of DPBS + Ca^{2+} + Mg^{2+} + 1% BSA + 5 mM EDTA + 0.01% sodium azide (DPBS*) and incubated with an excess of antibody, 10 μg antibody/15 x 10^6 cells, in 0.1 ml of DPBS* at 4°C for 30 min. The cells were then washed three times with DPBS* and 5 μg of a goat-anti-mouse $F(ab')_2$ flourescein conjugate (Tago, Burlingame, CA) was applied to a 0.1 ml cell suspension for 30 min at 4°C. The cells were again washed three times and then fixed with 0.5 ml of 1% paraformaldehyde. Flow cytometry analysis (FACScan; Becton Dickinson, San Jose, CA) was utilized to determine the relative fluorescence data for the various labeled molecules and provided an estimate of the level of adhesion receptor expression.

3.3 Endothelial Cell Preparation

3.3.1 Endothelial Cell Culture

Human umbilical vein endothelial cell (HUVEC) cultures[1] were obtained from single cord harvests and maintained in growth medium (EGM; Clonetics, San Diego, CA) supplemented with 10% FCS and 1% penicillin/streptomycin in fibronectin (Sigma Chemical, St. Louis, MO)-coated 75 cm^2 tissue culture flasks (Corning Glass Works, Corning, NY) in a 37°C humidified incubator containing 5% CO_2. Additional studies involving human dermal microvascular endothelial cell (HDMEC) cultures[2] were used and maintained under identical conditions. The use of the commercially available growth medium EGM provided insurance towards the standardization and reproducibility of the results [Watson, et al., 1995].

The endothelial cells used in the experiments of this thesis were of passage level 2 to 5. To maintain cultures for these extended periods, the endothelial cells were passaged by enzymatic detachment using trypsin/ethylenediaminetetraacetic acid (EDTA) and redistributed in a 1:3 proportion. The culture medium was changed every second day.

---

[1] The HUVEC cultures used for these experiments are a generous gift from Dr. Michael Gimbrone, Jr. of the Brigham and Women's Hospital [Gimbrone, et al., 1974].

[2] The HDMEC cultures used for these experiments are a generous gift from Dr. Michael Detmar of the Massachusetts General Hospital [Imcke, et al., 1991].

3.3.2 Endothelial Cell Monolayer Preparation

Preparation of the endothelial cell monolayers varied slightly depending on the application intended, i.e. expression assay or functional assay. For endothelial cells used in the functional adhesion assay, monolayers were grown on 3" x 1.5" sterile glass microscope slides (Fisherbrand, Fisher Scientific, Pittsburgh, PA) with plastic wells at a seeding concentration of 3×10^4/well and using EGM + 10% FCS. The monolayers were greater than 90% confluent and ready to use within 24 hours. The slides utilized were pre-treated with a siliconizing agent (Aquasil; Pierce Co., Rockford, IL) and coated with fibronectin (6 μg/cm^2) for 30 minutes at 37°C. The plastic wells were maintained on the slides by a 2% agarose preparation, permitting confinement of the monolayer and an accurate means for determining cytokine concentration (see Figure 3-1). The growth medium was subsequently replaced with serum-free RPMI and either cytokine, growth factor, and/or inhibitor was added for prescribed periods. Prior to use, the agarose was removed from the slides by using straight-edge extraction and the monolayer gently rinsed with HBSS before attaching to the flow chamber.
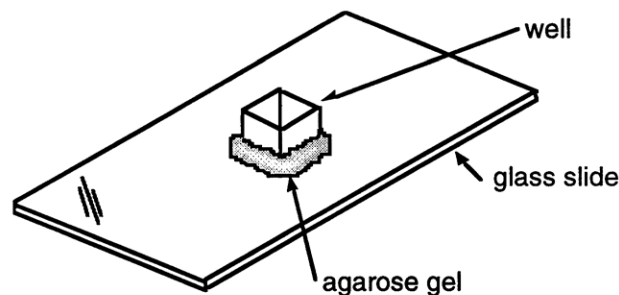
Figure 3-1. Slide preparation for monolayers to be used in the adhesion assay.

For endothelial cells used in the expression assays, HUVEC seeding varied depending on whether a well-plate or chamber slide was utilized. In either case, the substrate was pre-coated with 6 μg/cm^2 of fibronectin, and the monolayer grown to greater than 90% confluency in EGM medium over 24 hrs. Subsequently, the medium was replaced with serum-free RPMI and either cytokine, growth factor, and/or inhibitor was added. Complete descriptions of the preparations for each of the expression assays are described in their respective sections below.

3.4 Reagents

3.4.1 Cytokines and Growth Factors

The cytokines and growth factors used in the thesis were as follows: TNFα (Cetus, Emeryville, CA), IL-1β (R&D Systems), bFGF (Gibco BRL, Grand Island, NY), aFGF (R&D Systems), VEGF (Peprotech, Rocky Hill, NJ), and TGFβ (Genzyme, Cambridge, MA). The phorbol ester, phorbol 12-myristate, 13-acetate (PMA; Sigma Chemical, St. Louis, MO), was also utilized.

3.4.2 TIF Collection

Preparations of tumor interstitial fluid (TIF) were obtained from LS174T colon adenocarcinoma tumors (ATCC, Rockville, MD) grown in severe combined immunodeficient (SCID) mice by using the Gullino chamber, a semipermeable chamber [Gullino, 1970; Jain, et al., 1979; Melder, et al., 1996]. Essentially, a wafer-like chamber encased by a semipermeable membrane (0.45 μm mean pore size and typical porosity of 79%; type HA, Millipore, Bedford, MA) was inoculated with LS174T cells and implanted subcutaneously into SCID mice (see Figure 3-2). Following sufficient tumor growth, fluid accumulation within the internal cavity was sampled at 7, 10, and 14 days post-implantation and pooled from 3 mice, and was immediately stored at -70°C. Various dilutions of this fluid were used in both the expression and functional adhesion assays.
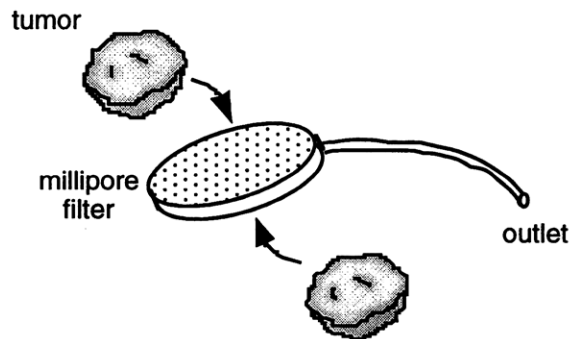
Figure 3-2. Schematic of the Gullino chamber used for the collection of tumor interstitial fluid.

3.4.3 Monoclonal Antibodies

Monoclonal antibodies used in the thesis were as follows: anti-ICAM-1 (CD54, clone LB-2; Becton Dickinson, San Jose, CA), anti-VCAM-1 (CD106, clone 1G11;

49

AMAC, Westbrook, ME), anti-E selectin (CD62E, clone H18/7; Becton Dickinson), anti-P selectin (CD62P, clone GA6; Becton Dickinson), anti-ICAM-2 (CD102, clone CBR-IC2/2; Endogen, Cambridge, MA), anti-sialyl Lewis X (clone CSLEX1, Becton Dickinson), anti-LECAM-1 (CD62L, clone SK11, Becton Dickinson), anti-CD15 (clone MMA, Becton Dickinson), anti-CD19 (Leu-12, clone 4G7, Becton Dickinson), IgG1 and IgG2a isotype control antibodies (clones X40 and X39; Becton Dickinson), anti-CD56 (Leu19, clone MY31, Becton Dickinson), anti-CD4 (clone IOT4a, Immunotech, Westbrook, ME), anti-CD8 (clone IOT8a, Immunotech), and anti-bFGF (R&D Systems, Minneapolis, MN).

3.4.4 Signaling Inhibitors

Sources for inhibitors to signaling molecules and transcription used in the thesis were as follows: methyl 2,5-dihydroxycinnamate (MDHC; Sigma Chemical), sodium orthovanadate (Na_3VO_4; Sigma Chemical), 2-nitro-4-carboxyphenyl N,N-diphenylcarbamate (NCDC; Sigma Chemical), propranolol DL (Sigma Chemical), calphostin C (Research Biochemicals International, Natick, MA), GF109203X (bisindolylmaleimide, Research Biochemicals International), and actinomycin D (Sigma Chemical).

3.5 Functional Adhesion Assay

In vitro adhesion characteristics between a suspension of lymphocytes (CD4+, CD8+, or CD56+) and endothelial cell monolayers were studied using a parallel-plate flow chamber [Munn, et al., 1994]. The flow chamber allows for the study of the kinetics of cellular binding in well-defined shear fields [Doroszewski, et al., 1979]. It consisted of a polycarbonate block, a silastic gasket and a transparent microscope slide, on which a confluent endothelial cell monolayer presided, all of which was held together by suction via a vacuum pump (see Figure 3-3).

A computer-driven (IBM PC; International Business Machines, Boca Raton, FL) variable speed syringe pump (Harvard Apparatus, South Natick, MA) drove the lymphocyte cell suspension from a reservoir through the chamber, which was stationed on an inverted microscope x, y stage (Nikon Diaphot TMD; Nikon, Garden City, NY) equipped with a 10x objective. Attached to the microscope was an I-CCD camera (Cohu 5000 Series, San Diego, CA) connected to a time code generator (Panasonic WJ-810, Secaucus, NJ), video cassette recorder (Sony SVO-9500MD, Park Ridge, NJ) and monitor (Ikegami PM205A, Maywood, NJ). Also directly connected to the microscope was an ultraviolent lamp (Nikon, Garden City, NY) for excitation of the fluorescently-labelled

lymphocytes. The system allowed for the simultaneous real-time visualization and recording of the flowing suspension and capture process of the lymphocytes, as well as the morphology and integrity of the endothelial cell monolayer. A schematic of the overall experimental set-up is presented in Figure 3-4.

(a)

(b)
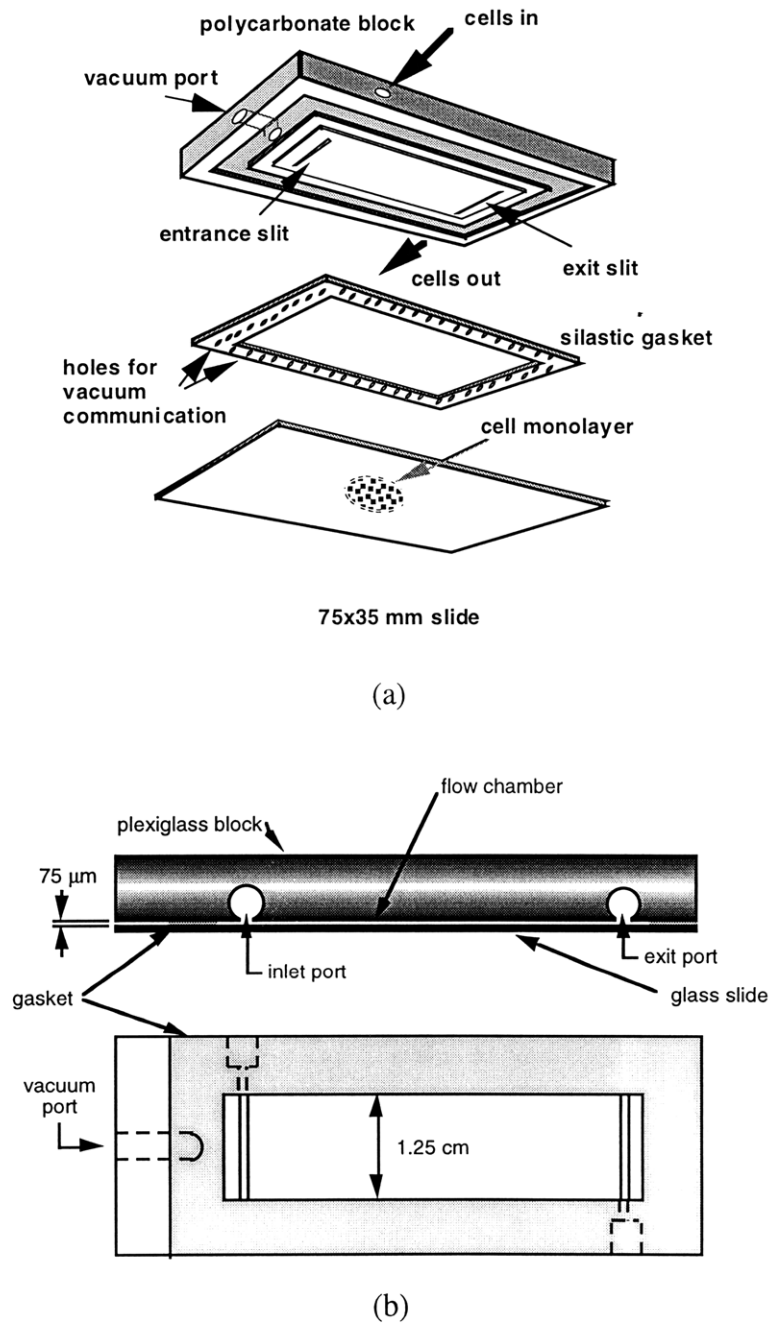
Figure 3-3. Parallel-plate flow chamber in a) an orthogonal representation, and b) a dimensional view point.
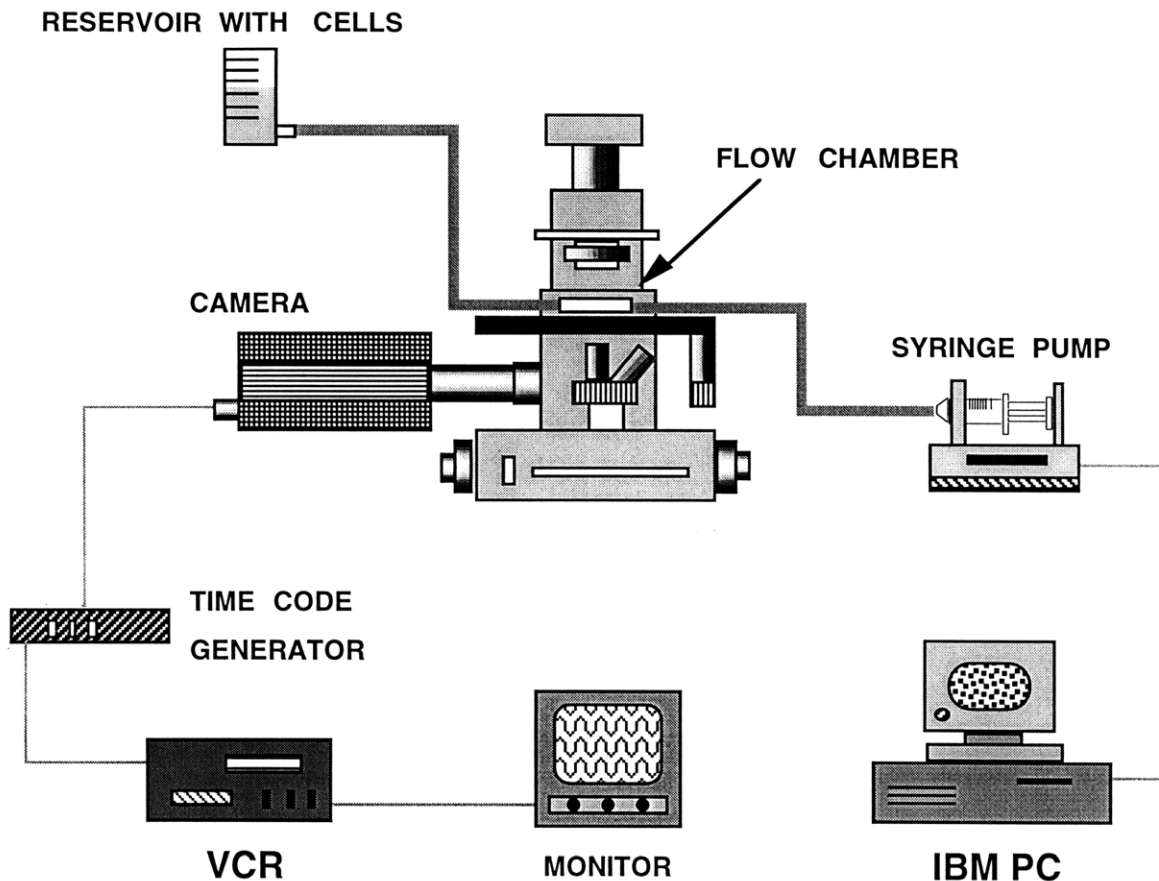
Figure 3-4. Schematic of the *in vitro* adhesion assay set-up.

The pump and chamber system allowed for a well-defined, unidirectional laminar flow to occur at single flow rates, typically 0.085 ml/min (corresponding to 1.0 dyne/cm^2 wall shear stress) applied for 6-8 minutes, or at multiple flow rates, ranging from 0.30 ml/min (3.51 dyne/cm^2) to 0.05 ml/min (0.59 dyne/cm^2) in steps of 0.05 ml/min. At each specific flow rate, steady-state was obtained, the corresponding run time adjusted to maintain equivalent cell flux [Munn, et al., 1994], and the stage was positioned to obtain 5-8 sample fields/flow rate. Each field was approximately 680 µm x 500 µm in size.

Off-line analysis using the video recordings was performed to determine the number of cells firmly bound per field, i.e. those cells which have not moved during the sampling period. In the case of multiple flow rates, a cumulative bound cell density was determined at each level of shear stress.

Antibody blocking experiments were also conducted with the lymphocyte subpopulation or the HUVEC monolayer being treated with an excess of antibody to

determine the role of each receptor-ligand pairing in cell adhesion. Activated and non-activated lymphocytes were suspended in 0.2 ml of HBSS and incubated with mAbs against CD18, VLA-4, sLeX, and IgG isotype control for 30 minutes at 4°C and resuspended in 1 ml immediately prior to experimentation. HUVEC monolayers were incubated in 0.2 ml medium with mAbs against ICAM-1, ICAM-2, VCAM-1, E-selectin, P-selectin, and IgG isotype control for 30 minutes at 37°C. The antibodies were used separately and in combination to assess the essential functional roles of the CAMs.

3.6 Protein Expression Assays

Four essential assays were used in this thesis to determine the level of protein expression. Three of the techniques involved cell surface protein expression of cell adhesion molecules on endothelial cells, namely targeted sampling fluorometry (TSF), flow cytometry, and fluorescence immunoassay. Each elicited their own advantages and disadvantages and were chosen based on these properties.

The fourth technique involved using enzyme-linked immunosorbent assays to quantify the levels of specific cytokines and growth factors in tumor interstitial fluid which may be essential in its modulatory characteristics of cell adhesion molecule expression.

3.6.1 Targeted Sampling Fluorometry

Targeted sampling fluorometry was specifically developed in the Steele Laboratory during this thesis to analyze the level and spatial profile of cell adhesion molecule expression on intact endothelial cell monolayers [Munn, et al., 1995]. The method utilizes standard immunostaining, fluorescence microscopy, and digital image analysis (see Figure 3-5).

In using TSF to measure cell adhesion molecule expression on the cell surface, HUVECs were grown in 8-chamber wells (Labtek; Nalge Nunc, Naperville, IL) on fibronectin-coated glass slides with a seeding density of 3 x 10^4 cells/well. The monolayers were greater than 90% confluent and ready to use within 24 hrs. At which time, the cells were washed 3 times with a serum-free solution of RPMI-1640 supplemented with 100 U/ml penicillin and 100 µg/ml streptomycin, and treated with a given cytokine and/or growth factor(s). After a selected incubation period, the cell monolayers were washed 3 times with PBS + Ca^{2+} + Mg^{2+}, fixed with paraformaldehyde (1 mg/ml in PBS) for 15 min, washed 4 times and then immunostained with a primary antibody directed against the given adhesion molecule (ICAM-1, ICAM-2, VCAM-1, E-selectin, P-selectin), followed by a secondary FITC-conjugated goat-anti-mouse antibody.

Both primary and secondary antibodies were added in excess, 10 µg primary antibody and 5 µg secondary antibody in 0.1 ml of PBS + 0.1% BSA, and incubated for 30 min. After the second incubation, the monolayers were washed 4 times and incubated with 1 mg/ml propidium iodide (PI) to stain for the cell nuclei. After a 15 minute period at 27˚C, the monolayers were washed and then mounted for microscopic observation using a buffer consisting of glycerol:PBS (2:8) with 1 mg/ml paraphenylenediamine (Aldrich Chemical, Milwaukee, WI) to inhibit photobleaching.
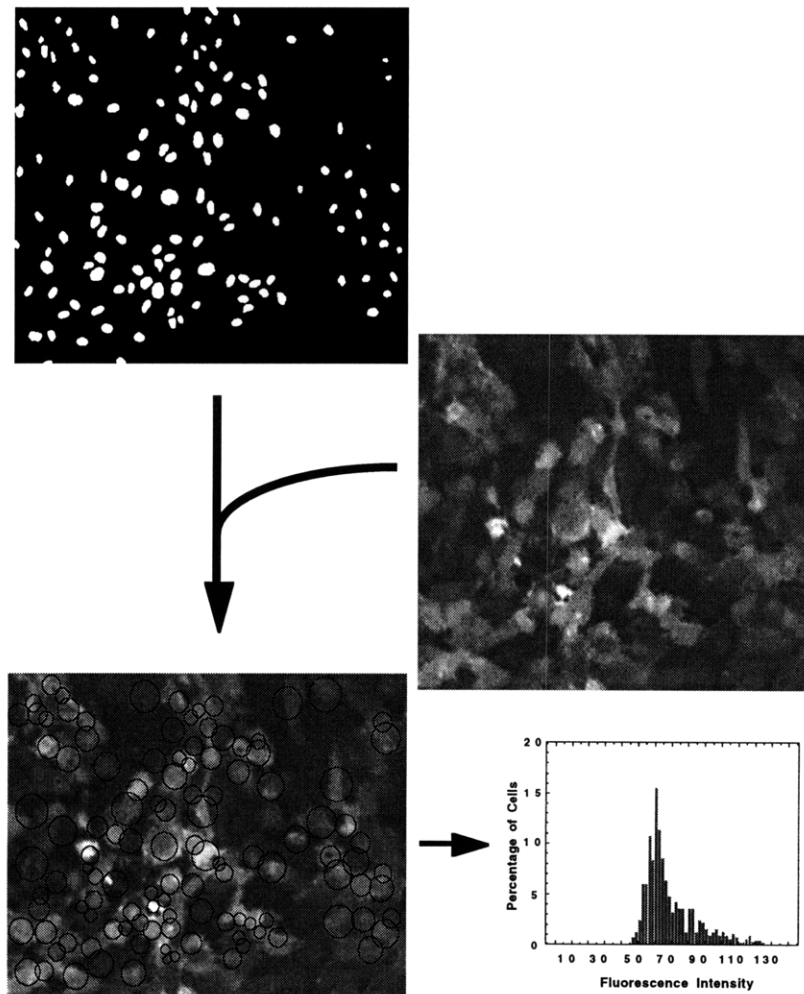
Figure 3-5. Targeted sampling fluorometry. Upper left image is that of the PI-stained nuclei and at right of center is the immunostained image. Bottom left image represents the sampled ROIs overlayed on the immunostained image and the corresponding histogram showing the distribution of intensity over the cell population.

Images of the stained monolayers were obtained using an epifluorescence microscope (Zeiss Axioplan, Oberkochen, Germany) with an I-CCD camera (Model C2400; Hamamatsu, Middlesex, NJ). Connected to this system was a frame grabber (DataTranslation, Marlboro, MA) installed on a Compaq® ProLinea 4/50 computer (Compaq Co., Houston, TX) for digitization and storage of images. A 20x, 0.40 N.A. objective was used which provided a field size of approximately 200-300 cells. Three fields were recorded per well, with each field providing two images: one image recorded in the 488/530 fluorescein channel and the other in the 488/600 channel (PI staining). No overlap was evident of the PI fluorescence in the fluorescein channel.

The images were processed and analyzed using a Macintosh® Quadra 650 (Apple Computer, Cupertino, CA) or a PowerWave 120 (Power Computing, Austin, TX) computer. The images representing the cell nuclei (PI staining) were initially recorded to determine the relative field coordinates of the cells. An algorithm had been written for the NIH Image 1.55 software (available through anonymous FTP at zippy.nih.nimh.gov) which segmented the gray-scale images into rectangular regions using a 20 x 20 grid and converted them into binary versions by pseudo-autothresholding (see Appendix B). This procedure effectively eliminated any problems due to shading and provided an accurate binary representation of the cell monolayer nuclei. The immunostained images were corrected for light intensity variations and shading effects by pixel-by-pixel division using an averaged background fluorescence image. The recorded x, y coordinates of the cell nuclei were then used by the algorithm to determine regions of interest (ROIs), which were representative of the area covered by each cell. These ROIs were adjusted to account for cell density variations on the monolayer to minimize sampling overlap. The mean gray level intensity for each ROI was then determined from the processed immunostained images, and histograms were formulated for the entire cell population. The method effectively provided the level of cell adhesion molecule expression on a per cell basis.

3.6.2 Flow Cytometry (FACS)

Confluent endothelial monolayers were formed on fibronectin-coated 3.5 cm culture dishes and incubated with treatments of growth factor and/or cytokine for prescribed periods of time. The monolayers were then trypsinized with trypsin-EDTA (Sigma Chemical), centrifuged, washed with a solution of DPBS + Ca^{2+} + Mg^{2+} + 1% BSA + 5 mM EDTA + 0.01% sodium azide (DPBS*), and resuspended in 0.1 ml of DPBS* with an excess of antibody, 10 μg antibody/15 x 10^6 cells, at 4°C for 30 min. The monoclonal antibodies used stained for the following receptors on the cells: ICAM-1, ICAM-2, VCAM-

1, E-selectin, P-selectin, and IgG_1 and IgG_{2a} isotype controls. The cells were then washed three times with DPBS* and 5 μg of a goat-anti-mouse F(ab')$_2$ flourescein conjugate (Tago, Burlingame, CA) was applied to a 0.1 ml cell suspension for 30 min at 4°C. The cells were again washed three times and then fixed with 0.5 ml of 1% paraformaldehyde. Flow cytometry analysis (FACScan) was utilized to determine the relative fluorescence data for the various labeled molecules and provided an estimate of the level of adhesion receptor expression.

3.6.3 Fluorescence Immunoassay (FIA)

The fluorescence immunoassay method was utilized for those studies involving the signaling pathway inhibitors. It provided a rapid and sensitive approach to measure the mean fluorescence, which directly correlated with the mean cell surface protein expression of a given CAM [Gerszten, et al., 1996].

In using FIA, HUVECs were seeded in 96-well, flat-bottom plates (Falcon; Becton Dickinson, Franklin Lakes, NJ) at concentrations of 2.25 x 10^4 cells/well in EGM medium at 37°C. Within 24 hrs, the monolayers were greater than 90% confluent and the cells were subsequently washed 3 times with a serum-free solution of RPMI-1640 supplemented with 100 U/ml penicillin and 100 μg/ml streptomycin, and treated with a given cytokine and/or growth factor(s). After a selected incubation period, the cell monolayers were washed 3 times with PBS + Ca^{2+} + Mg^{2+}, fixed with paraformaldehyde (1 mg/ml in PBS) for 15 min, washed 3 times and then immunostained with a primary antibody directed against the given adhesion molecule in 0.1 ml of RPMI + 1% FCS at 10 mg/ml for 45 min. The cells were then washed 3 times with RPMI + 1% FCS and incubated with an FITC-conjugated goat-anti-mouse antibody diluted 1:50 in DPBS at 4°C. After 45 minutes, the cells were washed twice with DPBS + 20% FCS and twice more with serum-free DPBS. The cells were then lysed with 0.01% NaOH in 0.1% sodium dodecyl sulfate (SDS) and transferred to 96-well, round-bottom plates (Corning) for optical clarity. A CytoFluor 2350 (PerSeptive Biosystems, Framingham, MA) fluorescent plate reader set at 485/535 was used to quantify the mean fluorescence from each well and provide the level of CAM expression on the cell surface.

3.6.4 Enzyme-Linked Immunosorbent Assay (ELISA)

ELISA kits (Quantikine, R&D Systems) were used to quantify the levels of TNFα, VEGF, and bFGF existing in several tumor interstitial fluid samples. This information was utilized in conjunction with the results obtained from the studies involving the individual

angiogenic factor treatments to postulate the effects of these factors within the tumor on cell adhesion molecule expression and lymphocyte adhesion.

The immunoassays used employed the quantitative sandwich enzyme immunoassay technique. The procedure followed began by first adding 50 μl of assay diluent, a buffered protein base, to the 96-well polystyrene microplates pre-coated with monoclonal antibody specific for the cytokine. A series of dilution standards and triplicate samples at a total volume of 200 μl were added and incubated for 2 hr at room temperature. The wells were then washed 3 times with wash buffer and 200 μl of conjugate was added. After 2 hrs of incubation at room temperature, the wells were washed 3 times with wash buffer and 200 μl of substrate solution, stabilized hydrogen peroxide and tetramethylbenzidine, was added to each well and incubated for 20 min at room temperature. A stop solution of 2N sulfuric acid was then added and the optical densities of each well was read at 450 nm using a microplate reader (Emax, Molecular Devices, Sunnyvale, CA).

3.7 Northern Blot Analysis

3.7.1 Blot Preparation and Hybridization

HUVEC were grown to confluency on 3.5 cm culture dishes (Corning) incubated with prescribed treatments of growth factor and/or cytokine in the presence or absence of a transcription blocker. Total RNA was isolated using TRIZOL reagent (Life Technologies, Grand Island, NY), a mono-phasic solution of phenol and guanidine isothiocyanate, and following the manufacture's instructions. RNA content and purity was quantified by measuring the optical densities at 260 λ and 280 λ using an UV spectrophotometer (Perkin-Elmer, Oak Brook, IL), and the isolated RNA was assured to have an $A_{260/280}$ ratio greater than 1.6.

For Northern transfer analysis, 15 μg of RNA was separated by electrophoresis on a 1% agarose formaldehyde denaturing gel containing 40 mM MOPS, 2 mM EDTA (pH 7.5), 5 mM Iodoacetamide, and 0.5 μg/ml ethidium bromide. After running for approximately 3 - 4 hrs at 100 V, the gel was soaked in 1 L of 50 mM NaOH and after 30 min, 75 mM of HOAc and 400 mM of NaCl was added and the gel was allowed to soak for another 30 min. RNA was then transferred to a nitrocellulose membrane by capillary transfer, and the blots were crosslinked by ultraviolet irradiation (FB-UVXL-1000, Fisher Scientific, Springfield, NY).

The membrane was then pre-hybridized in a hybridization cylinder with 6.5 ml of 0.77 M NaPO4 + 1 mM EDTA preboiled and 3.5 ml of 20% SDS and 40 μl of 0.5 M

Iodoacetamide for 1 hr at 65 °C. Labelled probe was added to the solution and allowed to hybridize at 65 °C for 18 - 24 hrs. Following hybridization, the blot was washed 3 times with 2X saline-sodium phosphate-EDTA (SSPE) + 1% SDS for 30 min each at 37 °C, and once with 0.2X SSPE + 1% SDS for 30 min at 65 °C (1X solution of SSPE consists of 150 mM NaCl, 10 mM NaH_2PO_4 and 1 mM EDTA). The blot was patted dry, placed in an autoradiography cassette (Fisher Scientific, Pittsburgh, PA), and exposed to a film (Eastman Kodak, Rochester, NY) for several hours, depending on the probe utilized. RNA levels were quantified by densitometry using NIH Image 1.55 and normalized with respect to the β-actin levels.

3.7.2 cDNA Probe Preparation

The cDNA constructs used in the Northern blot analysis were generously provided by the following individuals: a) ICAM-1 and E-selectin cDNA by Dr. Brian Seed, Department of Molecular Biology, Massachusetts General Hospital; b) β-actin cDNA by Dr. Toshihiro Shioda, Laboratory of Tumor Biology, Massachusetts General Hospital, c) VCAM-1 cDNA by Dr. Tucker Collins, Department of Pathology, Brigham and Women's Hospital, and d) ICAM-2 cDNA by Dr. Timothy Springer, Center for Blood Research, Harvard Medical School. The clones were all suitable for hybridization analysis of gene expression.

Extraction of the cDNA from the plasmid was performed using restriction enzymes appropriate for the given construct. More specifically, the cDNA of ICAM-1 and E-selectin were extracted from plasmid πH3M by incubating 1 μl of Hind III and Not I restriction enzymes, 3 μl of Buffer II, 20 μl of H_2O and 1.5 μg of construct for 1 hr at 37 °C. The product was then loaded in a low melting gel and the probe fragment cut at the specified molecular weight. Similarly, the cDNA of VCAM-1 was extracted from plasmid pBS M13+ using 1 μl of Kpn I and Sph I restriction enzymes, and the cDNA of ICAM-2 was extracted from plasmid CDM8 using 2 μl of Xba I restriction enzyme. The β-actin cDNA product was generated using reverse transcriptase-polymerase chain reaction (RT-PCR) and required no additional preparation.

Labelled probe was prepared from human ICAM-1, ICAM-2, VCAM-1, E-selectin, and β-actin cDNA with the Megaprime DNA labelling kit (Amersham Life Science, Buckinghamshire, England). Initially, 5 μl of template cDNA was added to 5 μl of primer and 23 μl of H_2O and denatured by heating to 100 °C for 5 min. Following a brief spin in a microcentrifuge, 10 μl of labelling buffer (dATP, dGTP, and dTTP in Tris/HCl (pH 7.5), 2-mercaptoethanol and $MgCl_2$), 2 μl of 1 U/μl DNA polymerase I Klenow fragment, and 5 μl of ^{32}P-dCTP was added and the solution was incubated for 30 min at 37 °C. The

reaction was subsequently stopped by the addition of 5 µl of 0.2M EDTA. The labelled DNA was then denatured by heating to 100 °C for 5 min, followed by placement on ice until hybridization with the membrane.

3.8 Signal Transduction Analysis

Studies were undertaken to determine essential signaling pathways used by the growth factor bFGF and cytokine TNFα in modifying CAM expression. The fluorescence immunoassay (FIA) method was used to determine the modulation of CAM expression on endothelial cells, and the adhesion assay was used to assess the functional correlation with signaling blockade.

In eliciting an effective blockade of the intracellular signaling pathways, the following drugs were placed 2 hr prior to and remained continuous with cytokine or growth factor treatment to deplete the cell of the signaling molecule's action: a) the FGF receptor tyrosine kinase inhibitor, MDHC, b) the phosphotyrosine phosphatase inhibitor, sodium orthovanadate, c) the phospholipase C inhibitor, NCDC, d) the phospholipase D inhibitor, propranolol DL, and e) the protein kinase C inhibitors, calphostin C and GF109203X.

Blockage of the high-affinity receptor-ligand interaction of bFGF:FGFR was obtained by initially adding 1 µg/ml of bFGF neutralizing antibody to a 10 ng/ml solution of bFGF, incubating for 1 hr at 37°C, and then applying the solution to the endothelial cells.

The influence of heparin, a low-affinity proteoglycan, was assessed by the supplemental addition of heparin (Elkins-Sinn, Cherry Hill, NJ) to the growth medium upon the application of cytokine or growth factor.

3.9 Statistical Analysis

Statistical comparison of means was performed by two-tailed unpaired Student's t test or Mann-Whitney test. The null hypothesis was considered rejected at $P < 0.05$.

Chapter 4

Lymphocyte Binding Kinetics

4.1 Introduction

The recruitment of lymphocytes, and more generally leukocytes, from the peripheral circulation is an essential process for the induction and maintenance of an effective immune and inflammatory response. Recruitment is mediated by specific receptor-ligand interactions between the leukocytes and vascular endothelium. Current models suggest a multi-step cascade involving members of the selectin, integrin, and immunoglobulin (Ig) gene families in the sequential process of initial attachment (capture and rolling), stable adhesion (arrest), cell spreading and diapedesis [Butcher, 1991; Carlos, et al., 1990; Springer, 1994; Cotran and Pober, 1990]. Interactions of molecules of the selectin family (E-, P-, L-selectin) with carbohydrate ligands (sialyl-Lewis X) mediate the initial step of leukocyte capture and rolling, while the subsequent firm adhesion and diapedesis requires activation-dependent engagement of integrins (LFA-1, VLA-4) with their endothelial ligands (ICAM-1, VCAM-1) [Lawrence and Springer, 1991; Luscinskas, et al., 1994].

Leukocyte populations have been shown to vary in their surface expression of cell adhesion receptors, and consequently differ in the specific molecular mechanisms they use in binding to the endothelium. For instance, polymorphonuclear (PMN) cells lack the β_1-integrin VLA-4, which is commonly expressed on T lymphocytes and monocytes, and thus do not recognize the counter-receptor VCAM-1 on endothelial cells. When compared to other leukocytes and in detailed, independent adhesion studies, T lymphocytes exhibited

inherent differences in their adhesive characteristics [Abassi, et al., 1993; Luscinskas and Lawler, 1994; Melder, et al., 1995], as described in section 2.1.

While these studies have provided a better understanding of the molecular mechanisms used by T cells in binding to the vascular endothelium, evidence has lacked as to a direct comparison of the adhesive binding kinetics among the individual lymphocyte subpopulations, namely CD4+, CD8+, and CD56+/CD3- cells. CD4+ cells, or helper T cells, mediate specific cell-mediated immune response that recognizes foreign antigen via major histocompatibility complex (MHC) class II complexes, and serve to secrete cytokines and provide stimuli for B cell differentiation. CD8+ cells, or cytotoxic T cells, constitute the specific immune effector response that recognizes foreign peptides via MHC class I complexes. In addition, the CD8+ cells act to lyse virus-infected cells, tumor cells, and allografts, as well as secrete various cytokines. CD56+ cells, or natural killer (NK) cells, participate in the innate immune response and act to lyse virus-infected cells and tumor cells by recognizing cells lacking MHC class I. Considering that the specificity of the cellular immune response varies for each subpopulation, adhesion receptor expression and their binding characteristics and efficiencies are also likely to vary.

Additionally, initial immunological responses are typically carried out by circulating lymphocytes in the resting or non-activated state. Only upon antigen recognition or extended cytokine exposure do the cells become activated, transform from the CD45RA+/CD45RO- to the CD45RA-/CD45RO+ phenotype, and produce stronger, more specified responses. The activation state is also known to alter the adhesive characteristics of lymphocytes by increasing integrin expression and the viscoelastic properties by decreasing cell deformability [Roth, 1994; Melder and Jain, 1992]. *In vivo* experimentation has shown an increased localization of IL-2 activated NK cells in normal and tumor tissues, and an increased accumulation of endogenous lymphocytes to tumor vessels following systemic IL-2 treatment [Melder, et al., 1993; Ohkubo, et al., 1991; Aronson, et al., 1988]. However, a detailed comparison analyzing the specific binding characteristics of IL-2 activated and non-activated lymphocyte subpopulations under physiological flow conditions has not been previously addressed.

Moreover, while CD3+ T lymphocyte molecular binding properties have been studied to a limited extent, the specific biophysical and molecular mechanisms of IL-2 activated CD56+ (NK) cells have not been defined under dynamic conditions. Under static conditions, IL-2 activated CD56+ cell adhesion to endothelial cells has been shown to involve the β_1 and β_2 integrins and their corresponding counter-receptor pairs, ICAM-1 and VCAM-1, but E-selectin-mediated interaction was found to be of no consequence [Allavena, et al., 1991]. However, static adhesion assays are limited in the their ability to

discriminate between differences in bond strengths or rate-limited binding events, which are characteristic of specific CAMs [Kojima, et al., 1992].

In this chapter, results are presented from experiments using the parallel-plate flow chamber which were designed to address the following essential issues: a) what differences are evident in the binding kinetics and efficiences to activated endothelial cells by the lymphocyte subpopulations CD4+, CD8+, and CD56+; b) what differences are present in the binding characteristics between IL-2 activated and non-activated lymphocyte subpopulations; and c) what are the molecular and biophysical mechanisms of IL-2 activated NK cell adhesion to activated endothelial cells? The findings from these studies provide additional insight to the immunological response of lymphocytes in normal and pathological conditions, such as tumor, inflammation and allograft rejection.

4.2 Non-Activated Lymphocyte Binding

To determine the binding characteristics of the individual subpopulations of resting lymphocytes, cumulative cell binding densities and capture efficiencies were obtained for each population of cells using the parallel-plate flow chamber under shear stress conditions ranging from 0.56 to 3.5 dyn/cm^2. The flow rates and shear stresses were representative of those found in physiological settings [Melder, et al., 1995]. Non-activated HUVEC monolayers were used to obtain basal adhesion characteristics. Monolayers activated with TNFα (50 ng/ml), a positive CAM modulator, bFGF (10 ng/ml), a negative CAM modulator (see Section 5.2), and a combination of the two factors were used to obtain *in vitro* binding profiles representative of those potentially found in tumors and inflammation.

The data obtained using the functional adhesion assay was plotted as the number of bound cells/mm^2 of monolayer area vs. the wall shear stress produced by the flow system (dynes/cm^2). This was used to describe the binding kinetics of the flowing lymphocytes over an intact endothelial cell monolayer. Additionally, capture efficiency plots were generated to provide further comparitive analysis between the subset of lymphocytes.

The initial set of experiments performed involved using non-activated endothelial cells to obtain basal adhesion kinetics. The cummulative bound cell densities of each lymphocyte subpopulation over the range of shear stresses are plotted in Figure 4-2-1. The results show a low, but significant accumulation of cells occuring only at the lowest shear stress employed, 0.56 dyn/cm^2. Higher wall shear stresses were not conducive for binding of any of the non-activated lymphocytes.

In comparing the lymphocyte sub-types, a significant difference was found in the number of bound CD56+ cells relative to both CD4+ and CD8+ cells at the lowest shear

stress (p < 0.05) (see Table 4-2-1). While relatively few in number, these cells are representative of a significant baseline adhesion to resting endothelium.

Figure 4-2-1. Cumulative binding curves of non-activated CD4+, CD8+, and CD56+ cells on non-activated HUVEC monolayers. Mean numbers ± SD of bound cells for five adjacent fields are shown for 1 of 3 representative flow experiments. * p < 0.05.

Table 4-2-1. Comparison of cell binding densities of non-activated CD4+, CD8+, and CD56+ cells on non-activated HUVEC monolayers. Mean values ± SD are shown for n = 3 flow experiments.

Shear stress (dyn/cm^2)	CD4+ (bound cells/mm^2)	CD8+ (bound cells/mm^2)	CD56+ (bound cells/mm^2)
3.51	0.00 ± 0.00	0.00 ± 0.00	0.00 ± 0.00
2.93	0.00 ± 0.00	0.00 ± 0.00	0.00 ± 0.00
2.34	0.00 ± 0.00	0.00 ± 0.00	0.00 ± 0.00
1.76	0.00 ± 0.00	0.00 ± 0.00	0.00 ± 0.00
1.17	0.00 ± 0.00	0.00 ± 0.00	0.00 ± 0.00
0.56	0.29 ± 0.93	0.59 ± 1.24	2.65 ± 2.17 ‡,¤

‡ Significant difference compared to CD4+ cells, p < 0.05.
¤ Significant difference compared to CD8+ cells, p < 0.05.

To provide a monolayer which was more conducive to cell binding, TNFα treatment was applied to the HUVEC monolayers for 24 hrs, allowing for sufficient ICAM-1 and VCAM-1 expression, while still maintaining an appreciable level of E-selectin. The cumulative binding curves for each of the lymphocyte subpopulations are shown in Figure

4-2-2. A significant increase in the level of binding above baseline was observed for each cell subtype for all flow rates considered (p < 0.05) (see Table 4.2.2). The number of bound cells on the TNFα-activated monolayer under the lowest shear stress, 0.56 dyn/cm^2, was approximately 50-fold higher for resting CD56+ cells, 150-fold higher for resting CD8+ cells, and 275-fold higher for resting CD4+ cells. The disproportionate increase in cell binding produced by the latter two cell subtypes may have been the result of the excessively low values found at baseline relative to the CD56+ cells, and therefore, are artifactual.

As another possibility for the disproportionate binding between cell subtypes, the TNFα-induced increase in CAM expression on the endothelial cells may have provided a critical level for the adhesion receptors on the CD4+ and CD8+ cells to interact and effectively bind.
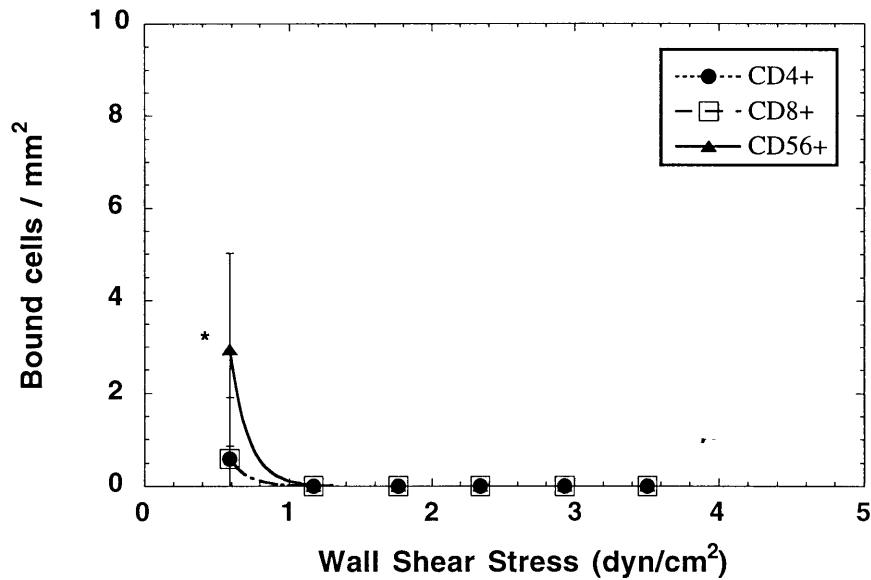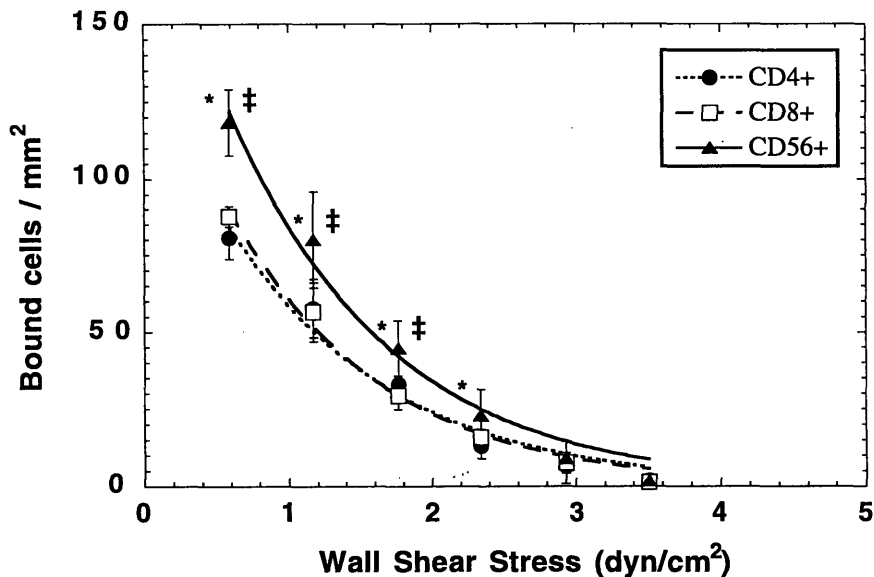

Figure 4-2-2. Cumulative binding curves of non-activated CD4+, CD8+, and CD56+ cells on TNFα-activated HUVEC monolayers. Mean numbers ± SD of bound cells for five adjacent fields are shown for 1 of 3 representative flow experiments. * significant difference between CD4+ and CD56+ cells, p < 0.05, and ‡ significant difference between CD8+ and CD56+ cells, p < 0.05.

In comparing the cell binding densities between the lymphocyte subpopulations, there was no statistically significant differences between the non-activated CD4+ and CD8+ cells for the complete range of flow rates. However, a greater number of CD56+ cells consistantly bound to the activated monolayers relative to both CD4+ and CD8+ cells for shear stresses ranging from 1.76 to 0.56 dyn/cm^2 (p < 0.05). At the lowest shear stress,

the level of CD56+ cell binding was approximately 30% greater than the levels obtained by both CD4+ and CD8+ cells. Considering the greater influence of integrin-mediated events contributing to the cell binding process at these low shear stresses, the results are consistent with the finding of differences in the β_2 integrin surface density on lymphocyte subsets [Pardi, et al., 1989]. Additionally, CD56+ cells are known to express significant levels of CD18 expression on their villi and podosomes, providing these cells with a topological advantage to binding [Burridge, et al., 1988; Marchisio, et al., 1988; Melder, et al., 1990].

Table 4-2-2. Comparison of cell binding densities of non-activated CD4+, CD8+, and CD56+ cells on HUVECs treated with TNFα for 24 hrs. Mean values ± SD are shown for n = 3 flow experiments.

Shear stress (dyn/cm^2)	CD4+ (bound cells/mm^2)	CD8+ (bound cells/mm^2)	CD56+ (bound cells/mm^2)
3.51	1.76 ± 1.86 *	1.37 ± 1.88 *	1.76 ± 1.86 *
2.93	5.88 ± 3.52 *	6.86 ± 4.26 *	7.84 ± 3.46 *
2.34	13.53 ± 3.10 *	16.86 ± 4.65 *	20.78 ± 6.33 *,‡
1.76	28.63 ± 7.24 *	32.35 ± 6.48 *	44.12 ± 6.39 *,‡,¤
1.17	55.69 ± 7.74 *	57.45 ± 10.77 *	80.20 ± 11.89 *,‡,¤
0.56	80.59 ± 9.55 *	86.47 ± 7.19 *	120.59 ± 10.01 *,‡,¤

* Significant difference from baseline of the respective cell type, p < 0.05.
‡ Significant difference compared to CD4+ cells, p < 0.05.
¤ Significant difference compared to CD8+ cells, p < 0.05.

To provide further insight into the different binding characteristics between the lymphocyte subtypes, capture efficiency plots for each of the cell types were generated and are shown in Figure 4-2-3. Changes in bound cell density with changing shear stress is directly related to the capture efficiency as a function of the force generated by the flow system. Fits of the bound cell density data were made to the function: $E = E_o e^{-\kappa S}$, where E is the capture efficiency at shear stress S. Additional parameters are: E_o, the efficiency at zero shear, and κ, the capture coefficient. E_o reflects the overall drag forces which promote cell arrest over a range of shear stress levels (integrin-mediated interactions), while κ is correlated with the change in capture rate with increasing shear stress (selectin-mediated process) [Melder, et al., 1995].

Binding efficiency plots derived from the cell accumulation curves reproducibly showed a reduction in binding efficiency that was uniform across the range of shear stresses examined for each of the lymphocyte subpopulations (see Figure 4-2-3). No statistical difference in the capture coefficient, κ, was evident between the three non-

activated lymphocyte subsets, and is plotted in Figure 4-2-4*a*. This finding indicates the non-activated lymphocyte subsets produce relatively similar adhesive forces at the time of initial contact with the endothelium.

A comparison of the fitted parameter E_o showed a statistically significant difference between CD56+ cells (0.879 ± 0.075) and CD4+ cells (0.597 ± 0.137), as well as CD8+ cells (0.601 ± 0.034) ($p < 0.05$), and is plotted in Figure 4-2-4b. No statistical difference was evident between the CD4+ and CD8+ cells. These findings indicate that the efficiency of the adhesion process after initial capture is greater for CD56+ cells, which is a direct function of their ligand-receptor affinity and integrin concentration.

$$E = E_o e^{-\kappa S}$$
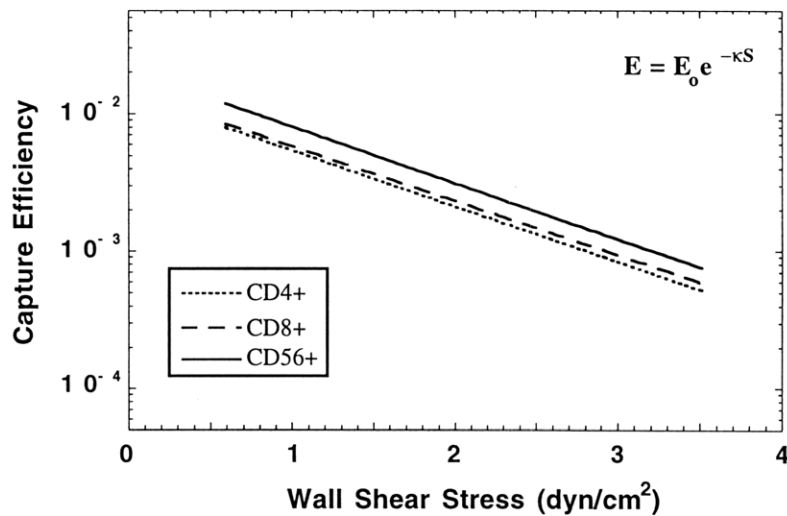
Figure 4-2-3. Comparison of binding efficiencies between non-activated CD4+, CD8+, and CD56+ cells on TNFα-activated HUVEC monolayers (n = 3).

(a)   (b)
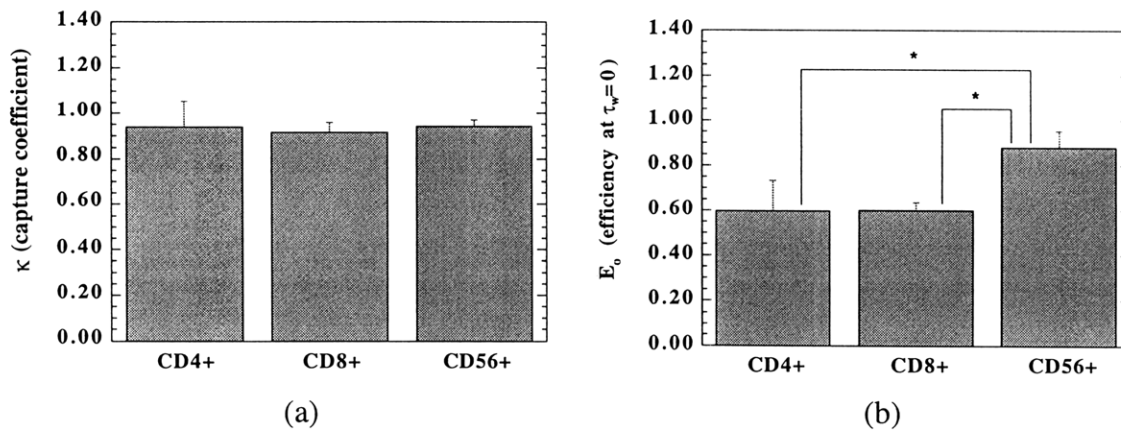
Figure 4-2-4. Comparison of the fitted parameters: a) κ, capture coefficient, and b) *Eo*, efficiency at zero shear generated from the capture efficiency plots of non-activated lymphocytes on TNFα-activated monolayers. R^2 greater than 0.96 in all cases. * $p < 0.05$.

66

As a source for providing a negative modulation of CAM expression on endothelial cells, in opposition to the positive modulation by TNFα, the binding characteristics of the non-activated lymphocyte populations were also studied on bFGF and TNFα + bFGF treated HUVEC monolayers. As will be discussed in further detail in Chapter 5, bFGF was found to inhibit the level of CAM expression on endothelial cells with optimal inhibitory kinetics around 24 hrs.

A representative set of binding curves of the lymphocyte subpopulations on bFGF (10 ng/ml)-activated HUVEC monolayers are shown in Figure 4-2-5. For the entire range of shear stresses imposed, lymphocyte binding of all three subsets was completely absent. A small, but statistically significant decrease in the level of CD56+ binding was found when compared to baseline levels from non-treated monolayers at the lowest shear stress (p < 0.05) (see Table 4-2-3). This suggests that a reduction of basal CAM expression by bFGF reduced the threshold of adhesive interaction below that which is necessary for stable adhesion under dynamic flow conditions.


Figure 4-2-5. Cumulative binding curves of non-activated CD4+, CD8+, and CD56+ cells on bFGF activated HUVEC monolayers. Mean numbers ± SD of bound cells for five adjacent fields are shown for 1 of 3 representative flow experiments.

To further examine the effects of the negative modulation of CAM expression on lymphocyte subpopulation binding kinetics, additional experiments were performed combining TNFα and bFGF. These experiments were based upon previous work

[Melder, et al., 1996] demonstrating reduced binding of activated lymphocytes to bFGF-treated endothelium. The following studies were designed to determine if the paradigm of bFGF-modulated adhesion could be extended to normal circulating (non-activated) lymphocyte populations. These experiments further elucidated differences in the molecular binding kinetics of distinct lymphocyte subpopulations. The experiments also represented a system in which to study the binding of circulating lymphocytes to vessels in or near tumor or inflammatory sites where several growth factors and cytokines simultaneously influence the microenvironment [Cotran and Pober, 1990; Blood and Zetter, 1990].

Table 4-2-3. Comparison of cell binding densities of non-activated CD4+, CD8+, and CD56+ cells on HUVECs treated with bFGF for 24 hrs. Mean values $\pm$ SD are shown for n = 3 flow experiments.

Shear stress (dyn/cm^2)	CD4+ (bound cells/mm^2)	CD8+ (bound cells/mm^2)	CD56+ (bound cells/mm^2)
3.51	0.00 $\pm$ 0.00	0.00 $\pm$ 0.00	0.00 $\pm$ 0.00
2.93	0.00 $\pm$ 0.00	0.00 $\pm$ 0.00	0.00 $\pm$ 0.00
2.34	0.00 $\pm$ 0.00	0.00 $\pm$ 0.00	0.00 $\pm$ 0.00
1.76	0.00 $\pm$ 0.00	0.00 $\pm$ 0.00	0.00 $\pm$ 0.00
1.17	0.00 $\pm$ 0.00	0.00 $\pm$ 0.00	0.00 $\pm$ 0.00
0.56	0.00 $\pm$ 0.00	0.00 $\pm$ 0.00	0.00 $\pm$ 0.00 *

* Significant difference from baseline of the respective cell type, $p < 0.05$.

The binding kinetics of non-activated lymphocytes to HUVEC monolayers activated with TNFα + bFGF are shown in Figure 4-2-6. Significant increases in lymphocyte binding above baseline levels were found for all cell subtypes for the range of shear stresses between 2.34 to 0.56 dyn/cm^2 ($p < 0.05$). Comparison of the cell binding densities between the subpopulations revealed significant differences and are shown in Table 4-2-4. Non-activated CD56+ cells consistantly showed binding levels above that of CD4+ and CD8+ cells for the imposed shear stresses between 1.17 to 0.56 dyn/cm^2 and 1.76 to 0.56 dyn/cm^2, respectively. At the lowest shear stress level, CD56+ cells bound to the activated endothelium on average 37% greater than both CD4+ and CD8+ cells. Differences between CD4+ and CD8+ cells were also observed, but were limited to the shear stresses ranging from 2.34 to 1.17 dyn/cm^2. Interestingly, no significant difference was found between these two cell subtypes at the lowest shear stress, possibly implying a critical range over which a particular molecular species, such as VLA-4, on the cell surface

may vary between the cells. VLA-4, a β_1 integrin, has been shown to have a potential overlapping role in the initial capture process and in stable adhesion [Melder, et al., 1995].
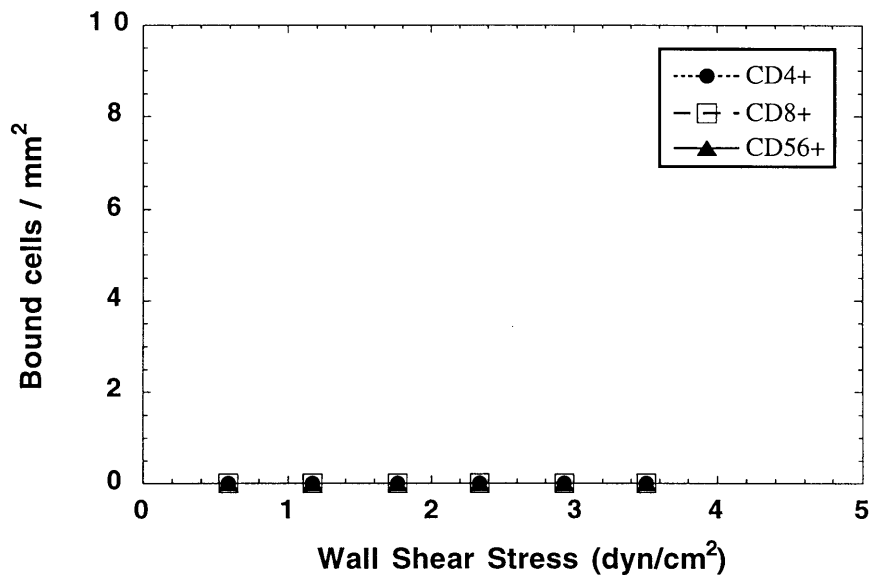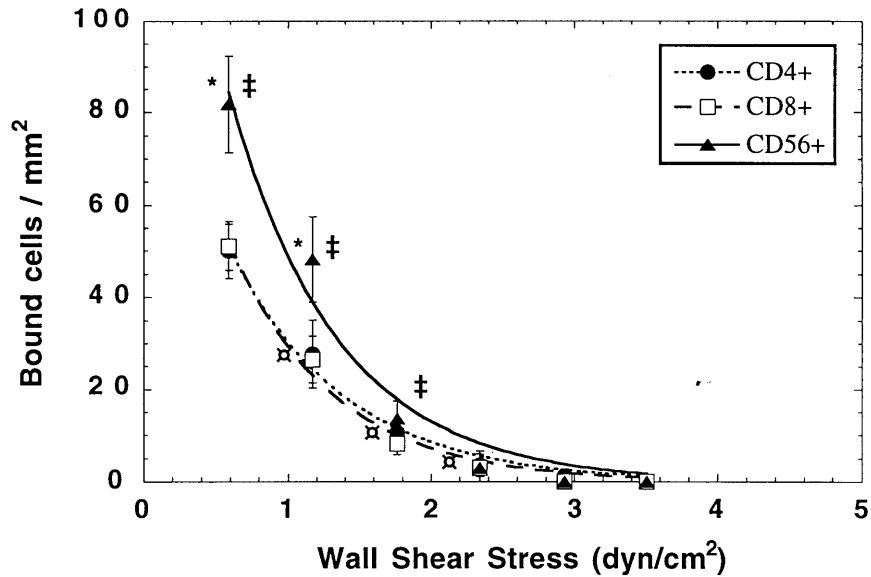

Figure 4-2-6. Cumulative binding curves of non-activated CD4+, CD8+, and CD56+ cells on TNFα + bFGF activated HUVEC monolayers. Mean numbers ± SD of bound cells for five adjacent fields are shown for 1 of 3 representative flow experiments. * significant difference between CD4+ and CD56+ cells, $p < 0.05$, ‡ significant difference between CD8+ and CD56+ cells, $p < 0.05$, and ¤ significant difference between CD4+ and CD8+ cells, $p < 0.05$.

Table 4-2-4. Comparison of cell binding densities of non-activated CD4+, CD8+, and CD56+ cells on HUVECs treated with TNFα+bFGF for 24 hrs. Mean values ± SD are shown for n = 3 flow experiments.

Shear stress (dyn/cm^2)	CD4+ (bound cells/mm^2)	CD8+ (bound cells/mm^2)	CD56+ (bound cells/mm^2)
3.51	0.00 ± 0.00 *	0.00 ± 0.00 *	0.00 ± 0.00 *
2.93	0.59 ± 1.22 *	0.00 ± 0.00 *	0.00 ± 0.00 *
2.34	3.53 ± 1.99 *,¤	1.76 ± 2.44 *	3.53 ± 2.98 *
1.76	12.16 ± 3.12 *,¤	6.08 ± 3.23 *	14.90 ± 4.37 *,¤
1.17	31.57 ± 7.07 *,¤	21.18 ± 7.88 *	43.14 ± 7.91 *,‡,¤
0.56	50.20 ± 7.50 *	50.20 ± 11.42 *	79.22 ± 10.34 *,‡,¤

* Significant difference from TNFα-activated monolayers of the respective cell type, $p < 0.05$.
‡ Significant difference compared to CD4+ cells, $p < 0.05$.
¤ Significant difference compared to CD8+ cells, $p < 0.05$.

In comparing the results obtained with TNFα-activated monolayers, several differences were found. First, for all shear stresses imposed and all cells tested, there was a significant reduction in the number of bound lymphocytes on the TNFα + bFGF treated monolayers (p < 0.05). Secondly, while CD56+ cells consistantly bound at higher levels compared to CD4+ and CD8+ for shear stresses between 1.76 to 0.56 dyn/cm^2, CD4+ cells were also found to bind at significantly greater levels than CD8+ cells for a selected range of shear stresses on TNFα + bFGF treated monolayers. This difference in binding between the two cell subtypes on the different monolayers implies a critical threshold at which one or more receptors on CD4+ cells are expressed in higher concentrations or possibly maintain higher affinities for CAMs that have been down-regulated on the endothelium by bFGF.

To further analyze the adhesion kinetics of the individual subpopulations, capture efficiencies were calculated and their plots are shown in Figure 4-2-7. As found for TNFα-activated monolayers, the cell accumulation curves reproducibly showed a reduction in binding efficiency that was uniform across the range of shear stresses examined for each of the lymphocyte subpopulations. A significantly lesser slope (κ) was observed for CD4+ cells (1.179 ± 0.072 cm^2/dyn) compared to CD8+ cells (1.709 ± 0.298 cm^2/dyn) and CD56+ cells (1.374 ± 0.097 cm^2/dyn), with no statistically significant difference between the latter two cell subtypes (see Figure 4-2-8a). The lower value of κ for CD4+ cells on the TNFα+bFGF activated monolayer indicates that these lymphocytes have a relatively stronger adhesive force at the time of contact with the endothelium. This results in a smaller decrease in the capture efficiency with increasing shear stress. Molecules such as L- and E-selectin have been shown to have dominant effects at high flow rates, especially when in high concentrations on the cell surface, and significantly affect the value of the capture coefficient, κ [Melder, et al., 1995]. These findings suggest that L-selectin or a functionally related receptor, such as sialyl Lewis X, may be elevated in non-activated CD4+ lymphocytes relative to CD8+ and CD56+ lymphocytes. Since this observation was evident only on TNFα + bFGF treated monolayers and not on TNFα treated monolayers, this might only be detectable when the CAM expression is reduced.

Comparison of the capture coefficients between TNFα and TNFα + bFGF treated monolayers for the lymphocyte subpopulations, showed significantly greater values for all three cell subtypes on TNFα + bFGF activated monolayers (p < 0.05). This finding is not unexpected based on the inhibitory effect which bFGF has on the expression of E-selectin, a counter-receptor for L-selectin and sialyl Lewis X, on the endothelial cells.

Evaluation of the fitted parameter E_O showed significantly higher values for CD56+ cells (0.937 ± 0.222) and CD8+ cells (0.825 ± 0.198) compared to CD4+ cells (0.495 ±

0.038) (see Figure 4-2-8b). The finding of increased efficiency of CD56+ cells over CD4+ cells is in agreement with that found for TNFα-activated monolayers, but the increased efficiency of CD8+ cells over CD4+ cells indicates a possible masking of this difference by high integrin concentration, which only becomes evident with the reduced CAM expression on the endothelium by bFGF.

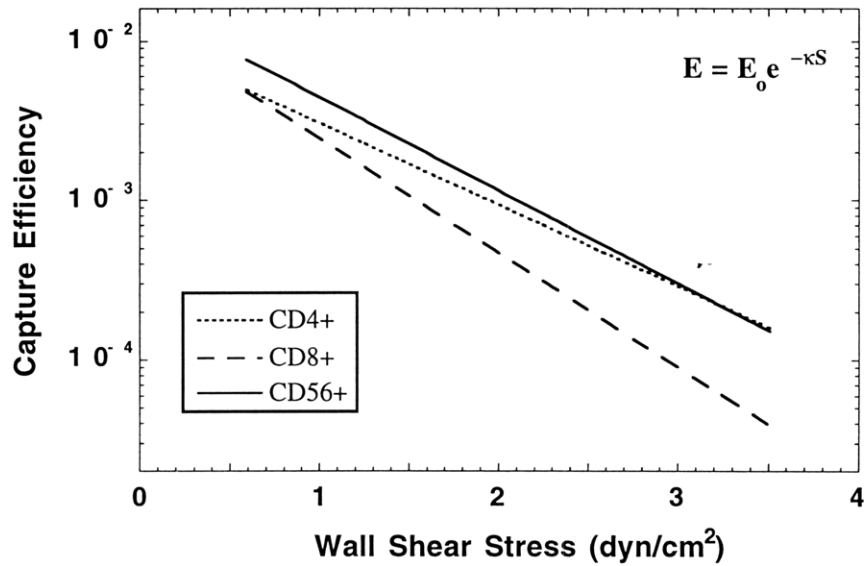Figure 4-2-7. Comparison of binding efficiencies between non-activated CD4+, CD8+, and CD56+ cells on TNFα + bFGF activated HUVEC monolayers (n = 3).
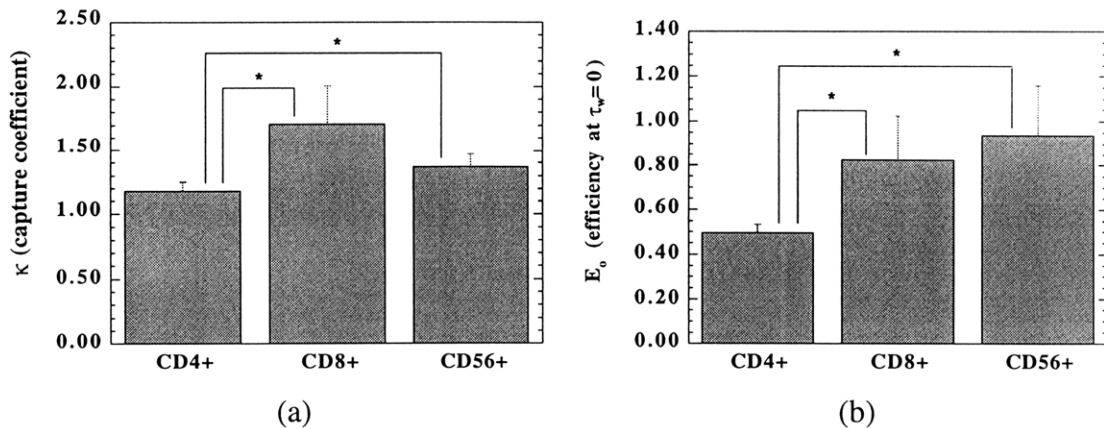

Figure 4-2-8. Comparison of the fitted parameters: a) κ, capture coefficient, and b) Eo, efficiency at zero shear generated from the capture efficiency plots of non-activated lymphocytes on TNFα + bFGF activated monolayers. R^2 greater than 0.96 in all cases. * p < 0.05.

4.3 IL-2 Activated Lymphocyte Binding

To determine the binding characteristics of the individual subpopulations of IL-2 activated lymphocytes, cumulative cell binding densities and capture efficiencies were obtained for each population using identitical conditions to that used for the analysis of the resting lymphocyte subpopulations in Section 4.2. Positive and negative controls for the level of adhesion on activated and non-activated endothelium provided an additional means for directly comparing the results between activated and non-activated lymphocyte subpopulations for a quantitative assessment of their binding kinetics and mechanisms of cell adhesion. A margin of error on the order of ± 5% was determined based on these controls.

Experiments using non-activated endothelial cells initially demonstrated a relatively low, but significant amount of adhesion at the lowest shear stress, 0.56 dyn/cm^2, by all three IL-2 activated lymphocyte subpopulations (see Figure 4-3-1 and Table 4-3-1). No statistical differences of the number of bound cells were noted between the CD4+, CD8+, and CD56+ cell types at this flow rate. Higher shear stresses resulted in no appreciable accumulation of any of the lymphocytes, consistant with the previous findings using non-activated endothelium. This emphasizes the importance of CAM modulation and shear stress on lymphocyte binding to endothelial substrate.
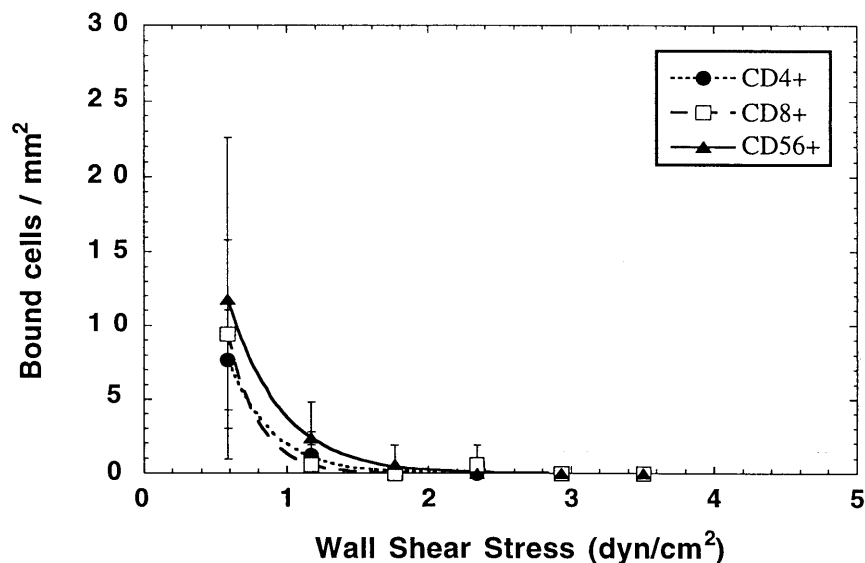

Figure 4-3-1. Cumulative binding curves of IL-2-activated CD4+, CD8+, and CD56+ cells on non-activated HUVEC monolayers. Mean numbers ± SD of bound cells for five adjacent fields are shown for 1 of 3 representative flow experiments.

Table 4-3-1. Comparison of cell binding densities of IL-2 activated CD4+, CD8+, and CD56+ cells on non-activated HUVEC monolayers. Mean values ± SD are shown for n = 3 flow experiments.

Shear stress (dyn/cm^2)	CD4+ (bound cells/mm^2)	CD8+ (bound cells/mm^2)	CD56+ (bound cells/mm^2)
3.51	0.00 ± 0.00	0.00 ± 0.00	0.00 ± 0.00
2.93	0.00 ± 0.00	0.00 ± 0.00	0.00 ± 0.00
2.34	0.00 ± 0.00	0.29 ± 0.93	0.00 ± 0.00
1.76	0.00 ± 0.00	0.29 ± 0.93	0.88 ± 1.42
1.17	2.06 ± 2.42	1.59 ± 1.24	3.53 ± 3.34
0.56	10.29 ± 4.65	9.71 ± 4.39	13.82 ± 7.85

Compared to the non-activated cells, each of the IL-2 activated lymphocyte subsets showed significant increases in their cumulative binding densities at the lowest shear stress. This finding is in agreement with the studies showing increased expression of integrin molecules on the cell surface of IL-2 activated lymphocytes.

When HUVEC monolayers were activated with TNFα for 24 hrs, significant increases in activated lymphocyte binding was found for all cell types above baseline levels for the entire range of flow rates studied. An exception was the activated CD4+ cells which failed to exhibit adhesion above baseline levels under the highest shear stress only (p < 0.05) (see Figure 4-3-2 and Table 4-3-2). The number of bound cells on the TNFα-activated monolayer at 0.56 dyn/cm^2 was approximately 10-fold higher than that found on the non-activated monolayer for all three subpopulations.

In comparing the cell binding densities between the subpopulations, significantly fewer CD4+ cells consistantly bound to the endothelial monolayer for the complete range of shear rates examined when compared to both CD8+ and CD56+ cells (p < 0.05). At the shear stress level of 0.56 dyn/cm^2, CD4+ cell binding levels were on average 13% and 22% less than the levels obtained by CD8+ and CD56+ cells, respectively.

Differences between CD8+ and CD56+ cells were also observed, but were limited to only the lowest shear rate, where on average a 10% greater number of CD56+ cells bound to the endothelial monolayer (p < 0.05). At this level of shear stress, the adhesion process is dominated by integrin-mediated binding. Therefore, the high levels of CD56+ binding was not suprising, since they are known to possess favorable molecular binding kinetics via high levels of integrin receptor expression on their cell surface and on their villi [Allavena, et al., 1991; Melder, et al., 1991]. Likewise, IL-2 activated CD8+ cells may

also exhibit relatively higher levels of integrin expression compared to CD4+ cells, resulting in their significantly greater binding.
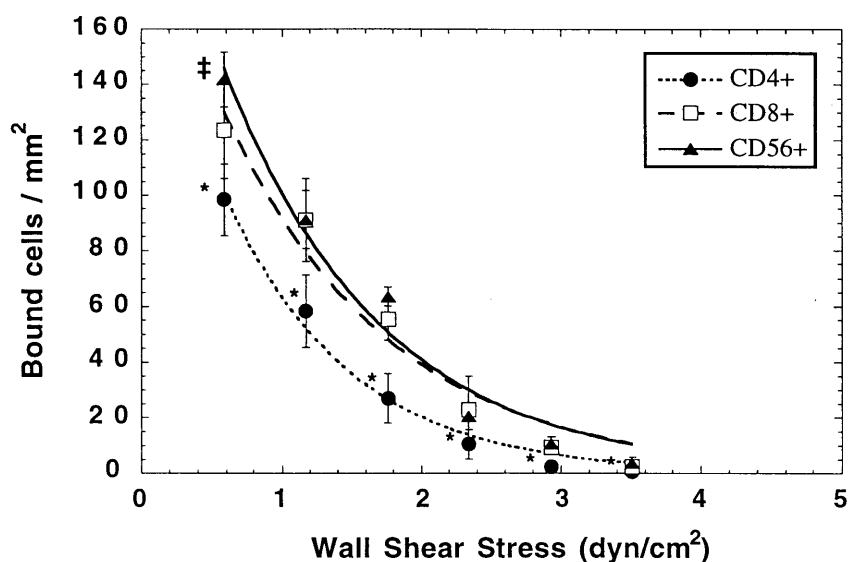
Figure 4-3-2. Cumulative binding curves of IL-2-activated CD4+, CD8+, and CD56+ cells on TNFα-activated HUVEC monolayers. Mean numbers ± SD of bound cells for five adjacent fields are shown for 1 of 3 representative flow experiments. * significant difference between CD4+ and CD8+ or CD56+ cells, $p < 0.05$, and ‡ significant difference between CD8+ and CD56+ cells, $p < 0.05$.

Table 4-3-2. Comparison of cell binding densities of IL-2 activated CD4+, CD8+, and CD56+ cells on HUVECs treated with TNFα for 24 hrs. Mean values ± SD are shown for n = 3 flow experiments.

Shear stress (dyn/cm^2)	CD4+ (bound cells/mm^2)	CD8+ (bound cells/mm^2)	CD56+ (bound cells/mm^2)
3.51	0.59 ± 1.22	1.96 ± 2.13 *,‡	3.53 ± 2.32 *,‡
2.93	2.35 ± 2.28 *	8.04 ± 3.76 *,‡	9.41 ± 3.34 *,‡
2.34	10.20 ± 4.43 *	20.00 ± 7.47 *,‡	25.59 ± 7.97 *,‡
1.76	27.65 ± 12.42 *	51.08 ± 13.65 *,‡	57.94 ± 7.85 *,‡
1.17	66.67 ± 13.51 *	82.75 ± 18.09 *,‡	87.94 ± 11.13 *,‡
0.56	108.04 ± 16.80 *	124.31 ± 19.62 *,‡	137.65 ± 9.78 *,‡,¤

* Significant difference from baseline of the respective cell type, $p < 0.05$.
‡ Significant difference compared to CD4+ cells, $p < 0.05$.
¤ Significant difference compared to CD8+ cells, $p < 0.05$.

In agreement with these observations are the findings that IL-2 lymphocyte populations were able to bind at significantly greater levels than the non-activated populations for the low shear conditions. For instance, at the lowest shear stress of 0.56 dyn/cm^2, IL-2 activated CD56+, CD8+, and CD4+ cells bound at levels on average 15%, 43%, and 34% greater than the non-activated populations, respectively. Additionally, the significantly greater levels of activated CD8+ cells which bound compared to activated CD4+ cells, but which bound at equivalent levels in the non-activated state, suggests a differential level of integrin upregulation by IL-2 activation on T cell subsets.

To provide further insight into the different binding characteristics between the lymphocyte subpopulations, capture efficiency plots for each of the cell types were generated and are shown in Figure 4-3-3.

Binding efficiency plots derived from the cell accumulation curves reproducibly showed a reduction in binding efficiency that was uniform across the range of shear stresses examined for each of the lymphocyte subpopulations (see Figure 4-3-3). A significantly greater slope (κ) of the capture efficiency plot was observed for CD4+ cells (1.169 $\pm$ 0.081 cm^2/dyn) compared to CD8+ cells (0.974 $\pm$ 0.089 cm^2/dyn), as well as CD56+ cells (0.898 $\pm$ 0.016 cm^2/dyn) ($p < 0.05$) (see Figure 4-3-4a). No statistical difference of the parameter κ was evident between CD8+ and CD56+ cells. The increased value of κ for activated CD4+ cells indicates that these lymphocytes have a greater sensitivity to shear stress by possessing a relatively weaker adhesive force at the time of contact with the endothelium. As mentioned previously, specific selectin molecules have been shown to effect capture rates under high flow conditions. To account for the reduced binding efficiencies observed, these molecules may be significantly reduced in activated CD4+ lymphocytes relative to activated CD8+ and CD56+ lymphocytes. A comparison between the activated and non-activated cell subtypes showed no significant differences for CD56+ and CD8+ cells, but a statistically significant difference between IL-2 activated CD4+ cells (1.169 $\pm$ 0.081 cm^2/dyn) and non-activated cells (0.938 $\pm$ 0.118 cm^2/dyn) ($p < 0.05$). The increased value of κ observed by CD4+ cells activated by IL-2 was in accordance with the previously hypothesized state of selectin alteration in these cells.

An analysis of the fitted parameter Eo showed no statistical difference between any of the activated lymphocyte subpopulations (see Figure 4-3-4b). This result was somewhat suprising considering the high level of integrin expression on IL-2 activated, as well as the non-activated, CD56+ cells, which would act to stabilize the adhesion complex and increase the efficiency of the adhesion process after initial capture. However, upon activation by IL-2, CD4+ and CD8+ cells may increase their integrin surface expression to levels approaching that of the activated CD56+ cells. Additionally, cells utilize multiple

75

molecular species to maintain adhesion which are dependent on specific receptor-ligand affinities and concentrations. It is conceivable that on TNFα-activated endothelium, the binding advantages activated CD56+ cells and CD8+ cells have over CD4+ populations may be over-shadowed by the high level expression of ICAM-1, VCAM-1, and E-selectin. Modifications to the level of CAM expression on the endothelial surface may provide further insight to these mechanisms.
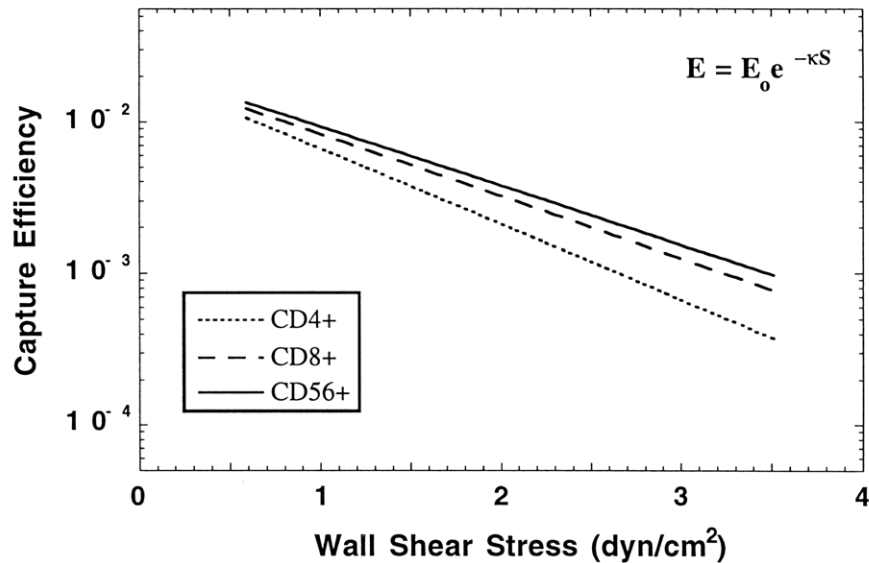

Figure 4-3-3. Comparison of binding efficiencies between IL-2-activated CD4+, CD8+, and CD56+ cells on TNFα-activated HUVEC monolayers (n = 3).
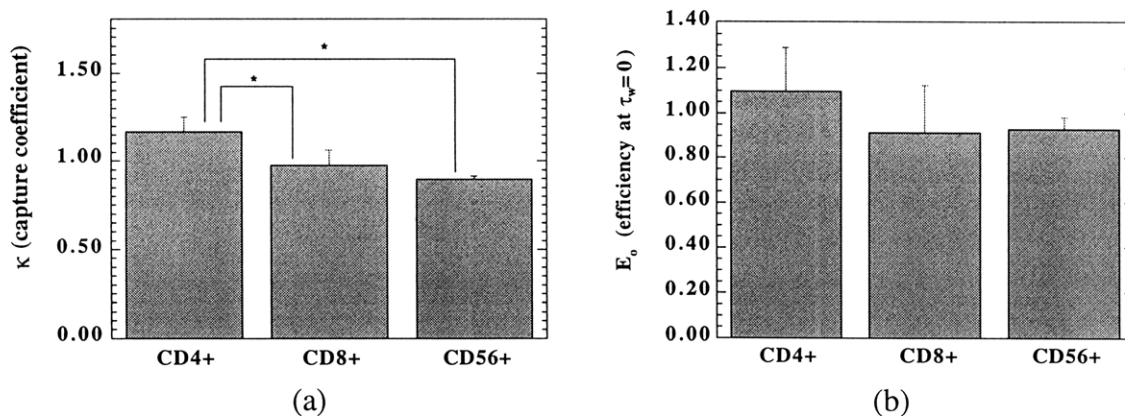

Figure 4-3-4. Comparison of the fitted parameters: a) κ, capture coefficient, and b) Eo, efficiency at zero shear generated from the capture efficiency plots of activated lymphocytes on TNFα-activated monolayers. R^2 greater than 0.96 in all cases. * $p < 0.05$.

76

The binding characteristics of the activated lymphocyte populations were also studied on bFGF and TNFα + bFGF treated HUVEC monolayers, as a means of providing a negative modulation of CAM expression on endothelial cells. The binding characteristics of the lymphocyte subpopulations on bFGF (10 ng/ml)-treated HUVEC monolayers are shown in Figure 4-3-5. A low level of adhesion was evident by all three cell types at only the lowest shear stress, 0.56 dyn/cm^2, with no statistical difference in the level of binding between the cells. Higher shear stresses resulted in no appreciable accumulation of any of the lymphocytes.

Comparison of the binding levels on non-activated and TNFα-activated monolayers indicated a statistical difference at the shear stress levels between 0.56 to 1.17 dyn/cm^2 for CD4+ and CD56+ cells, and at 0.56 dyn/cm^2 for CD8+ cells ($p < 0.05$) (see Table 4-3-3). The number of lymphocytes binding on the bFGF-treated endothelium at the lowest shear rate was, on average, 8- to 15-fold less than that observed for the non-activated endothelium. This inhibition of binding was found to be directly associated with the level of CAM expression on the monolayers and is described in further detail in Chapter 5.
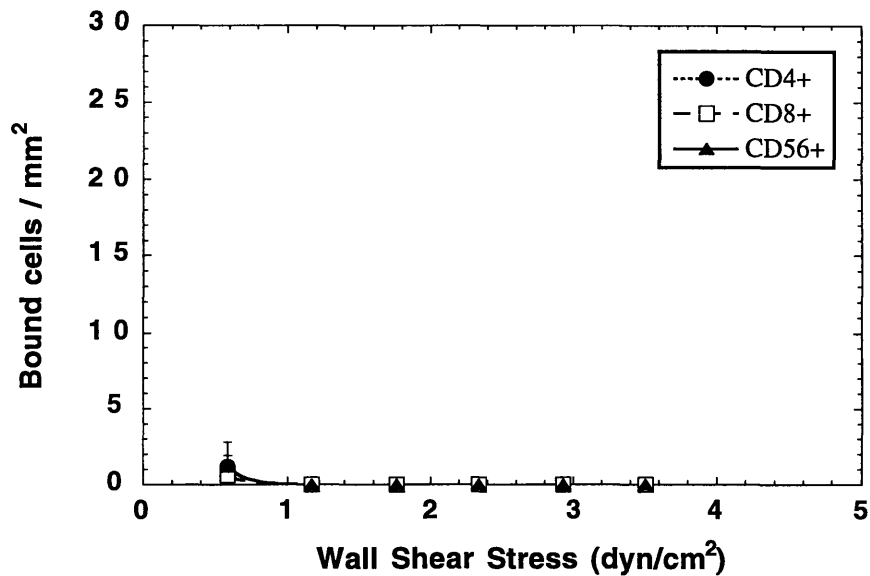

Figure 4-3-5. Cumulative binding curves of IL-2-activated CD4+, CD8+, and CD56+ cells on bFGF activated HUVEC monolayers. Mean numbers ± SD of bound cells for five adjacent fields are shown for 1 of 3 representative flow experiments.

Table 4-3-3. Comparison of cell binding densities of IL-2 activated CD4+, CD8+, and CD56+ cells on HUVECs treated with bFGF for 24 hrs. Mean values ± SD are shown for n = 3 flow experiments.

Shear stress (dyn/cm^2)	CD4+ (bound cells/mm^2)	CD8+ (bound cells/mm^2)	CD56+ (bound cells/mm^2)
3.51	0.00 ± 0.00	0.00 ± 0.00	0.00 ± 0.00
2.93	0.00 ± 0.00	0.00 ± 0.00	0.00 ± 0.00
2.34	0.00 ± 0.00	0.00 ± 0.00	0.00 ± 0.00
1.76	0.00 ± 0.00	0.29 ± 0.93	0.00 ± 0.00
1.17	0.00 ± 0.00 *	0.00 ± 0.00	0.00 ± 0.00 *
0.56	1.18 ± 1.52 *	1.18 ± 1.52 *	0.88 ± 1.42 *

* Significant difference from baseline of the respective cell type, $p < 0.05$.

To further examine the effects of the negative modulation of CAM expression on lymphocyte subpopulation binding kinetics, additional experiments were performed combining TNFα and bFGF treatment, as previously described for the non-activated lymphocyte subpopulations. These experiments were designed to further examine the differences in the binding kinetics between activated lymphocyte subpopulations, and to provide a binding substrate for circulating activated lymphocytes which may effect their binding efficiencies differently than non-activated lymphocytes.

When HUVEC monolayers were activated with TNFα + bFGF for 24 hrs, significant increases in activated lymphocyte binding was found for all cell types above baseline levels for the range of shear stresses between 2.93 to 0.56 dyn/cm^2 ($p < 0.05$) (see Figure 4-3-6 and Table 4-3-4). The number of cell which bound on the TNFα + bFGF activated monolayer at 0.56 dyn/cm^2 shear stress was approximately 6- to 9-fold higher than that found on the non-activated monolayer for CD4+, CD56+, and CD8+ cells, respectively. Indicating the importance of CAM modulation on lymphocyte binding characteristics.

The binding characteristics of the activated lymphocyte subpopulations on TNFα + bFGF treated monolayers were comparable to those found on TNFα-treated monolayers. However, key differences were noted in several specific aspects. First, differences in the binding levels at the lowest shear stress between CD4+ cells and CD8+ cells were significantly greater on the TNFα + bFGF activated monolayers than on the TNFα activated monolayers, 33% vs. 13%, respectively. Similar effects were evident between CD4+ and CD56+ cells on the TNFα + bFGF and TNFα activated monolayers, with differences in binding levels of 40% vs. 22%, respectively. Second, there was a greater

range of shear stresses over which statistical differences were found between the CD8+ and CD56+ cells on the TNFα + bFGF activated monolayers. However, at the lowest shear stress, the difference in the binding levels between these two subpopulations were not found to be statistically significant between TNFα and TNFα + bFGF treated monolayers.
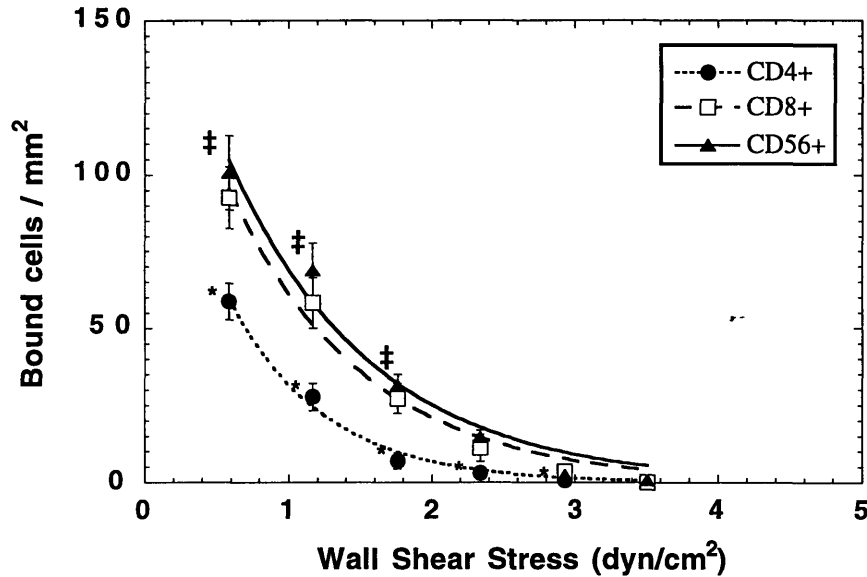

Figure 4-3-6. Cumulative binding curves of IL-2-activated CD4+, CD8+, and CD56+ cells on TNFα + bFGF activated HUVEC monolayers. Mean numbers ± SD of bound cells for five adjacent fields are shown for 1 of 3 representative flow experiments. * significant difference between CD4+ and CD8+ or CD56+ cells, p < 0.05, and ‡ significant difference between CD8+ and CD56+ cells, p < 0.05.

Table 4-3-4. Comparison of cell binding densities of IL-2 activated CD4+, CD8+, and CD56+ cells on HUVECs treated with TNFα+bFGF for 24 hrs. Mean values ± SD are shown for n = 3 flow experiments.

Shear stress (dyn/cm^2)	CD4+ (bound cells/mm^2)	CD8+ (bound cells/mm^2)	CD56+ (bound cells/mm^2)
3.51	0.00 ± 0.00	0.20 ± 0.76 *	0.78 ± 1.35 *,‡
2.93	0.59 ± 1.22 *	3.92 ± 3.08 *,‡	3.14 ± 2.07 *,‡
2.34	2.94 ± 2.49 *	10.39 ± 4.43 *,‡	13.53 ± 3.98 *,‡
1.76	8.82 ± 4.31 *	27.26 ± 4.90 *,‡	33.14 ± 8.79 *,‡,¤
1.17	30.78 ± 8.23 *	54.90 ± 9.35 *,‡	70.59 ± 10.95 *,‡,¤
0.56	60.98 ± 8.50 *	90.39 ± 13.45 *,‡	100.00 ± 9.37 *,‡,¤

* Significant difference from TNFα-activated monolayers of the respective cell type, p < 0.05.
‡ Significant difference compared to CD4+ cells, p < 0.05.
¤ Significant difference compared to CD8+ cells, p < 0.05.

These findings are suggestive that the lower CAM expression on TNFα + bFGF treated monolayers are reaching a threshold in which the favorable molecular binding kinetics of CD56+ and CD8+ cells are significantly advantageous over CD4+ cells, and CD56+ cells are advantageous over CD8+ cells.

In comparing the cell binding densities between the subpopulations on TNFα + bFGF treated monolayers, fewer CD4+ cells consistantly bound to the endothelial monolayer for the complete range of shear rates examined, compared to both CD8+ and CD56+ cells ($p < 0.05$). The only exception occurring at 3.51 dyn/cm^2 shear stress for the CD8+ cells. At 0.56 dyn/cm^2 shear stress, CD4+ cell binding levels were on average 33% and 40% less than the levels obtained by CD8+ and CD56+ cells, respectively. Differences between CD8+ and CD56+ cells were also observed, but were limited to the shear stresses ranging from 1.76 to 0.56 dyn/cm^2 ($p < 0.05$). At the lowest shear rate, a 10% greater number of CD56+ cells than CD8+ cells bound to the endothelial monolayer. These findings suggest that IL-2 activated CD4+ cells do not increase their integrin expression as greatly as IL-2 activated CD8+ and CD56+ cells. In addition, the CD4+ cells may also have a lower selectin expression upon activation compared to CD8+ and CD56+ cells, thus accounting for their lower binding levels at the higher shear stresses.

These results contrasted with those found for the non-activated cell subtypes. Activated CD8+ cells dramatically increased their adhesiveness above the levels attained by activated CD4+ cells for nearly the entire range of shear stresses. However, non-activated CD4+ cells maintained higher binding levels for the mid-range shear stresses compared to non-activated CD8+ cells. These findings indicate that the binding advantage which CD4+ cells have over CD8+ cells in the non-activated state can apparently be overcome by the differential increase in integrin expression in favor of the CD8+ cells in the IL-2 activated state.

Plots of the capture efficiencies for each of the lymphocyte subpopulations were generated to further examine the adhesion kinetics on TNFα + bFGF activated monolayers, and are shown in Figure 4-3-7. The cell accumulation curves reproducibly showed a reduction in binding efficiency that was uniform across the range of shear stresses examined for each of the lymphocyte subpopulations. A significantly greater slope (κ) of the capture efficiency plot was observed for CD4+ cells (1.452 ± 0.076 cm^2/dyn) compared to CD8+ cells (1.079 ± 0.066 cm^2/dyn), as well as CD56+ cells (0.992 ± 0.027 cm^2/dyn) ($p < 0.05$), and is plotted in Figure 4-3-8a. No statistical difference of the parameter κ was evident between CD8+ and CD56+ cells. These results are consistent with those found using TNFα alone, but significant differences in the capture coefficient values between the two monolayer treatments were found for both CD4+ and CD56+ cells

80

(p < 0.05). The increased value of κ on TNFα + bFGF treated monolayers indicates that the CD4+ and CD56+ cells experience a relatively weaker initial binding to the endothelium, which is the result of the decreased expression of selectins on the monolayer surface. While the κ value for CD8+ cells was not found to be significantly different between the two treatment groups, there was a similar trend towards a larger κ value on TNFα + bFGF treated monolayers, and consequently a weaker initial binding force. These results are in agreement with the findings that monolayers treated with TNFα + bFGF approach a threshold of CAM expression, whereby variations in the binding kinetics for each of the activated lymphocyte subpopulations become evident for a relatively broad range of physiological shear stresses.

In comparison with the non-activated lymphocyte subsets, the activated lymphocytes showed a differential effect on the value of the capture coefficient. Activated CD4+ cells demonstrated a significantly increased value for κ (1.452 $\pm$ 0.076 vs 1.179 $\pm$ 0.072 cm^2/dyn). As was hypothesized in the comparison between binding characteristics of CD4+ cells on TNFα-activated endothelium, this may be attributable to a reduced level of selectin expression maintained by CD4+ cells in the activated state. In contrast, CD8+ and CD56+ cells showed significant decreases in their κ values between the activated and non-activated states. A possible reason for this occurrance may be the increased expression of a β_1 integrin (VLA-4) on the activated lymphocytes, which has been shown to have an overlapping role in the capture process.
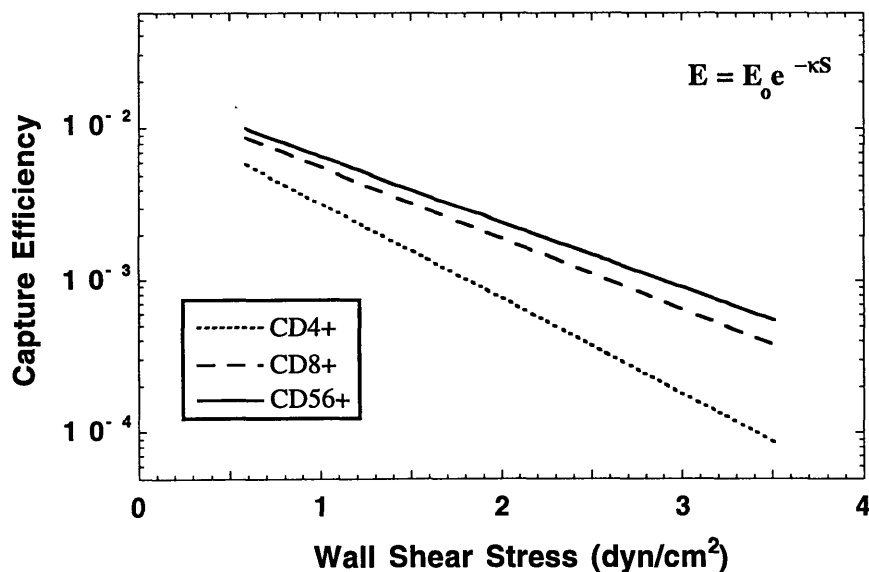

Figure 4-3-7. Comparison of binding efficiencies between IL-2-activated CD4+, CD8+, and CD56+ cells on TNFα + bFGF activated HUVEC monolayers (n = 3).
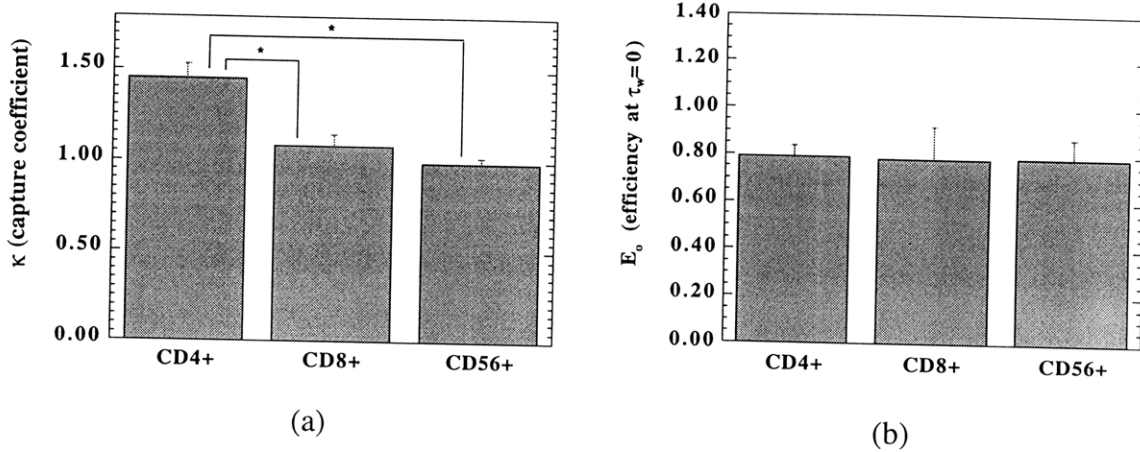
Figure 4-3-8. Comparison of the fitted parameters: a) κ, capture coefficient, and b) Eo, efficiency at zero shear generated from the capture efficiency plots of activated lymphocytes on TNFα + bFGF activated monolayers. R^2 greater than 0.96 in all cases. * $p < 0.05$.

An analysis of the fitted parameter Eo showed no statistically significant difference between any of the activated lymphocyte subpopulations or between the two monolayer groups for the respective lymphocytes (see Figure 4-3-8b). Therefore, the differences found in the binding kinetics and in the capture coefficient between the lymphocyte subpopulations may be the result of selective molecular interactions. The selectins and β_1 integrins are functionally more dominant at the higher flow rates, and would explain the differences observed. The increased binding efficiency found when comparing non-activated and IL-2 activated CD8+ and CD56+ cells provides additional evidence to the role of β_1 integrins in this process.

4.4 IL-2 Activated Natural Killer Cell Binding Mechanisms

To further elucidate the molecular mechanisms mediating activated CD56+ or A-NK cell adhesion under a range of physiological shear stress conditions, additional studies were performed using monoclonal antibodies (mAbs) as blocking agents against selective CAMs. For these studies, HUVEC monolayers were activated with either TNFα (50 ng/ml) or tumor interstitial fluid (TIF, 1:50 dilution) for 24 hrs, and unactivated monolayers were used as baseline controls. Monoclonal antibodies were added in excess 30 min prior to use in the flow assay, as described in Section 3.5. Cumulative cell binding

densities of A-NK cells were determined using the flow chamber under shear stress conditions ranging from 0.56 to 3.5 dyn/cm^2.

The use of tumor interstitial fluid, a milieu of growth factors and other tumor products, provided an *in vitro* model for the potential microenvironmental conditions experienced by endothelial cells in a tumor. The incubation time of 24 hrs was selected to reflect prolonged exposure of the endothelium to tumor fluid, and was accordingly analyzed for its ability to alter CAM expression (see Section 5.2).

Experiments involving TIF-mediated activation demonstrated increased A-NK cell adhesion to the endothelium, with significant increases in binding between 2.0 and 0.56 dyn/cm^2 (see Figure 4-4-1). The number of bound cells on the TIF-activated monolayer at 0.56 dyn/cm^2 was approximately 10-fold higher than that on the untreated monolayer.
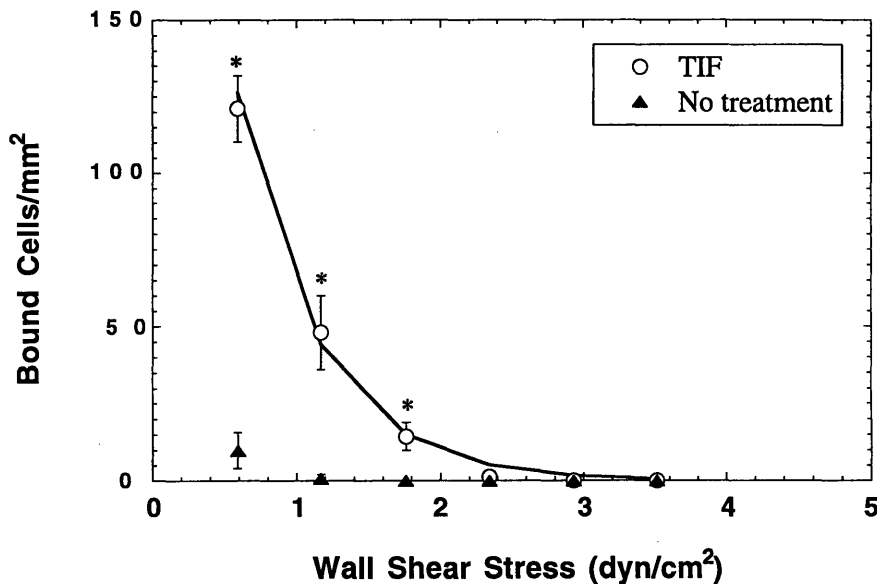

Figure 4-4-1. Cumulative binding curves of A-NK cells on TIF-activated and non-activated endothelial cell monolayers. Mean numbers ± SD of bound cells for five adjacent fields are shown. * p < 0.05.

The relative influence of the receptor-ligand interaction between CD18, ICAM-1 and ICAM-2 was found to provide a significant contribution to A-NK cell binding, as demonstrated by mAb blocking (see Figures 4-4-2 and 4-4-3). The effect of independently blocking ICAM-1 and ICAM-2 produced a 40-50% decrease in the number of cells bound under a wall shear stress of 0.56 dyn/cm^2 compared to TIF only treated monolayers. Blocking of the shared receptor, CD18, showed an average decrease of 70-75%. This

reduction was significant between 0.56 to 2.0 dyn/cm^2 for LFA-1 and corresponding counter-receptor blocking (p < 0.05). When ICAM-1 and ICAM-2 were blocked simultaneously, the level of binding was reduced further to a total of 65-70% from controls, and reached levels attained by CD18 blocking. This result was consistent with the involvement of the two ICAM molecules in interacting with lymphocyte-associated LFA-1 in forming stable adhesion at low shear stresses.

The β_1-integrin, VLA-4 (CD49d), and its corresponding ligand on the endothelium, VCAM-1, was found to also produce a significant effect on cell binding (see Figure 4-4-4). Blocking of VCAM-1 produced a 45-55% decrease in the number of cells bound under a wall shear stress of 0.56 dyn/cm^2 compared to TIF controls, while blocking of VLA-4 produced an average decrease of 70-80%. The reduction in binding was significant up to shear stresses as high as 2.0 dyn/cm^2 (p < 0.05). The discrepancy between the relative contributions of VLA-4 and VCAM-1 on A-NK adhesion was found to be statistically significant (p < 0.05). This suggests that an additional ligand may exist on endothelial cells which interacts with the β_1-integrin, or that the blocking antibodies may have different affinities or blocking efficiencies.
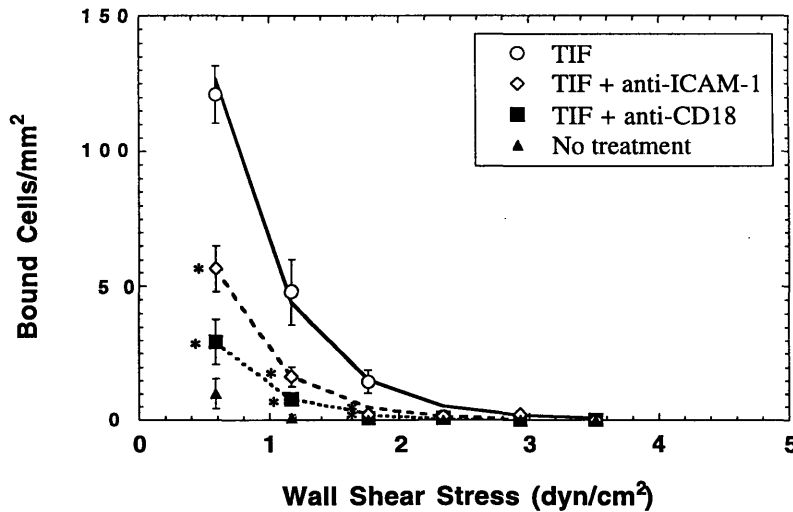

Figure 4-4-2. A-NK cell adhesion to TIF-activated HUVEC monolayers showing the role of CD18:ICAM-1 using monoclonal antibody blocking. Mean numbers ± SD of bound cells for five adjacent fields are shown. * p < 0.05.
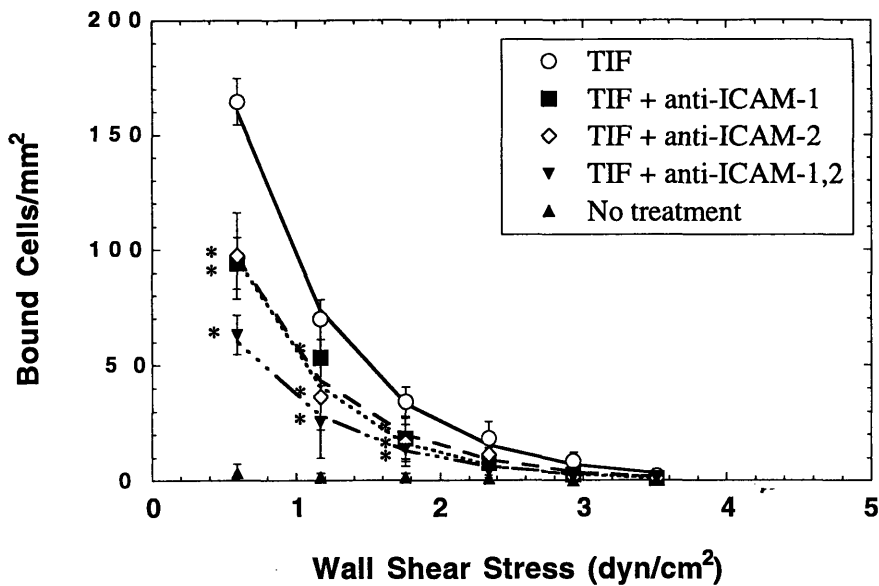
84

Figure 4-4-3. A-NK cell adhesion to TIF-activated HUVEC monolayers showing the role of ICAM-1:ICAM-2 using monoclonal antibody blocking. Mean numbers ± SD of bound cells for five adjacent fields are shown. * p < 0.05.
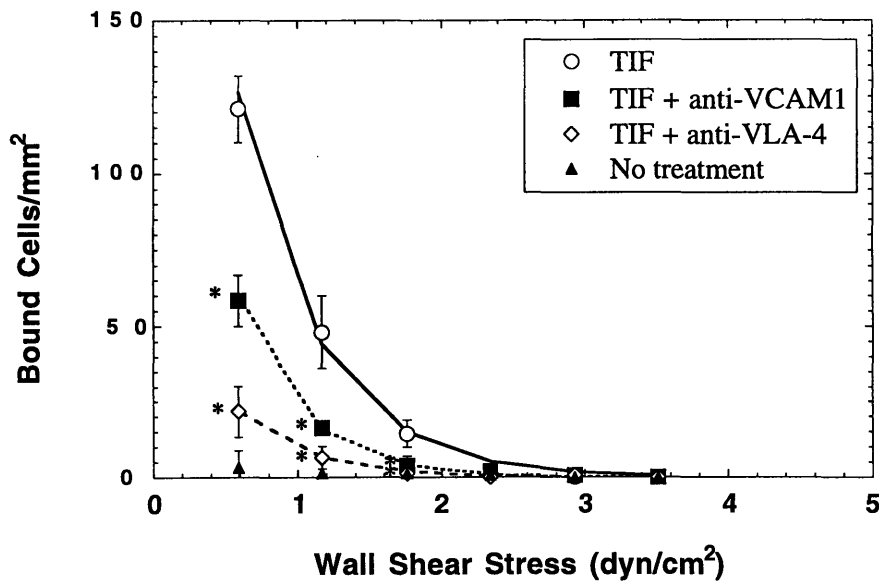

Figure 4-4-4. A-NK cell adhesion to TIF-activated HUVEC monolayers showing the roles of VLA-4:VCAM-1 using monoclonal antibody blocking. Mean numbers ± SD of bound cells for five adjacent fields are shown. * p < 0.05.

The relative contribution of the selectin molecules, namely E- and P-selectin, and their common ligand, sialyl Lewis X, was found to produce modest effects on A-NK cell adhesion only at the lowest levels of shear stress examined (see Figure 4-4-5 and Figure 4-4-6). The slight but significant ($p < 0.05$) reduction in adhesion of A-NK cells at 0.6 dyn/cm^2 was by 15%, 7%, and 7% for sialyl-Lewis X, E- and P-selectin mAb treatment, respectively. As was found with the anti-integrin antibody treatments, stable adhesion of the flowing cells on the activated endothelium occurred rapidly and displayed no significant rolling interactions even after prolonged arrest. This provided further evidence of a process which is largely independent of a selectin-mediated mechanism. However, it is unprecedented that a modest level of inhibition of A-NK cell binding occurred at the low shear stress by antibody blocking of the E- and P-selectin, as well as their counter-receptor, sLeX. These molecules have been characterized as principally mediating the inital phase of capture, which is most relevant at the higher shear states [von Andrian, et al., 1991]. Additional studies will be needed to further characterize their possible role in A-NK cell adhesion.
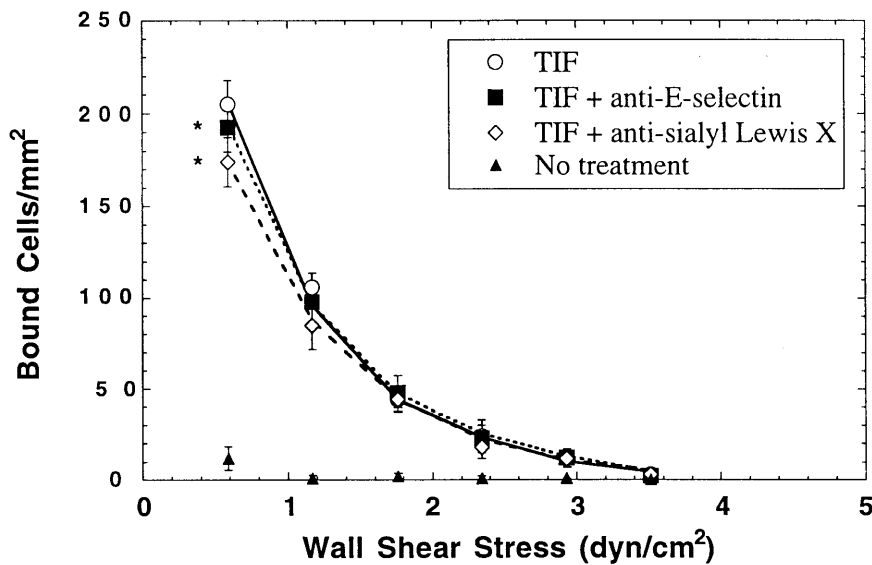

Figure 4-4-5. A-NK cell adhesion to TIF-activated HUVEC monolayers showing the role of E-selectin and sialyl-Lewis X using monoclonal antibody blocking. Mean numbers ± SD of bound cells for five adjacent fields are shown. * $p < 0.05$.
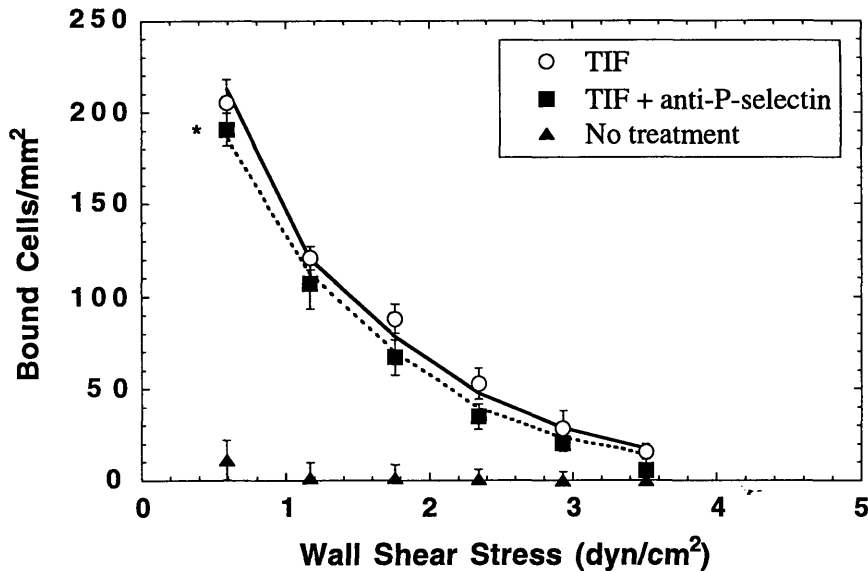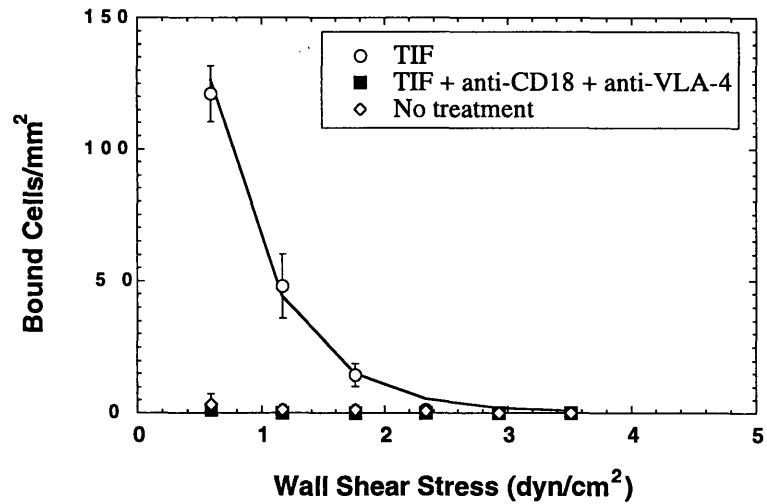
Figure 4-4-6. A-NK cell adhesion to TIF-activated HUVEC monolayers showing the role of P-selectin using monoclonal antibody blocking. Mean numbers ± SD of bound cells for five adjacent fields are shown. * p < 0.05.

To define the cooperative function of the β_1 and β_2 integrins in the adhesion of A-NK cells to vascular endothelium, A-NK cells were treated with a combination of anti-CD18 and anti-VLA-4. As shown in Figure 4-4-7a, the combined treatment resulted in fewer bound cells than either antibody treatment alone (p < 0.05), and the overall number of bound cells reached baseline levels for all shear stress examined (p > 0.1). Identical results were obtained by blocking the corresponding ligands on the endothelial cells, i.e. ICAM-1 and VCAM-1 (see Figure 4-4-7b).

While the results obtained with TIF-activation of HUVEC monolayers conclusively demonstrated an integrin-dominated cell capture process by A-NK cells, a multiple number of factors may contribute to the effect produced by TIF, and provide an inherent kinetic advantage of A-NK cells to utilize a strongly integrin-dominated binding process. To provide additional support to the findings, binding studies identical to those performed with TIF were conducted using TNFα to further verify the molecular mechanisms used by A-NK cells in binding to endothelial cell monolayers.

Results involving TNFα-activation of the endothelium, which causes an uniform upregulation of ICAM-1, VCAM-1 and E-selectin, demonstrated significantly increased A-NK cell adhesion between 2.0 and 0.56 dyn/cm^2 (see Figure 4-4-8). The number of bound cells on the TNFα-activated monolayer at 0.56 dyn/cm^2 was also approximately 10-

fold higher than that on the non-activated monolayer, a finding similar to that which was seen with TIF treatment.
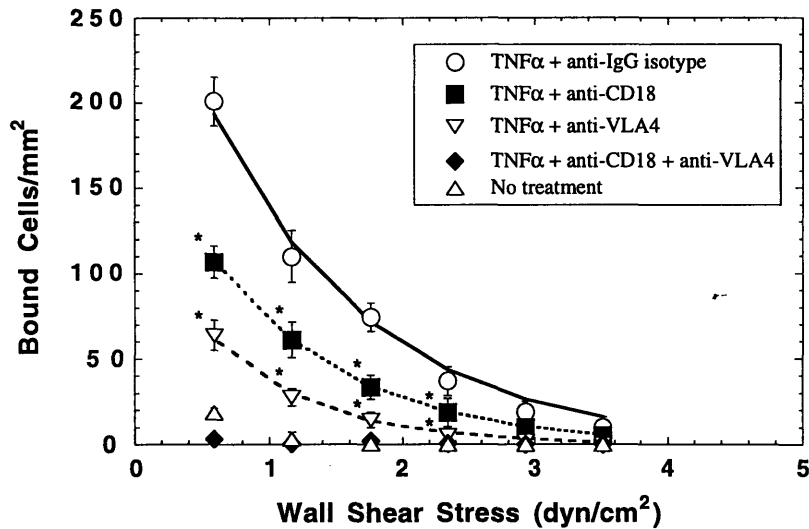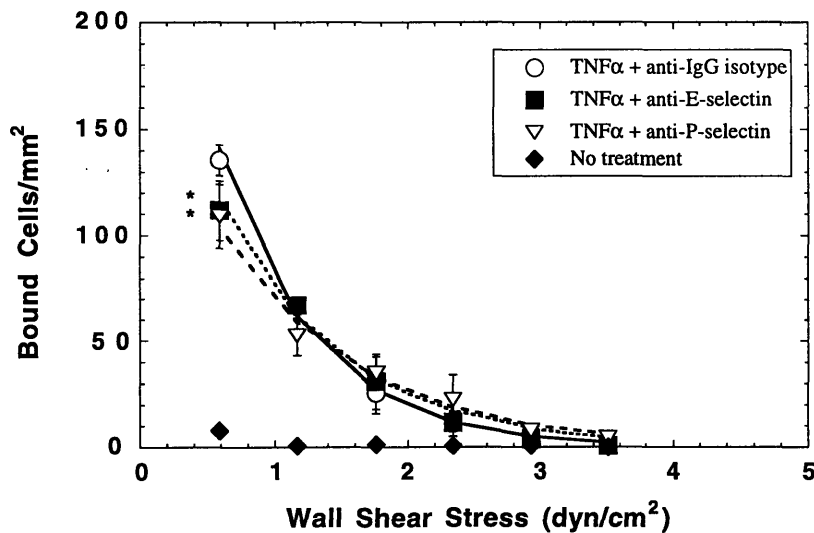

(a)
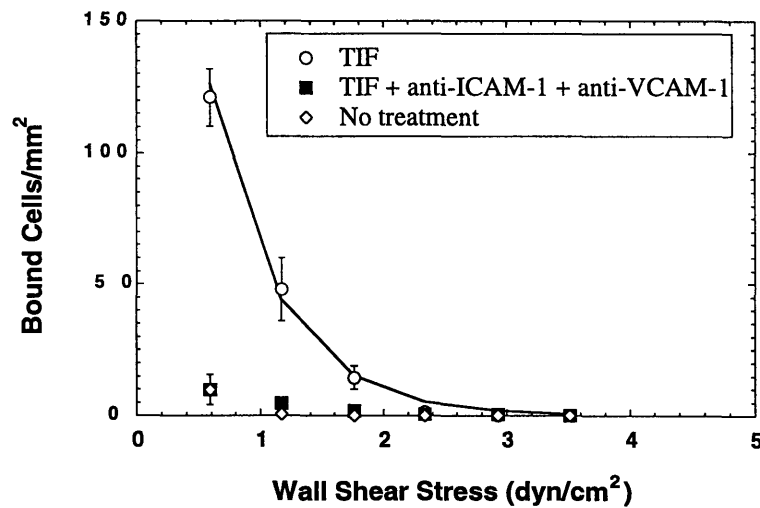
(b)

Figure 4-4-7. A-NK cell adhesion to TIF-activated HUVEC monolayers showing the combined effects of blocking a) CD18 and VLA-4 on A-NK cells, and b) ICAM-1 and VCAM-1 on endothelial cells. Mean numbers ± SD of bound cells for five adjacent fields are shown.

Antibody blocking experiments corroborated the findings that A-NK cells adhere to activated endothelium by an integrin-mediated interaction process involving CD18/ICAM-1 and VLA-4/VCAM-1 (Figure 4-4-8a and b). Pretreatment of the endothelial cells with anti-

E- or anti-P-selectin showed only a slight, but significant inhibition of A-NK binding at the low shear stress ($p < 0.05$). This was in agreement with the previous findings demonstrating that A-NK cells largely use a selectin-independent binding process. In addition, as was found with flowing cells on TIF-activated monolayers, rapid arrest occurred independently of rolling interactions.

(a)

Legend:
- ○ TNFα + anti-IgG isotype
- ■ TNFα + anti-CD18
- ▽ TNFα + anti-VLA4
- ◆ TNFα + anti-CD18 + anti-VLA4
- △ No treatment

Y-axis: Bound Cells/mm² (0, 50, 100, 150, 200, 250)
X-axis: Wall Shear Stress (dyn/cm²) (0, 1, 2, 3, 4, 5)

(b)

Legend:
- ○ TNFα + anti-IgG isotype
- ■ TNFα + anti-E-selectin
- ▽ TNFα + anti-P-selectin
- ◆ No treatment

Y-axis: Bound Cells/mm² (0, 50, 100, 150, 200)
X-axis: Wall Shear Stress (dyn/cm²) (0, 1, 2, 3, 4, 5)

Figure 4-4-8. A-NK cell adhesion to TNFα-activated HUVEC monolayers showing the roles of a) β_1 and β_2 integrins, and b) E- and P-selectin using monoclonal antibody blocking. Mean numbers ± SD of bound cells for five adjacent fields are shown. * $p < 0.05$.

To quantify the level of adhesion receptors available for A-NK cells to bind to activated endothelial cell monolayers, flow cytometric analysis was periodically performed to several cultures. Results consistently showed high levels of β_1 (VLA-4) and β_2 (CD18) integrin expression, 50-80% and 90-95%, respectively (see Figure 4-4-9). Levels of L-selectin (35-45%) and sialyl-Lewis X (10-20%), counter-receptors for E- and P-selectin, were also significantly present but in lower quantities. For the period of time in which the NK cultures were utilized, between 1.5 to 4 weeks, there was no appreciable shedding or increase in expression of any of the receptors analyzed.
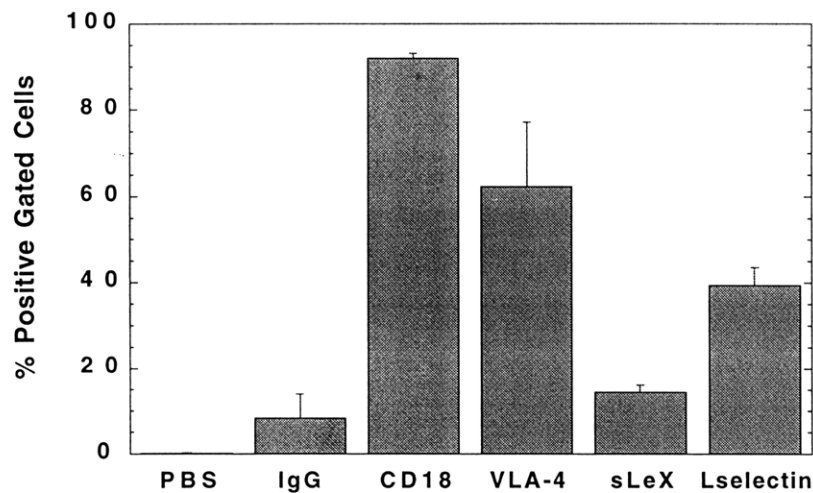

Figure 4-4-9. A-NK expression levels of CD18, VLA-4, L-selectin, and sialyl Lewis X. PBS and IgG isotype staining are provided as controls. Percentage of positive gated cells ± SD for three separate IL-2 activated NK cultures are shown. Gates for positive cells were arbitrarily placed based upon the IgG isotype control fluorescence. See Appendix A for the flow cytometric histograms.

4.5   Conclusions

The important results obtained from the *in vitro* studies presented in this chapter can be generally summarized into the following: a) the lymphocyte subpopulations CD4+, CD8+, and CD56+, vary in their ability to adhere to activated vascular endothelium, b) IL-2 activated lymphocytes differ in their ability to bind to vascular endothelium compared to non-activated populations, with lymphocyte subset variability, and c) IL-2 activated natural killer cells (CD56+) largely utilize an integrin-dependent (β_1 and β_2), selectin-independent adhesion process in binding to activated vascular endothelium.

The lymphocyte subset binding characteristics broadly demonstrated the increased ability of CD56+ cells, compared CD8+ and CD4+ cells, to adhere to HUVEC monolayers under a wide range of shear stresses. In the unactivated state, CD4+ and CD8+ cells bound to the endothelium with relatively equivalent kinetics under high levels of CAM expression. However, increased binding levels of CD4+ cells were obtained under reduced levels of counter-receptor expression on the endothelium. Non-activated CD4+ cells may be more dependent on a selectin-mediated mechanism, while non-activated CD8+ cells may utilize a greater integrin-mediated mechanism in binding, as suggested by the capture efficiency studies.

However, in the IL-2 activated state, CD8+ cells clearly demonstrated an increased binding level over CD4+ cells, regardless of the extent of counter-receptor expression. This is consistent with previous studies on tumor-infiltrating lymphocytes containing proportionally greater levels of CD8+ cells compared to CD4+ cells [Takagi, et al., 1989; Yoo, et al., 1990]. The findings in these experiments are likely to be associated with a decrease in selectin expression on CD4+ cells and a significantly increased integrin expression on CD8+ cells following IL-2 mediated activation.

The overall effect of IL-2 activation was found to increase the binding efficiencies of each of the lymphocyte subsets. Based on the findings of others demonstrating increased integrin expression by lymphocytes following IL-2 activation [Roth, 1994; Melder and Jain, 1992], this may be the major contributor to the increased binding effect. Additionally, the demonstration of the greater reduction or shedding of L-selectin by activated CD4+ cells compared to CD8+ cells [Biselli, et al., 1992], may also be appreciably relevant to the binding characteristics observed.

Further definition of the specific molecular mechanisms used by IL-2 A-NK cells under dynamic flow conditions complimented previous studies characterizing T cell (CD3+) capture and adhesion on activated endothelium. While T cells have demonstrated a significant involvement of selectins in cell capture and the integrins, β_1 and β_2, in stable arrest, NK cells were shown in this investigation to largely involve β_1 (VLA-4) and β_2 (CD18) interactions, with minimal contribution from the selectins. Additionally, monolayers activated with tumor interstitial fluid were able to retain A-NK cells under physiological shear stress conditions, providing an *in vitro* model to the localization of A-NK cells in tumor vessels.

Several *in vivo* studies were conducted in collaboration with this work to provide validation of the *in vitro* findings [Melder, et al., 1996]. Using LS174T tumors grown in the cranial window of SCID mice, human A-NK cells treated with a combination of anti-CD18 and anti-VLA-4 mAbs were adoptively transfered and shown to significantly

decrease their retention in tumor vessels. These studies also showed rapid binding of the A-NK cells without rolling interaction in the control mice, providing further support to the *in vitro* findings.

Contributions of this work to the field of cell adhesion will have impact on: a) improving current modeling schemes which attempt to predict the biodistribution of effector cell populations by providing essential binding kinetic data for each of the subpopulations; b) providing additional insight into the binding kinetics of helper and effector cell populations in areas of active immunological response; and c) contributing to a better understanding of the biophysical and molecular mechanisms used by lymphocytes to potentially improve or modify current adoptive immunotherapy techniques for cancer treatment.

Chapter 5

CAM Modulation by Angiogenic Factors

5.1 Introduction

The adherence of lymphocytes and tumor cells to vascular endothelium is a necessary step in producing an effective immune response and developing metastases, respectively. The process requires adhesion receptors found on the lymphocytes or cancer cells to bind to complementary counter-receptors or ligands on endothelial cells. The cell adhesion molecules (CAMs) on the endothelium are grouped into two distinct families: selectins (E- and P-), which primarily mediate the initial capture and rolling of cells; and the immunoglobulin gene superfamily members, ICAM-1, ICAM-2, and VCAM-1, which mediate stable adhesion [Springer, 1995; Butcher, 1991]. The expression of the CAMs on the endothelium can be modulated and regulated by cytokines and growth factors released by resident tissue cells, infiltrating leukocytes, and/or cancer cells during inflammatory, immune, and tumor responses [Pober and Cotran, 1990; Freeman, et al., 1995; Jain, et al., 1996]. Many of these same cytokines and growth factors mediate angiogenesis, and are conjointly termed angiogenic factors [Folkman, 1995; Fidler and Ellis, 1994]. TNFα, VEGF, bFGF, and TGFβ are four widely documented angiogenic factors which are present in sites of inflammation, healing wound, and tumor growth [Pober and Cotran, 1990]. The temporal kinetics of CAM modulation by the individual factors alone, or in combination with each other, have only been explored to a limited extent and are not well defined.

The expression of both constitutive and inducible CAMs on normal endothelium has been found to be tissue or organ dependent [Kuzu, et al., 1993]. Specifically, the expression of CAMs in the tumor vasculature has been shown to be heterogeneous, both intra-tumorally and inter-tumorally [Jain, et al., 1996]. A positive correlation between the accumulation of inflammatory cells and the expression of specific CAMs in tumor vessels have been demonstrated [Suzuki, et al., 1995]. These observations are suggestive of the tumor microenvironment providing a significant contribution to modulating CAM expression and, thereby, regulating the infiltration of leukocytes. Insight into the regulation of adhesion molecule expression and leukocyte-endothelial interactions by angiogenic factors found in tumor has been significantly limited.

In this chapter, results are presented from several experiments using targeted sampling fluorometry, flow cytometry, and the parallel-plate flow chamber to address the following essential issues: a) what effect does the interstitial fluid from tumors (TIF), a model of the tumor microenvironment, have on CAM expression in endothelial cells; b) what are the levels of angiogenic factors in the tumor fluid, which may establish a mechanism for its ability to modulate CAM expression; c) what are the kinetics of CAM expression in endothelial cells treated independently, or in combination, with the known angiogenic factors TNFα, VEGF, bFGF, and TGFβ; and d) what is the functional significance of the effects of TIF and angiogenic factors on lymphocyte binding to treated endothelial cells under dynamic flow conditions?

The findings from these studies provide additional understanding of the role of angiogenic factors in regulating the host response to sites of tumor growth and inflammation, as well as in modifying the metastatic potential of tumors.

5.2 Surface Expression and Activation Kinetics

The first objective of this investigation was to determine the level and kinetics of cell surface adhesion molecule expression on endothelial cells activated by TIF and various angiogenic factors. Two expression assays were used to perform this task: a) flow cytometric analysis (FACScan), and b) targeted sampling fluorometry (TSF). The results are presented as intensity histograms with the number of counts or percentage of cells compared to the fluorescence intensity measured. The temporal kinetics of activation or inhibition, whichever the case may be, were analyzed at 6 and 24 hr time points. These time points were selected based on preliminary experiments demonstrating that 6 and 24 hrs were representative of early and long-term responses, respectively.

5.2.1 Tumor Interstitial Fluid (TIF)

The use of tumor interstitial fluid to activate the endothelial monolayer was initially performed to determine whether the expression of CAMs on the endothelium could be modulated by the modeled tumor microenvironment. An incubation time of 24 hrs was selected to reflect prolonged or chronic exposure of the endothelium to tumor fluid.

The resulting expression profiles of ICAM-1, VCAM-1, E-selectin and P-selectin are shown in Figure 5-2-1a-d. In response to TIF activation, surface expression of ICAM-1 and VCAM-1 was significantly upregulated compared to untreated cells. E-selectin also showed a slight increase in expression, but P-selectin expression was not altered by the TIF. These findings provide distinct evidence that within and locally around a tumor, CAM expression on endothelial cells can be altered by factors existing in the tumor microenvironment.

Various agents may exist in the tumor microenvironment that could potentially mediate the increased CAM expression on endothelial cells, including inflammatory cytokines and angiogenic factors. To ascertain the possible constituents present in the TIF, an enzyme-linked immunosorbent assay was utilized to determine the levels of VEGF, bFGF, and TNFα in the fluid. These cytokines or angiogenic factors were selected based on previous findings of their expression within tumors [Senger, et al., 1993; Rodeck, et al., 1991; Bebok, et al., 1994; Dalal, et al., 1993; Folkman, 1995].

As shown in Figure 5-2-2, the level of VEGF, bFGF, and TNFα was found to be 14.23 ± 2.55 ng/ml, < 0.40 ng/ml, and < 0.10 ng/ml, respectively. Due to the relatively small quantities of fluid available with each collection, which is estimated at less than 50 μl per mouse, and the heterogeneity which exists between samples, the lower limit of accurate detection was obtained for the latter two samples. However, functional analysis using the adhesion assay, as well as published results using various angiogenic assays [Frater-Schroder, et al., 1987; Montesano, et al., 1986], have shown these levels to be at the lower limit of biological responsiveness for endothelial cells. Additionally, the concentration of the TIF used in the expression experiments was at a dilution of 1:50, further lowering the relative dosage of growth factor experienced by the endothelial cells. Therefore, the TIF sampled can be cautiously interpreted as having significant levels of VEGF, but significantly low concentrations of bFGF and TNFα. Additional studies using Northern blot analysis to determine the RNA levels of VEGF and bFGF in LS174T tumors have shown a strong correlation with these protein expression results[3].

---

[3] Communicated by Dr. Kyungran Park, Department of Radiation Oncology, Massachusetts General Hospital.
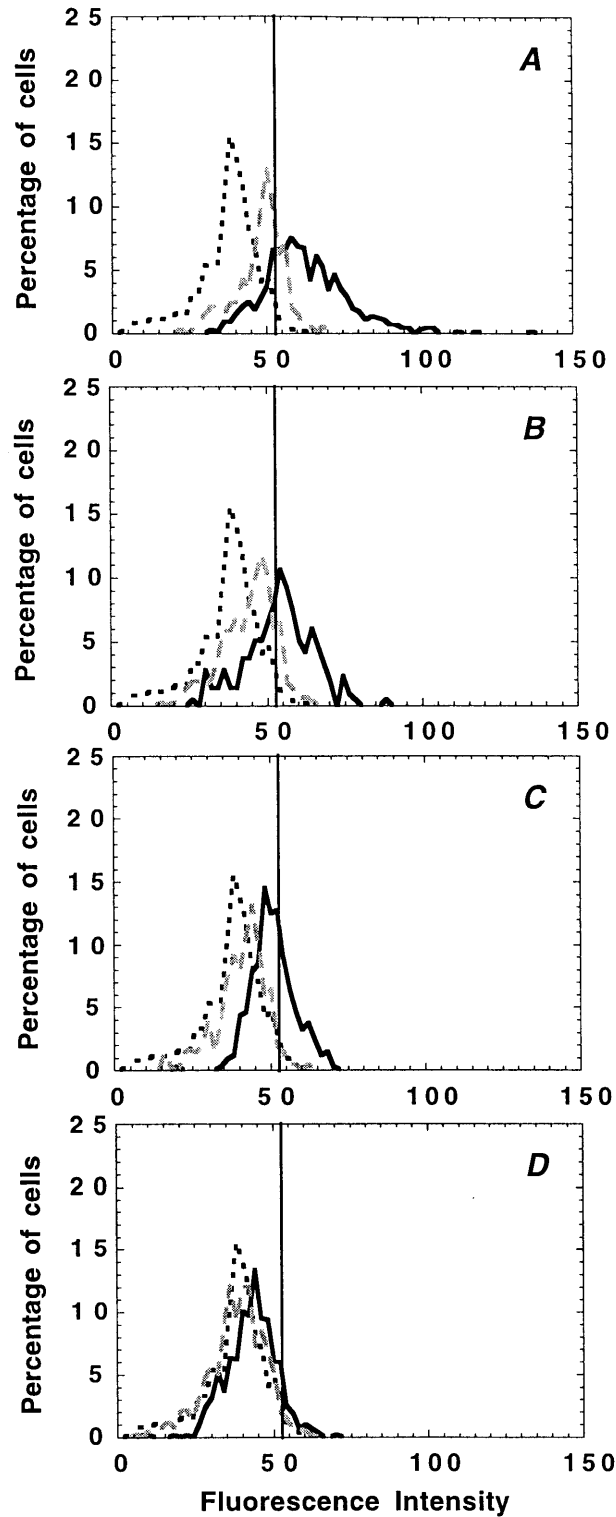
95

Figure 5-2-1. Kinetics of CAM expression on HUVEC monolayers treated with LS174T TIF for 24 hrs using targeted sampling fluorometry: a) ICAM-1, b) VCAM-1, c) E-selectin, and d) P-selectin. — = TIF treatment (1:50), - - = no treatment (baseline), ⋯ = IgG isotype control.
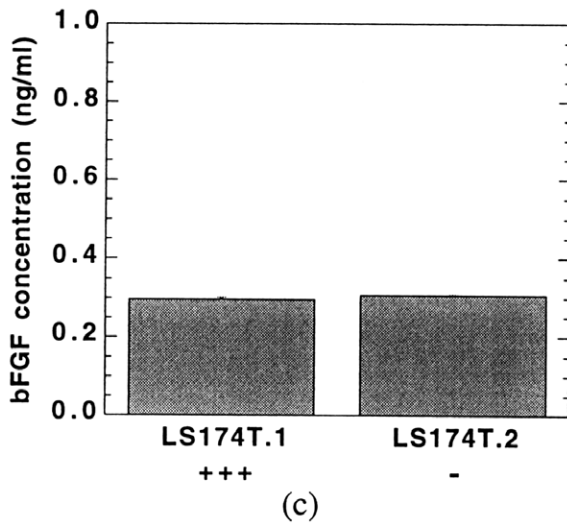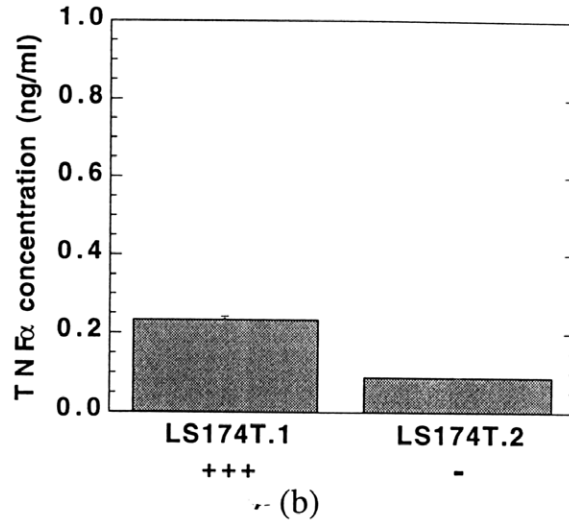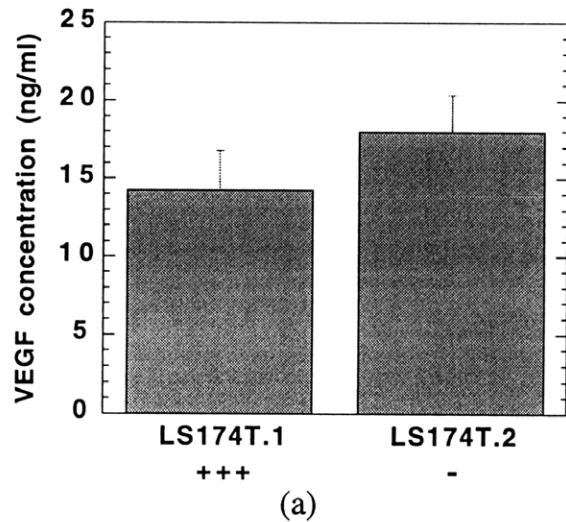
(a)

(b)

(c)

Figure 5-2-2. Concentration of a) human VEGF, b) human TNFα, and c) human bFGF in the tumor interstitial fluid of LS174T xenotransplants. Mean numbers ± SD for n = 3 samples. +/- represents a relative index for the ability of A-NK cells to bind to monolayers treated with the TIF sample, which directly correlated with the level of CAM expression on the endothelial cells.

However, relative caution should be considered in interpreting these results due to several limitations in the overall analysis. Firstly, the viability of the protein within the fluid has not been determined, only the overall level of protein expression. Significant levels of proteases within the tumor may modulate the effectiveness of the growth factor at its receptor binding site, but not at the epitope site for antibody binding. Secondly, cross-reactivity issues may be a factor since the fluid is extracted from xenotransplanted tumors. There may be sufficient amounts of growth factor produced by the host cells of the mouse that are influencing the tumor microenvironment, and thus the responsiveness of the endothelial cells to the TIF in culture. Thirdly, other potent factors, such as IL-1β, IFN-γ, and TGFβ, may exist in the tumor fluid and provide a major regulatory mechanism to the CAM expression observed. Additionally, the fluid collected using the Gullino chamber

represents the minimum level of protein present in the tumor interstitial compartment. The absence of growth factor in the TIF collected does not negate its presence in the tumor, but rather may be a limitation of the collection technique. Lastly, the tumor fluid extracted is an average, global representation of the environment within a tumor, rather than a local microenvironmental representation. Given the fact that tumors are exceptionally heterogeneous and that CAM expression has been shown to vary from one region to the other, local variation in the level of growth factor may not be representative of the global milieu. To this end, there was also found a general lack of correlation between the level of VEGF produced by these tumors and their ability to regulate lymphocyte-endothelial interaction, as indexed in Figure 5-2-2a.

Considering these limitations and the finding that of the growth factors analyzed, only significant levels of VEGF, and not bFGF or TNFα, were produced by the LS174T tumor line, a detailed analysis was performed on the kinetics of CAM expression on endothelial cells activated with the individual angiogenic factors TNFα, VEGF, bFGF and TGFβ. Other tumors, such as mammary carcinomas and melanomas, have been shown to express high levels of these angiogenic factors, and thus warrant their investigation.

5.2.2 TNFα

Tumor necrosis factor-α, a pro-inflammatory cytokine, at a concentration of 50 ng/ml was placed on HUVEC monolayers. The temporal kinetics were determined for ICAM-1, VCAM-1, E-selectin, and P-selectin. Although the kinetics of this endogenous stimulator have been well characterized, differences in culture medium conditions (serum-free), endothelial cell phenotype (HUVEC), and confluency level (greater than 90%) may have altered the responsiveness of the endothelial cells to the cytokines and growth factors examined. These variables were utilized as controls.

As shown in Figure 5-2-3 using flow cytometric analysis, the expression of ICAM-1, VCAM-1 and E-selectin were all substantially increased above baseline levels by 6 hrs, while P-selectin showed no significant difference from controls. By 24 hrs, ICAM-1, VCAM-1 and E-selectin levels for the TNFα-activated monolayer continued to be significantly above the non-treated controls, and P-selectin remained at baseline levels.

These results are in agreement with those previously documented [Osborn, 1990; Munn, et al., 1995], and indicate that TNFα is a rapid and potent inducer of CAMs on the endothelium.
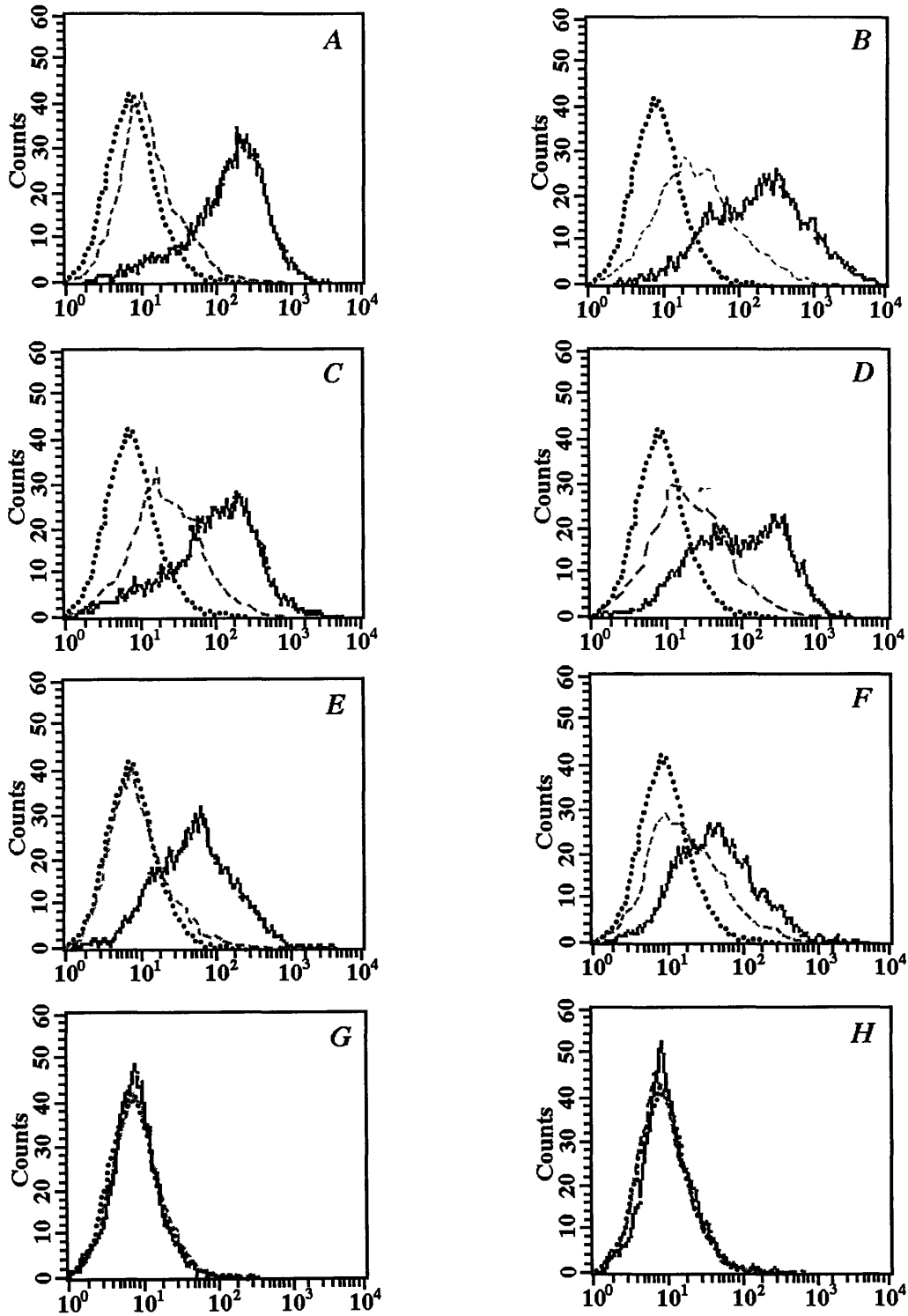
Figure 5-2-3. Kinetics of CAM expression on HUVEC monolayers treated with TNFα for 6 and 24 hrs using flow cytometry: a) ICAM-1 (6 hr), b) ICAM-1 (24 hr), c) VCAM-1 (6 hr), d) VCAM-1 (24 hr), e) E-selectin (6 hr), f) E-selectin (24 hr), g) P-selectin (6 hr), and h) P-selectin (24 hr). — = TNFα treatment (50 ng/ml), - - = no treatment (baseline), ⋯ = IgG isotype control.

99

5.2.3 VEGF

Vascular endothelial growth factor was the next angiogenic factor considered in this investigation. While VEGF is widely known for its mitogenic and permeability enhancing activity, its capability for altering CAM expression has largely been ignored. Using a concentration of 35 ng/ml, as conjectured from studies on its angiogenic activity, the temporal kinetics were determined for each of the CAMs and the results are shown in Figure 5-2-4.

As was found for the TNFα experiments, VEGF induced increased levels of ICAM-1, VCAM-1 and E-selectin by 6 hrs of incubation on endothelial cells. P-selectin was found to be unchanged from control levels. By 24 hrs of treatment, ICAM-1 remained at substantially higher levels above controls, while P-selectin remained at baseline levels. The expression of VCAM-1 and E-selectin, while reduced compared to their respective levels at 6 hrs, remained significantly above the non-treated levels at 24 hrs.

Since a) VEGF can induce increased ICAM-1, VCAM-1 and E-selectin expression on endothelial cells, similar to TIF, and that b) VEGF was found in substantial quantities in the tumor fluid, suggests that VEGF may be a mediator TIF modulation of CAM expression in tumors. However, the concentration of VEGF in the TIF was found not to correlate with the ability of TIF to modify CAM expression. This suggests that another mediator may be involved which either inhibits the action of VEGF or is a co-activator of VEGF in altering CAM expression on endothelial cells. Basic FGF and TGFβ were studied next as possible inhibitory agents of CAM expression.

5.2.4 bFGF

Basic fibroblast growth factor, another potent mitogenic and angiogenic factor, has been shown to increase the expression of several alpha and beta integrins [Klein, et al., 1993], but its effect on CAM modulation is poorly understood [Kitayama, et al., 1994; Griffioen, et al., 1996]. Using a concentration of 10 ng/ml, as determined from several angiogenic studies, the temporal kinetics were determined for each of the CAMs and the results are shown in Figure 5-2-5.

Basic FGF was found to produce a biphasic effect on ICAM-1 expression. After 6 hrs of activation with bFGF, endothelial cells expressed a slight, but significant increase in ICAM-1 expression. However, after 24 hrs of treatment, the endothelial cells showed a slight, but significant decrease in the basal expression of ICAM-1 compared to non-treated controls. The levels of VCAM-1, E-selectin and P-selectin were unaffected by bFGF treatment at 6 and 24 hrs compared to baseline expression.
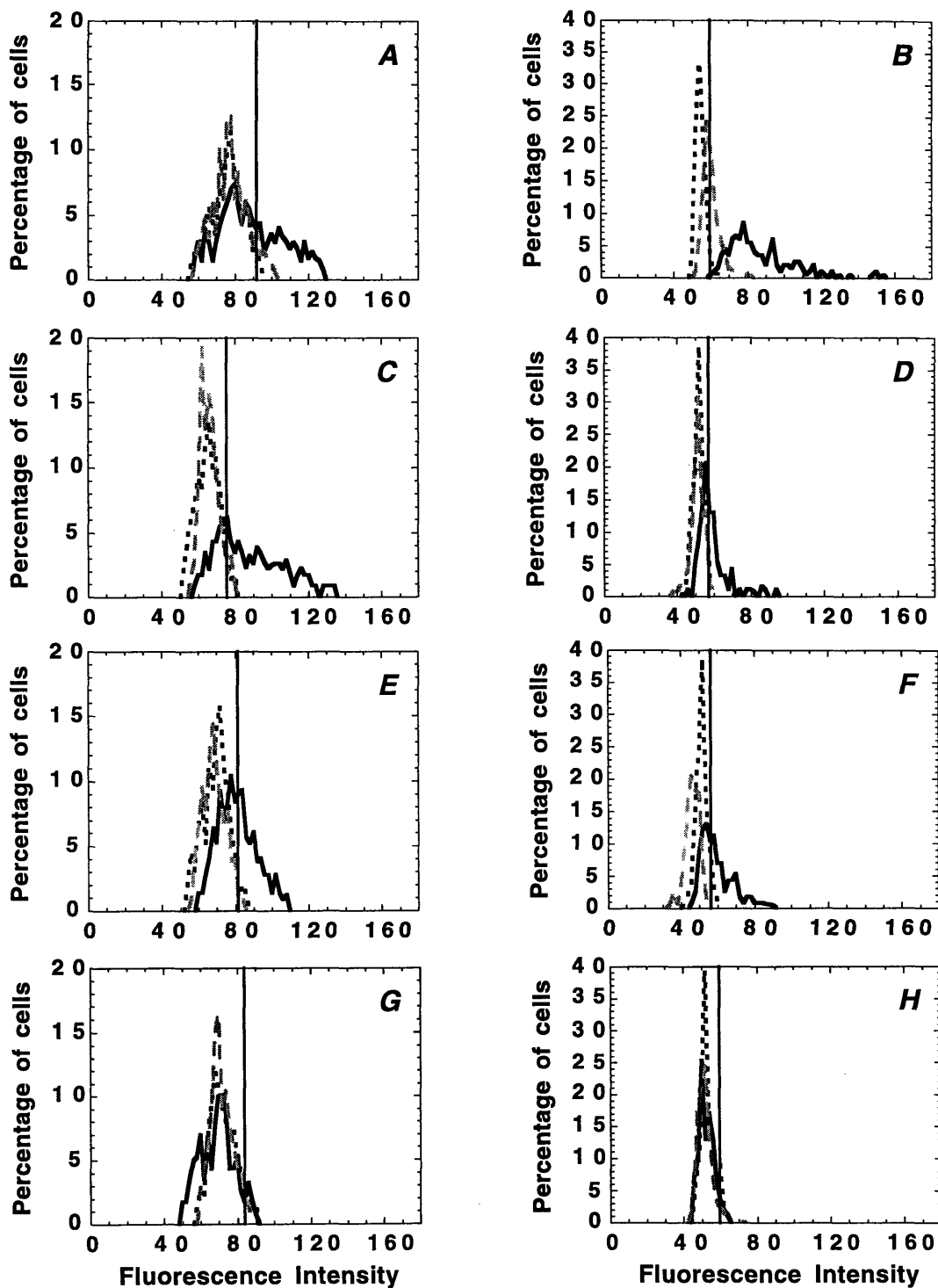
Figure 5-2-4. Kinetics of CAM expression on HUVEC monolayers treated with VEGF for 6 and 24 hrs using TSF: a) ICAM-1 (6 hr), b) ICAM-1 (24 hr), c) VCAM-1 (6 hr), d) VCAM-1 (24 hr), e) E-selectin (6 hr), f) E-selectin (24 hr), g) P-selectin (6 hr), and h) P-selectin (24 hr). — = VEGF treatment (35 ng/ml), - - = no treatment (baseline), ⋯ = IgG isotype control.
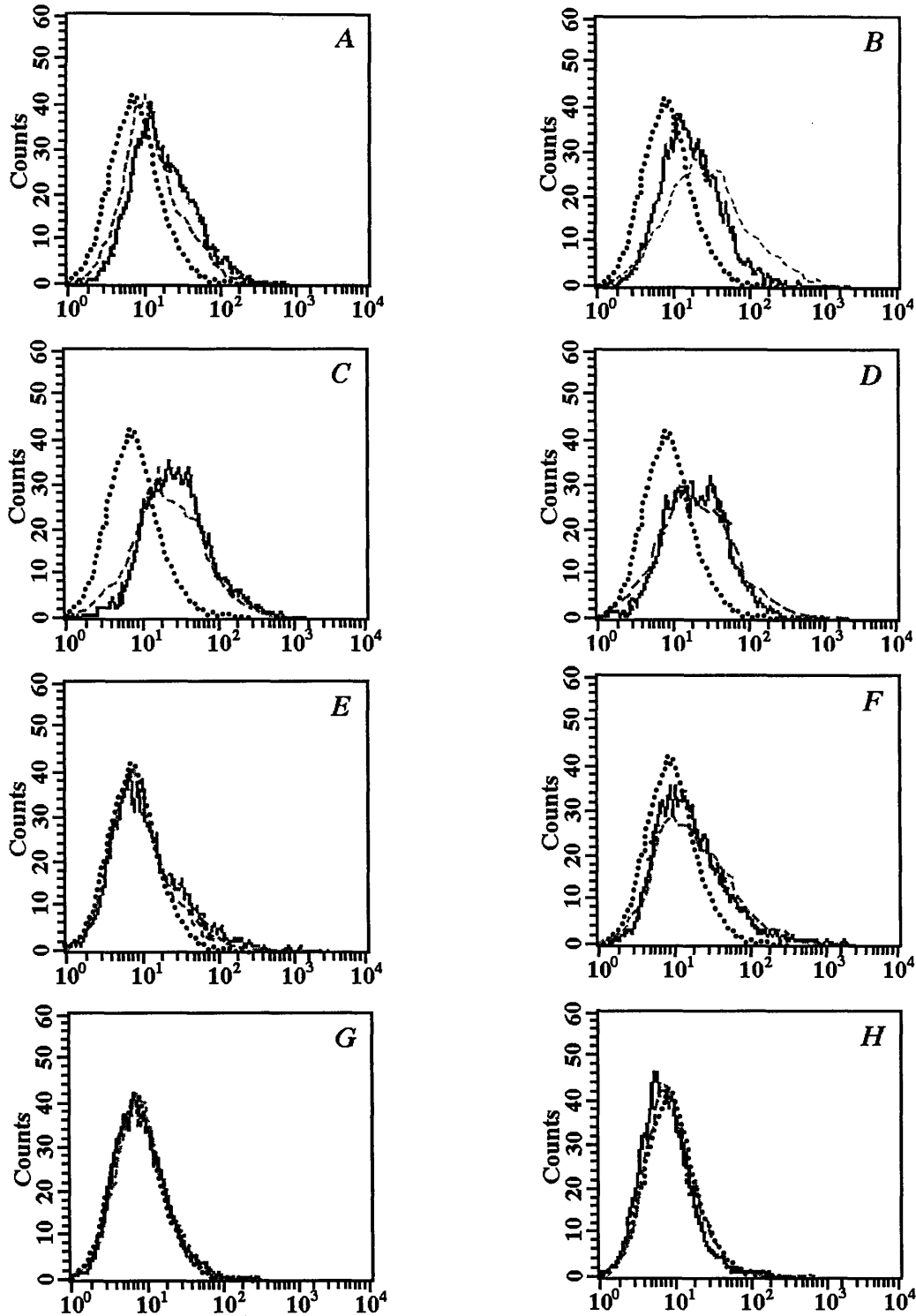
Figure 5-2-5. Kinetics of CAM expression on HUVEC monolayers treated with bFGF for 6 and 24 hrs using flow cytometry: a) ICAM-1 (6 hr), b) ICAM-1 (24 hr), c) VCAM-1 (6 hr), d) VCAM-1 (24 hr), e) E-selectin (6 hr), f) E-selectin (24 hr), g) P-selectin (6 hr), and h) P-selectin (24 hr). —— = bFGF treatment (10 ng/ml), - - = no treatment (baseline), ··· = IgG isotype control.

The unique biphasic regulation of ICAM-1 expression by bFGF has been simultaneously verified by others [Griffioen, et al., 1996], but the kinetics of the response profile have been shown to lag that found in this investigation. One explanation for this discrepancy is that under serum-free conditions, as was used in the studies presented here, endothelial cells showed an accelerated response to bFGF compared to endothelial cells in the continued presence of serum. Since serum contains significant levels of various growth factors, including bFGF, exogenous stimulation by additional growth factor may result in a longer response time by the endothelial cells.

While the modulation of ICAM-1 by bFGF alone may be used to explain the minor variability observed in ICAM-1 expression within various tumors, bFGF appears not to play a significant role in the expression characteristics found using the LS174T tumor interstitial fluid, as suggested by the ELISA results (see Section 5.2.1).

5.2.5 TGFβ

Transforming growth factor-β (TGFβ), a multifunctional agent eliciting a broad range of pleiotropic responses, was examined as a final possible mediator of CAM expression in angiogenic tissue. TGFβ has been previously shown to inhibit the adhesion of T lymphocytes and neutrophils to untreated and TNFα-treated human endothelium, respectively, through an E-selectin-mediated mechanism [Gamble and Vadas, 1988; Gamble and Vadas, 1991]. However, the kinetics of the CAM regulation in this system have not been explored in detail.

To this end, the temporal kinetics of CAM expression on HUVEC monolayers treated with TGFβ (10 ng/ml) were studied and the results are shown in Figure 5-2-6. Compared to baseline levels of non-treated controls, monolayers treated for 6 hrs with TGFβ demonstrated no significant differences in the expression of ICAM-1, VCAM-1, E-selectin and P-selectin. Similarly, no significant differences were observed at 24 hrs.

While the absence of a change in ICAM-1, VCAM-1 and P-selectin expression was in agreement with previous findings, the ability of TGFβ to reduce E-selectin expression was not evident in this investigation. The baseline level of E-selectin expression was also sufficiently low that an accurate comparative analysis could not be performed and may explain this discrepancy. Differences in culture conditions, including the addition of serum to the culture medium, did not produce any significant changes to baseline levels and the results remained indifferent.

These findings suggest that TGFβ is not one of the major mediators which may be acting to regulate the CAM expression on endothelial cells by TIF, even in lieu of its reported E-selectin modulation.
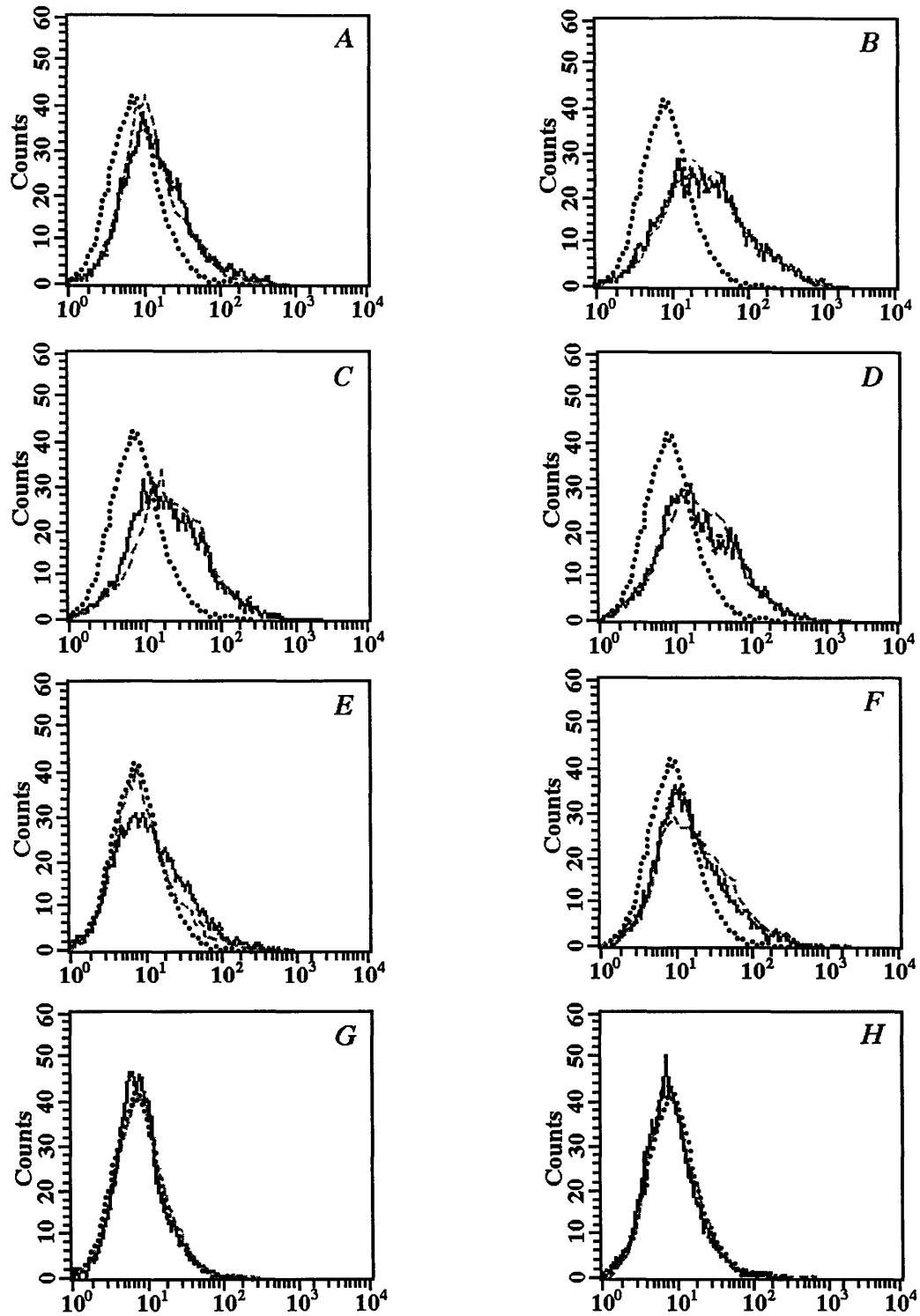
103

Figure 5-2-6. Kinetics of CAM expression on HUVEC monolayers treated with TGFβ for 6 and 24 hrs using flow cytometry: a) ICAM-1 (6 hr), b) ICAM-1 (24 hr), c) VCAM-1 (6 hr), d) VCAM-1 (24 hr), e) E-selectin (6 hr), f) E-selectin (24 hr), g) P-selectin (6 hr), and h) P-selectin (24 hr). — = TGFβ treatment (10 ng/ml), - - = no treatment (baseline), ··· = IgG isotype control.

5.2.6 Combination of Angiogenic Factors

While the characterization of the kinetics of cell surface adhesion molecule expression by the individual cytokines and growth factors is essential for their fundamental understanding, several growth factors and cytokines may be acting simultaneously to influence the microenvironment in tumor or inflammation [Cotran and Pober, 1990]. The individual angiogenic factors may synergize, augment or inhibit the responsiveness of endothelial cells to other factors, and thus influence the expression of CAMs on the cell surface [Jain, et al., 1996]. To further study the responsiveness of endothelial cells to positive modulators of CAM expression, namely TNFα and VEGF, the angiogenic factor basic FGF was simultaneously applied to the monolayers. The levels of ICAM-1, VCAM-1, E-selectin, and ICAM-2 (a constitutively expressed adhesion molecule [Stauton, et al., 1989]) were measured. The analysis also provided a means for overcoming the limitation of observing the effect of bFGF on CAMs expressed at low baseline levels.

The expression kinetics of HUVEC monolayers activated with TNFα (50 ng/ml), bFGF (10 ng/ml), and the combination of TNFα + bFGF are shown in Figures 5-2-7 and 5-2-8. Following 6 hrs of incubation, there was no significant difference in the levels of ICAM-1 or VCAM-1 induced by TNFα in the presence of bFGF. The slight increase in ICAM-1 expression produced by bFGF alone compared to controls, did not augment the level produced by TNFα. The exceptionally potent effects of TNFα on ICAM-1 expression may provide an overwhelming stimulus to the endothelial cells and limit their sensitivity to a far less potent stimulus.

However, slight differences were observed in the levels of E-selectin expressed by the endothelial cells when exposed to TNFα alone and TNFα + bFGF. The significant inhibition of TNFα-induced E-selectin by bFGF was not observed when HUVECs were treated with bFGF alone. However, as observed for TGFβ, this may have been the result of low baseline levels of E-selectin expression.

No differences were found in the alteration of the constitutively expressed ICAM-2 molecule by TNFα, bFGF, or the combination of the two angiogenic factors. Therefore, a selective modulation of the CAMs is imposed by bFGF at 6 hrs post-treatment on activated endothelium.

Following 24 hrs of co-incubation, significant differences were observed in several of the CAMs studied (Figure 5-2-8). The levels of TNFα-induced ICAM-1, VCAM-1 and E-selectin expression were significantly reduced on monolayers treated with bFGF. No differences in the level of ICAM-2 expression for the co-incubated monolayers compared to controls were observed at 24 hrs post-treatment.
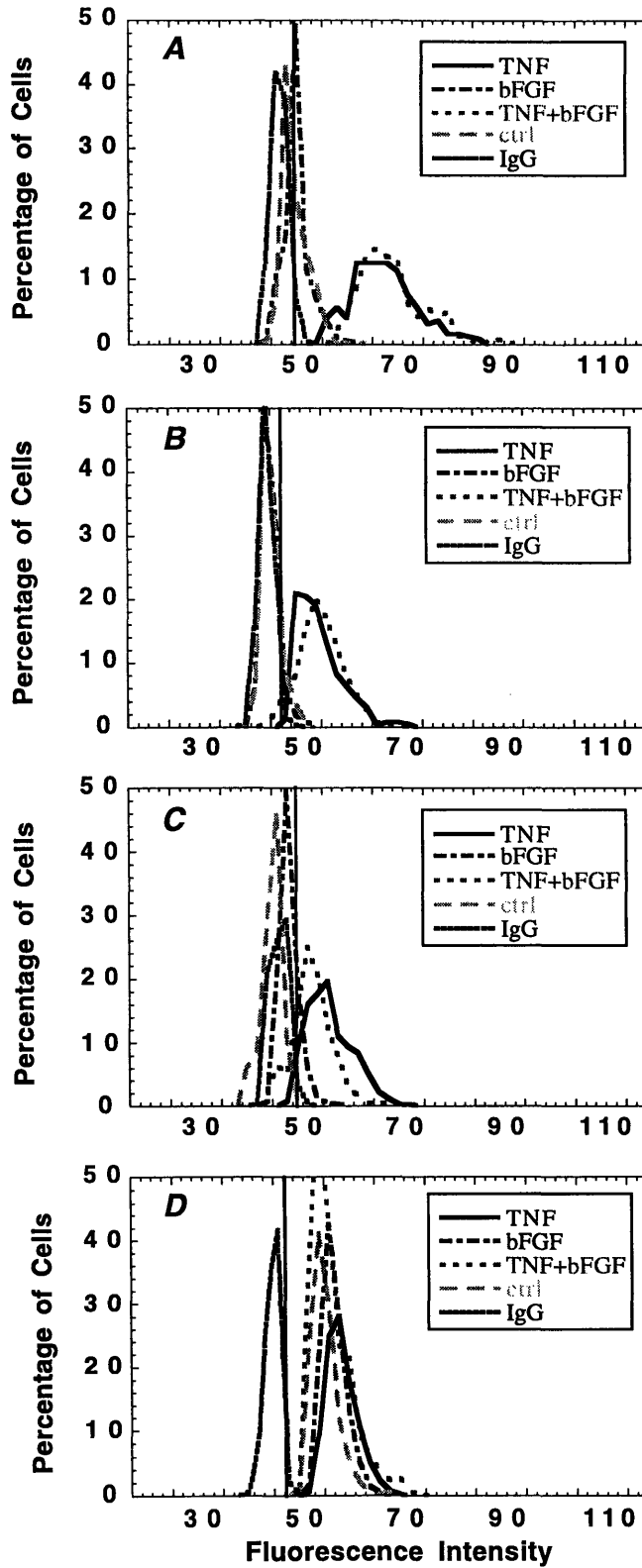
Figure 5-2-7. Kinetics of CAM expression on HUVEC monolayers treated with a combination of TNFα (50 ng/ml) and bFGF (10 ng/ml) for 6 hrs using TSF: a) ICAM-1, b) VCAM-1, c) E-selectin, and d) ICAM-2.
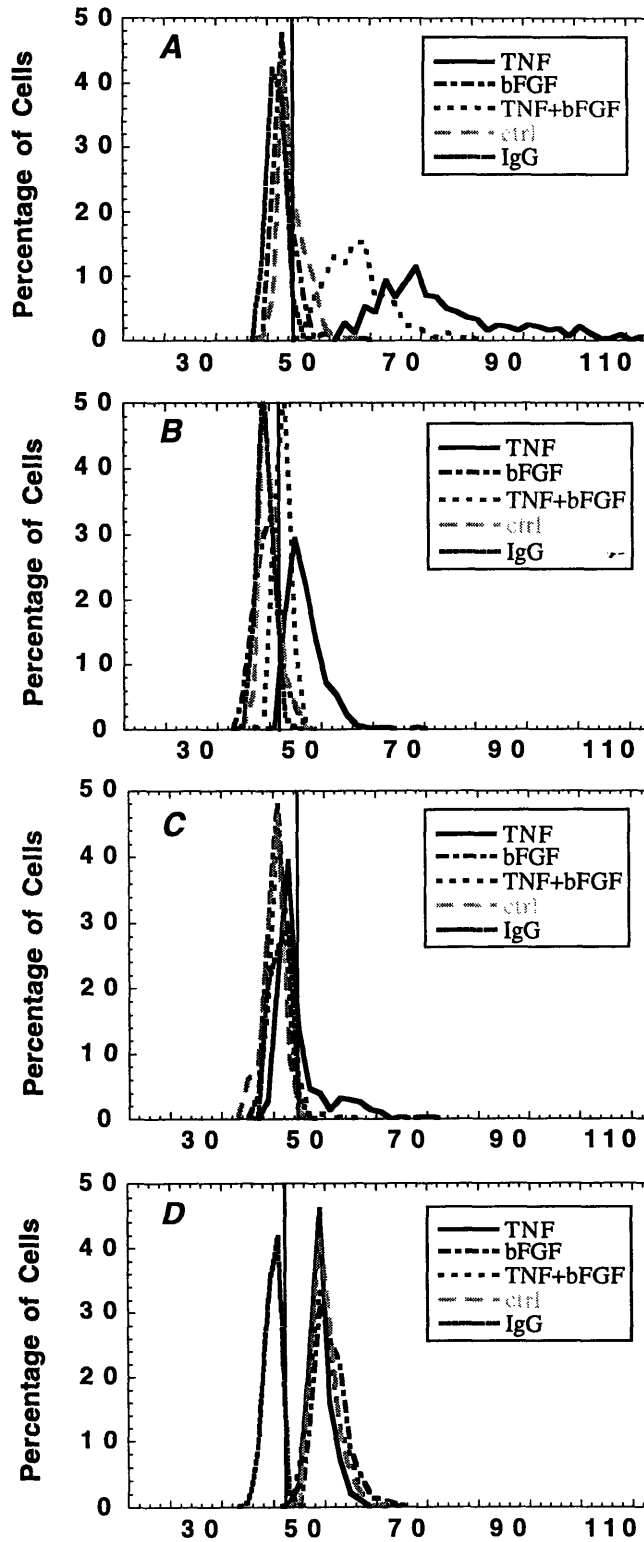
Figure 5-2-8. Kinetics of CAM expression on HUVEC monolayers treated with a combination of TNFα (50 ng/ml) and bFGF (10 ng/ml) for 24 hrs using TSF: a) ICAM-1, b) VCAM-1, c) E-selectin, and d) ICAM-2.

107

As was found for the individual treatments, bFGF acts to inhibit or decrease the sensitivity of endothelial cells to the expression of ICAM-1 by 24 hrs. Also, the slight suppressive effect which bFGF elicited on E-selectin at 6 hrs, continued through the 24 hr period. The additional finding that VCAM-1 expression is inhibited by bFGF at 24 hrs, and not at 6 hrs post-treatment, suggests a possible difference in the response kinetics of selectives CAMs to bFGF.

Combined studies with VEGF and bFGF were also performed and demonstrated similar results to those found for TNFα and bFGF. Considering the similar temporal kinetics of CAM expression by VEGF and TNFα, and the potential use of similar downstream secondary messengers in regulating CAM expression, these results seemed reasonable. However, the results were especially interesting since VEGF and bFGF are known to synergistically cause endothelial cell proliferation and act via similar receptor tyrosine kinase signaling pathways [Goto, et al., 1993; Carpenter, 1987]. Further elucidation of the signaling pathways used by the two molecules is needed to explain these results and is described in Chapter 6.

5.3 Functional Correlation

The expression studies described above demonstrated differential regulation of the CAMs on the endothelial cells by the angiogenic factors and are suggestive of the induction of functional changes in lymphocyte-endothelial cell adhesion. To provide functional relevance of the expression findings, the adhesion assay involving the parallel-plate flow chamber was utilized. Activated natural killer cells, whose specific molecular mechanisms of cell adhesion have been defined in Chapter 4, served as the lymphocyte effector population.

5.3.1 TIF

As demonstrated in Chapter 4, activation of HUVEC monolayers with TIF (diluted 1:50) for 24 hrs resulted in significant accumulation of A-NK cells under physiological flow conditions (see Figure 5-3-1). The greatest increase in binding was observed for the low shear rate ranges, the kinetics of which are suggestive of integrin-mediated binding. Antibody blocking experiments demonstrated that ICAM-1 and VCAM-1 were the major adhesion molecules involved in the adhesion process, which strongly correlated with significant increases in ICAM-1 and VCAM-1 expression induced by TIF on the endothelial cells.

5.3.2 Individual Angiogenic Factors

To determine the functional relevance of the expression results for the individual angiogenic factors TNFα, VEGF, bFGF and TGFβ, adhesion studies were performed. Dose response curves were initially determined for each of the factors and are shown in Figures 5-3-2 (TNFα, TGFβ) and 5-3-3 (VEGF, bFGF). Non-activated monolayers served as the baseline control, and A-NK adhesion was measured under flow conditions producing a wall shear stress of 1 dyn/cm². Total incubation time for all of the cytokines and growth factors was kept constant at 24 hr.
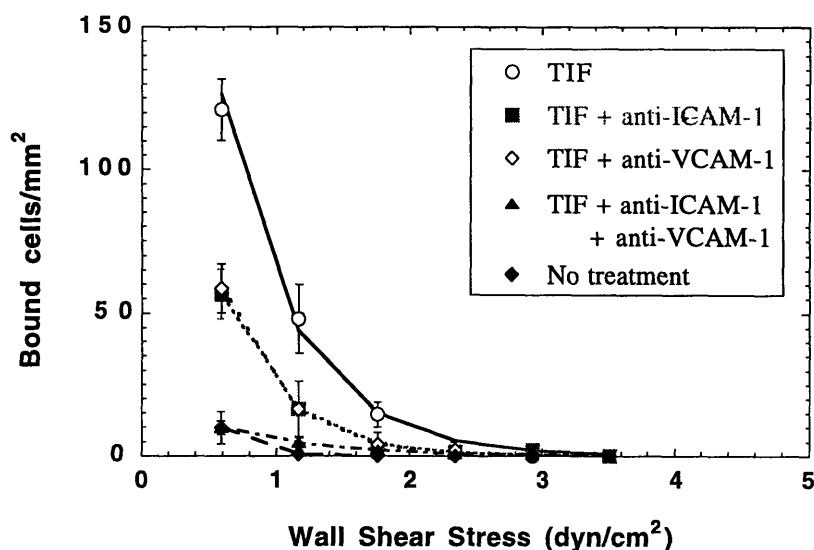
Figure 5-3-1. Cumulative binding curves of A-NK cells on TIF-activated (24 hr) and non-activated endothelial cell monolayers. Monoclonal antibody blocking of ICAM-1 and VCAM-1 are additionally shown. Mean numbers ± SD of bound cells for five adjacent fields are shown.

The dose response of TNFα-activated monolayers showed significantly elevated levels of A-NK binding for concentrations as low as 1 ng/ml, with optimal levels between 20 and 40 ng/ml. The concentration of 50 ng/ml used in the expression assay correlated well with the functional response at this dosage. The elevated levels of ICAM-1 and VCAM-1 induced by TNFα following 24 hr of incubation could readily explain these functional results, and additional antibody blocking experiments confirmed this hypothesis.

Titrations of the growth factor TGFβ, ranging from 100 pg/ml to 50 ng/ml, showed no statistically significant differences from baseline controls (Figure 5-3-2). This finding correlated well with the expression results showing no changes in the baseline expression of ICAM-1, VCAM-1 and E-selectin following 24 hrs of TGFβ treatment.
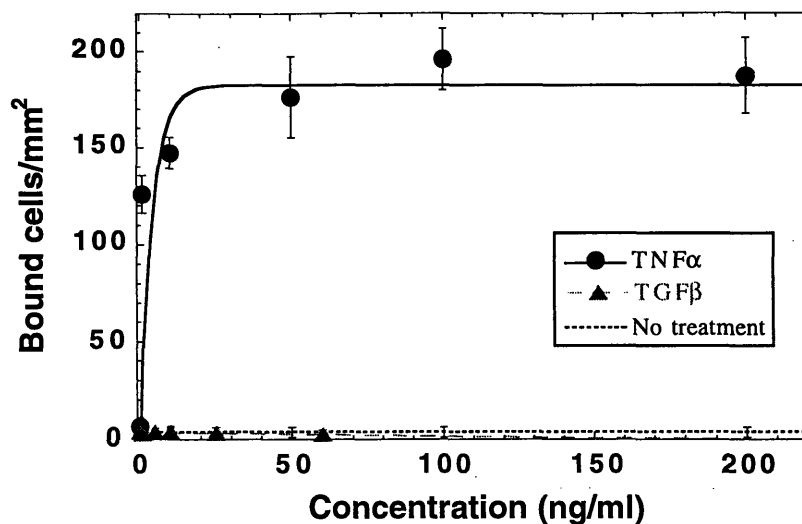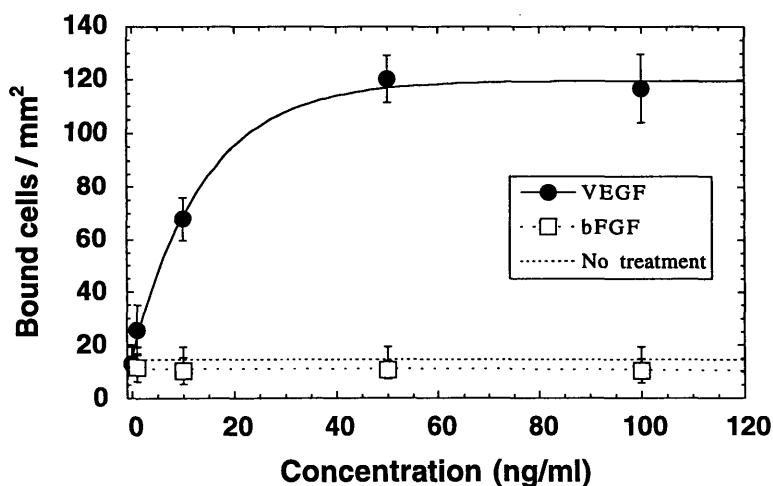
Figure 5-3-2. TNFα and TGFβ dose response curves of activated NK cell binding to HUVEC monolayers treated with the cytokines for 24 hr. A flow rate corresponding to 1 dyn/cm^2 wall shear stress was imposed. Mean numbers ± SD of bound cells for eight adjacent fields are shown for 1 of 3 representative flow experiments.

HUVEC monolayers treated with a broad range of dosages of VEGF for 24 hrs demonstrated significant levels of A-NK binding (Figure 5-3-3). The optimal concentration was found to be approximately 35 ng/ml, similar to that used for the expression analysis. The VEGF-induced upregulation of ICAM-1 and VCAM-1 correlated well with the lymphocyte binding levels found using the adhesion assay.

Figure 5-3-3. VEGF and bFGF dose response curves of activated NK cell binding to HUVEC monolayers treated with the angiogenic factors for 24 hr. A flow rate corresponding to 1 dyn/cm^2 wall shear stress was imposed. Mean numbers ± SD of bound cells for eight adjacent fields are shown for 1 of 3 representative flow experiments.

110

The dose response curve showing the effect of bFGF was found to produce slight, but statistically significant decreases in the level of A-NK binding to the activated endothelium (Figure 5-3-3). Concentrations as low as 1 ng/ml were able to elicit a reduction in the binding, and correlated with the slightly decreased level of ICAM-1 induced by bFGF.

Using the information obtained from the dose response analysis, the time course of activation was then studied for each of the individual angiogenic factors and correlated with the results on the CAM expression kinetics.

The time course of activation of TNFα on A-NK cell binding was initially performed and the results are shown in Figure 5-3-4. TNFα was found to rapidly activate the monolayer over a 4 to 6 hr period resulting in significant A-NK cell binding. The continued presence of TNFα maintained the level of cell adhesion for up to 24 hrs. These results are in agreement with the findings of increased ICAM-1, VCAM-1, and E-selectin on the TNFα-activated monolayer occurring within the initial 6 hrs and sustained over the 24 hr period.

The temporal kinetics of bFGF activation on A-NK cell binding was studied next and the results are also shown in Figure 5-3-4. Correlating with the slightly increased levels of ICAM-1 expression demonstrated in the expression assay, A-NK cells showed small, but significant levels of increased adhesion to monolayers activated with bFGF for 6 hrs. This level of binding was found to be approximately 10% of that found for monolayers activated with TNFα-activated monolayers for an equivalent period of time. The prolonged exposure of endothelial cells to bFGF resulted in a rapid decrease in the level of adhesion by 16 hrs and lasting for up to 24 hrs. As demonstrated in the expression assays (see Section 5.2.4), these results corresponded to the decrease in ICAM-1 expression on the monolayers treated with bFGF for 24 hrs.

The ability of A-NK cells to adhere to endothelial cells as a function of VEGF exposure time is shown in Figure 5-3-5. Following 6 hrs of VEGF treatment, lymphocyte adhesion to the monolayer was significantly above baseline levels, and comparable to the kinetics of TNFα activation. These results agree with the expression studies showing increased ICAM-1, VCAM-1, and modestly E-selectin expression on the monolayers after 6 hrs of exposure. Cell binding levels remained elevated up to 24 hrs of VEGF stimulation, correlating with the continued elevated expression of the CAMs. The overall binding level of A-NK cells on VEGF-activated monolayers was found to be less than that on TNFα-activated monolayers, and correlated with lower levels of CAM expression (see Section 5.2).

111

The temporal kinetics of TGFβ on lymphocyte adhesion was performed and the results are shown in Figure 5-3-5. Monolayers exposed to 10 ng/ml of TGFβ for up to 24 hrs showed no significant differences from baseline levels of A-NK adhesion. This directly correlated with a lack of detectable CAM modulation by TGFβ treatment shown in the expression experiments (see Section 5.2.5).
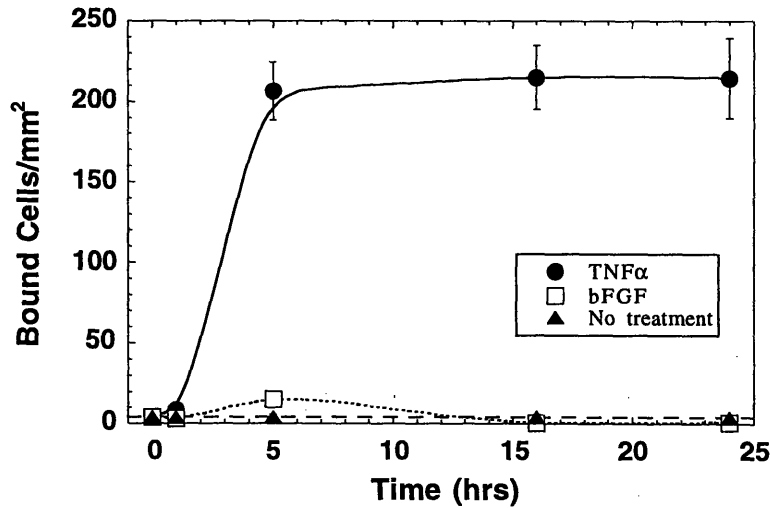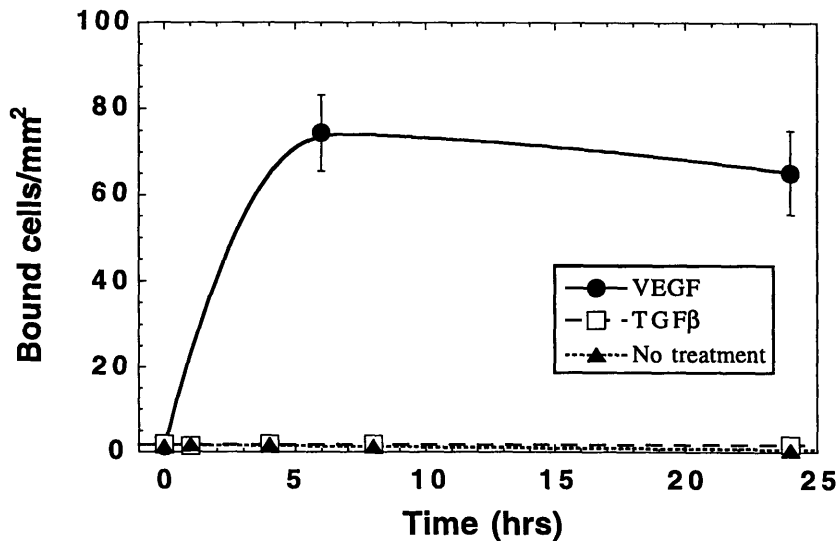

Figure 5-3-4. Temporal kinetics of 50 ng/ml TNFα and 10 ng/ml bFGF on A-NK cell binding to activated HUVEC monolayers. A flow rate corresponding to 1 dyn/cm^2 wall shear stress was imposed. Mean numbers ± SD of bound cells for eight adjacent fields are shown.

Figure 5-3-5. Temporal kinetics of 35 ng/ml VEGF and 10 ng/ml TGFβ on A-NK cell binding to activated HUVEC monolayers. A flow rate corresponding to 1 dyn/cm^2 wall shear stress was imposed. Mean numbers ± SD of bound cells for eight adjacent fields are shown.

112

5.3.3 Combined Angiogenic Factors

To further determine the biological significance of bFGF and TGFβ inhibition on cytokine and growth factor enhanced leukocyte-endothelial interaction, functional adhesion studies were designed to simulate these conditions. Dose requirements and kinetics of the response were analyzed to further define the responsiveness of endothelial cells to scenarios involving multiple stimuli. The results were then correlated with the regulatory effects of the angiogenic factors on CAM expression. To limit the range of possible considerations, a specific focus was placed on the interaction between TNFα and bFGF. Combinations of the other angiogenic factors are noted for their influences in specific cases.

The dose response profiles of A-NK cell binding to endothelial cells activated for 24 hrs with broadly varying concentrations of TNFα and bFGF combinations were determined under flow conditions (1 dyn/cm^2) and the results are shown in Figure 5-3-6. Basic FGF was shown to produce a dose-dependent inhibitory effect on TNFα-mediated A-NK cell adhesion. The inhibitory response consistently showed similar profiles for the full range of concentrations analyzed, which were between 0 and 50 ng/ml of bFGF and between 0 and 200 ng/ml of TNFα. A concentration of 10 ng/ml of bFGF was found to produce optimal levels of inhibition (46.0 ± 10.6%, $p < 0.05$) for TNFα concentrations ≥ 50 ng/ml.
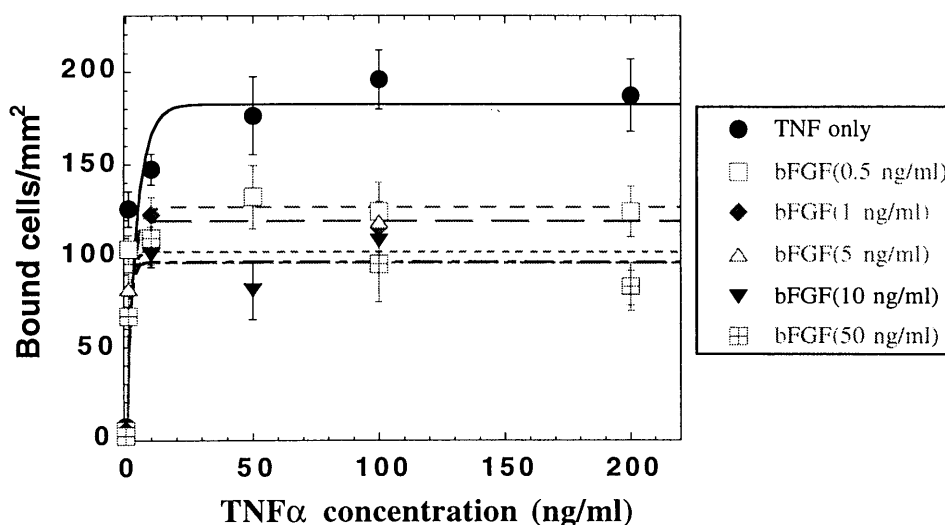
Figure 5-3-6. Dose response curve of activated NK cell binding to HUVEC monolayers treated simultaneously with TNFα and bFGF for 24 hr. A flow rate corresponding to 1 dyn/cm^2 wall shear stress was imposed. Mean numbers ± SD of bound cells for eight adjacent fields are shown.

Similar inhibitory dose responses were obtained on HUVECs treated with VEGF (35 ng/ml) and bFGF (Figure 5-3-7). At a concentration of 10 ng/ml of bFGF, optimal levels of inhibition (52.5 ± 12.6%, $p < 0.05$) were obtained, indicating that the sensitivity of endothelial cells to the inhibitory effect of bFGF is constant despite different positive modulators of CAM expression.
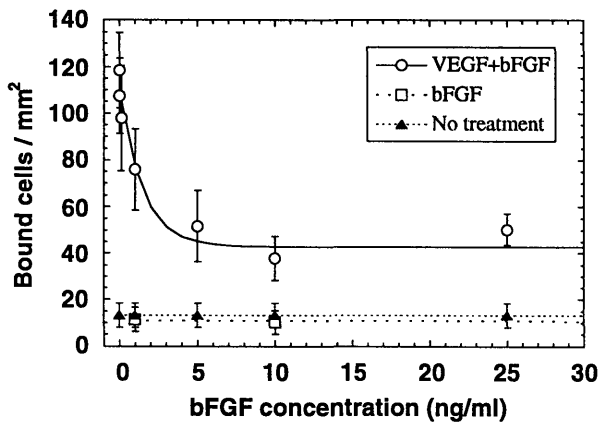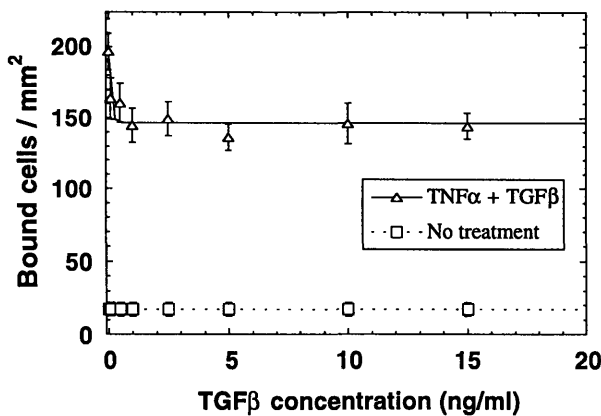

Figure 5-3-7. Dose response curve of activated NK cell binding to HUVEC monolayers treated simultaneously with VEGF (35 ng/ml) and bFGF for 24 hr. A flow rate corresponding to 1 dyn/cm^2 wall shear stress was imposed. Mean numbers ± SD of bound cells for eight adjacent fields are shown.

The influence of TGFβ on endothelial cell monolayers treated with TNFα was also documented and found to inhibit the binding level of A-NK cells under flow conditions (Figure 5-3-8). A concentration of 1 ng/ml of TGFβ caused a 15.7 ± 4.2% inhibition of A-NK binding to HUVECs treated with 50 ng/ml TNFα. This level of inhibition is close to the level obtained by antibody blocking of E-selectin on TNFα-activated monolayers, and provides support to its effect being limited to the regulation of E-selectin expression [Gamble and Khew-Goodall, 1993].

Figure 5-3-8. Dose response curve of activated NK cell binding to HUVEC monolayers treated simultaneously with TNFα (50 ng/ml) and TGFβ for 24 hr. A flow rate corresponding to 1 dyn/cm^2 wall shear stress was imposed. Mean numbers ± SD of bound cells for eight adjacent fields are shown.

Using the information obtained from the dose response analysis, the time course of inhibition was then specifically studied for bFGF on TNFα-activated endothelial cell monolayers and correlated with the results on the CAM expression kinetics.

Upon simultaneous application of bFGF and TNFα, a decrease in the level of A-NK binding became evident after 6 hrs of treatment, with significant levels occurring after 12 hrs ($p < 0.05$) (Figure 5-3-9). The total inhibition obtained was accomplished after 24 to 48 hrs of initial exposure. The time course of A-NK cell binding inhibition directly correlated with the expression assay results, which showed that ICAM-1 and VCAM-1 levels were not reduced until 6 hrs following bFGF exposure.
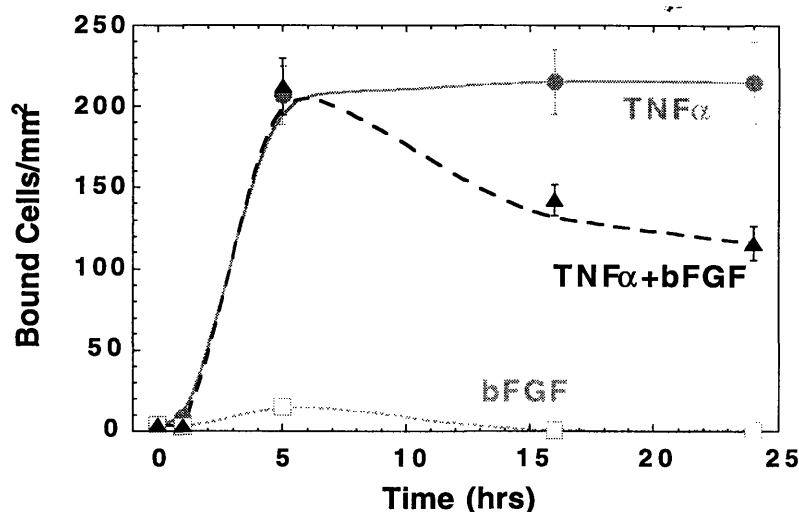
Figure 5-3-9. Inhibition kinetics of A-NK cell binding to HUVEC monolayers treated simultaneously with 50 ng/ml TNFα and 10 ng/ml bFGF. A flow rate corresponding to 1 dyn/cm² wall shear stress was imposed. Mean numbers ± SD of bound cells for eight adjacent fields are shown.

To provide additional evidence for a direct correlation between CAM expression and lymphocyte binding inhibition by bFGF on TNFα-treated monolayers, antibody blocking experiments were performed. As shown in Figure 5-3-10, addition of anti-ICAM-1 mAb or anti-VCAM-1 mAb to TNFα and TNFα + bFGF treated monolayers showed significant differences between the two treatment groups ($p < 0.05$). This directly indicated that both molecules were essential in the reduced level of binding of A-NK cells to bFGF-treated monolayers. Also, a combination of both blocking antibodies effectively

eliminated differences in the TNFα and TNFα + bFGF treated monolayers, demonstrating that ICAM-1 and VCAM-1 were the principal molecules involved in the functional adhesion process for both treatment groups.

To test whether previous exposure of the endothelial cells to either of the factors influenced the kinetics of the response, experiments were conducted where either TNFα was applied prior to bFGF exposure or bFGF was applied at various times prior to TNFα activation for 5 hrs. The results of these two sets of experiments are shown in Figure 5-3-11. Regardless of prior sensitization of the endothelial cells to cytokine or growth factor exposure, the kinetics of bFGF inhibition on TNFα-induced CAM expression required greater than 6 hrs of exposure of the endothelial cells to bFGF. This indicates that signaling induced by bFGF on endothelial cells defines the time course of CAM expression, and that exposure to other angiogenic factors or inflammatory cytokines does not dramatically influence it.
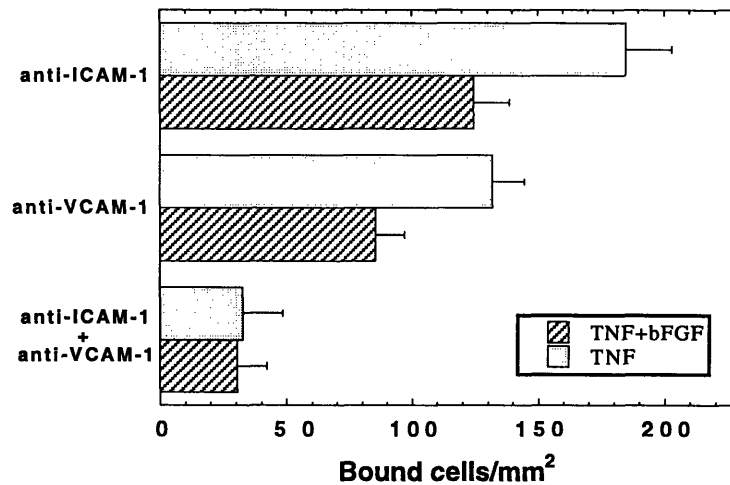
Figure 5-3-10. Antibody blocking experiments demonstrating a direct correlation between ICAM-1 and VCAM-1 expression and A-NK cell binding to HUVEC monolayers treated simultaneously with 50 ng/ml TNFα and 10 ng/ml bFGF. A flow rate corresponding to 1 dyn/cm^2 wall shear stress was imposed. Mean numbers ± SD of bound cells for eight adjacent fields are shown. * p < 0.05. Treatment and antibody controls showed no significant effect on A-NK cell binding.

116
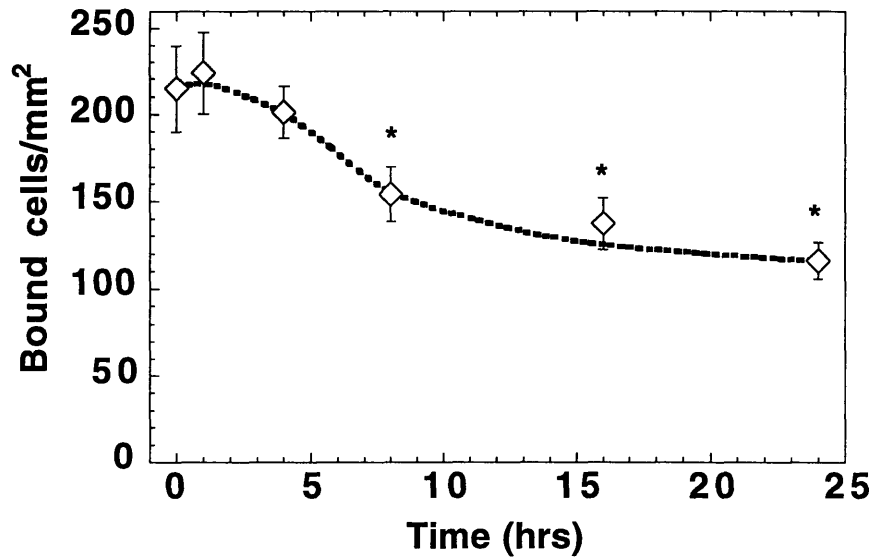
(a)
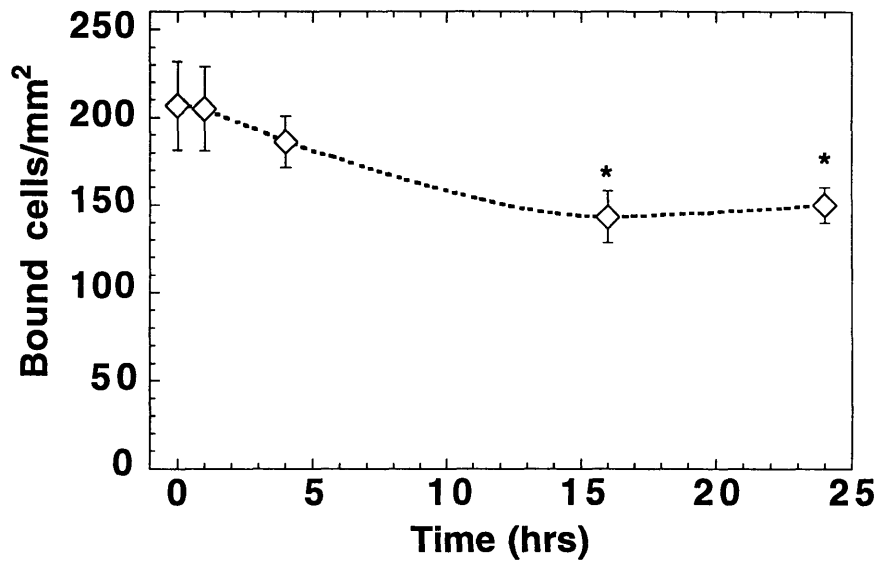
(b)

Figure 5-3-11. Inhibition kinetics of A-NK cell binding to activated HUVEC monolayers pretreated with either a) 50 ng/ml TNFα (24 hr total exposure time) and then 10 ng/ml bFGF for the time indicated, or b) 10 ng/ml bFGF for the time indicated and then 50 ng/ml TNFα for 5 hrs. A flow rate corresponding to 1 dyn/cm^2 wall shear stress was imposed. Mean numbers ± SD of bound cells for eight adjacent fields are shown. * $p <$ 0.05.

5.4 Conclusions

The key findings obtained from the *in vitro* investigations presented in this chapter can be generally summarized as follows: a) the interstitial fluid (TIF) from xenotransplanted adenocarcinomas provides a model of the tumor microenvironment which increases the expression of specific CAMs in endothelial cells; b) the TIF used in these studies contains significant levels of the angiogenic factor VEGF, but low or absent levels of bFGF and TNFα, and level of VEGF in the TIF does not directly correlate with its ability to modulate CAM expression; c) the angiogenic factors TNFα and VEGF are able to upregulate the expression of specific CAMs in endothelial cells in a dose-dependent manner, while bFGF has a biphasic effect on ICAM-1 expression only, and TGFβ has no observable effect on CAM expression; d) combined treatment of bFGF and TNFα or VEGF show significantly reduced levels of CAM expression in a time-dependent process which is independent of prior sensitization; and e) the biological modulation of CAM expression by the TIF and angiogenic factors has functional relevance as determined by lymphocyte binding characteristics under physiological flow conditions.

The ability of the TIF to simulate the microenvironment experienced by endothelial cells in a tumor and for selected samples to significantly increase ICAM-1, VCAM-1, and E-selectin expression provided invaluable information to the mechanisms used by leukocytes to adhere to the tumor vasculature. The presence of various angiogenic factors within the tumor for the development of an increased vascular blood supply, may be the primary response elements responsible for the alteration in CAM expression by the TIF. The finding that VEGF was expressed in significant levels in the tumor fluid and that it induced the upregulation of ICAM-1, VCAM-1 and E-selectin, with kinetics similar to that of TNFα, was suggestive of it being an essential mediator. However, while significant variability existed in the ability of TIF samples to influence lymphocyte adhesion, VEGF levels remained consistently elevated. Co-activators or inhibitory factors present in the TIF may explain the discrepancy.

Along those lines, basic FGF, another angiogenic factor produced by various neoplastic cells [Moscatelli, et al., 1986], was found to significantly decrease the expression of ICAM-1, VCAM-1, and E-selectin in a time-dependent manner, and to also functionally reduce the level of lymphocyte adhesion to TNFα and VEGF stimulated endothelium. The decrease in the counter-receptor expression by bFGF has been shown in Chapter 4 to differentially affect the ability of lymphocyte subpopulations to bind to activated endothelial cells. Infiltrating lymphocytes and macrophages in the tumor vasculature, in addition to the angiogenic factors produced by the cancer cells and

surrounding normal tissue, may further influence the tissue microenvironment and the products of the immune response to a tumor or inflammatory site. While bFGF was found not to be present in sufficient levels in the TIF sampled, the aforementioned underscores the influence the growth factor may have in the protective mechanisms found in other tumors and angiogenic tissue towards reducing exposure to leukocytes by downregulation of CAM expression and decreasing the response to inflammatory cytokines.

TGFβ may also be influential in mediating the immunological response to tumors. While its concentration within the TIF was not examined, it was demonstrated that it can produce a modest decrease in the ability of lymphocytes to adhere to cytokine-stimulated endothelial cells. However, its mediating effects has been shown by others to be limited to E-selectin expression and cannot explain the global variance experienced by the TIF samples.

Several *in vivo* studies were also conducted in collaboration with this work to provide validation of the *in vitro* findings [Melder, et al., 1996; Detmar, et al., 1998]. One set of *in vivo* studies used LS174T tumors grown in the cranial window of SCID mice. Human A-NK cells were adoptively transferred and shown to preferentially adhere to the tumor vasculature, providing validation to the TIF findings. In addition, bFGF was exogenously perfused onto the tumors and a significant reduction in the number of bound cells to the tumor vasculature was observed, providing supporting evidence that bFGF can inhibit lymphocyte adhesion *in vivo*.

In another set of *in vivo* experiments, transgenic mice were generated which selectively overexpressed VEGF in the epidermis. Dramatic increases were found in leukocyte rolling and adhesion to the postcapillary skin venules, which were significantly inhibited by antibody combinations of anti-E-/P-selectin and anti-ICAM-1/VCAM-1, respectively. These studies provided supporting evidence that VEGF can promote leukocyte rolling and adhesion *in vivo*, in accordance with the *in vitro* findings provided in this thesis.

Implications for the results presented in this chapter include the following: a) providing insight into the regulatory and protective mechanisms potentially found in tumors, as well as in inflammation and wound healing, by the action of the various angiogenic factors present; b) contributing to the better understanding of metastasis and the role of angiogenic factors in the process; c) providing additional information towards formulating a comprehensive paradigm of the microenvironmental effects on tumor growth and evasiveness; and d) offering potential possibilities towards improving current anti-tumor immunotherapies and treatments for inflammatory diseases.

Chapter 6

Molecular Mechanisms of bFGF in CAM Modulation

6.1 Introduction

The adhesion of circulating lymphocytes to the endothelium is mediated by the expression of adhesion molecules on the lymphocyte surface and their interaction with counter-receptors expressed on the endothelial cell surface [Butcher, 1991]. The cell adhesion molecules on the endothelium include ICAM-1, VCAM-1, and E-selectin, with each performing distinct functions [Oppenheimer-Marks, et al., 1991]. As was demonstrated in Chapter 5 of this thesis, TNFα induces the protein expression of all three of these adhesion molecules in endothelial cells, while bFGF inhibits their expression and biological function. In general, the surface expression of these CAMs is known to correlate with the transcriptional activation of their genes and corresponding increases in their mRNA levels when activated by TNFα. However, the particular molecular mechanisms used by bFGF in altering TNFα-induced CAM expression has not been studied.

Previous studies examining the signaling pathways used by bFGF in modifying other cellular responses, such as cell proliferation and angiogenesis in endothelial cells, have shown it to involve a specific interaction with its high affinity, transmembrane receptor and low affinity, membrane-bound heparin sulfate polysaccharides [Jaye, et al., 1992]. The ternary complex causes autophosphorylation of its receptor tyrosine kinases, leading to the direct phosphorylation of phospholipase C-γ1 (PLC-γ1) and subsequent breakdown of phosphatidylinositol bisphosphate (PIP$_2$) to generate inositol 1,4,5-triphosphate (IP$_3$) and diacylglycerol (DAG) [Mohammadi, et al., 1992; Ullrich and

Schlessinger, 1990]. IP_3 causes the mobilization of Ca^{2+} from intracellular stores, which combines with DAG to activate protein kinase C (PKC). The secondary messengers generated in this cascade have been implicated in controlling many of the physiological responses produced by bFGF. However, the specific role of each messenger in mediating the cellular functions of bFGF are strongly cell-type dependent and function-dependent [Jaye, et al., 1992; Peters, et al., 1992].

To date, the intracellular signals by which TNFα regulates adhesion molecule gene transcription in endothelial cells have been studied to a modest extent. Investigations have shown that it interacts with two distinct receptors, TR55 and TR75, and that the complex triggers PLC-phosphatidylcholine (PC) to produce DAG, and subsequently the activation of PKC and acidic sphingomyelinase (SMase) [Schütze, et al., 1991; Schütze, et al., 1992]. These two secondary messengers then go on to induce NF-κB activity, which may be involved with the transcriptional regulation of ICAM-1, VCAM-1, and E-selectin by TNFα [Read, et al., 1994]. However, the actions of the two enzymes are cell-type dependent and differ in the kinetics and in subunit composition and function of NF-κB activation.

In this chapter, results are presented from several experiments using Northern blot analysis, fluorescence immunoassay, and the parallel-plate flow chamber to address the following essential issues regarding the molecular mechanisms used by bFGF to inhibit CAM expression and function: a) does bFGF act directly or indirectly through an extracellular or paracrine mechanism to modify CAM expression and function; b) what effect does bFGF have on CAM mRNA levels and expression kinetics; c) does bFGF alter CAM mRNA expression at the transcriptional or translational levels; d) what are the proximal signaling pathways used by bFGF in producing its inhibitory effect on CAM function; and e) what are the broader implications of the inhibitory effect of FGF?

Investigation into these specific questions and the importance of knowing the kinetics and molecular mechanisms of the action of bFGF may prove to be essential for improved disease treatment and cancer therapy.

6.2   Characterization of bFGF-Mediated Inhibition

6.2.1 Protein and Functional Level

In the studies carried out in Chapter 5, it was demonstrated that with TNFα as the stimulus, bFGF inhibits the surface protein expression of ICAM-1, VCAM-1, and E-selectin. The constitutively expressed ICAM-2 molecule was not shown to be effected by

121

the presence of bFGF nor TNFα. In addition, kinetic analysis showed that bFGF inhibited surface CAM expression and biological function only after 8-12 hrs of exposure, and reached optimal inhibitory levels after 24 hrs. Therefore, bFGF acts to selectively inhibit specific CAMs on the surface of endothelial cells after a sufficiently latent period of exposure. The question that now remains to be answered is how bFGF actually acts to reduce CAM expression?

For one possible explanation of these findings it can be suggested that bFGF acts indirectly and induces the production of a second substance, possibly another growth factor or cytokine, which is the actual mediator of the observed effects on CAM expression. This would be consistent with the latency of the bFGF-mediated effect observed in this investigation, and concordant with its known ability to induce the production of urokinase-type plasminogen activator and release of arachidonate from endothelial cells to elicit multiple physiological and pathophysiological responses [Sa and Fox, 1994; Gualandris and Presta, 1995].

To investigate a possible paracrine mechanism for the inhibitory action of bFGF, conditioned medium transferred from HUVEC monolayers treated for 6 hrs with 10 ng/ml bFGF was placed on a second monolayer and treated with TNFα for several time periods ranging from 5 to 24 hrs. As a negative control, the supernatant from sham-treated HUVEC monolayers, where bFGF was added just prior to collection, was transferred to a second monolayer and subsequently treated with TNFα. Additionally, another set of monolayers were exposed to medium collected from non-treated HUVEC monolayers for 6 hrs and subsequently treated with or without TNFα. These served as positive and baseline controls, respectively. The treated monolayers were then placed in the parallel-plate flow chamber and assessed for their ability to bind A-NK cells under flow conditions, which has already been shown to directly correlate to the expression of CAMs on the endothelial cells. The results of this experiment are shown in Figure 6-2-1.

Monolayers treated with bFGF-conditioned medium were found to produce similar temporal binding kinetics of A-NK cells as sham-treated controls, and both showed significant differences from the positive control group. The inability of the conditioned medium to elicit a kinetically faster inhibitory response compared to the sham controls is strongly suggestive that bFGF does not produce a secondary product which is inhibitory to CAM expression and the functional binding of lymphocytes. However, these results must be interpreted cautiously and are not absolutely conclusive of bFGF eliciting a direct inhibitory effect on the endothelial cells.

The cells may be responsive to only high, local concentrations of a secondary substance produced by bFGF treatment, and may be insufficiently sensitive to the global

122

concentrations present in the conditioned medium. Also, the cells may be producing an intracellular protein which effectively elicits the inhibitory response and, thus, would not be present in the conditioned medium.
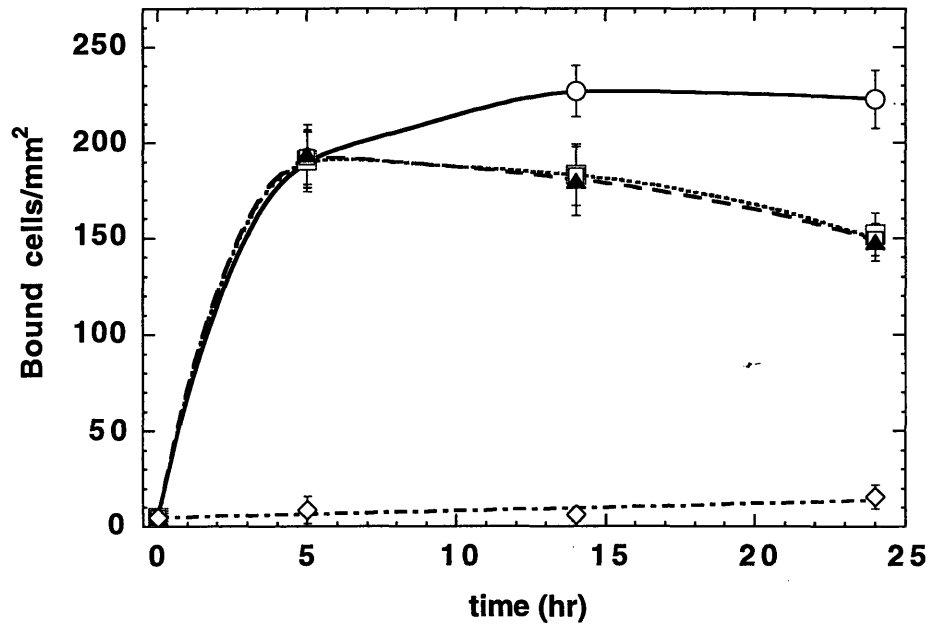

Figure 6-2-1. Kinetics of A-NK cell binding to HUVEC monolayers treated with bFGF-conditioned medium and 50 ng/ml TNFα. A flow rate corresponding to 1 dyn/cm^2 wall shear stress was imposed. — = TNFα positive control, - - - = TNFα+bFGF-conditioned medium, $\cdots$ = TNFα+bFGF sham, - $\cdot$ - = no treatment (baseline). Mean numbers ± SD of bound cells for eight adjacent fields are shown for n = 3 experiments.

As another possible mechanism for the inhibitory action mediated by bFGF, specific interaction between bFGF and one of its receptors may cause a downregulation of the expression of TNFα receptors on the cell. This would also be consistent with the latency of the bFGF-mediated effect observed, and in agreement with its known ability to attenuate the *in vitro* growth inhibitory effect of TGFβ by downregulating the 85 kDa TGFβ receptor subtype in a dose-dependent manner [Fafeur, et al., 1990]. However, preliminary experiments have found no alteration in the levels of TNFp55R and TNFp75R expressed on endothelial cells treated with bFGF for extended periods [Griffioen, et al., 1996].

Basic FGF has also been found to decrease the level of ICAM-1 expression on non-activated endothelial cells (Chapter 5), thus not requiring specific cytokine activation of the CAMs to produce its response. Additionally, bFGF inhibits lymphocyte binding to

123

monolayers activated by other inflammatory cytokines (IL-1β; Section 6.5) as well, which utilize distinct receptors. Therefore, bFGF does not appear to affect cytokine receptor levels as a mechanism for its CAM regulation.

Experiments were conducted to examine the effect bFGF has on the protein synthesis, as well as on the degradation rate, of the CAMs. Since the level of protein expressed in a cell is a function of the continuously opposing processes of protein degradation and synthesis, an effect on either process could elicit the response seen for bFGF. Also, the cell surface adhesion molecules are inducible proteins dependent on the translation of their mRNA and, consequently, the transcription of their genes. Alteration in the transcriptional or translational process effectively influences the level of protein expressed and provides a potential pathway through which bFGF acts.

To study whether bFGF effects the rate of degradation of the CAMs, HUVEC monolayers initially treated with TNFα for 6 hrs were washed with serum-free medium to remove the TNFα and then exposed to either the presence or absence of bFGF. Initial exposure of the endothelial cells to TNFα results in the transcriptional activation of the genes for ICAM-1, VCAM-1 and E-selectin, and upregulation of their protein expression. The subsequent removal of TNFα effectively prevents additional CAM gene transcription, and by 24 hrs, results in the downregulation of the CAM proteins to baseline levels [Read, et al., 1994].

Using the functional adhesion assay as an indirect gauge of the CAM expression conducive to lymphocyte binding, the kinetics of A-NK adhesion to the treated monolayers were analyzed. As shown in Figure 6-2-2, removal of TNFα from the activated monolayers resulted in a dramatic decrease in the ability of lymphocytes to bind, which reached baseline levels by 24 hrs. This finding directly correlated with the CAM downregulation pattern observed under similar treatment conditions [Read, et al., 1994]. The addition of bFGF to the monolayers demonstrated no significant difference in the rate of decrease of lymphocyte binding compared to the appropriate controls ($p > 0.1$), suggestive that bFGF does not act to increase the rate of degradation of CAM proteins on the cell surface.

6.2.2 mRNA Level

To confirm that the specific effect of bFGF was to inhibit protein synthesis and to determine whether the effect on synthesis occurred before translation, Northern blot analysis was performed to directly measure the mRNA levels and kinetics of expression of

ICAM-1, VCAM-1, E-selectin and ICAM-2 in endothelial cells treated with TNFα, bFGF, and the simultaneous combination of TNFα and bFGF.
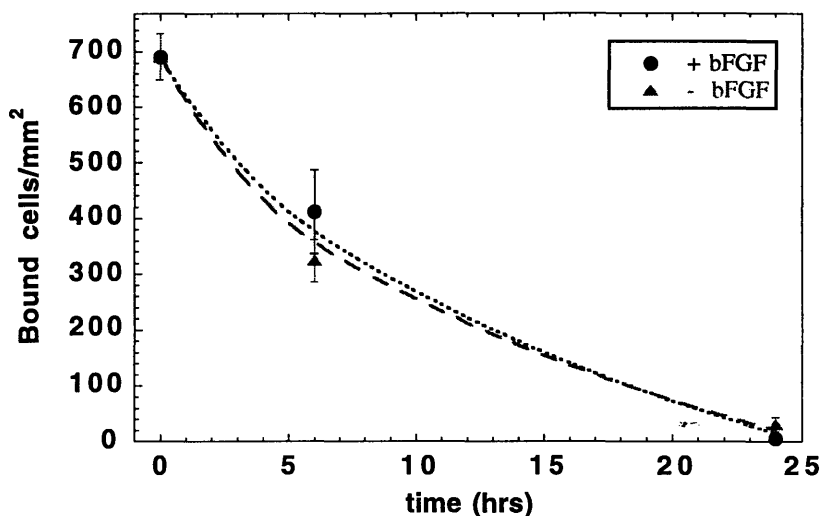
Figure 6-2-2. Kinetics of A-NK cell binding to HUVEC monolayers initially treated with 50 ng/ml TNFα for 6 hrs (t = 0) and then subsequently washed and treated with ± 10 ng/ml bFGF. A flow rate corresponding to 1 dyn/cm^2 wall shear stress was imposed. ··· = presence of bFGF, - - - = absence of bFGF. Mean numbers ± SD of bound cells for eight adjacent fields are shown for 1 of 3 representative experiments.

As shown in Figure 6-2-3 and 6-2-4a, treatment of HUVEC monolayers with TNFα resulted in an initial rapid induction of ICAM-1 mRNA expression that peaked around 4 hrs of treatment, followed by a steady and gradual decrease over 24 hrs. Treatment with bFGF produced a rapid, but transient increase in ICAM-1 mRNA in the first 4 hrs that reduced to baseline levels by 8 hrs. The HUVEC response to combined treatment generally showed similar kinetics as that of TNFα treated monolayers, but with lower levels of ICAM-1 expression consistently occurring after 8 hrs of treatment. In two sets of experiments, significant differences were noted only after 8 hrs of bFGF exposure, while a third showed differences occurring as early as 4 hrs (shown in Figure 6-2-4a). The results obtained for the individual treatment groups were consistent with the responses observed at the protein and functional levels for the CAMs. The combined treatment of the cells with TNFα and bFGF generally demonstrated a reduction in the level of ICAM-1 mRNA expression which was sufficiently delayed to explain the kinetics of the decreased protein levels observed.
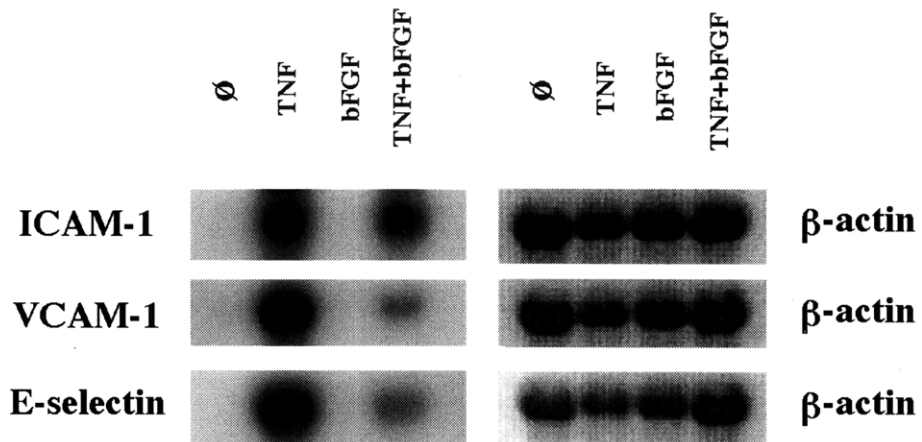
(a) 24 hrs
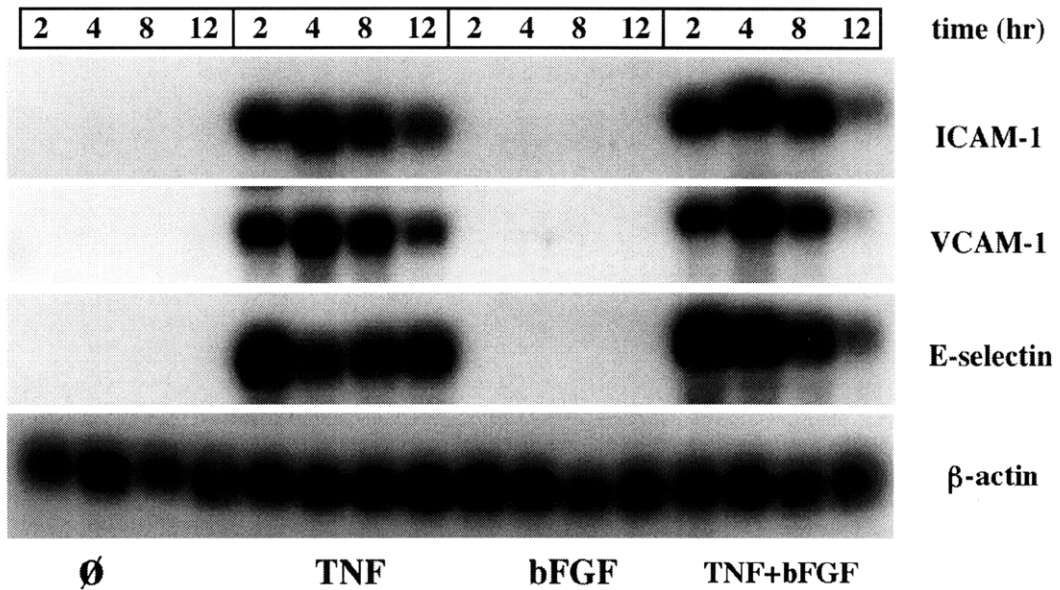
(b) 2 - 12 hrs

Figure 6-2-3. Northern blot analysis showing the kinetics of bFGF (10 ng/ml)-induced inhibition of ICAM-1, VCAM-1, and E-selectin mRNA levels in HUVECs simultaneously activated by TNFα (50 ng/ml). Northern blots are shown for (a) 24 hr treatment, and (b) 2 to 12 hrs of treatment. Data are representative of 1 of at least 2 similar experiments.
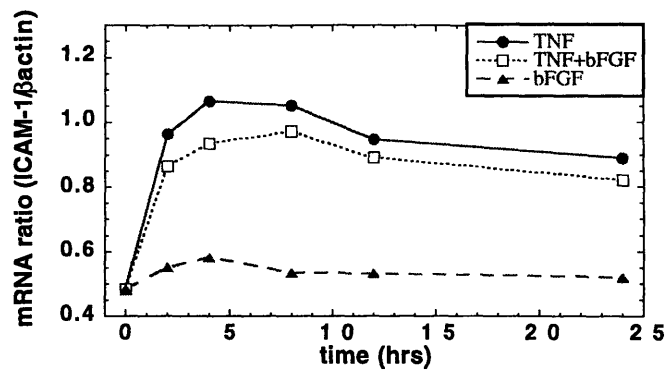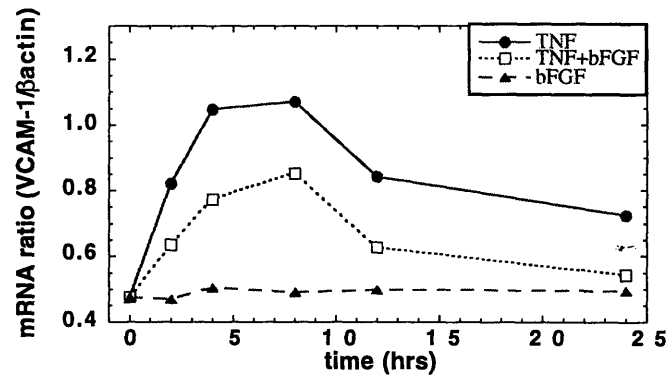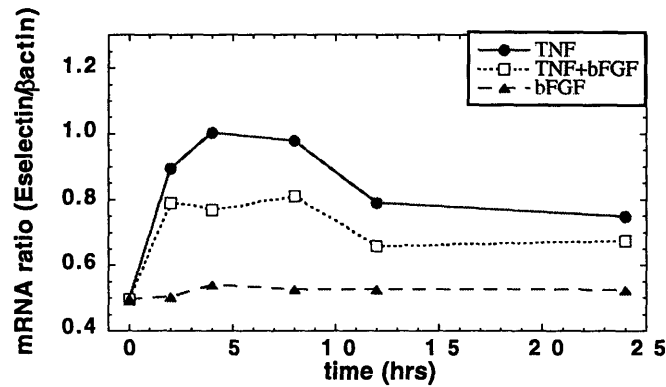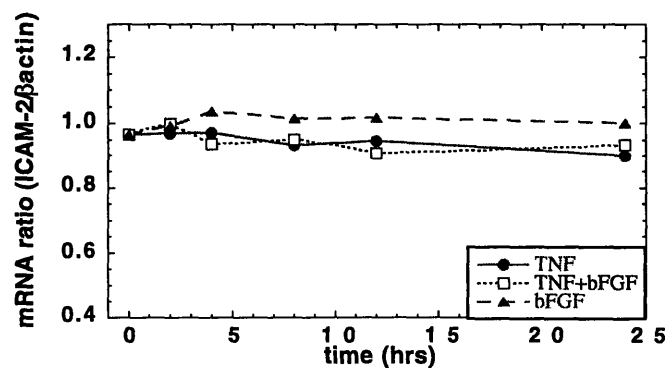
Figure 6-2-4. Graphic representation of the kinetics of bFGF (10 ng/ml)-induced inhibition of (a) ICAM-1, (b) VCAM-1, (c) E-selectin, and (d) ICAM-2 mRNA levels in HUVECs simultaneously activated by TNFα (50 ng/ml). CAM RNA levels are shown with respect to β-actin RNA levels as determined by densitometric measurement of Northern blots. Data are representative of 1 of at least 2 similar experiments.

The effects of TNFα on both VCAM-1 and E-selectin mRNA expression showed characteristically similar kinetics, with a rapid initial increase peaking between 4 and 8 hrs and then decreasing to a steady-state level after 12 hrs. Treatment with bFGF resulted in no significant change in the mRNA levels of both CAMs even 24 hrs after initial exposure. The combination of both TNFα and bFGF produced rather similar kinetics as that of TNFα treated monolayers, but with significantly lower levels of expression occurring even prior to 2 hrs of treatment and lasting for the complete 24 hrs. The results of the E-selectin expression correlated well with the kinetics observed at the protein level for all of the treatment groups. However, while TNFα and bFGF induction kinetics of VCAM-1 mRNA expression were consistent with those observed at the protein level, the combined treatment using TNFα and bFGF demonstrated reductions in the level of VCAM-1 mRNA expression which significantly preceded any changes on the protein level. As a possible explanation for this finding, the combined treatment may produce a sufficient threshold of VCAM-1 expression at the protein level, such that initial differences relative to TNFα controls are not apparent at the mRNA level until a longer exposure duration.

The effect of the treatment groups on the constitutively expressed molecule ICAM-2 produced profound differences compared to the inducible CAMs. While treatment with either TNFα or TNFα combined with bFGF did not alter the level of ICAM-2 mRNA expression, treatment with bFGF alone resulted in a slight increase in ICAM-2 expression after 4 hrs and remained for up to 24 hrs. This effect of bFGF on ICAM-2 mRNA levels was not evident at the protein level, which showed no significant differences between the treatment groups.

Possible reasons for the discrepancy between the protein and mRNA levels are: a) ICAM-2 may have a sufficient half-life that increases in its mRNA expression do not become evident within 24 hrs, b) there may be a threshold of ICAM-2 which is continually present on the cell surface and do not reflect changes in its mRNA expression, or c) the sensitivity of the protein expression assay may have been insufficient to detect the small differences in ICAM-2 levels which possibly were produced.

6.3 mRNA Regulation

The suppression of the TNFα-inducible CAM mRNAs by bFGF indicates that its effect does not occur on the post-translational level, but rather on the pre-translational or transcriptional level. In an effort to further understand the molecular regulation of the selected CAM mRNA, a set of experiments were conducted to determine whether bFGF

128

affects the stability, a post-transcriptional event, of ICAM-1, VCAM-1, E-selectin, and ICAM-2 mRNA.

To this end, HUVECs were initially treated with TNFα (50 ng/ml) for 4 hrs, to increase the level of the inducible CAM mRNA within the cell, as determined by the previous kinetic analysis. Actinomycin D (10 µg/ml) was then added to block transcriptional activity, in the presence or absence of bFGF (10 ng/ml). Total RNA was isolated at various times (2, 4, 8, 12, and 24 hrs) after addition of the actinomycin D and subjected to Northern blot analysis.

As shown in Figure 6-3-1, when transcriptional activity was blocked, the suppressive effect of bFGF on ICAM-1, VCAM-1, and E-selectin was effectively inhibited. Additionally, the expression of ICAM-2 mRNA was unaffected relative to the TNFα treated cells, demonstrating that the addition of actinomycin D does not alter overall constitutive protein expression.

The control groups for these experiments are shown in Figure 6-3-2, and represent the endothelial cells that were treated with TNFα for 4 hrs prior to the exposure to bFGF and without the addition of actinomycin D. As was found with the kinetic analysis using simultaneous treatments, significant differences in all three of the inducible CAMs were evident after 2 to 4 hrs of treatment with bFGF, and maintained over a 24 hr duration. Also, the mRNA levels of ICAM-2 remained unaltered by the continued exposure to TNFα or TNFα combined with bFGF.

The findings of this study are suggestive that the stability of TNFα-induced ICAM-1, VCAM-1, and E-selectin mRNA are not affected by the presence of bFGF. Therefore, the inhibition of the protein and mRNA levels of these CAMs may likely be regulated by bFGF at the transcriptional level, and not significantly at the translational or post-translational levels. Additional investigation using transcription run-on assays to examine the changes in promoter activity of the CAM genes by bFGF are needed to determine whether the rate of transcription is actually affected [Neish, et al., 1992].

It has also been previously shown that TNFα activates NF-κB transcriptional regulatory proteins, which are capable of inducing the transcription of ICAM-1, VCAM-1, and E-selectin genes via NF-κB binding sites located on their promoter regions [Collins, et al., 1995]. NF-κB is a heterodimer of two proteins, p50 and p65, which upon activation translocates from the cytoplasm to the nucleus. Basic FGF may suppress the activation of this transcription factor through second or third messengers activated by one of its intracellular signaling pathways. Electrophoretic mobility shift assays using nuclear extracts from TNFα induced HUVECs are needed in defining this as a possible mechanism [Marui, et al., 1993].
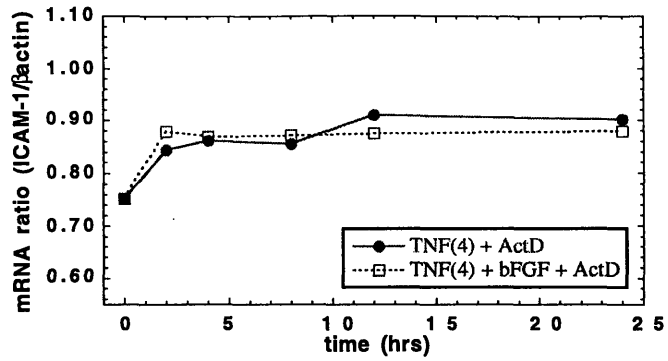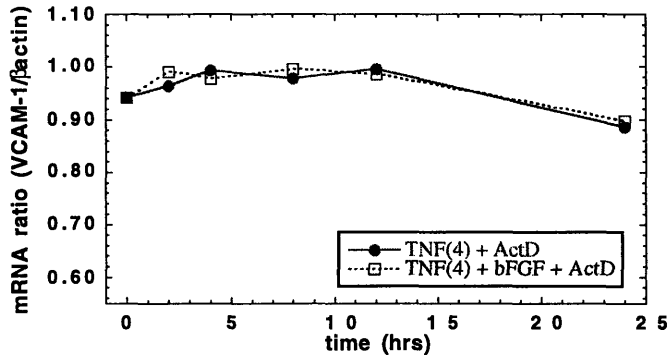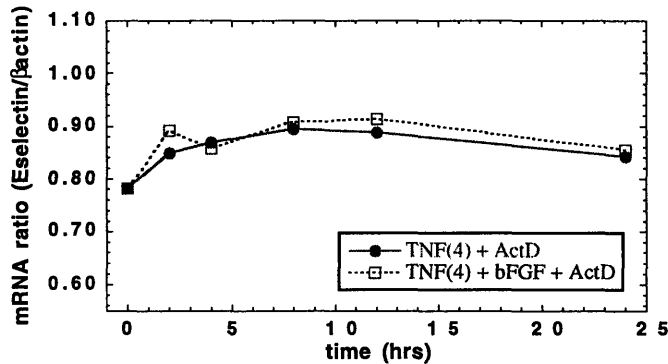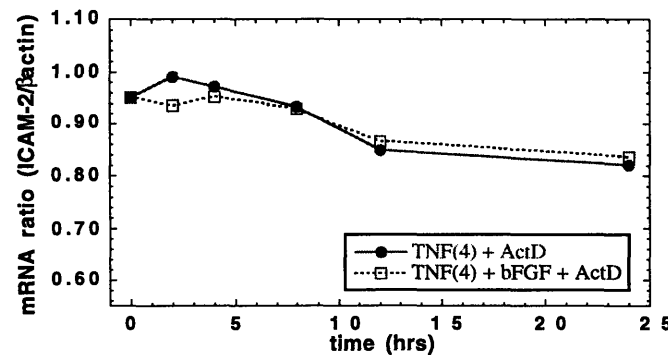
Figure 6-3-1. Graphic representation of the effects of bFGF (10 ng/ml) on the stability of (a) ICAM-1, (b) VCAM-1, (c) E-selectin, and (d) ICAM-2 mRNA in HUVECs initially activated with TNFα (50 ng/ml) for 4 hrs. The CAM RNA levels are shown with respect to β-actin RNA levels as determined by densitometric measurement of Northern blots. Data are representative of 1 of 3 similar experiments.
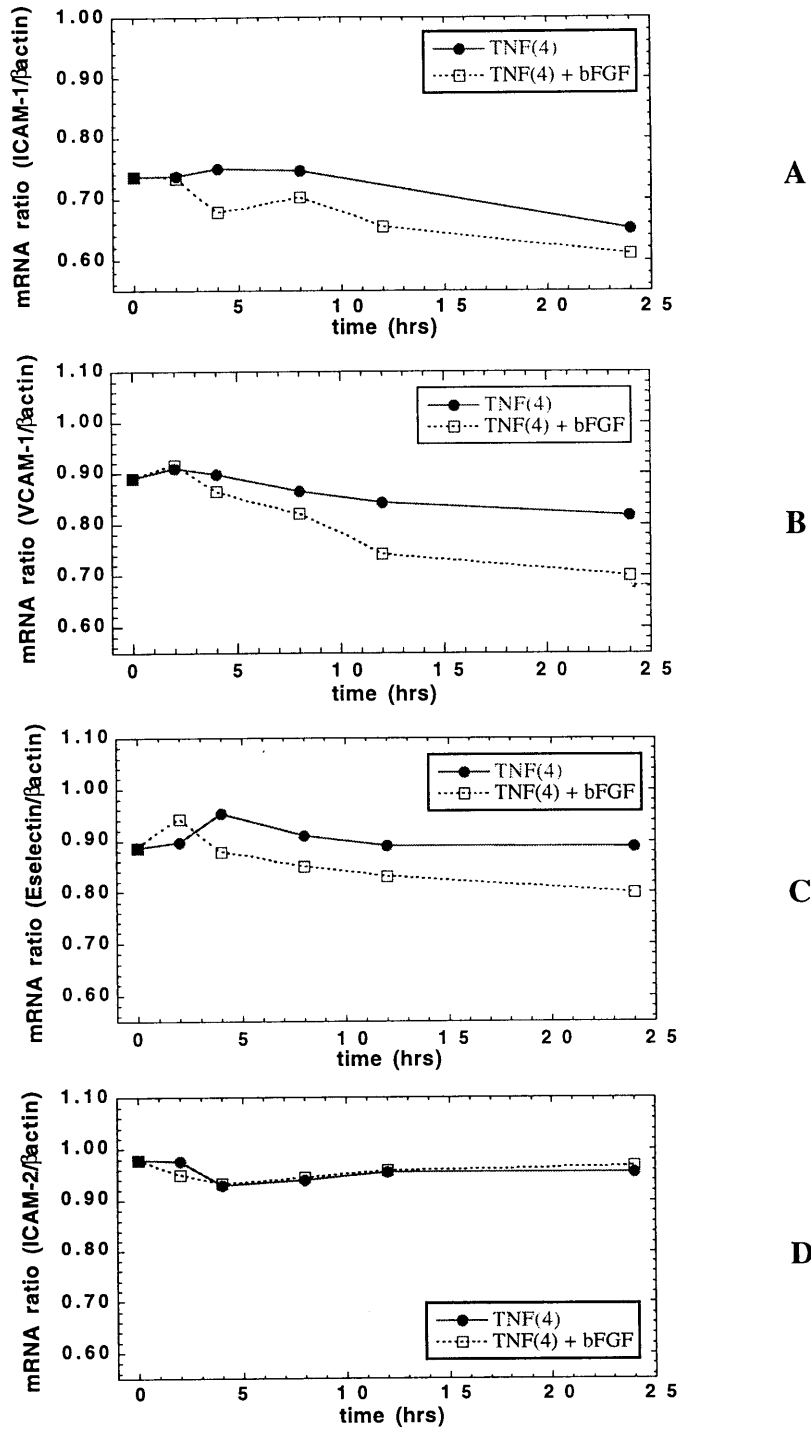
Figure 6-3-2. Graphic representation of the effects of bFGF (10 ng/ml) on (a) ICAM-1, (b) VCAM-1, (c) E-selectin, and (d) ICAM-2 mRNA in HUVECs initially activated with TNFα (50 ng/ml) for 4 hrs. These served as control groups for the stability analysis study, and the CAM RNA levels are shown with respect to β-actin RNA levels as determined by densitometric measurement of Northern blots. Data are representative of 1 of 3 similar experiments.

6.4 Signaling Pathways

In an effort to further define the mechanisms employed by bFGF in its regulation of the transcriptional activity of the inducible CAM genes, studies were conducted to investigate the specific early signaling pathways used by bFGF in modulating CAM expression and function. Utilizing information obtained from previous studies examining the signaling pathways used by bFGF in modifying other physiological responses, an axis was established to narrow the focus of the investigation. Sufficient scope was maintained to provide essential understanding of the specific signal transmission pathway(s) linking bFGF to several intracellular mediators, as well as its potential interaction with the signaling pathways used by TNFα in activating CAM expression.

An illustration of the bFGF-mediated pathways considered and the plausible interaction with TNFα signaling is shown in Figure 6-4-1. The paradigm to be considered involves the following specific interactions: a) bFGF with its high affinity receptors (bFGF:FGFR), b) bFGF with the low affinity heparin sulfate polysaccharide, c) receptor tyrosine kinase activation, d) protein tyrosine phosphatase function, e) phospholipase C-γ1 activation, f) phospholipase D activation, and g) protein kinase C activation. Selective, commercially available blocking agents and antibodies were used to determine the role of each of these interactions and are listed in Table 6-1 along with their specific modes of action. Dose response curves were conducted for the blocking agents using the functional adhesion assay to determine the effective concentrations for use in the expression and functional analysis, and are shown in Appendix C for reference.

6.4.1 Surface Protein Expression

To study the influence of each of the various signaling components on TNFα- and bFGF-induced modulation of adhesion molecule expression on endothelial cells, the fluorescence immunoassay (FIA) method was used in conjunction with the appropriate signal transduction blockers.

Experiments were first conducted to determine the role of the high-affinity receptor-ligand interaction of bFGF:FGFR. HUVEC monolayers were initially treated with a solution consisting of 1 µg/ml bFGF neutralizing antibody and 10 ng/ml of bFGF and/or TNFα for 24 hrs and then assessed for the level of CAM expression. As shown in Figure 6-4-2, the neutralizing antibody showed no significant effect on TNFα activated ICAM-1, VCAM-1 or E-selectin expression, as well as no effect on non-treated baseline controls.

132
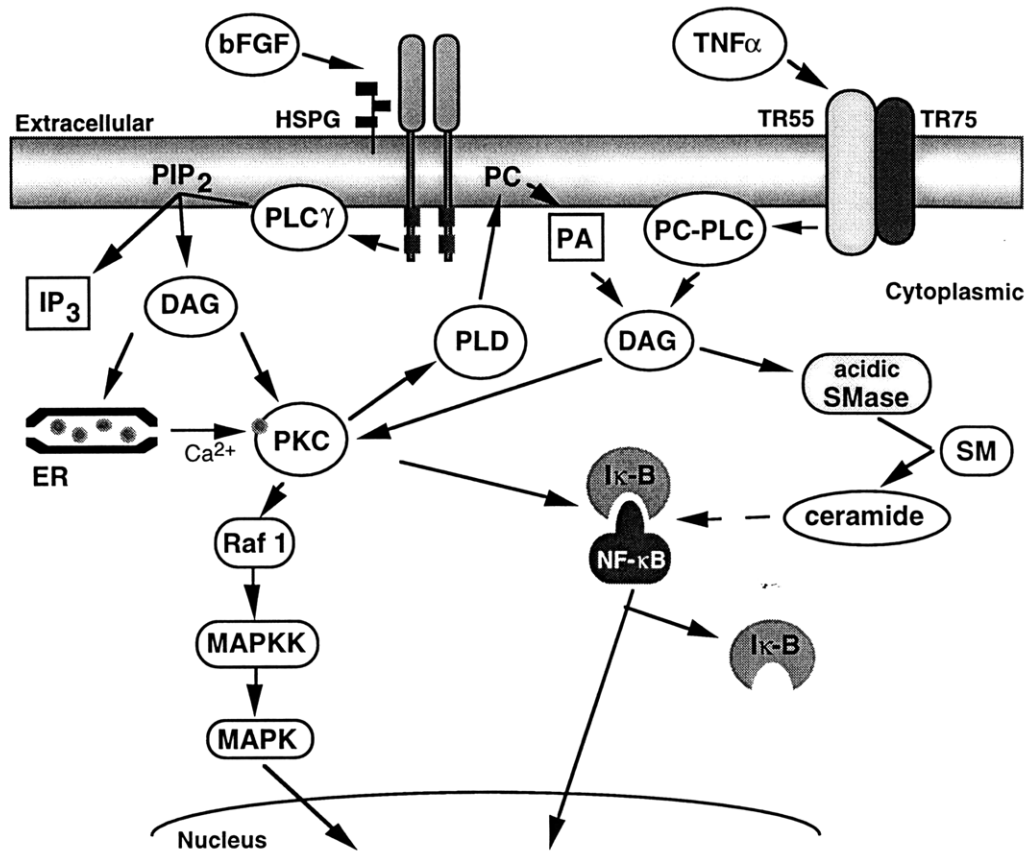
Figure 6-4-1. Simplified schematic of the TNFα and bFGF signaling pathways.

Table 6-1. Specific signal transduction inhibitors and their modes of action.

Agent	Selectivity	Mode of action
anti-bFGF mAb	bFGF:FGFR	bFGF-specific neutralizing antibody
Methyl 2,5-dihydroxycinnamate (MDHC)	Tyrosine kinase	Erbstatin analog, a competitive inhibitor of FGF receptor-associated tyrosine kinase
Sodium orthovanadate (Na_3VO_4)	Protein tyrosine phosphatase	Broad-spectrum potent inhibitor of protein tyrosine phosphatases
2-nitro-4-carboxyphenyl N,N-diphenylcarbamate (NCDC)	Phospholipase C	Blocks hydrolysis of PPI to IP_3
1-[isopropylamino]-3-[1-naphthyloxy]-2-propanol (propranolol)	Phospholipase D	Blocks phospholipase D-derived DAG by inhibiting phosphatidate phosphohydrolase
Calphostin C	Protein kinase C	Highly specific inhibitor of PKC, competes at the binding site of DAG and phorbol esters
Bisindolylmaleimide (GF109203X)	Protein kinase C	Highly selective inhibitor of PKC, competes at the ATP-binding site

133

Due to the relative insensitivity of the assay system for low levels of expression, small differences in CAM expression on monolayers treated with bFGF were not evident, nor were the effects of the neutralizing antibody on the response of bFGF. However, in comparison with TNFα treatment, monolayers treated with both TNFα and bFGF showed significant reversal of CAM inhibition by the addition of the bFGF antibody. Therefore, the results demonstrate that bFGF acts through its receptor in mediating the inhibitory action on ICAM-1, VCAM-1 and E-selectin protein expression induced by TNFα.
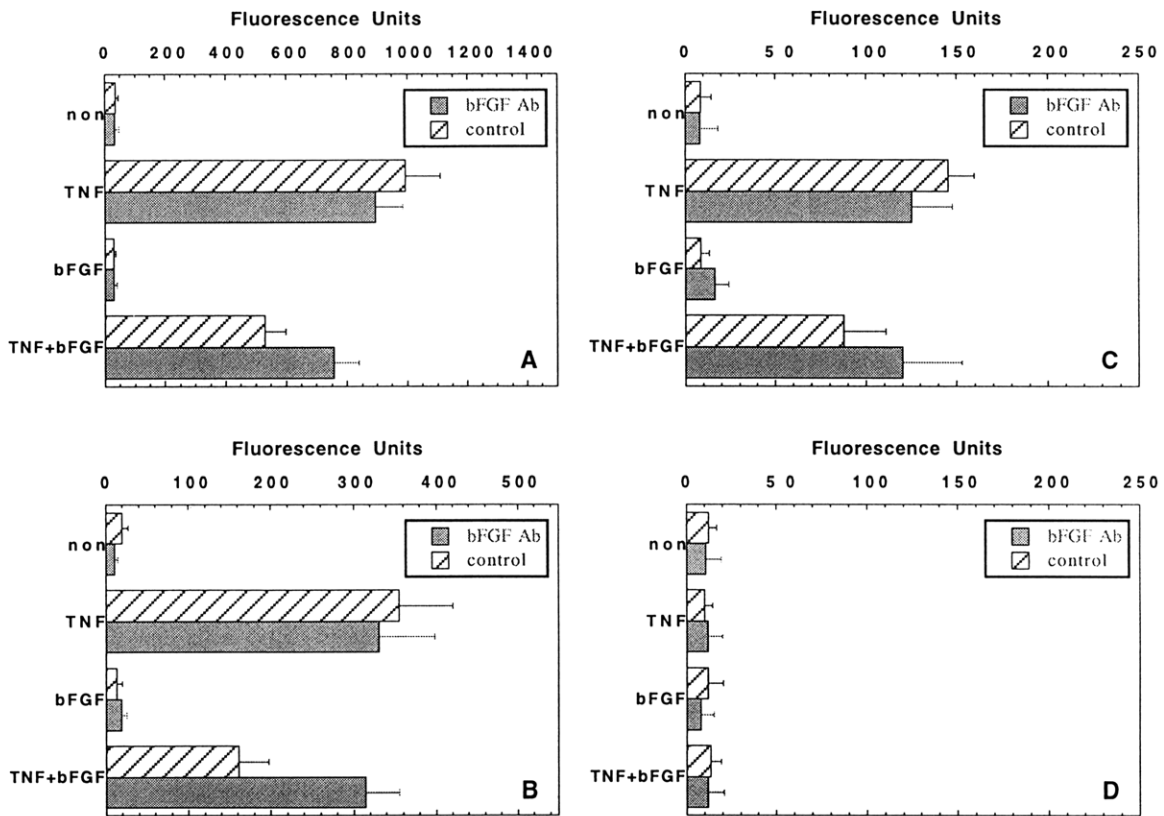
Figure 6-4-2. Effect of bFGF neutralizing antibody on TNFα and bFGF induced HUVEC protein expression of a) ICAM-1, b) VCAM-1, c) E-selectin, and d) IgG isotype control. Data represent means ± SEM from triplicate wells.

In addition to the high-affinity interaction which bFGF has with its receptor, low-affinity receptors for bFGF exist that are predominantly proteoglycans carrying heparan sulphate side chains [Klagsburn, 1990]. While unable to activate a signal transduction by themselves, heparin and heparan sulphates sequester and present bFGF to its high-affinity receptors and facilitate efficient binding. To explore the potential of heparin to modulate the

inhibitory effect of bFGF, experiments were conducted in which supplemental heparin (10 µg/ml) was added to endothelial cell monolayers along with cytokine and growth factor treatment for 24 hrs. As shown in Figure 6-4-3, heparin treatment did not alter the level of ICAM-1, VCAM-1, or E-selectin induced by TNFα, nor did it significantly affect the ability of bFGF to inhibit their expression. Baseline levels for each of the CAMs were also unaffected by the exogenous addition of heparin. These results indicate that, under the conditions used in this investigation, supplemental heparin does not change the effectiveness of bFGF to alter CAM expression on TNFα treated monolayers.
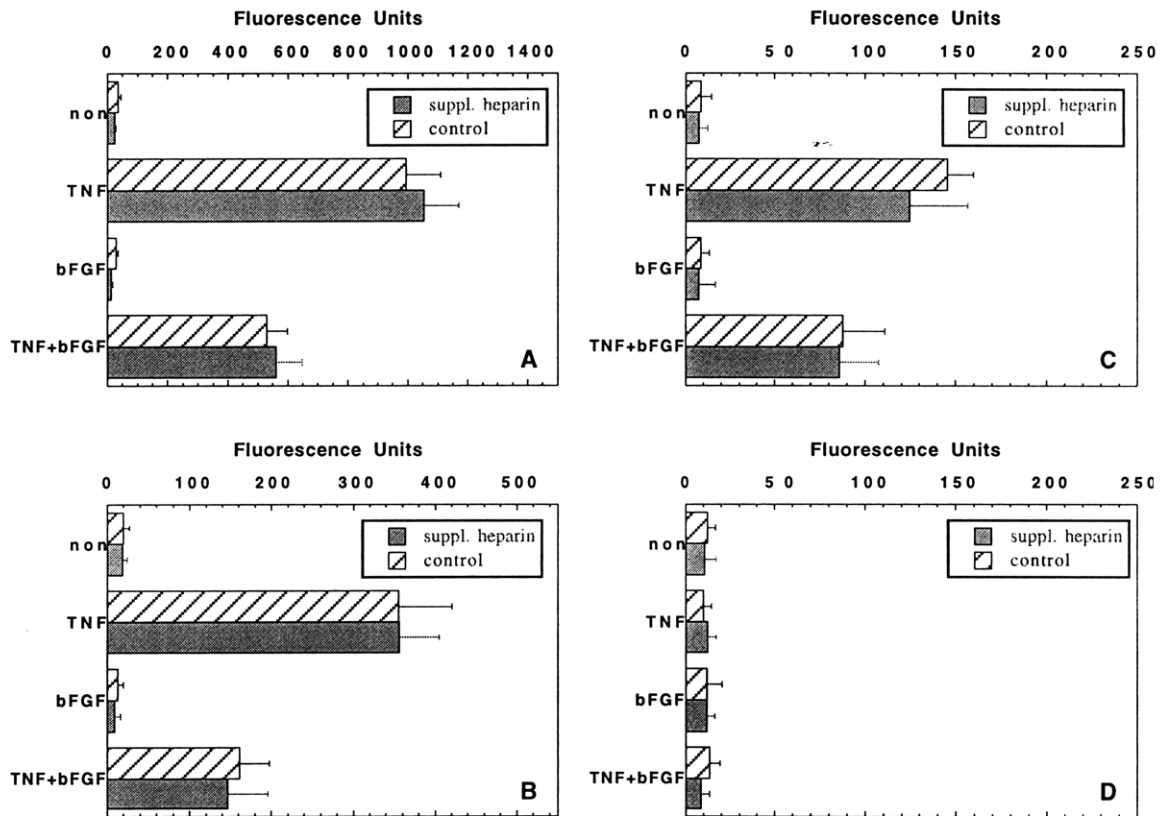
Figure 6-4-3. Effect of supplemental heparin on TNFα and bFGF induced HUVEC protein expression of a) ICAM-1, b) VCAM-1, c) E-selectin, and d) IgG isotype control. Data represent means ± SEM from triplicate wells.

As the next step in the signaling cascade, autophosphorylation of the tyrosine kinase domain on the cytoplasmic portion of the FGF receptor is known to occur, which, in turn, leads to the tyrosine phosphorylation of a number of intracellular proteins. The ability of the receptor tyrosine kinase to transduce the inhibitory signal of bFGF was studied using MDHC as the blocking agent. Following a 2 hr pretreatment with 5 µM of

MDHC, TNFα and/or bFGF was applied to HUVEC monolayers for a 24 hr period in the continued presence of the inhibitor. Their ability to alter endothelial cell surface expression of all three CAMs was then assessed. As shown in Figure 6-4-4, the blockage of receptor tyrosine kinase (RTK) phosphorylation resulted in a significant decrease in the ability of TNFα to induce the expression of ICAM-1, VCAM-1, and E-selectin. Although cytoplasmic amino acid sequences of TNFα receptors demonstrate a lack of intrinsic protein tyrosine kinase activity [Loetscher, et al., 1990], TNFα has been shown to induce rapid protein tyrosine phosphorylation in PMN [Fuortes, et al., 1993], and be required for NF-κB mobilization and induction of VCAM-1 and E-selectin by TNFα [Weber, et al., 1995]. The attenuation of ICAM-1 induction may be attributed to a distinct inhibitory mechanism of the particular blocking agent used in this investigation.
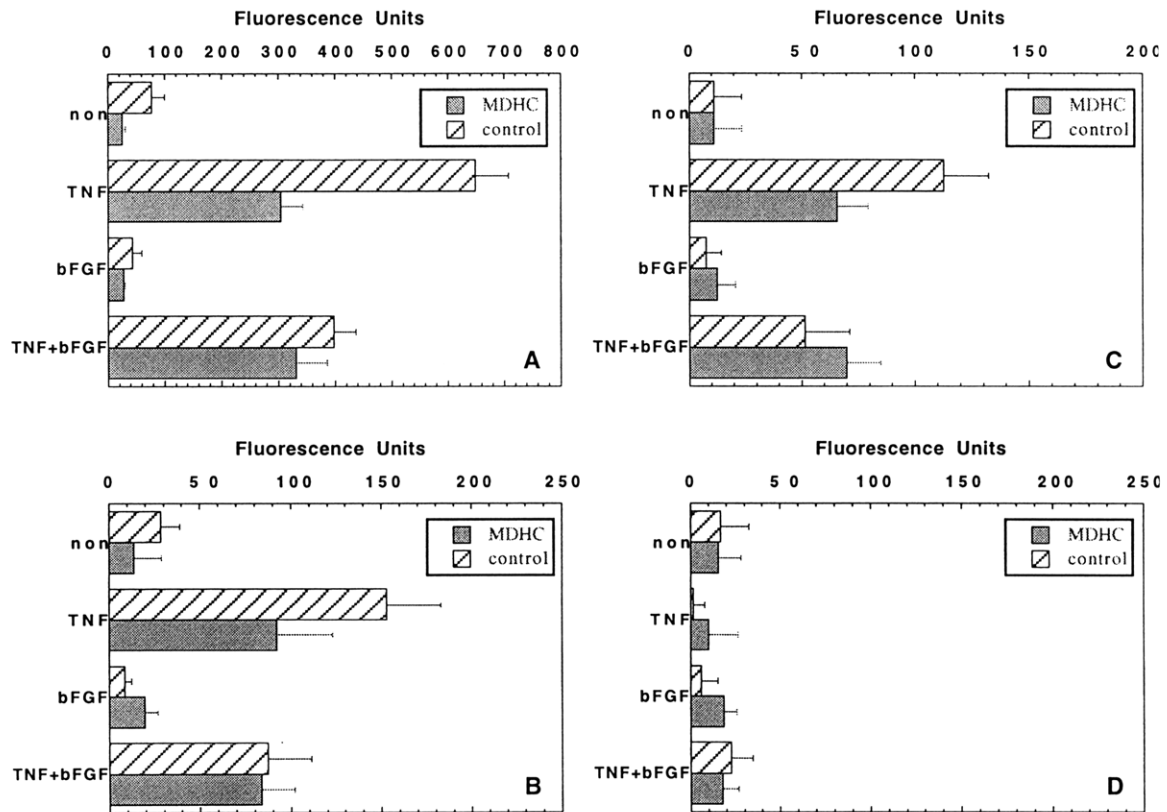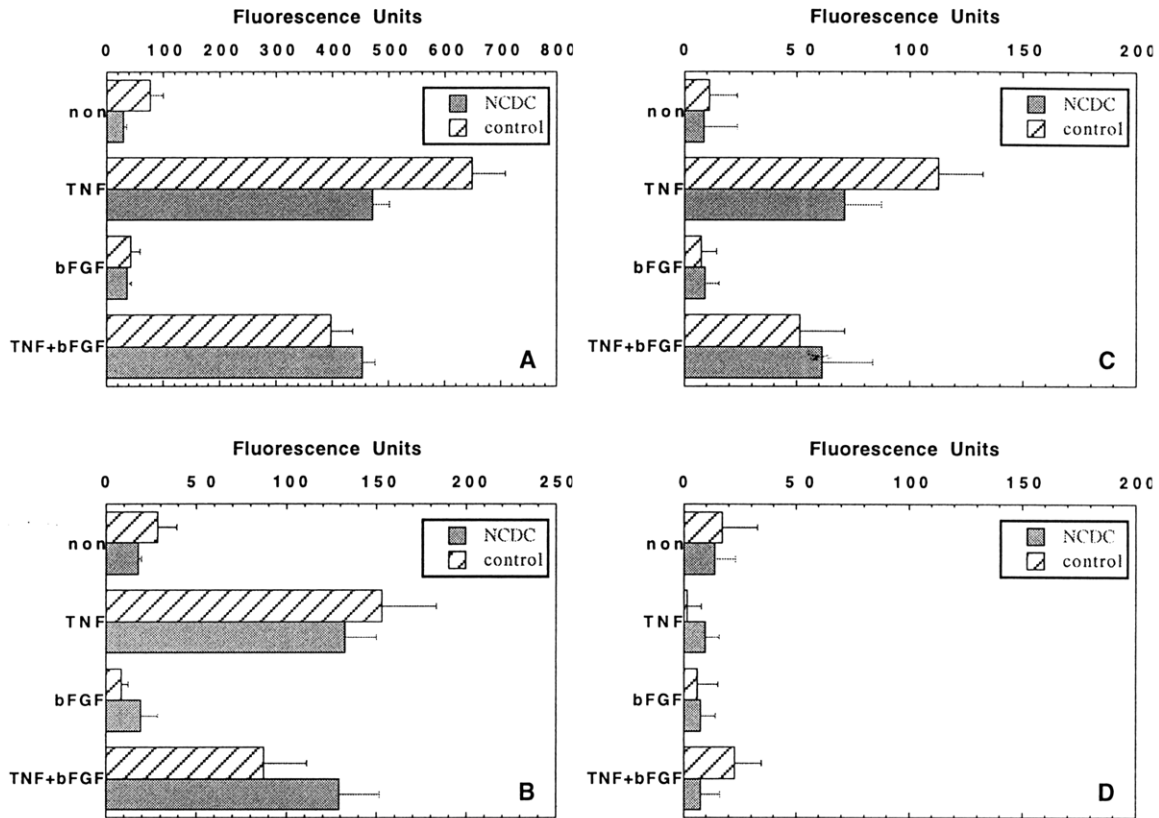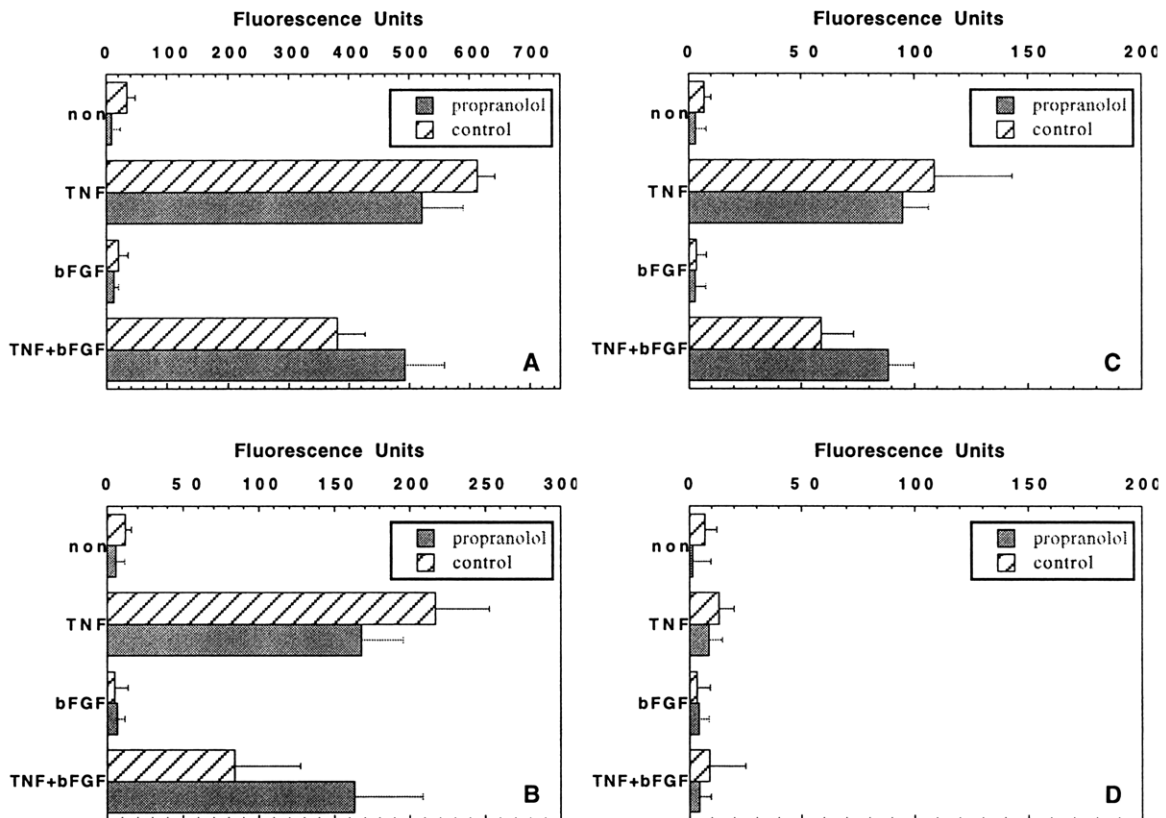

Figure 6-4-4. Effect of the receptor tyrosine kinase inhibitor MDHC on TNFα and bFGF induced HUVEC protein expression of a) ICAM-1, b) VCAM-1, c) E-selectin, and d) IgG isotype control. Data represent means ± SEM from triplicate wells.

136

The RTK inhibitor did not elicit a significant effect on the CAM expression of bFGF treated monolayers, as well as the baseline controls, except for a modest decrease in the baseline level of ICAM-1. However, there was observed a significant inability of bFGF to inhibit all three of the CAMs induced by TNFα, suggesting that bFGF acts via the specific phosphorylation of its receptor tyrosine kinase in producing its effect on inducible CAM expression. This specific activity has been demonstrated to be essential for bFGF to initiate DNA synthesis and mitogenic signaling in endothelial cells [Hawker and Granger, 1994].

To further assess the role of tyrosine phosphorylation in the induction of adhesion molecules by TNFα and in the inhibitory effect elicited by bFGF, expression studies were performed on monolayers treated with sodium orthovanadate, a protein tyrosine phosphatase (PTP) inhibitor. HUVEC monolayers were treated for 2 hrs with 30 μM of sodium orthovanadate and then incubated with TNFα and/or bFGF for a further 24 hrs in the continued presence of the PTP-inhibiting agent. The results obtained showed a significant decrease in TNFα-induced VCAM-1 expression by vanadate, while exhibiting no significant effect on ICAM-1 or E-selectin (Figure 6-4-5). In addition, vanadate produced slightly increased basal levels of VCAM-1 and E-selectin expression, correlating with previous studies using HUVECs [May, et al., 1996].

Blockage of tyrosine phosphatase activity elicited only a small effect on the ability of bFGF to inhibit the expression of VCAM-1 by TNFα, and did not produce differences in the inhibition of ICAM-1 or E-selectin. Most likely this was due to the significant reduction in the control levels of TNFα-induced VCAM-1 expression, which was evident in the presence of sodium orthovanadate. No significant differences were also observed for the CAMs on monolayers treated with bFGF alone. Therefore, in agreement with the studies blocking the receptor tyrosine kinase function, further evidence is provided in favor of bFGF mediating its CAM inhibition through the tyrosine phosphorylation activity of its receptor.

Phospholipase C-γ (PLC-γ) is a RTK substrate (SH2 domain) possessing catalytic activity and regulated by tyrosine phosphorylation [Burgess, et al., 1990]. As a potential next step in the signal transduction cascade leading to CAM inhibition by bFGF, the role of PLC-γ was studied. Using the known PLC inhibitor, NCDC, HUVEC monolayers were treated with 50μM of the blocking agent and exposed to TNFα and/or bFGF for 24 hrs. As shown in Figure 6-4-6, inhibition of PLC activity was shown to produce a decrease in the levels of ICAM-1 and E-selectin induced by TNFα, with no significant change in VCAM-1 expression. While NCDC acts to inhibit the action of PI-PLC in producing DAG, a PLC-γ-mediated mechanism used by bFGF, it may non-specifically interfere with

137

the action of PC-PLC in producing DAG, which is used by TNFα in mediating CAM expression.
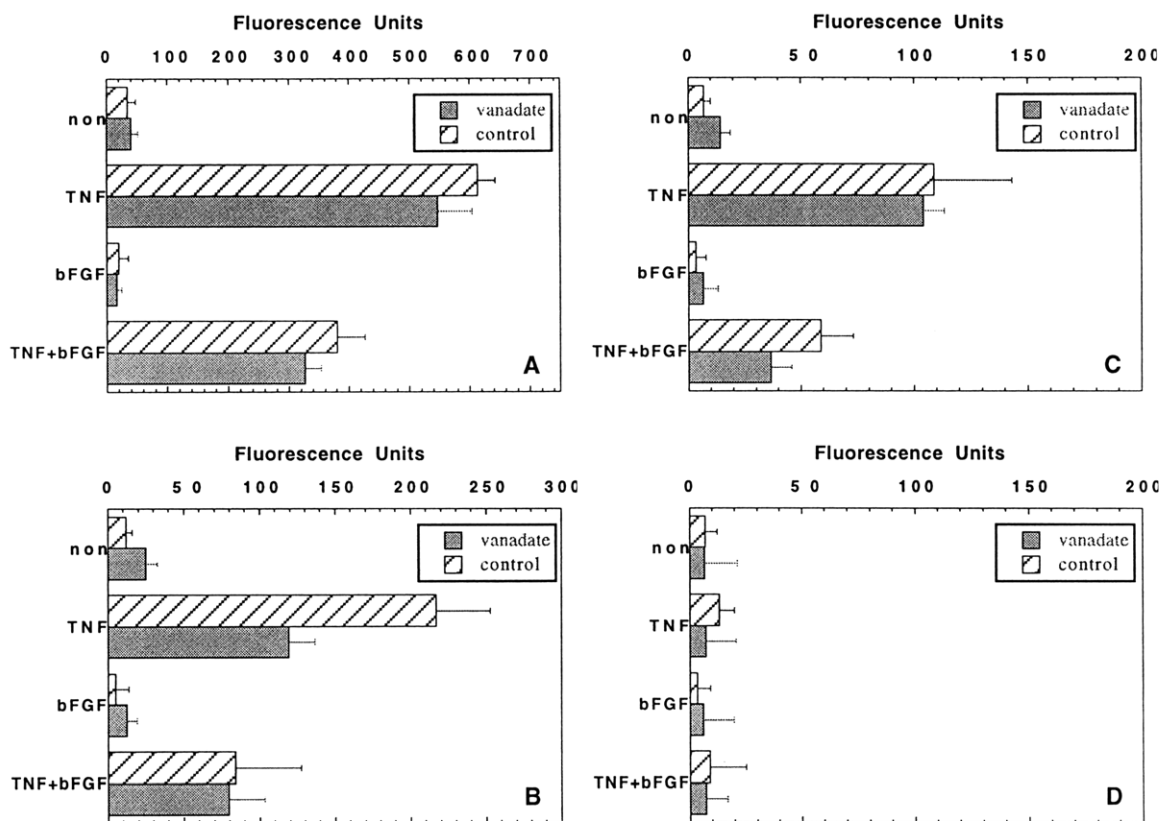
Figure 6-4-5. Effect of the protein tyrosine phosphatase inhibitor sodium orthovanadate on TNFα and bFGF induced HUVEC protein expression of a) ICAM-1, b) VCAM-1, c) E-selectin, and d) IgG isotype control. Data represent means ± SEM from triplicate wells.

Blockage of PLC-γ was also demonstrated to effectively prevent the inhibition of all three CAMs by bFGF. No significant differences were noted in the baseline controls or in the monolayers treated with bFGF alone. Therefore, these findings are suggestive that bFGF acts, in part, through a PLC-γ-mediated mechanism in eliciting its inhibitory response to CAM expression.

Another possible pathway which bFGF may incorporate is one involving phospholipase D (PLD). Activation of PLD by bFGF is known to catalyze the hydrolysis of phosphatidylcholine (PC) to produce a precursor of diacylglycerol in either a PKC-dependent or an inositol-lipid hydrolysis-independent mechanism [Billah and Anthes, 1990; Ahmed, et al., 1994]. PC is also hydrolyzed by a TNFα-responsive PLC to produce the second messenger DAG, a known activator of PKC and acidic

sphingomyelinase, and signifies one of the early signaling interactions between bFGF and TNFα. To further elucidate the role of PLD in CAM regulation by bFGF, propranolol was used as the specific PLD antagonist.

Figure 6-4-6. Effect of the phospholipase C inhibitor NCDC on TNFα and bFGF induced HUVEC protein expression of a) ICAM-1, b) VCAM-1, c) E-selectin, and d) IgG isotype control. Data represent means ± SEM from triplicate wells.

HUVEC monolayers treated with 50 μM of propranolol were found to show no difference in their ability to upregulate the expression of ICAM-1, VCAM-1 or E-selectin induced by TNFα (Figure 6-4-7). Baseline and bFGF controls also remained unaltered by the treatment with propranolol. However, significant reduction in the bFGF-mediated suppression of all three inducible CAMs was evident.

These results demonstrate that PLD is a significant contributor to the bFGF response. In conjunction with the finding that PLC-γ also provides a significant contribution, it would appear that bFGF acts to hydrolyze phosphoinositides by PLC-γ to

form DAG and the eventual activation of PKC. PKC may, in turn, activate PLD to contribute to the inhibitory signaling by bFGF and directly compete with TNFα signaling.

To determine the specific role of PKC in mediating the bFGF response to CAM regulation, experiments were conducted using the specific PKC inhibitors, calphostin C and bisindolylmaleimide (BIM). The two independent blocking agents were separately utilized in order to provide a better perspective on the influence of PKC, which consists of seven isoforms that differ in their dependence on calcium and phospholipid cofactor activity.
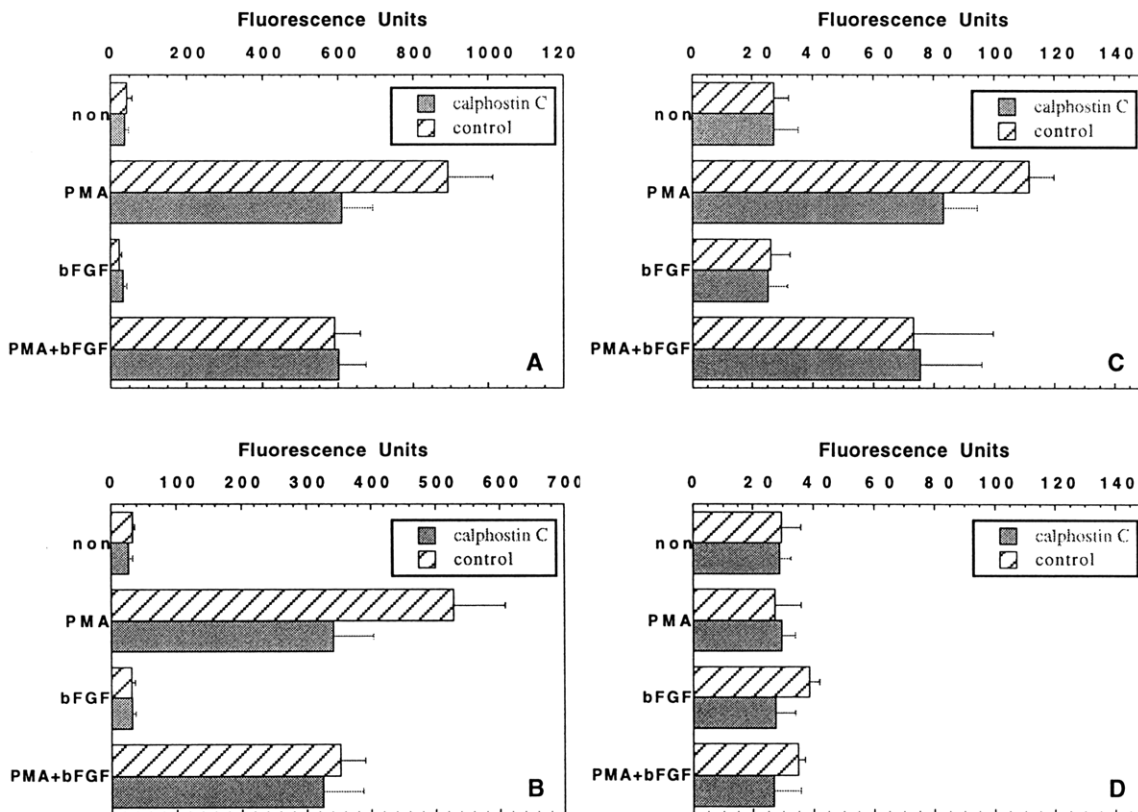

Figure 6-4-7. Effect of the phospholipase D inhibitor propranolol on TNFα and bFGF induced HUVEC protein expression of a) ICAM-1, b) VCAM-1, c) E-selectin, and d) IgG isotype control. Data represent means ± SEM from triplicate wells.

The results of the blocking experiments are shown in Figure 6-4-8. Both agents reduced TNFα-induced surface expression of VCAM-1, 38% by calphostin C and 63% by BIM. However, neither agent was influential in modifying ICAM-1 or E-selectin expression, consistent with the known effects using other PKC inhibitors on TNFα signaling [Ritchie, et al., 1991; Deisher, et al., 1993]. The inhibitory effect elicited by bFGF on TNFα-induced VCAM-1 expression was also effectively reduced by BIM

140

(30%), but less so by calphostin C (10%). Moreover, the ability of bFGF to inhibit induced ICAM-1 and E-selectin expression was essentially unaltered by both agents. Baseline controls were found to be unaffected by blocking PKC activity with either compound. The differences found between the two agents may partly be the result of their specific inhibitory action on PKC, with BIM acting as a competitive inhibitor for the ATP-binding site, and calphostin C competing at the binding site of diacylglycerol and phorbol esters. Additionally, the selectivity for the various PKC isozymes may vary between the two compounds.

Based on the results obtained it would appear that bFGF may act through PKC to mediate its inhibitory action on TNFα-induced VCAM-1 expression only, and not ICAM-1 or E-selectin. The fact that TNFα utilizes a PKC-dependent mechanism only for the selective upregulation of VCAM-1, and a PKC-independent mechanism for the induction of ICAM-1 and E-selectin on endothelial cells, is suggestive that bFGF uses a diverse scheme in modulating the CAMs induced by TNFα.
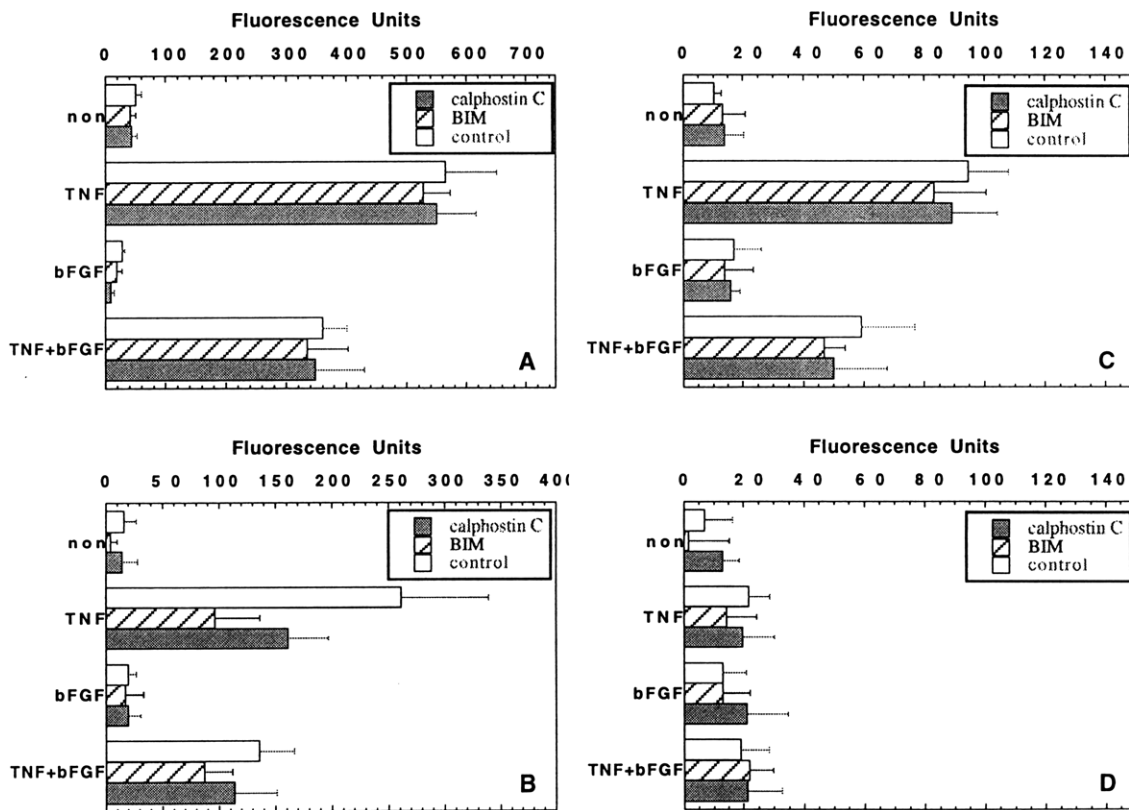
Figure 6-4-8. Effects of the protein kinase C inhibitors calphostin C and bisindolylmaleimide (BIM) on TNFα and bFGF induced HUVEC protein expression of a) ICAM-1, b) VCAM-1, c) E-selectin, and d) IgG isotype control. Data represent means ± SEM from triplicate wells.

141

However, it does leave unanswered the possibility that bFGF may still utilize PKC for reducing ICAM-1 and E-selectin expression by cytokines using the PKC pathway for their induction. To address this possible mechanism, the phorbol ester, PMA, a known activator of PKC and inducer of ICAM-1, VCAM-1 and E-selectin expression, was utilized and the effect of bFGF on suppressing its ability to activate the CAMs via PKC was examined. Calphostin C was used as the blocking agent, as it interacts with the regulatory domain of PKC by competing directly at the binding site for the phorbol ester. As shown in Figure 6-4-9, PMA induces the expression ICAM-1, VCAM-1, and E-selectin, and that addition of calphostin C effectively reduces the expression of all three CAMs by 32%, 35%, and 25%, respectively. Addition of bFGF to PMA-treated endothelial cells also caused a reduction in the level of the inducible CAMs, which was effectively blocked by using calphostin C. Therefore, it would appear evident that bFGF can act through both a PKC-dependent and independent means to reduce the expression of adhesion molecules by positive modulators, depending on the pathway used by the specific inducer. This may be the result of a competitive effect by bFGF in its activation of second messengers for eliciting other cellular processes, such as cell proliferation and migration.

Figure 6-4-9. Effects of the protein kinase C inhibitor calphostin C on PMA and bFGF induced HUVEC protein expression of a) ICAM-1, b) VCAM-1, c) E-selectin, and d) IgG isotype control. Data represent means ± SEM from triplicate wells.

6.4.2 Functional Correlation

Having established a set of early signaling pathway mediators used by bFGF in inhibiting the expression of selective CAM proteins, adhesion assay studies using the parallel-plate flow chamber were conducted to demonstrate the functional relevance of the biological findings. IL-2 activated natural killers cells served as the lymphocyte model and were analyzed for their ability to bind to HUVEC monolayers treated with TNFα and/or bFGF in combination with the signal transduction blocking agents under dynamic flow conditions (1.0 dyn/cm^2).

Initial studies performed examined the interaction of bFGF with its receptor using identical conditions as that for the expression assay. The results obtained showed no effect by the neutralizing bFGF Ab on A-NK binding to TNFα-activated or non-treated monolayers (Figure 6-4-10). However, the antibody did significantly suppress the ability of bFGF to inhibit ANK binding to the activated monolayers compared to the control group ($p < 0.05$). These findings directly correlate with the expression assay results showing significant reversal of CAM inhibition by addition of the bFGF antibody, and thus further demonstrate that bFGF acts through its high-affinity receptor to modulate A-NK adhesion.
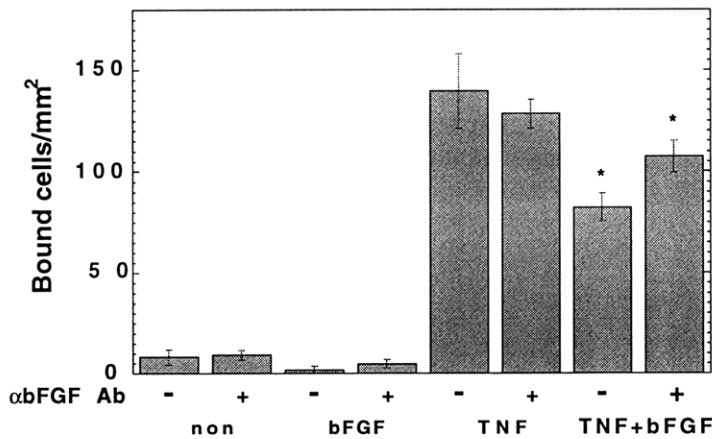
Figure 6-4-10. Effect of neutralizing bFGF Ab (10 μg) on A-NK cell binding to HUVEC monolayers treated with bFGF, TNFα, and TNFα + bFGF. Mean numbers ± SD of bound cells for eight adjacent fields are shown for 1 of 3 representative flow experiments. * $p < 0.05$ compared to control values.

To determine a possible functional influence of a low affinity interaction of bFGF with heparin, a facilitator of increased bFGF binding to its receptor, on the ability of bFGF to inhibit A-NK binding, flow experiments were performed on monolayers treated with supplemental heparin under conditions matching those used in the expression assay.

As shown in Figure 6-4-11, the addition of exogenous heparin did not increase the level of inhibition produced by bFGF on A-NK adhesion to TNFα-activated monolayers, as might be expected if the bFGF signal was particularly sensitive to low affinity complementation. In fact, there was a slight, but statistically insignificant, increase in A-NK binding, which most likely was attributable to the soluble binding of bFGF. This

143

overall effect of heparin was evident for a broad range of heparin dosages, varying from 1 to 200 µg/ml, and did not influence the level of binding to the treatment control groups. These results are strongly supportive of the expression assay findings that CAM inhibition by bFGF was unaltered by the presence of supplemental heparin.
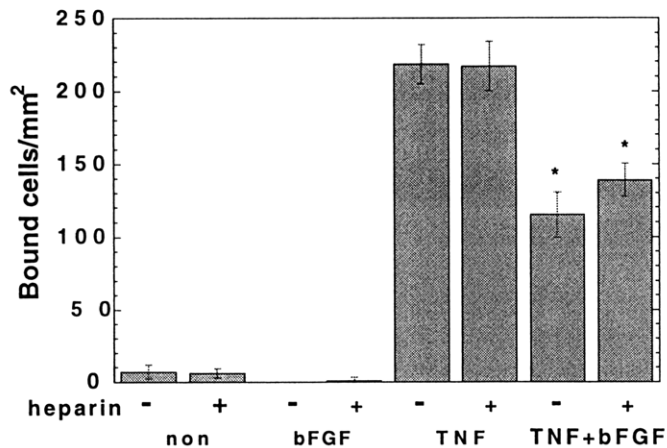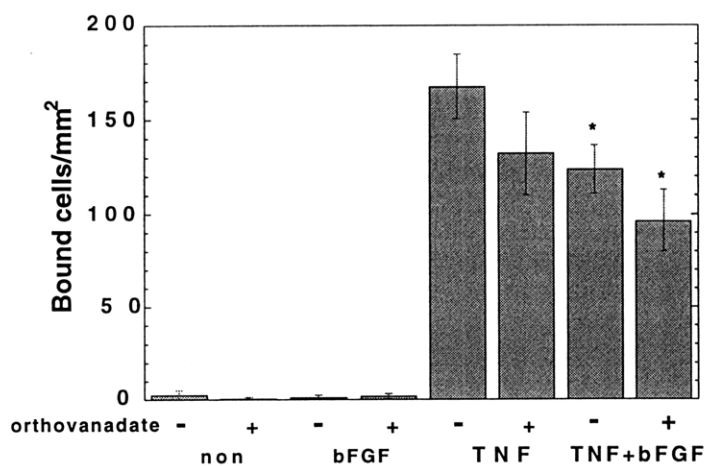

Figure 6-4-11. Effect of exogenous heparin (10 µg/ml) on A-NK cell binding to HUVEC monolayers treated with bFGF, TNFα, and TNFα + bFGF. Mean numbers ± SD of bound cells for eight adjacent fields are shown for 1 of 3 representative flow experiments. * p < 0.05 compared to control values.

The activation of the bFGF receptor tyrosine kinase, the third stage in the signal transduction cascade analyzed using the expression assay, was next explored for its functional significance on A-NK binding. In agreement with the reduced levels of ICAM-1, VCAM-1, and E-selectin found upon blockage of the RTK by MDHC on TNFα-treated monolayers, decreased A-NK cell binding was demonstrated to occur at significant levels, with approximately a 30% reduction compared to controls (Figure 6-4-12). While changes in baseline levels were found to be insignificant, the ability of bFGF to inhibit lymphocyte binding to TNFα-treated monolayers was abrogated by blocking RTK activation. Therefore, specific phosphorylation of its receptor tyrosine kinase is essential for both the inhibition of CAM expression and function under physiological flow conditions.
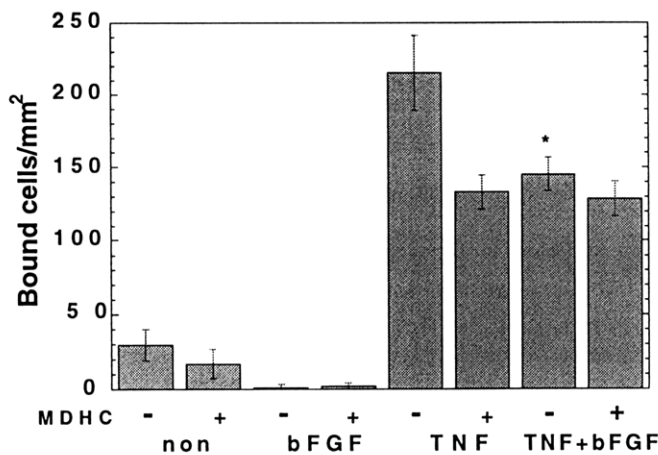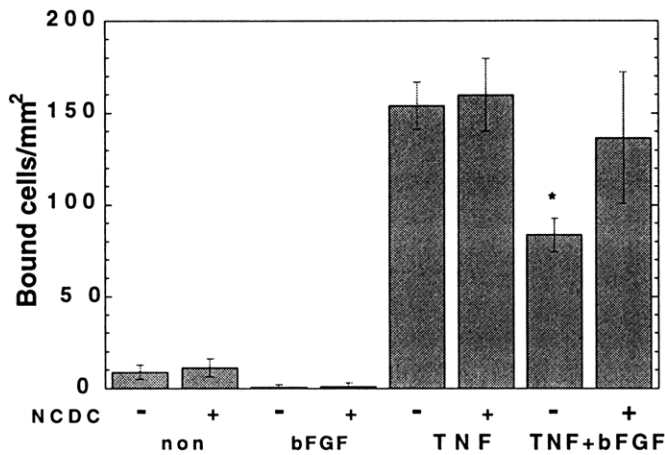

Figure 6-4-12. Effect of MDHC (5 µM) on A-NK cell binding to HUVEC monolayers treated with bFGF, TNFα, and TNFα + bFGF. Mean numbers ± SD of bound cells for eight adjacent fields are shown for 1 of 3 representative flow experiments. * p < 0.05 compared to control values.

In an effort to place further emphasis on the role of tyrosine kinase phosphorylation by both bFGF, in mediating its inhibitory response, and TNFα, in mediating its excitatory response, sodium orthovanadate was used as the particular blocking compound against tyrosine phosphatase activity and studied under flow conditions. The results obtained, which are shown in Figure 6-4-13, were found to correlate reasonably well with the expression data. Namely, the reduction in TNFα-induced VCAM-1 expression by vanadate (40%) was associated with a corresponding decrease (18%) in the A-NK cell binding to the monolayer, emphasizing the importance of tyrosine phosphorylation on TNFα-mediated VCAM-1 expression and function. Also, by blocking the phosphatase action, the inhibitory action of bFGF was not only found to remain active, but was even enhanced. However, this enhancement was more likely the result of decreased VCAM-1 induction by TNFα on PTP inhibited monolayers, as demonstrated by FIA analysis, than an actual increase in the proficiency of bFGF-mediated reduction in lymphocyte binding. Lastly, the slight increase in baseline VCAM-1 and E-selectin expression that was found to occur by PTP inhibition did not contribute significantly to A-NK cell binding. This was likely due to the increased CAM levels being below kinetically favorable concentrations for cell binding. Therefore, it can be concluded that the phosphorylation of tyrosine kinases is necessary for the bFGF-mediated inhibitory process, as well as being contributory to TNFα-induced VCAM-1 expression and function.
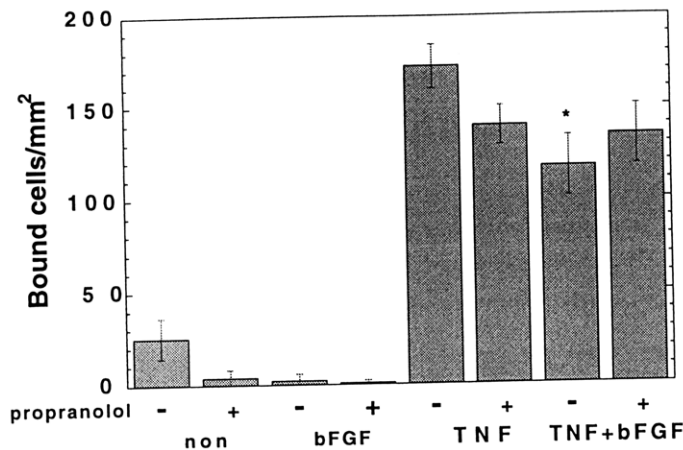

Figure 6-4-13. Effect of sodium orthovanadate (30 µM) on A-NK cell binding to HUVEC monolayers treated with bFGF, TNFα, and TNFα + bFGF. Mean numbers ± SD of bound cells for eight adjacent fields are shown for 1 of 3 representative flow experiments. * $p < 0.05$ compared to control values.

With the role of the receptor tyrosine kinase having been found to be essential for bFGF-mediated regulation of both protein expression and lymphocyte adhesion, the functional relevance of the biologically effective PLC activation, a RTK substrate, was

145

subsequently studied. HUVEC monolayers treated with TNFα and exposed to the PLC blocking agent, NCDC, demonstrated no difference in their ability to bind A-NK cells (Figure 6-4-14). Although in contrast to the finding that ICAM-1 and E-selectin were suppressed by PLC blockage, the relative level of downregulation may not have been sufficient to elicit a functional response to lymphocyte binding, thereby accounting for the indifferent cell binding densities on the monolayers. As for the bFGF response, blocking the action of PLC resulted in significant suppression of the inhibitory effect of bFGF on both TNFα-treated and non-treated monolayers, with A-NK binding reaching levels nearly equivalent to TNFα and baseline controls. These findings were in direct correlation with the expression results, and provides additional support to the contributory role of this mediator in bFGF signaling.
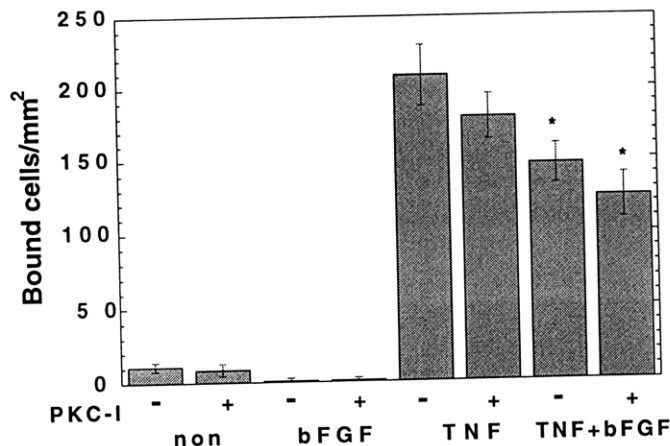

Figure 6-4-14. Effect of NCDC (50μM) on A-NK cell binding to HUVEC monolayers treated with bFGF, TNFα, and TNFα + bFGF. Mean numbers ± SD of bound cells for eight adjacent fields are shown for 1 of 3 representative flow experiments. * $p < 0.05$ compared to control values.

As found for phospholipase C, phospholipase D was also demonstrated to provide a significant role in the bFGF-mediated reduction in A-NK cell binding and CAM expression. As shown in Figure 6-4-15, when HUVEC monolayers were exposed to the phospholipase D inhibitor, propranolol, the inhibitory action of bFGF on lymphocyte binding was abolished and effectively reached the levels obtained by the TNFα control group. Results obtained from FIA analysis were in close agreement with these functional findings.

As for the effect of the blocking agent on TNFα signaling, it was also found to be modestly inhibitory. A-NK cell binding to TNFα-treated monolayers were reduced by 15% compared to unblocked TNFα controls. This was in agreement with the decreased levels of VCAM-1 demonstrated in the expression analysis.

146

Figure 6-4-15. Effect of propranolol (50 μM) on A-NK cell binding to HUVEC monolayers treated with bFGF, TNFα, and TNFα + bFGF. Mean numbers $\pm$ SD of bound cells for eight adjacent fields are shown for 1 of 3 representative flow experiments. * $p < 0.05$ compared to control values.

With the involvement of both PLC and PLD in the bFGF response, and partly to the TNFα response, it becomes circumspect as to the scope of the downstream second messenger PKC in contributing to the response. Functional studies were conducted to provide additional insight, as well as biological relevance, to the expression results obtained earlier. As shown in Figure 6-4-16, monolayers treated with TNFα were found to be slightly less conducive to A-NK cell binding when PKC activity was blocked by calphostin C. This effect could be attributed to the decreased VCAM-1 expression which was found to occur when PKC activity was blocked.

As for the bFGF response, blocking of PKC actually further decreased the level of A-NK binding to the endothelial cell monolayers. Although the inhibition of TNFα-induced VCAM-1 expression by bFGF is slightly reduced by blocking PKC activity, the overall effect of calphostin C causes a significant reduction in the level of VCAM-1 expression. When compounded by the PKC-independent decrease of ICAM-1 and E-selectin by bFGF, the overall decrease in the binding levels observed can be explained by the expression results.

Figure 6-4-16. Effect of calphostin C (50 nM) on A-NK cell binding to HUVEC monolayers treated with bFGF, TNFα, and TNFα + bFGF. Mean numbers $\pm$ SD of bound cells for eight adjacent fields are shown for 1 of 3 representative flow experiments. * $p < 0.05$ compared to control values.

For additional insight into the involvement of PKC in mediating the inhibitory response of bFGF at the functional level, the phorbol ester PMA was utilized for its ability to increase CAM expression largely through PKC. As shown in Figure 6-4-17, a 3 hr, low dose PMA treatment effectively enhanced the ability of A-NK cells to bind to the monolayers, producing a near 15-fold increase. Additionally, monolayers pretreated with bFGF for 24 hrs showed significant reduction in the ability of PMA to elicit cell binding. These findings directly correlated with the expression results, which demonstrated increased levels of ICAM-1, VCAM-1 and E-selectin following short term PMA treatment, and their effective suppression upon pretreatment with bFGF.

When calphostin C was added 2 hrs prior to PMA treatment, the resultant level of A-NK adhesion was effectively reduced, in agreement with the expression results showing decreased levels of expression of all three CAMs. Moreover, monolayers treated with calphostin C obviated the ability of bFGF to inhibit PMA-induced cell adhesion. In concordance with the expression results involving PMA, it would appear evident that bFGF acts at least partly through PKC signaling in mediating its inhibitory response.
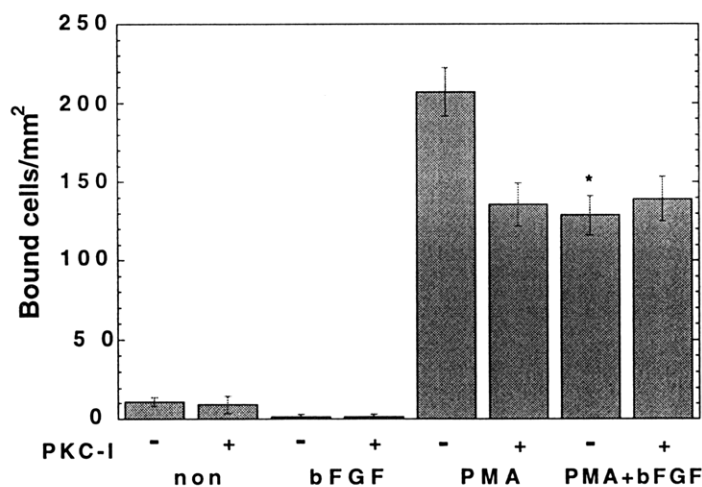
Figure 6-4-17. Effect of calphostin C (50 nM) on A-NK cell binding to HUVEC monolayers treated with bFGF (10 ng/ml), PMA (100 nM), and PMA + bFGF. Mean numbers ± SD of bound cells for eight adjacent fields are shown for 1 of 3 representative flow experiments. * $p < 0.05$ compared to control values.

To provide an additional means for assessing bFGF and TNFα signaling, a long term (48 hrs), high dose (200 nM) PMA treatment was also given to the HUVEC monolayers to effectively deplete the cells of intracellular PKC. Monolayers subsequently given TNFα treatment for 24 hrs showed reduced, but significant levels of A-NK cell binding (Figure 6-4-18). Presumably, the increase in cell binding was the result of TNFα utilizing its PKC-indpendent mechanism to upregulate ICAM-1 and E-selectin expression.

Addition of bFGF to these monolayers demonstrated significant reduction in A-NK cell binding, providing additional evidence that bFGF also utilizes a PKC-independent pathway in its functional inhibition of lymphocyte binding.
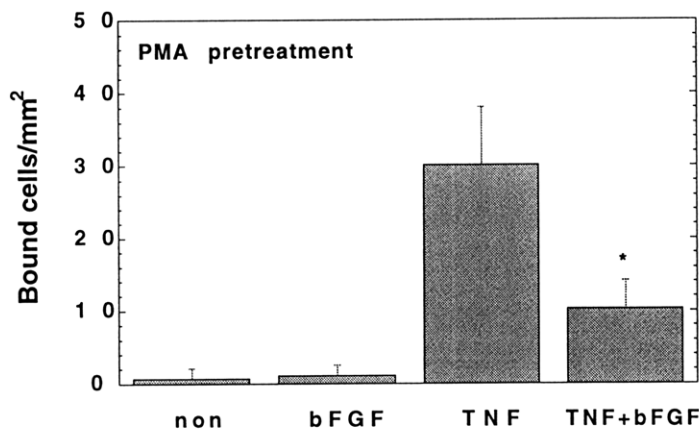
Figure 6-4-18. Effect of A-NK cell binding by long term, high dose PMA treatment of HUVEC monolayers treated with bFGF, TNFα, and TNFα + bFGF. Mean numbers ± SD of bound cells for eight adjacent fields are shown. * p < 0.05 compared to control values.

6.5 Generalization of Findings

The findings above provide significant insight into the particular mechanisms by which bFGF is able to regulate CAM expression and function on TNFα- and PMA-treated monolayers. While this provides invaluable information to the potential role of bFGF in normal physiology, as well as pathological disease, the scope of the work presented in this chapter has been rather limited to specific cell-types and CAM excitatory/inhibitory agents. To provide an increased breadth to the work, four specific questions were addressed: a) does bFGF act to inhibit lymphocyte binding to HUVECs treated with a cytokine or growth factor other than TNFα; b) do other members of the FGF family exhibit similar inhibition responses in endothelial cells; c) are other endothelial cell-types responsive to the inhibitory action of bFGF; and d) are other lymphocyte subpopulations inhibited from binding to activated endothelial cells?

Preliminary studies were first conducted using the proinflammatory cytokine IL-1β as an alternative positive modulator of CAM expression. HUVEC monolayers treated with 50 ng/ml of the cytokine for 24 hrs were able to increase A-NK cell binding by 10-fold compared to baseline levels (Figure 6-5-1a). Moreover, the addition of 10 ng/ml of bFGF resulted in a significant decrease (45%) compared to positive controls. This inhibitory effect was not only associated with proinflammatory cytokines, but also shown to exist on HUVEC monolayers treated with the angiogenic factor VEGF (see Chapter 5). Therefore, the inhibitory influence which bFGF partakes on the cells is not dependent on the specific

positive modulator utilized, but rather by the competitive inhibition of converging downstream intracellular signals or the regulation of transcriptional activity of the CAM genes.

(A)

(B)

(C)
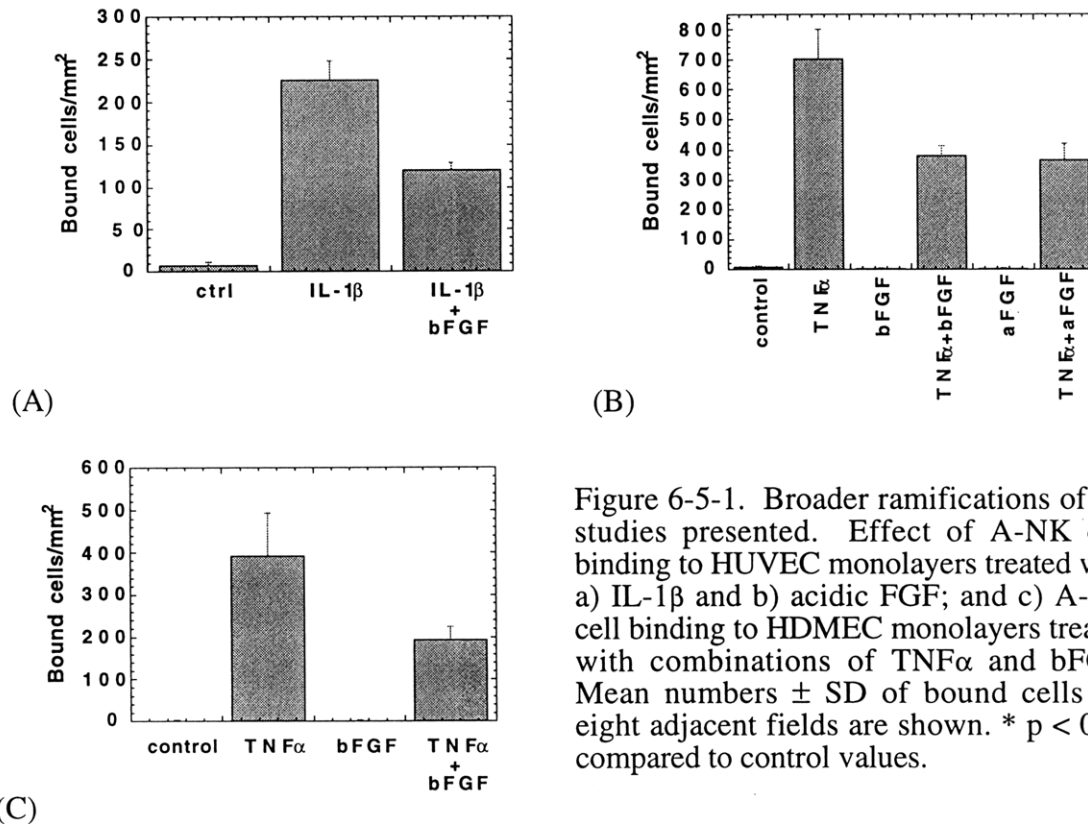
Figure 6-5-1. Broader ramifications of the studies presented. Effect of A-NK cell binding to HUVEC monolayers treated with a) IL-1β and b) acidic FGF; and c) A-NK cell binding to HDMEC monolayers treated with combinations of TNFα and bFGF. Mean numbers ± SD of bound cells for eight adjacent fields are shown. * $p < 0.05$ compared to control values.

As one of the prototypical members of the FGF family, bFGF (FGF-2) may utilize similar signal transduction pathways as other members in eliciting its response on endothelial cells. To explore this possibility, HUVEC monolayers were treated with acidic FGF (FGF-1) for a 24 hr period and tested for their ability to inhibit TNFα-induced A-NK cell binding. As shown in Figure 6-5-1b, acidic FGF at a concentration of 10 ng/ml was able to significantly suppress the level of A-NK binding to the monolayers treated with TNFα, and the reduction was equivalent to that obtained by basic FGF. Also, treatment schemes combining both aFGF and bFGF showed no additional influence on cell binding, suggestive of similar signaling pathways being utilized. These results imply that FGF-family proteins may globally produce inhibitory regulation of CAM expression and function. Additional experiments are needed to explore this potential using other, non-prototypical, members of the family.

150

Also critical to the understanding of FGF-mediated inhibition is the cell-type in which it is studied. The specific role of each messenger in mediating the cellular functions of bFGF, as well as TNFα and other cytokines, are strongly cell-type dependent [Jaye, et al., 1992; Schütze, et al., 1992]. In keeping with the endothelial cell model, human dermal microvascular endothelial cells (HDMECs) were utilized to examine whether bFGF is able to elicit similar inhibitory characteristics on A-NK cell binding. As shown in Figure 6-5-1c, monolayers treated with bFGF were found to significantly reduce the level of binding on TNFα-activated HDMEC monolayers. Therefore, similar signaling characteristics and responses may exist in the two venular endothelial cells with respect to bFGF, which may, in turn, imply similar potential in other endothelial cell subtypes.

Lastly, the biological relevance of the CAM modulation by bFGF on endothelial cells has largely been studied using A-NK cells. While t his lymphocyte subpopulation possess distinct binding kinetics compared to others, the general binding characteristics are similar and there is universal inhibition in binding under modified counter-receptor levels. A more complete and detailed analysis is provided in Chapter 4.

6.6 Conclusions

The important results obtained from the studies performed in this chapter on the molecular mechanisms of bFGF inhibition of CAM expression and function can be generally summarized as follows: a) bFGF does not appear to act through a paracrine mechanism to inhibit the functional binding of lymphocytes to activated endothelium; b) bFGF acts to inhibit protein synthesis, as opposed to increasing the rate of protein degradation, by suppressing TNFα-induced mRNA expression of ICAM-1, VCAM-1, and E-selectin; c) the decrease in mRNA expression by bFGF is not due to changes in mRNA stability, but rather a reduction in the rate of transcription of the CAM genes; d) bFGF utilizes a signal transduction pathway which involves the activation of its receptor, phospholipase C-γ, phospholipase D, and partially protein kinase C; and e) the inhibitory effect on A-NK cell binding can be extended to other members of the FGF family, and the response is effective on other endothelial cell types, lymphocyte subpopulations, and inflammatory cytokines.

Results obtained from the previous chapter demonstrated a significant delay in the ability of bFGF to inhibit ICAM-1 and VCAM-1 protein expression induced by TNFα, which was directly correlated with functional studies using the parallel-plate flow chamber. The significant time delay raised speculation on the mechanism used by bFGF in regulating the response.

151

When bFGF binds to its receptor, the bFGF-FGFR complex is internalized and the surface receptors are downregulated. Unlike other growth factors, bFGF is not degraded through the lysosomal pathway, but is taken up in the nucleus [Baldin, et al., 1990; Moscatelli, 1988]. While it remains to be elucidated as to how the nuclear translocation of bFGF affects signal transduction, the delayed inhibitory response of bFGF on the protein level found in the previous chapter was suggestive of a ligand/receptor complex being a rate-limiting step, as hypothesized for the long-term exposure required for bFGF to induce proliferation in endothelial cells [Hawker and Granger, 1994]. However, the mRNA expression kinetics analyzed in this investigation using Northern blot analysis were shown not to be in agreement with such a limitation. For instance, VCAM-1 mRNA was found to be reduced within 2 to 4 hrs of exposure to monolayers treated with both TNFα and bFGF, compared to monolayers just treated with TNFα, which is comparatively faster than the time suggested by the protein studies. This may be hypothesized as a result of a threshold limitation being evident on the protein level, and would not appear to be the result of a transport limitation of the receptor complex.

As another source of the latency observed at the protein level, bFGF was suggested as possibly inducing the production of a second substance which actually mediated the observed effects in a paracrine-type mechanism. However, functional studies performed in this investigation using conditioned medium from bFGF-treated monolayers demonstrated no discernible increase in the kinetic response. Additionally, the mRNA kinetics were more suggestive of a direct response by the endothelial cells than to a secondary effect.

The direct evidence of the regulation of inducible CAM expression at the mRNA level by bFGF additionally raised the question of whether it acted at the transcriptional or translational level. Specific experiments using a transcriptional blocking agent found that the decrease in the ICAM-1, VCAM-1 and E-selectin mRNA levels were due to a reduction in the rate of transcription of the CAM genes and not from changes in the stability of the mRNA. A possible mechanism may involve the inhibition of the activation of the transcriptional factor NF-κB, which has been shown to be used by TNFα in its induction of ICAM-1, VCAM-1 and E-selectin expression [Collins, et al., 1995]. Additional studies are needed using nuclear run-on assays and electrophoretic mobility shift assays to specifically characterize the transcriptional regulation by bFGF and the potential involvement of a NF-κB-dependent mechanism.

A portion of the early signaling pathways used by bFGF in regulating the surface protein expression and function of the TNFα-inducible CAMs was also uncovered in this investigation. It was demonstrated that bFGF specifically interacts with its high affinity tyrosine kinase receptor and does not require additional low affinity interaction with

supplemental heparin in effectively transducing its signal. Based on studies using the specific blocking agents MDHC and sodium orthovanadate, the autophosphorylation of the receptor and its activation of tyrosine residues was found to be essential in further transduction of the signal. In addition, it was shown that NCDC and propranolol, inhibitors of phospholipase C-γ and phospholipase D, respectively, effectively inhibited the bFGF-induced suppression of CAM protein expression and function. These two molecules have been shown to be interconnected in their signaling activity. PLD catalyzes the hydrolysis of phosphatidylcholine, producing a precursor to the formation of diacylglycerol, which activates PKC to further activate PC-PLD. PLC-γ, activated by tyrosine phosphorylation, catalyzes the hydrolysis of phosphoinositides to produce diacylglycerol and inositol phosphates, which activate PKC and potentially PC-PLD. Subsequent analyses using two specific inhibitors of PKC, calphostin C and bisindolylmaleimide, were shown to produce a partial inhibition of the bFGF-mediated suppression of TNFα-induced CAM expression, but complete inhibition of the bFGF-mediated suppression of PMA-induced CAM expression.

Implications for the results presented in this chapter include the following: a) contributing to a better understanding of the signaling pathways used by bFGF to modify cell adhesion molecule expression, and the relation to its other physiological functions, such as cell proliferation, migration, and angiogenesis; b) providing insight into angiogenic processes and the kinetic responses elicited by specific growth factors in the microenvironment; c) improving current cancer therapies by providing potential mechanisms for drug intervention to control CAM expression in tumors, regulate metastatic potential, and increase immune cell localization; and d) improving current therapies for immunologically-based complications, such as auto-immune diseases, graft and transplant rejection, and even atherosclerotic plaque formation.

Chapter 7

Conclusions

7.1 Summary

The investigations carried out in this thesis used a combination of engineering and biological principles to provide an improved understanding of the *in vitro* binding mechanisms of lymphocyte subpopulations, regulation of cell adhesion molecule (CAM) expression by angiogenic factors, and the intracellular signaling mechanisms used by bFGF to modulate CAM expression on vascular endothelial cells.

The following conclusions were formulated from the studies performed in this thesis:

(i) *Lymphocyte binding kinetics.*

Using the parallel-plate flow chamber, it was determined that IL-2 activated and non-activated lymphocyte subpopulations (CD4+, CD8+, and CD56+ cells) vary in their ability to adhere to activated vascular endothelial cells. More specifically, CD56+ cells demonstrate an increased binding avidity over the other cell subtypes for a wide-range of physiological flow rates. Also, activated lymphocytes are able to bind to endothelial cell monolayers at increased levels of efficiency over the non-activated populations. The lymphocyte subset binding kinetics were found to depend on the level of counter-ligand expression on the endothelium and the state of activation of the lymphocytes. Additional studies demonstrated that IL-2 activated natural killer cells (CD56+) principally utilize an integrin-dependent (β_1 and β_2), selectin-independent adhesion process in binding to activated vascular endothelium.

(ii) *CAM modulation by angiogenic factors.*

Using targeted sampling fluorometry and flow cytometry, it was determined that fluid extracted from the tumor interstitium (TIF) increases specific CAMs on endothelial cells *in vitro*, which is conducive to lymphocyte binding. These results correlate with the *in vivo* findings demonstrating increased adhesion of activated natural killer cells to certain regions of the tumor vasculature, and thus provides an *in vitro* model of the tumor microenvironment. Analysis of the TIF contents revealed it contains significant levels of VEGF, but low or absent levels of bFGF and TNFα. Expression studies on these individual angiogenic factors, as well as TGFβ, showed that TNFα and VEGF are able to upregulate specific cell surface CAMs in a dose-dependent manner with similar temporal kinetics. However, bFGF produces a biphasic effect on ICAM-1 regulation fails to produce an observable effect on the expression of other CAMs. Monolayers treated with TGFβ showed no significant change in the level of CAM expression. Treatment regimens combining bFGF with TNFα or VEGF showed reduced levels of induced CAM expression in a time-dependent process, independent of prior treatment. Also, the biological regulation of surface CAM expression by the angiogenic factors is functionally relevant to lymphocyte binding.

(iii) *Molecular mechanisms of CAM modulation by bFGF.*

The inhibitory effect of bFGF does not appear to act through a paracrine-type mechanism or a rate-limited degradation of the surface proteins. Rather it acts to inhibit new protein synthesis by suppressing the mRNA expression of ICAM-1, VCAM-1, and E-selectin induced by TNFα. The decrease in mRNA levels by bFGF is due to a reduction in the rate of transcription of the CAM genes, and not the result of changes in mRNA stability. The early signaling events involved in this regulation consist of receptor tyrosine kinase activation, followed by the activation of phospholipase C-γ, phospholipase D, and protein kinase C. Additionally, the effects of bFGF can be extended to other members of the FGF family, and are similarly effective on other endothelial cell types, lymphocyte subsets, and proinflammatory cytokines.

7.2 Future Work

The studies presented in this thesis provide important advances in the fields of angiogenesis, vascular biology, tumor physiology and immunology. However, a good deal more remains to be elucidated and understood. Firstly, several of the studies

conducted and the underlying assumptions used are distinctly limited and serve as avenues for further study. Secondly, the results presented provide directive for future studies to expand upon the work and offer new insights to the respective fields. The discussion which follows briefly addresses these possibilities and future directions.

The diversity of the lymphocyte binding kinetics was hypothesized to be the result of differences in the expression of adhesion receptors on the lymphocytes. This was based on the characteristics of the capture efficiencies and the fitted parameters κ and E_o. Additionally, the hypothesis was consistent with findings on β_2 integrin surface density variation between lymphocyte subsets [Pardi, et al., 1989]. To provide a definitive answer, studies are needed using flow cytometry to characterize the surface expression of the adhesion receptors on both IL-2 activated and non-activated lymphocyte subpopulations. Also, antibody blocking experiments would provide functional relevance to the expression data and cast additional insight to receptor-ligand interaction.

As a possible extension to this work, alteration of the receptor expression on specific lymphocyte subsets could be performed using gene transfection or biochemical modification. The former could be done by either directly altering the genetic production of the receptors or incorporating genetic stimulators, such as IL-2, to induce receptor gene expression. This may provide a means for improving the responsiveness and localization of these cells to sites requiring an immunological response.

The results presented in this thesis also showed that the TIF extracted from LS174T tumors contain substantial levels of VEGF, but no detectable levels of bFGF or TNFα. While VEGF was shown to be a positive modulator of CAM expression and function, variability between the TIF samples to promote lymphocyte adhesion did not correlate with VEGF concentration. Further experiments are needed to determine whether other cytokines or growth factors exist within the TIF that can modulate the response. As a possible factor, TGFβ was shown in this study to be a significant inhibitory agent to A-NK cell adhesion, although less than bFGF (46.0 $\pm$ 10.6% for bFGF vs. 15.7 $\pm$ 4.2% for TGFβ). Others have demonstrated that TGFβ suppresses the expression of basal and TNFα-induced E-selectin, but with no observable effects on ICAM-1 or VCAM-1 [Gamble and Khew-Goodall, 1993]. Consequently, TGFβ cannot independently explain the results obtained with the TIF. Further study may reveal that it may either synergize with bFGF or act to suppress VEGF receptor expression in eliciting its response.

As another possible explanation for the TIF effect, additional experiments measuring the viability of the VEGF in the TIF may provide valuable insight. Since a variety of proteases are essential for tumor angiogenesis and migration of tumor cells, VEGF may have a variable susceptibility to these proteases and their heterogeneous

presence. Therefore, the alteration in CAM expression may not be a function of the level of inhibitors or correlate with the level of positive stimulators. This may prove to be a remarkable feature of tumors which has important ramifications for cancer therapies.

To further expand upon the present work, tumors normally lacking the ability to produce bFGF, or another angiogenic factor, may be genetically-engineered to express the specific growth factor. Interstitial fluid collected from these tumors could be compared to unaltered tumors for their specific lymphocyte binding capacities. Addition of high concentrations of exogenous bFGF has already been shown to elicit a suppressive effect on A-NK binding *in vivo* [Melder, et al., 1996], and is suggestive that inherent bFGF production may produce similar results.

The analysis performed on the molecular mechanisms of bFGF-mediated CAM inhibition is also open to further study. The present work has suggested that bFGF acts at the transcriptional level to regulate CAM expression. This was concluded after having shown no significant effect by bFGF on CAM mRNA stability. To provide definitive evidence of the ability of bFGF to alter the rate of CAM gene transcription, nuclear run-on assays are needed to measure the promoter activities of each CAM gene. These studies would preclude additional experiments exploring the potential of bFGF to inhibit NF-κB-dependent transactivation of the CAM genes. This has been proposed as a possible mechanism based on the central role which NF-κB maintains in cytokine-mediated upregulation of CAMs [Collins, et al., 1995]. To address this possibility and provide a conclusive result, electrophoretic mobility shift assays are needed to be performed.

The early signaling pathways used by bFGF in modulating CAM expression may also be studied in further detail. While specific transmembrane molecules and second messengers have been shown to be necessary for the inhibition of CAM expression and function, these studies were limited to using selective inhibitors. These results must be cautiously interpreted due to non-specific effects occurring with other pathways and mediators. Other techniques are available which permit direct measurement of the activation of these messengers, and thus better define their role. Additionally, specific second messenger agonists may be used to provide further validation of the results.

Nevertheless, *in vivo* experiments using similar blocking agents as presented in this thesis need to be conducted in the future. Although many of these agents have already been used in cancer studies, their application has largely been directed towards altering tumor cell growth and proliferation. By specifically focusing their action to the vascular endothelium, it may increase the localization of host immune cells, as well as adoptively transferred lymphocytes. Also, the alteration in counter-receptor expression on the

endothelium may be sufficient to improve lymphocyte subset diversity, as found in the *in vitro* cell binding studies presented.

Similar studies may be performed in analyzing the effect of CAM alteration on metastatic potential. Since the same CAMs are potentially used by metastasizing tumor cells as immune cells, increasing CAM expression may increase the metastatic potential of tumors. To date, this important question has not been specifically addressed and remains essential for future cancer therapies incorporating this strategy.

Another possible extension of this thesis work would be to further define the differences between the VEGF and bFGF signaling pathways. Both growth factors act through similar receptors having intrinsic tyrosine kinase activity. Consequently, many of the same early signaling events are used by both factors and have been shown to mediate their proliferative responses in vascular cells. However, it has been demonstrated in this thesis that the two growth factors have quite different effects on CAM regulation. Additional pathways may exist which have not been well explored that may explain the differences. Kinetic analysis of their signaling activation may also be useful in revealing specific sequencing patterns that are unique to each factor and prove essential for eliciting its response. Clearly, distinct differences exist in the intracellular signaling pathways utilized, and their elucidation would provide an invaluable contribution to tumor physiology, as well as to basic vascular biology.

7.3   Clinical Significance and Implications

For the first time the American Cancer Society has reported a decline in the total number of new cancer cases, with a decrease of more than 11% compared to 1997, and a reduction in the cancer death rates among many cancers [Landis, et al., 1998]. While a significant trend, it has largely been attributed to new early detection and prevention techniques. This fact provides greater incentive for continued research in the treatment of cancer and its effective implementation into the clinic, so that future trends continue on this path. As a contribution to this undertaking, several findings presented in this thesis provide important implications for new insights and strategies.

The strategy of immune-based therapies, or adoptive immunotherapy, continues to hold promise as a systemic-based strategy against cancer. Clinical trials using lymphokine-activated killer cell- and tumor infiltrating lymphocyte-based adoptive immunotherapy have found limited success in treating patients with malignant melanoma and renal cell carcinoma [Rosenberg, 1990]. However, it has been largely unsuccessful in treating other cancers,

and the mechanisms remain to be elucidated. The results obtained in this thesis contribute to a better understanding of the biophysical and molecular mechanisms used by lymphocytes in localizing to the tumor vasculature. Additional insight is also provided to the regulatory and protective mechanisms potentially found in specific tumors by the action of the various angiogenic factors present. This information augments current paradigms of the microenvironmental effects on the evasiveness of tumors, and provides potential mechanisms for drug intervention to increase immune cell localization. These may ultimately improve or modify current adoptive immunotherapy techniques.

Another exciting new area of cancer therapy involves altering the vasculature in a growing tumor. The genomic stability and homogeneity of the endothelial cells make them particularly alluring targets compared to the high genetic instability and heterogeneity of tumor cells. Two primary methods have arisen using this strategy. One uses anti-angiogenic compounds directed against a tumor's endothelial cells [Boehm, et al., 1997], and the other genetically alters endothelial cells to increase the immune response. Several findings presented in this thesis have direct relation to the latter therapeutic option. Firstly, specific intracellular signaling agonists or antagonists may be used to alter the level of CAM expression induced on the endothelium, thereby enhancing the capture rates of circulating immune cells. Additionally, induction of specific counter-ligands on the endothelium may further enhance selective lymphocyte localization and kinetics of binding. These therapies have the benefit of being relatively non-cytotoxic, and may be combined with other tumor-specific agents to enhance their selectivity for the tumor vasculature. However, a potential limitation of this technique is that many of the same CAMs used by immune cells are also used by tumor cells which are metastasizing.

In terms of clinical treatment planning options, physiologically-based pharmacokinetic models continue to be improved and offer invaluable use for optimization and efficacy potential [Zhu, et al., 1996]. Essential to the effectiveness of these models is the accurate prediction or assessment of the kinetic parameters. The studies performed in this thesis on the lymphocyte binding kinetics may serve to enhance the ability of these models to accurately predict the biodistribution of the effector cell populations used in adoptive immunotherapy schemes. Additionally, the new treatment strategies proposed may be applied to the models and assessed for their potential efficacy *in vivo*.

Of even greater potential significance of this thesis are the ramifications of its findings beyond the field of cancer. Numerous other pathophysiological conditions, as well as normal physiological processes, may benefit from its findings. For instance, heart disease continues to have the highest overall mortality rate in the U.S. (32% of all yearly deaths), and is associated with an inflammatory process involving the progressive

formation of atherosclerotic plaques. The plaques eventually lead to the blockage of coronary arteries and formation of ischemic myocardial tissue, and/or the production of emboli resulting in stroke. Consistent with the early events of the disease is the expression of adhesion molecules on the endothelium and the local production of a variety of cytokines. Early therapeutic interventions may serve to prevent destructive downstream consequences.

As a possible therapeutic intervention, stents incorporating the controlled-release of a negative CAM modulator, such as bFGF or similar analogue, may be used to regulate the local CAM expression. Additionally, the angiogenic factor would support the re-endothelialization of the stent by providing a mitogenic stimulus to the cells.

Another therapy which has recently received acclaim is the use of VEGF in enhancing collateral circulation and improving regional perfusion in patients with obstructed coronary arteries. However, a potential drawback to this therapy may be the increased ability of leukocytes to adhere to the local vasculature and eventually lead to the occlusion of the collateral circulation. This may occur by either directly obstructing the blood flow or by initiating the subsequent plaque formation. Use of specific signaling antagonists uncovered in this thesis or by combining treatment with bFGF may serve to provide adequate CAM regulation, while still maintaining angiogenic potential.

Additional implications of this thesis are:

a) providing additional understanding of the binding kinetics of helper and effector cell populations in areas of active immunological response;

b) providing insight to the regulatory and protective mechanisms potentially found in inflammation, ischemic-reperfusion injury and wound healing, by the action of the various angiogenic factors present;

c) providing insight into the angiogenic process and the kinetic responses elicited by specific growth factors in the microenvironment;

d) potentially improving current therapies for immunologically-based complications, such as autoimmune diseases, graft vs. host disease, and transplant rejection.

Appendix A

Binding Kinetics Data

The following supplemental sections present the experimental plots of the IL-2 and non-activated lymphocyte subpopulation binding kinetics. Each set was performed in triplicate under identical flow conditions using the parallel-plate flow chamber. Four treatment groups were analyzed: TNFα, bFGF, TNFα+bFGF and non-treatment. Total activation time for all runs was 24 hr.

A.1 Non-Activated Lymphocyte Binding Data
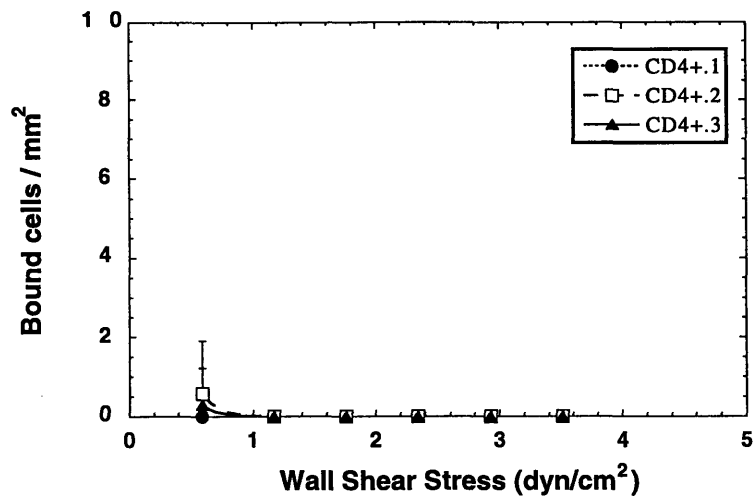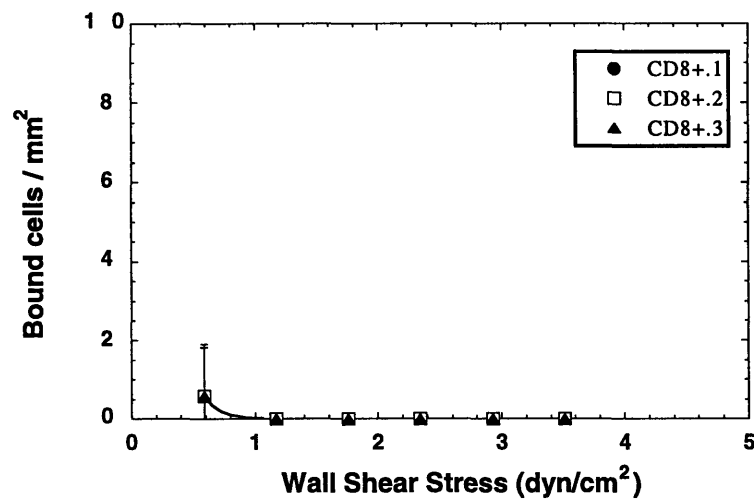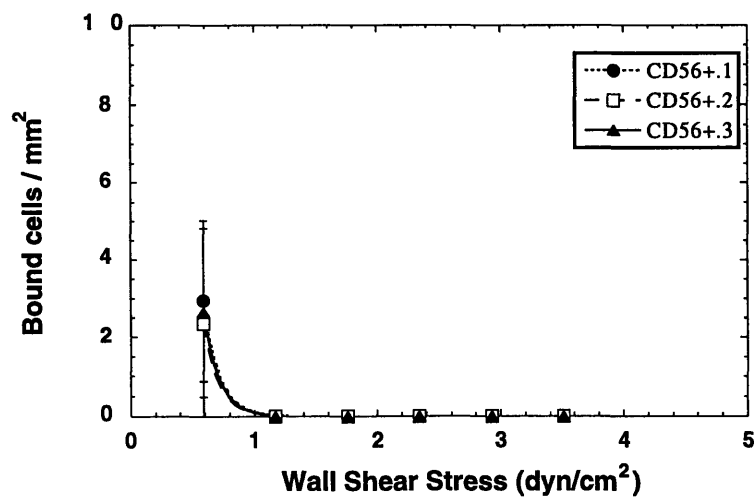
Figure A-1-1. Non-activated lymphocyte binding kinetics on non-treated HUVEC monolayers: (a) CD4+, (b) CD8+, and (c) CD56+.
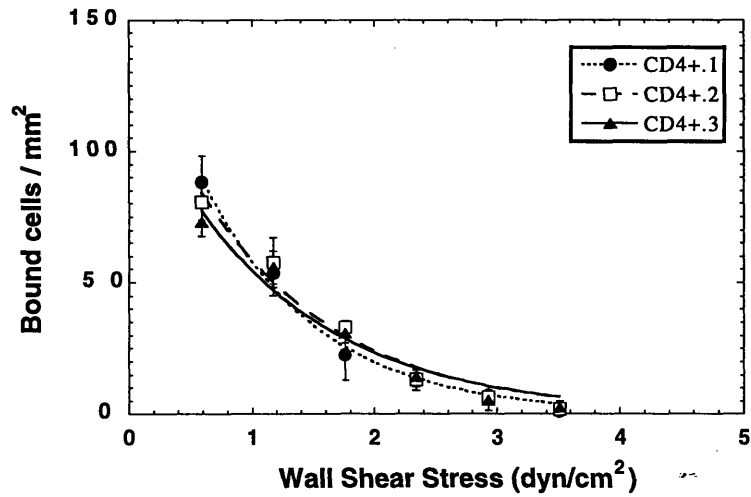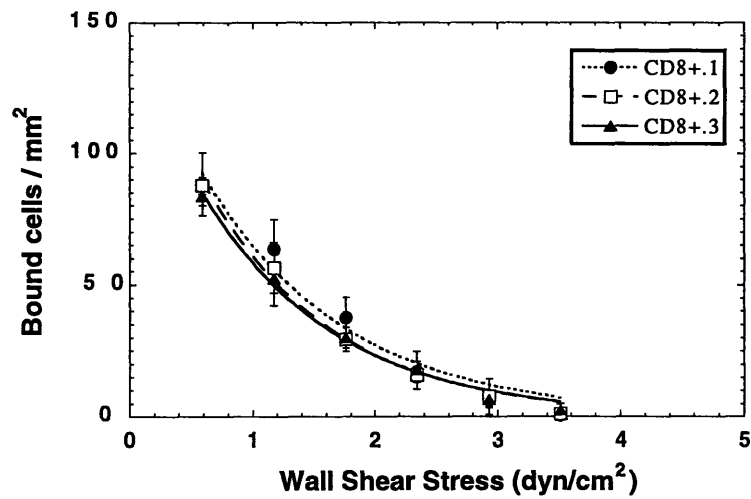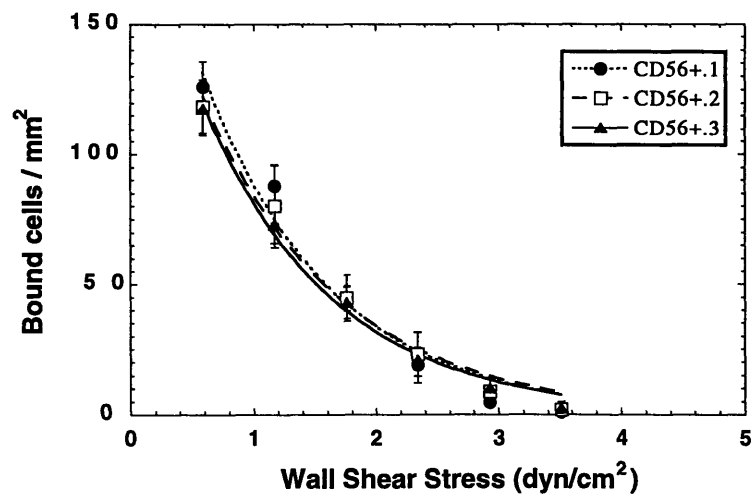
Figure A-1-2. Non-activated lymphocyte binding kinetics on TNFα-treated HUVEC monolayers: (a) CD4+, (b) CD8+, and (c) CD56+.
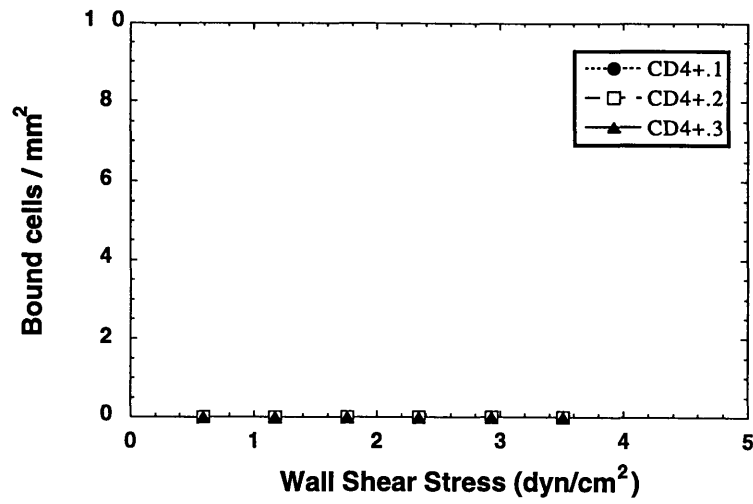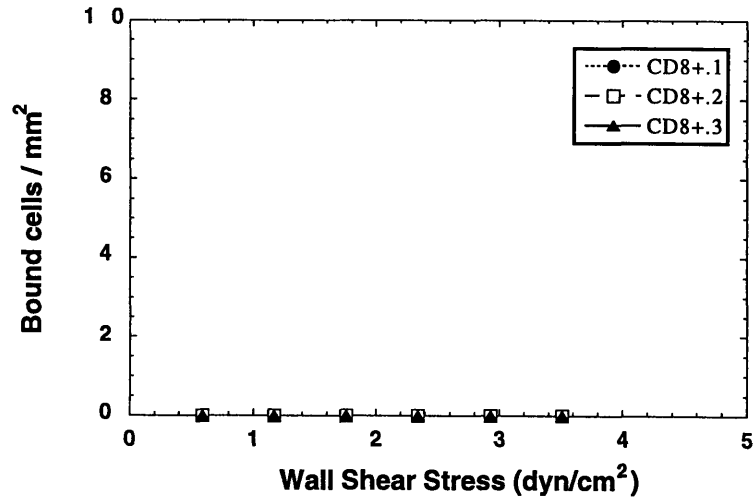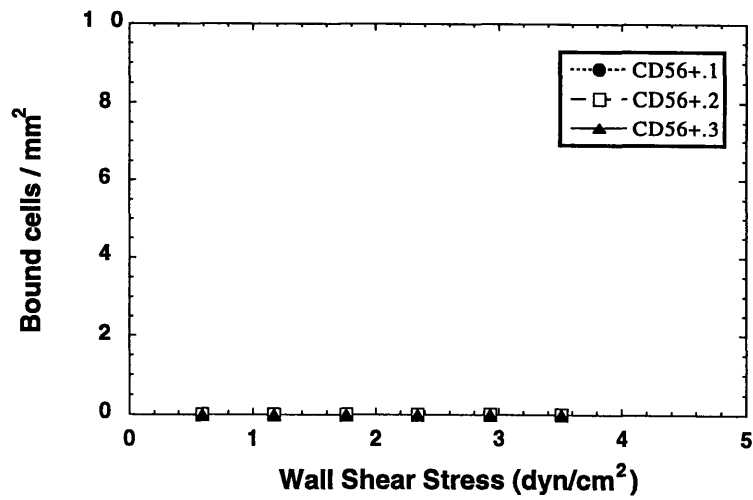
Figure A-1-3. Non-activated lymphocyte binding kinetics on bFGF-treated HUVEC monolayers: (a) CD4+, (b) CD8+, and (c) CD56+.
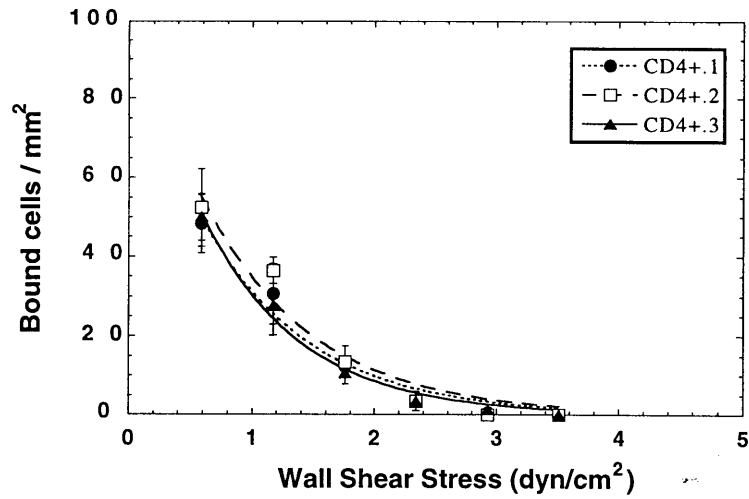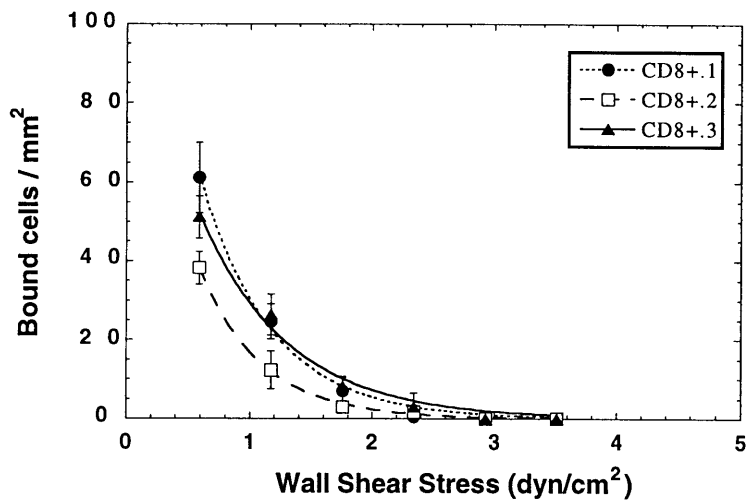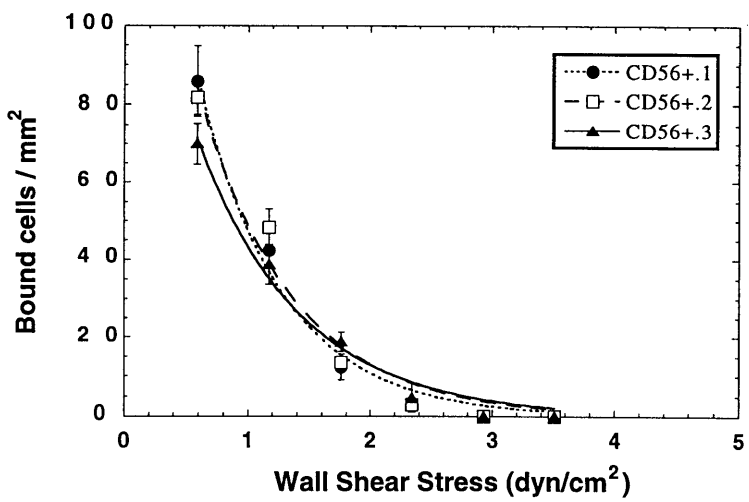
Figure A-1-4. Non-activated lymphocyte binding kinetics on TNFα+bFGF-treated HUVEC monolayers: (a) CD4+, (b) CD8+, and (c) CD56+.

A.2 IL-2 Activated Lymphocyte Binding Data
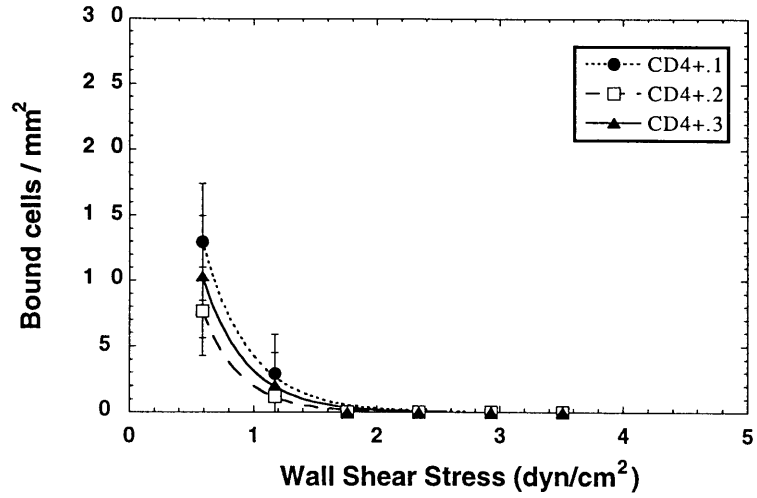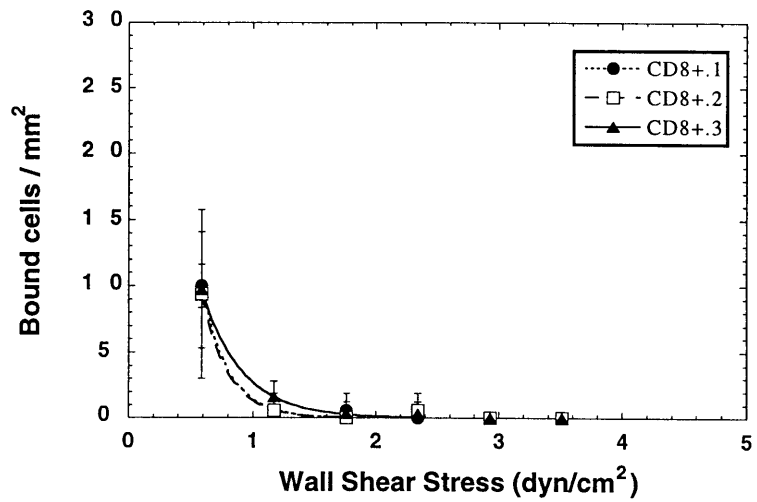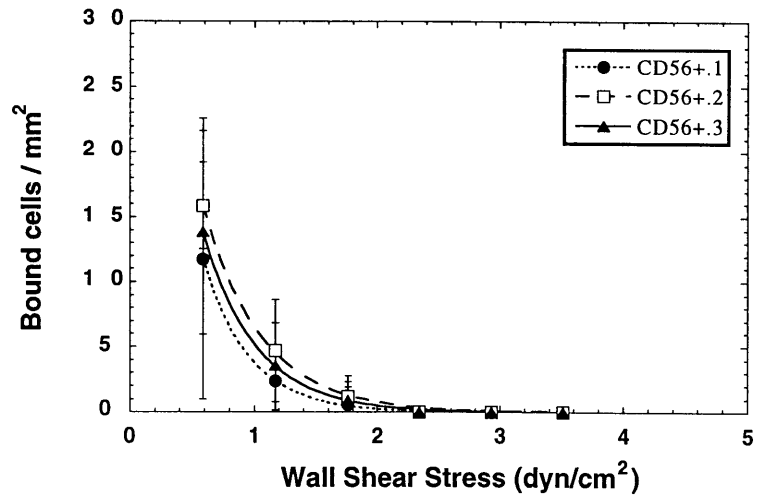
Figure A-2-1. IL-2 activated lymphocyte binding kinetics on non-treated
HUVEC monolayers: (a) CD4+, (b) CD8+, and (c) CD56+.
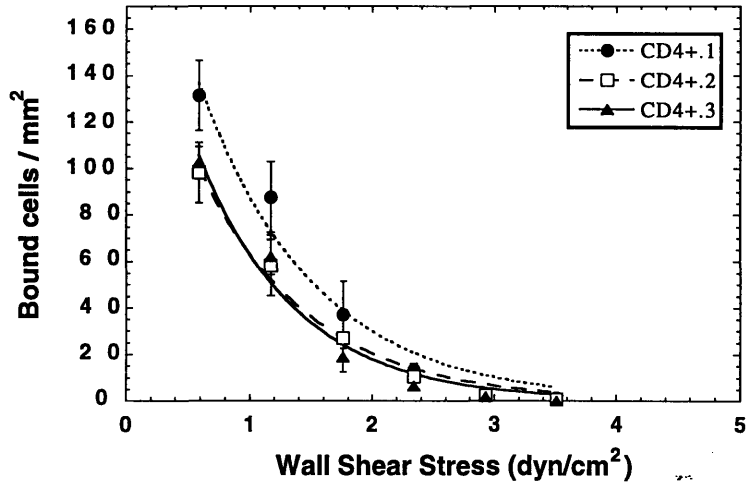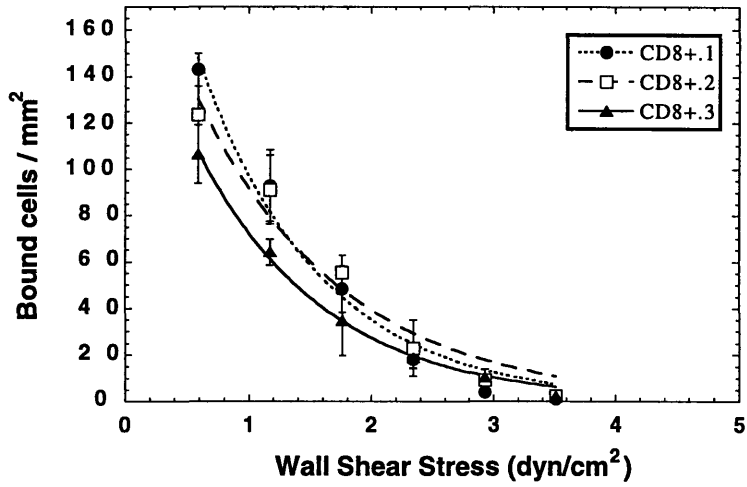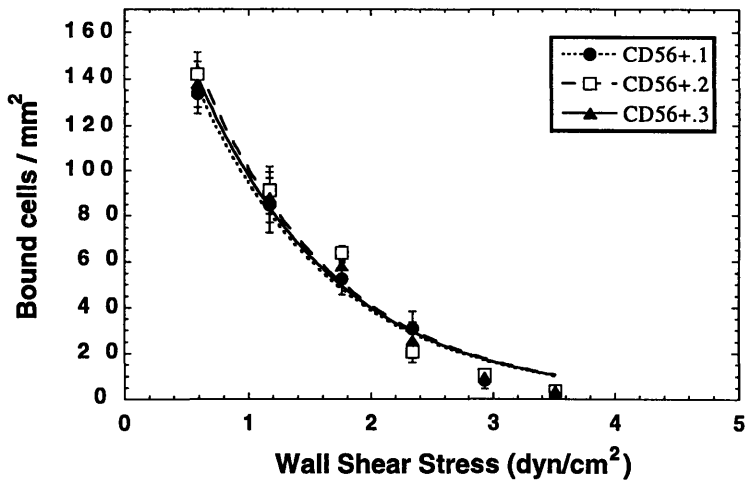
Figure A-2-2. IL-2 activated lymphocyte binding kinetics on TNFα-treated HUVEC monolayers: (a) CD4+, (b) CD8+, and (c) CD56+.
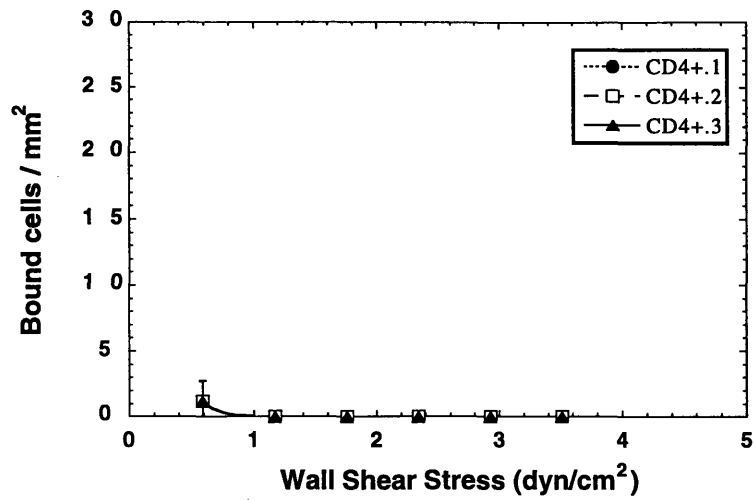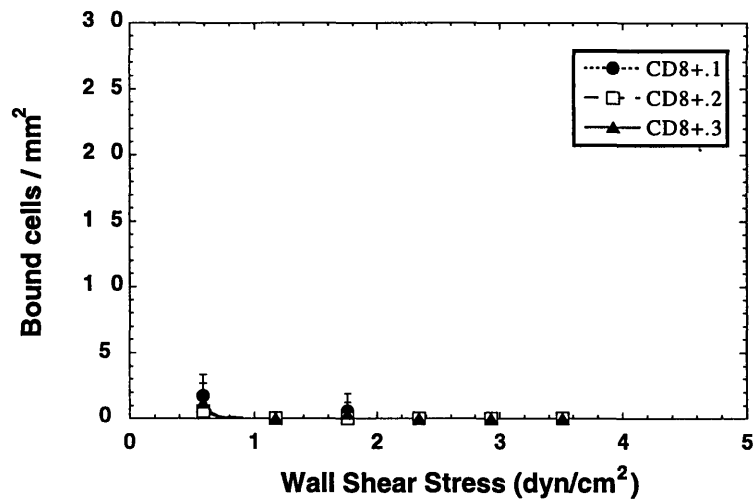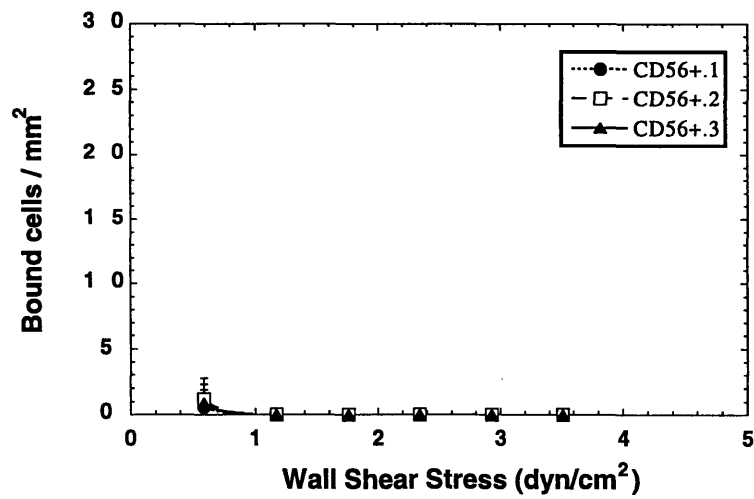
Figure A-2-3. IL-2 activated lymphocyte binding kinetics on bFGF-treated HUVEC monolayers: (a) CD4+, (b) CD8+, and (c) CD56+.
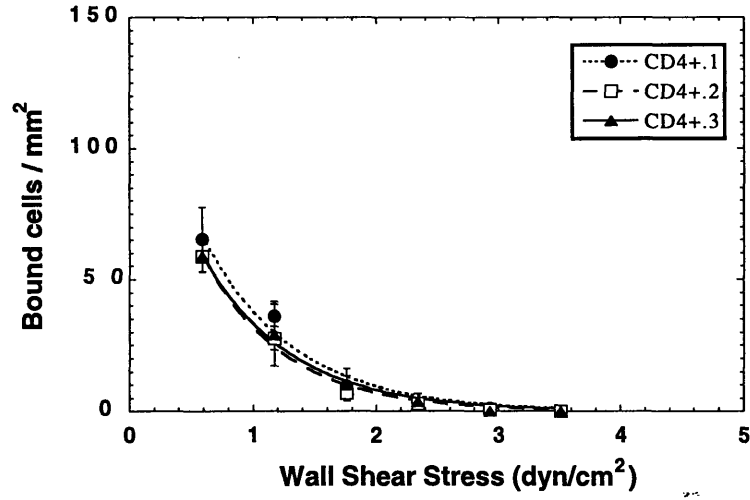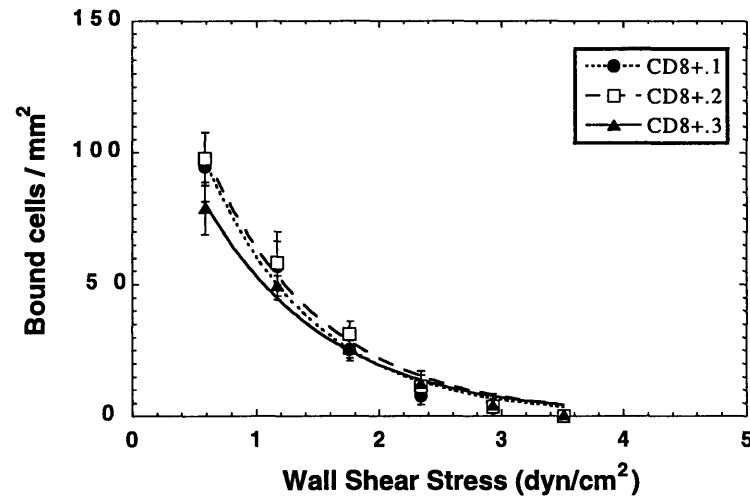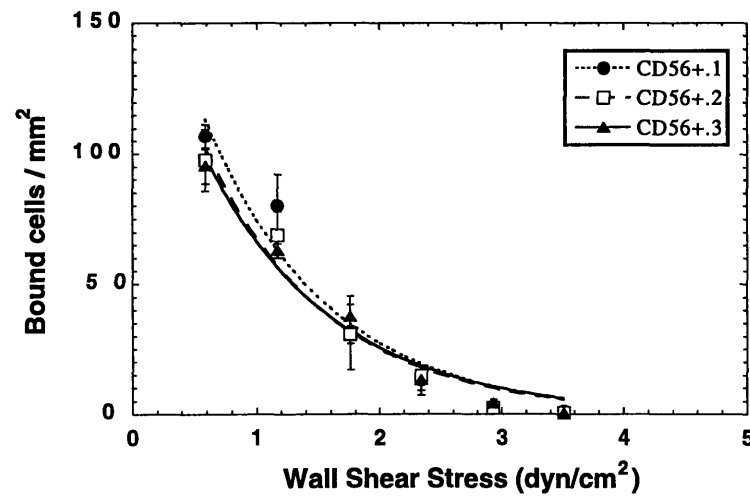
Figure A-2-4. IL-2 activated lymphocyte binding kinetics on TNFα+bFGF-treated HUVEC monolayers: (a) CD4+, (b) CD8+, and (c) CD56+.

A.3   A-NK Receptor Expression Data
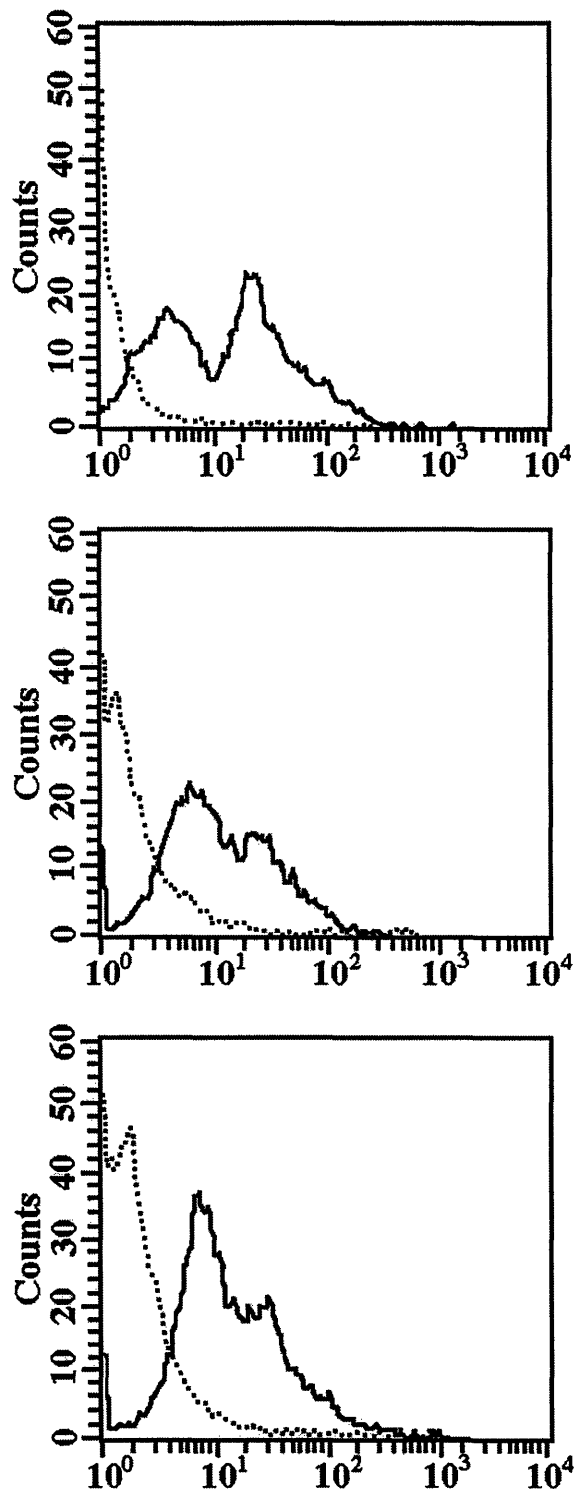
Figure A-3-1. IL-2 activated NK cell expression of CD18. Data sets from three separate experiments shown. IgG istoype control staining represented as dotted lines.
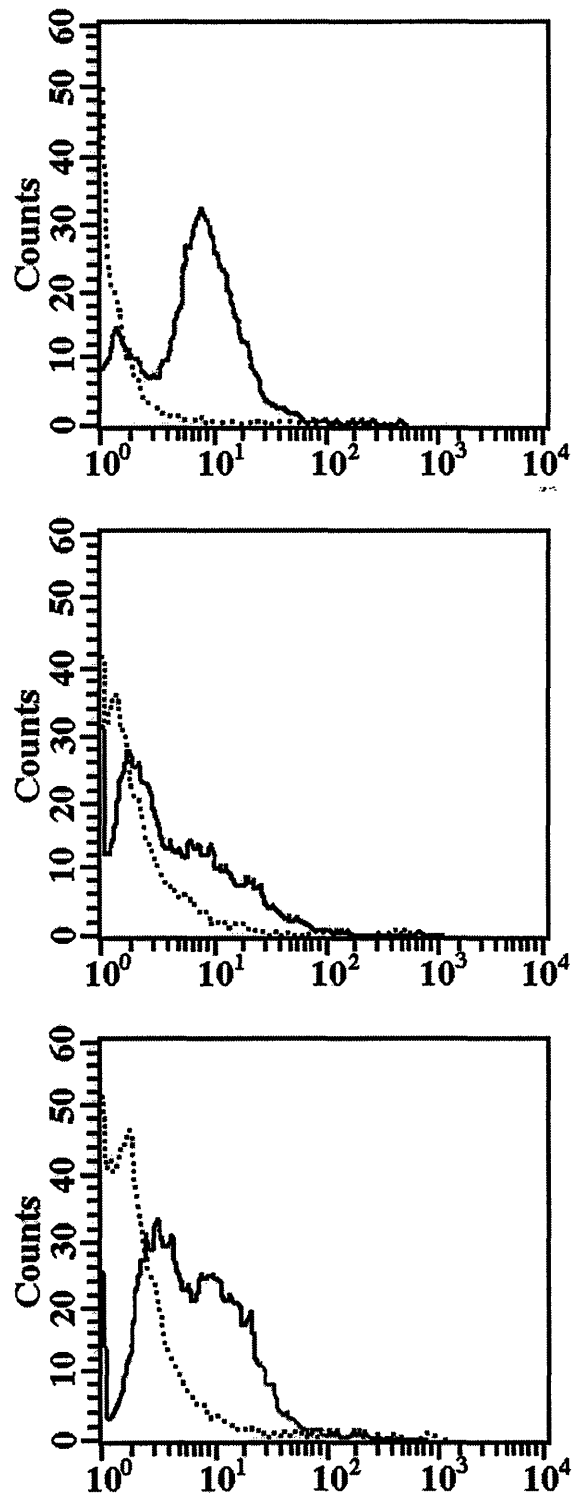
Figure A-3-2. IL-2 activated NK cell expression of VLA-4. Data sets from three separate experiments shown. IgG istoype control staining represented as dotted lines.
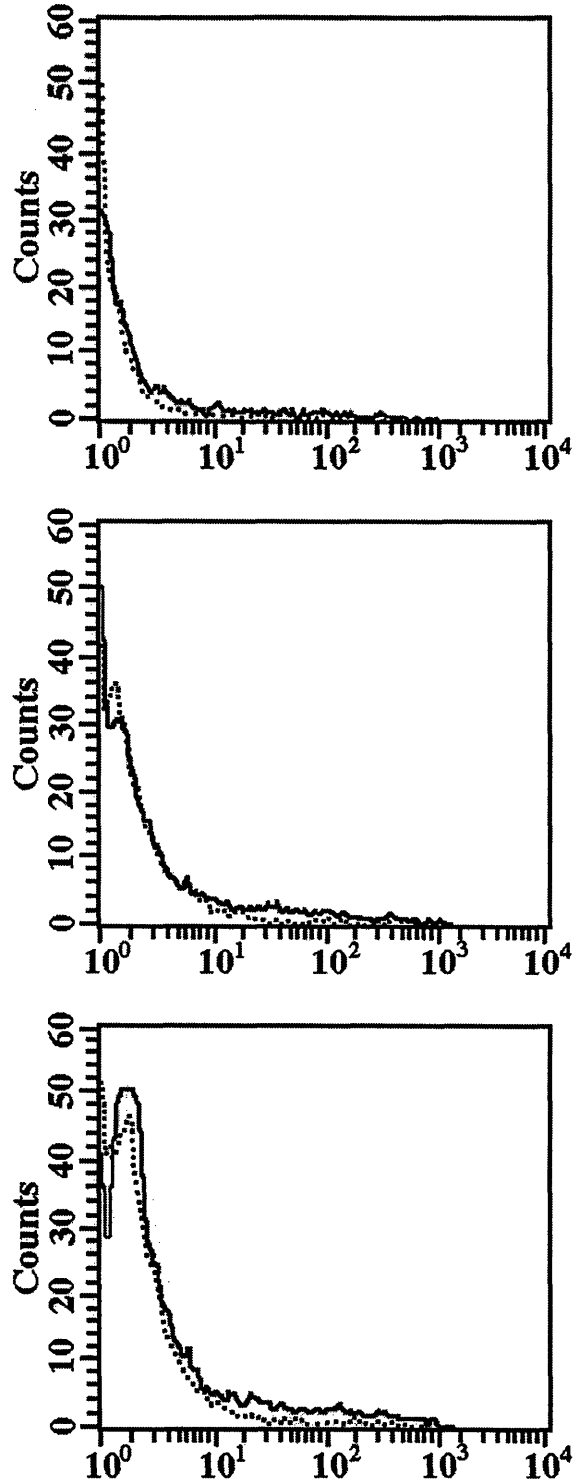
Figure A-3-3. IL-2 activated NK cell expression of sLeX. Data sets from three separate experiments shown. IgG istoype control staining represented as dotted lines.
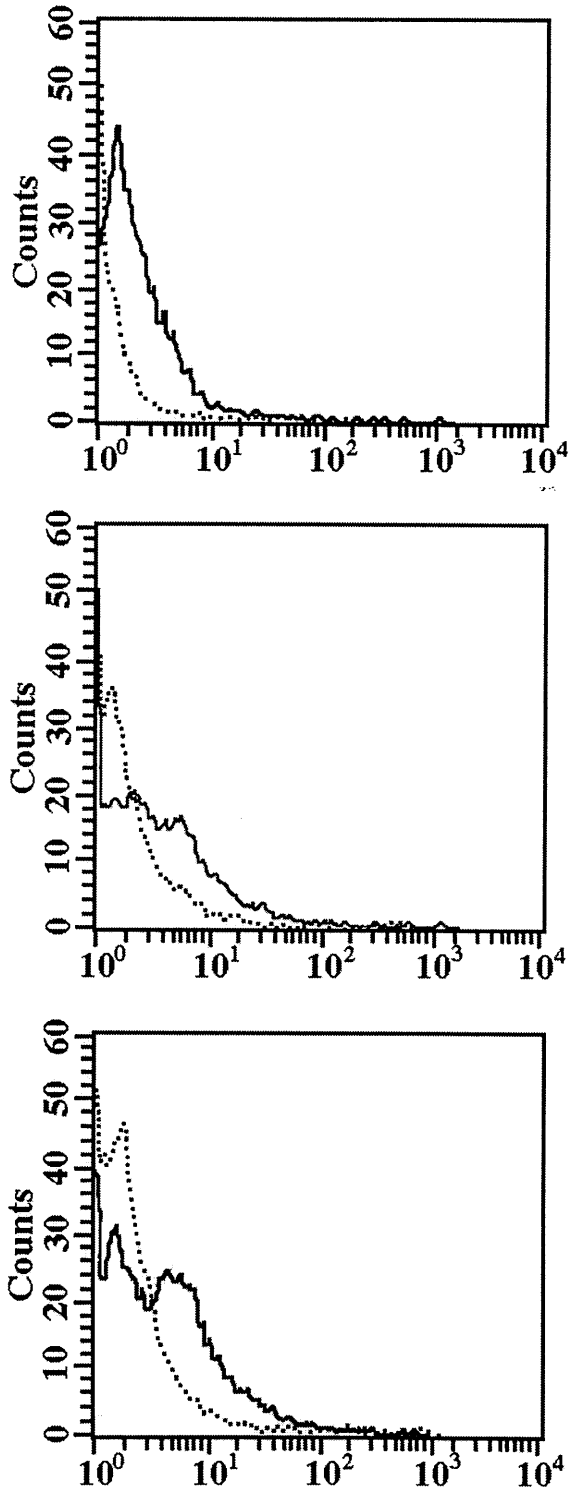
Figure A-3-4. IL-2 activated NK cell expression of L-selectin. Data sets from three separate experiments shown. IgG istoype control staining represented as dotted lines.

Appendix B

CAM Expression Data

The following sections provide supplemental data to the CAM surface expression analyses for HUVEC monolayers treated with tumor interstitial fluid (TIF), TNFα, VEGF, bFGF, TGFβ, and TNFα+bFGF. In addition, the computer algorithm written and used in this research for processing the TSF images using the NIH Image software[4] is provided.

B.1   TSF Algorithm for NIH Image

Macro algorithm for targeted sampling fluorometry (TSF)
By: G.C. Koenig and L.L. Munn
Copyright 1995

This macro is used to retrieve a series of files for obtaining an optimal regional thresholding of nuclear stained images.   In addition, this macro features an automatic ROI sizing routine to accomodate varying cell diameters. It was developed for 20x objective. All images must be located in the same folder and the directory path to this folder must be entered in lines 2 and 3 of the macro (after 'begin'). Images should be labeled with Slide # as the first digit, well# as the second digit, and field# as the third digit (SWF; for example 352 would be the 2nd field from the 5th well of the third slide analyzed). There should be both an image (in our case, green) of the stained surface proteins, and a corresponding image of the nuclear stain (in our case, red), labeled SWFg.tif and SWFr.tif, respectively. The macro was written to analyze images from experiments done in 8 well chamber slides, and it therefore keeps track of the slide, well and field#s. You can change the loop indices for these

---

[4] The NIH Image software and all supporting information are available by anonymous ftp from zippy.nimh.nih.gov.

parameters to suit your application. The "process images" option will do basic noise reduction and background subtraction of the immunostained images. To use this, include a background image labeled "calib" in the image folder. The macro can save a number of the intermediate images as well as the resulting data. If you want, you can supress some of the save commands by enclosing them in brackets. Results for each field are stored in files labeled .data. They include the ROI area (nPix), the average intensity for each ROI (cmean), the modal intensity (cmode), the minimum pixel value (cmin), and the maximum pixel value (cmax). In addition, a running summary file (sum data) is kept that records the filename, the mean pixel value for the entire image (tmean), the average of the ROI means for the field (avg), the associated sstandard deviation (sd), the total area covered by the ROIs (totalarea), and the mean ROI diameter (avgdiam). The parameters listed above are in column order as stated: no headings are supplied }

```
var
        filered, fileg, outfileb,filed:string;
        infileg, infilered,infiler,
        filename2,infilename2,outfilename2,outname1:string;
        outfiled, outfiler, outfileg,test,outfilepg,filepgname:string;
        indirect,indirect2,outdirect,calfilename,file,filegreen,
        filegname,prcalfn:string;
        i,j,c,f,k,mm,opt,temp,image1,tpix,tmax,tmin,totalmean,cal,grnimg,nPixels:
        integer;
        pp,ppp,nfields,process,image2,count,icount,cmode,cmin,cmax,mode,regions:
        integer;
        kkk,m,n,width,height,x,y,w,h,Tlow,Tup,nPix,total,ihigh,ilow,kk,jj,fact,tick,p:
        integer;
        cPix, calibmean, cmode, cmin, cmax: integer;
        dx,dy,tmean,tmode,diameter,max,min,min2,dtotal,tarea,totalarea:real;
        sd,variance,avg,total,cmean,mean,totalmeansqr,con,tdiam,avgdiam:real;

begin
        {**** Input file and folder location ****}
        indirect:=concat('STORAGE:test:');
        outdirect:=concat('Storage:Output files:');
        test:=concat(outdirect,'greet');
        NewTextWindow(test,330,50);
        writeln('Begin Program');
        Wait(1.8);
        SaveAs(test);
        Dispose;
        process:=GetNumber('shading correction? (1=yes, 0=no)', 1);
        nfields:=GetNumber('number of fields per well?', 3);
        NewTextWindow('sum data');

for m:= 1 to 1 do begin {4= number of slides}

                if (process=1) then begin
                calfilename:=concat(indirect,'calib');
                Import(calfilename);
                Smooth;
                SelectAll;
                Measure;
                GetResults(cPix, calibmean, cmode, cmin, cmax);
```

```
                prcalfn:=concat(outdirect,'prcal.1');
                SetPicName(prcalfn);
                {SaveAs(prcalfn);}
                cal:=PicNumber;
        end; {process shading}

        for n:= 1 to 1 do begin  {# of wells}
                for k:= 1 to nfields do begin  {# of fields per well}

                file:=concat( m:1, n:1, k:1);
                filered:=concat(file, 'r.tif');
                filegreen:=concat(file, 'g.tif');
                filegname:=concat(file, 'g');
                filepgname:=concat(file, 'pg');
                infiler:=concat(indirect, filered);
                infileg:=concat(indirect, filegreen);
                outfileg:=concat(outdirect, file,'g');
                outfilepg:=concat(outdirect, file,'pg');
                outfiler:=concat(outdirect, file,'r');
                outfiled:=concat(outdirect, file,'.data');
                outfileb:=concat(outdirect, file,'.bin');

                Import(infileg);
                SetPicName(outfileg);
                SaveAs(outfileg);
                grnimg:=PicNumber;

{ ********* Processing Image Files ********* }

                if (process=1) then begin
                                SelectAll;
                                f:=calibmean;
                                ImageMath('div', grnimg, cal, f, 0, 'Result');
                                ReduceNoise;
                                Smooth;
                                SelectWindow('Result');
                                SaveAs(outfilepg);
                                SelectWindow(filegname);
                                Dispose;
                end; {process}

                Import(infiler);
                SetPicName(outfiler);
                SaveAs(outfiler);
                GetPicSize(width,height);
                image1:=PicNumber;
                SetNewSize(width,height);
                MakeNewWindow('Temporary');
                temp:=PicNumber;
                MakeNewWindow('Optimum');
                opt:=PicNumber;

{ **** Optimal Grid Code **** }
```

```
regions:=5;
dx:=width/regions;
dy:=height/regions;
for x:=0 to (regions-1) do begin
        for y:=0 to (regions-1) do begin
                ChoosePic(image1);
                SelectAll;
                copy;
                ChoosePic(temp);
                paste;
                MakeRoi(x*dx,y*dy,dx,dy);
                AutoThreshold;
                GetThreshold(Tlow,Tup);
                Tlow:=Tlow-0.05*Tlow;
                if Tlow<0 then Tlow:=0;
                if Tlow>255 then Tlow:=255;
                SetThreshold(Tlow);
                MakeBinary;
                copy;
                SelectAll;
                SetThreshold(-1);
                Clear;
                ChoosePic(opt);
                MakeRoi(x*dx,y*dy,dx,dy);
                paste;
        end;
end;
SelectPic(temp);
Dispose;
SelectPic(image1);
Dispose;
SelectWindow('Optimum');
SelectAll;
Invert;
SetBinaryCount(4);
Erode;
SaveAs(outfileb);
```

{***** Setting up Particle Analysis of Binary PI Image *****}

```
SetOptions('X-Y Center');
LabelParticles(false);
OutlineParticles(true);
IgnoreParticlesTouchingEdge(true);
IncludeInteriorHoles(false);
SetParticleSize(50,900);
SelectAll;
AnalyzeParticles;
count:=rCount;
Dispose;
```

{**** Input fluorescent stained image and folder location ****}

```
image2:=grnimg;
```

177

```
if (process =1) then SelectWindow(filepgname) else
        SelectWindow(filegname);
Measure;
GetResults(tPix, tmean, tmode, tmin, tmax);
Undo;
SetUser1Label('ROI intensity.');
SetUser2Label('ROI area');
diameter:=40;
max:=diameter/2;
total:=0; tdiam:=0;
totalarea:=0;
fact:=0.5;
totalmean:=0; totalmeansqr:=0;
for i:=1 to count do begin
        min:=max;
        min2:=max;
        ilow:= i - 100;
        ihigh:= i + 100;
        if ilow < 1 then ilow:=1;
        if ihigh > count then ihigh:=count;
        for j:= ilow to ihigh do begin
                dx:= abs(rX[i] - rX[j]);
                dy:= abs(rY[i] - rY[j]);
                if i = j then dx:=30;
                if i = j then dy:=30;
                dtotal:= fact*sqrt(dx*dx + dy*dy);
                if dtotal < min then begin
                        min2:=min;
                        min:=dtotal;
                end;    {if}
        end; {j}
        diameter:=min+min2;
        if diameter < 30 then diameter:=30.0;
        SetOptions('X-YCenter;Area;Mean;Std.Dev.;User1;User2');
        if ((rX[i] - diameter/2) > 0) and ((rY[i] - diameter/2) > 0) and
                ((rX[i] + diameter/2) < width) and ((rY[i] +
                diameter/2) < height) then begin
        MakeOvalRoi(rX[i]-diameter/2,rY[i]
                diameter/2,diameter,diameter);
        Measure;
                GetResults(nPix,cmean,cmode,cmin,cmax);
                rUser1[i]:=cmean;
                rUser2[i]:=npix;
                Undo;
        tdiam:=tdiam + diameter;
        total:=total + 1;
                totalarea:=totalarea +npix;
                totalmean:=totalmean + cmean;
                totalmeansqr:=totalmeansqr + cmean*cmean;
        end else begin
        rUser1[i]:=0;
         rUser2[i]:=0;
        end; {if}
end; {i}
```

```
                            SetExport('measurements');
                            SetOptions('X-Y Center;User1;User2');
                            Export(outfiled);
                            avg:=totalmean/total;
                            avgdiam:=tdiam/total;
                            variance:=(total*totalmeansqr-(totalmean*totalmean))/
                                    ((total1)*total);
                            sd:=sqrt(variance);
                            SelectWindow('sum data');
                            Writeln(file, tmean:9:2, avg:9:2, sd:9:2, totalarea:14:2,
                                    avgdiam:9:2);
                                    SetText('centered');
                                    Import(outfileb);
                                    for i:=1 to count do begin
                                    MoveTo(rX[i],rY[i]);
                                    SetForegroundColor(80);
                                    Write(i);
                                    end;
                            SaveAs(outfileb);
                            Dispose;
                            Beep;
                            SelectPic(image2);
                            ResetCounter;
                            Dispose;
    end;  { k }
    end;  { n }
            if (process=1) then begin
                    SelectWindow(prcalfn);
                    Dispose;
            end; {if}
    end; { m}
    end; {begin}
```

B.2 CAM Expression Kinetics by TIF and Angiogenic Factors
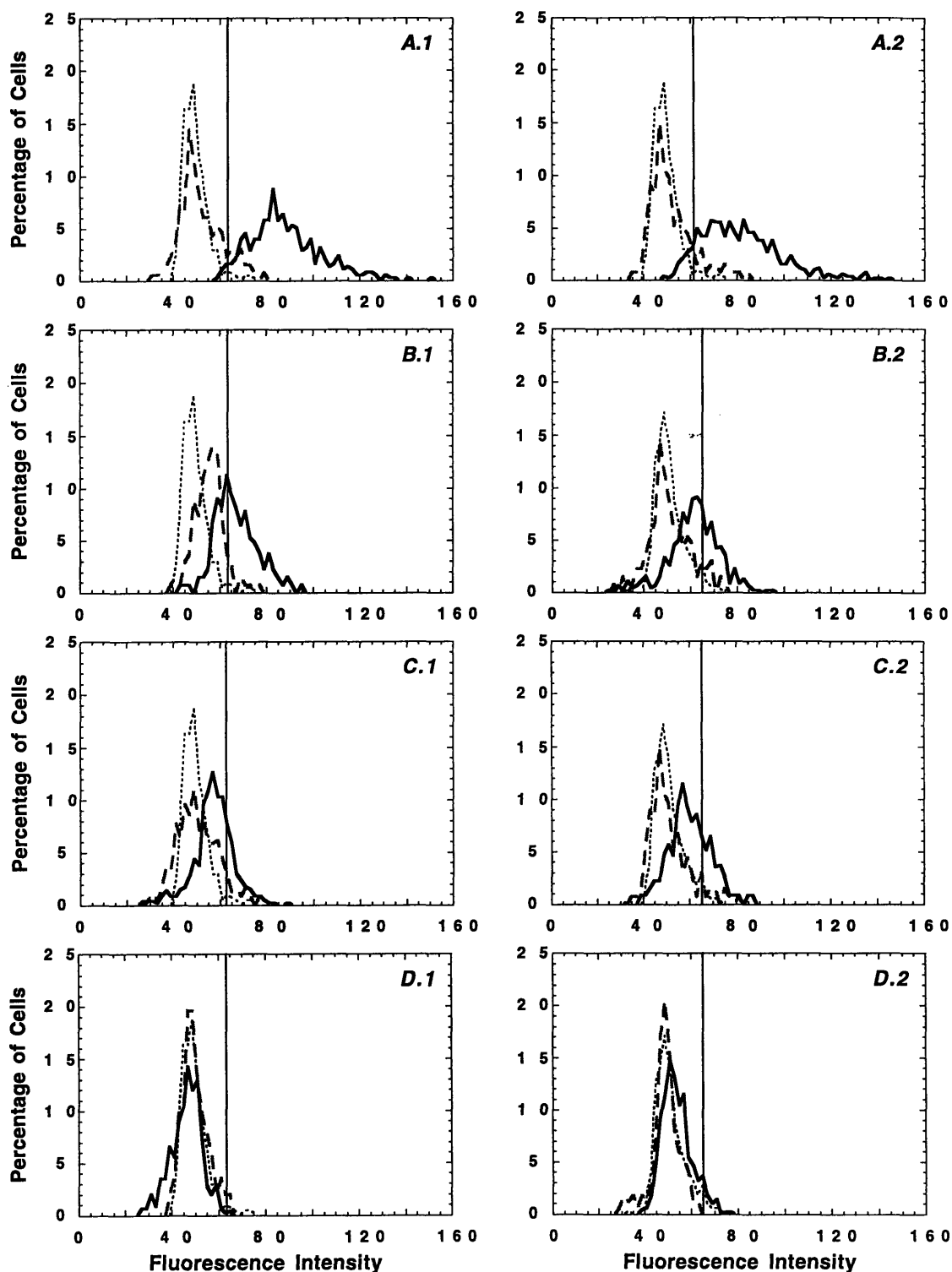
Figure B-2-1. CAM expression on HUVECs treated with TIF for 24 hrs. Two sets of each group representing: a) ICAM-1, b) VCAM-1, c) E-selectin, and d) P-selectin. — = TIF, - - = non, ⋯ = IgG control.
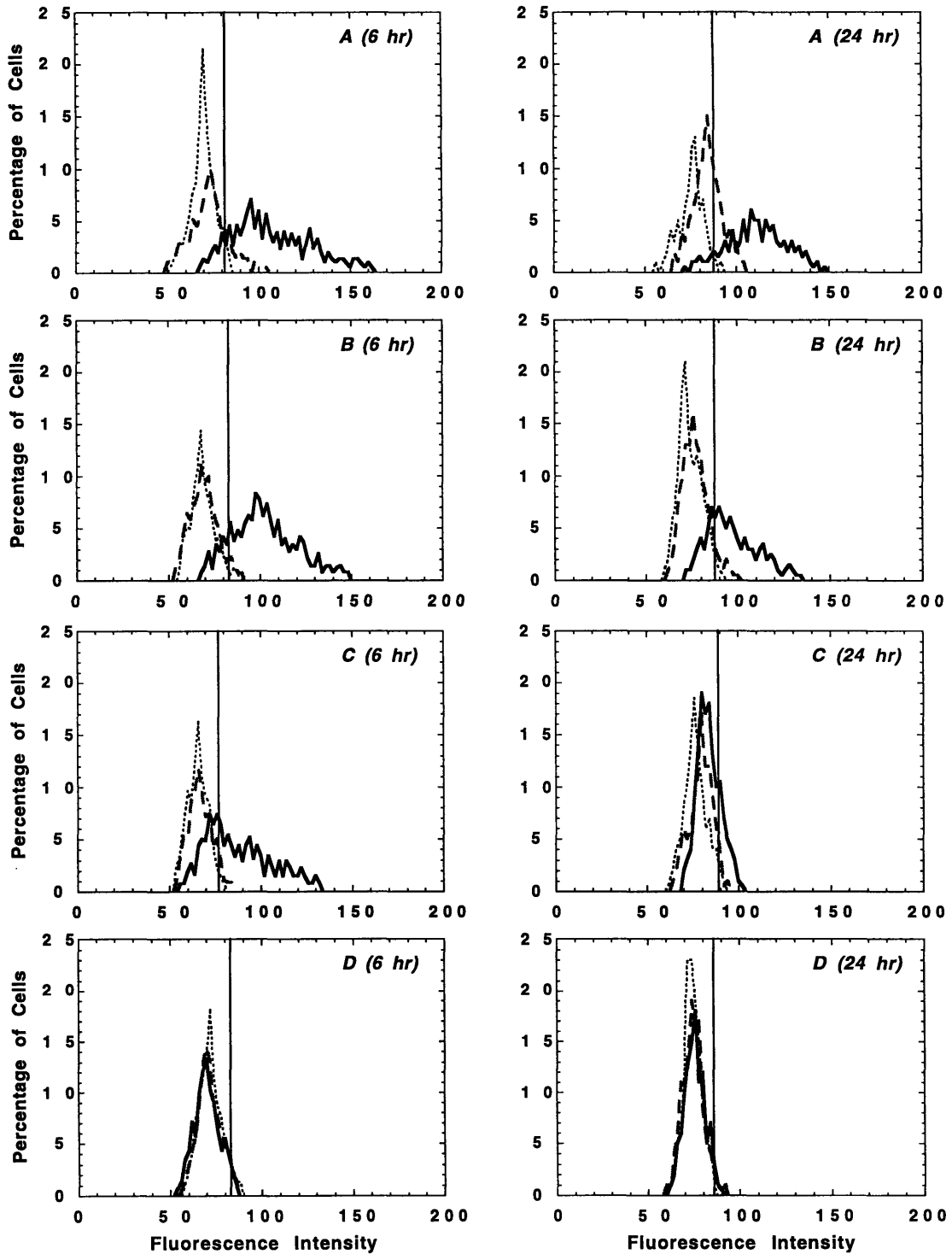
Figure B-2-2. CAM expression on HUVECs treated with TNFα for 6 and 24 hrs. Each time period shown for: a) ICAM-1, b) VCAM-1, c) E-selectin, and d) P-selectin. — = TNFα, - - = non, ··· = IgG control.
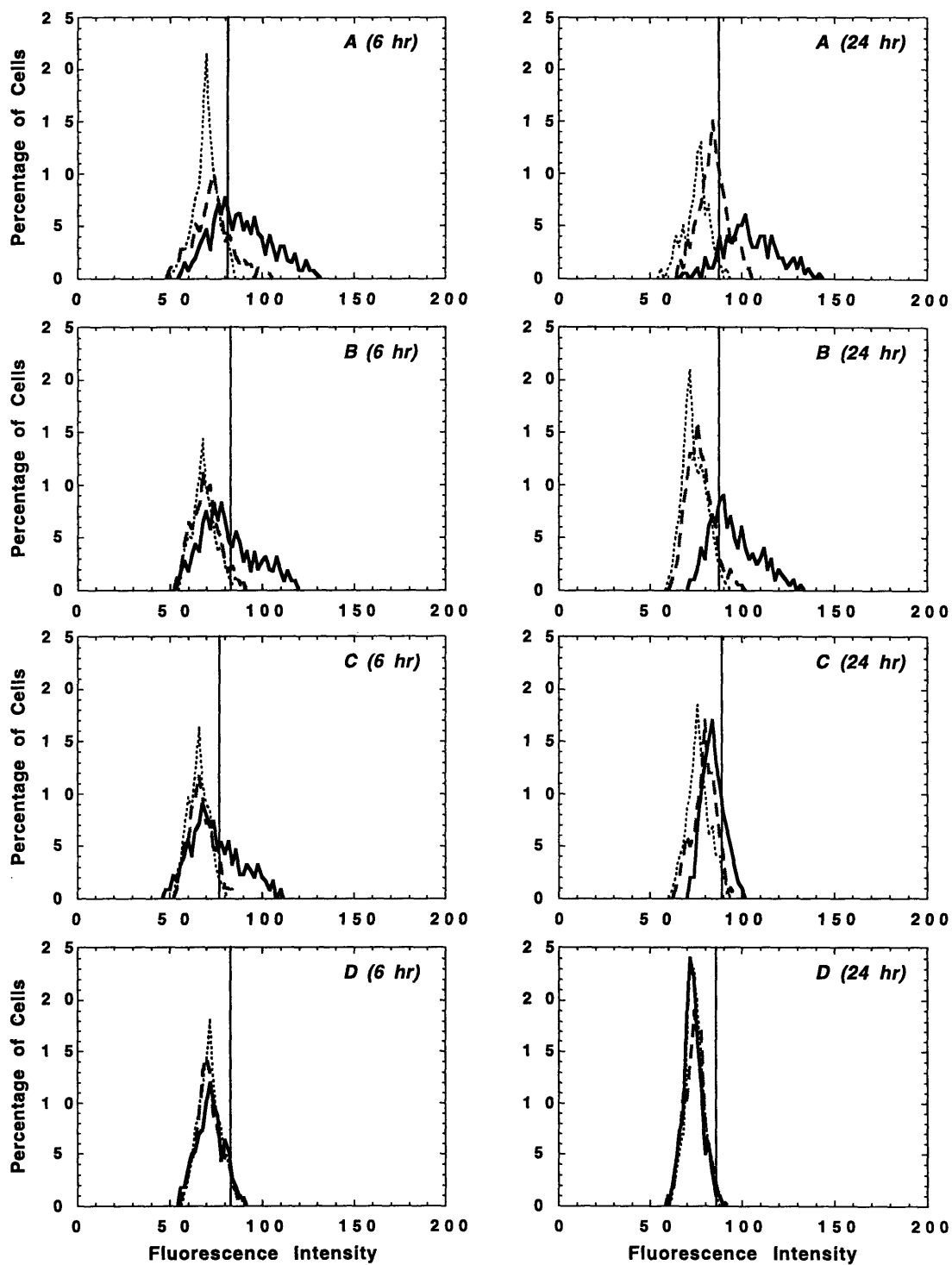
Figure B-2-3. CAM expression on HUVECs treated with VEGF for 6 and 24 hrs. Each time period shown for: a) ICAM-1, b) VCAM-1, c) E-selectin, and d) P-selectin. — = VEGF, - - = non, ⋯ = IgG control.
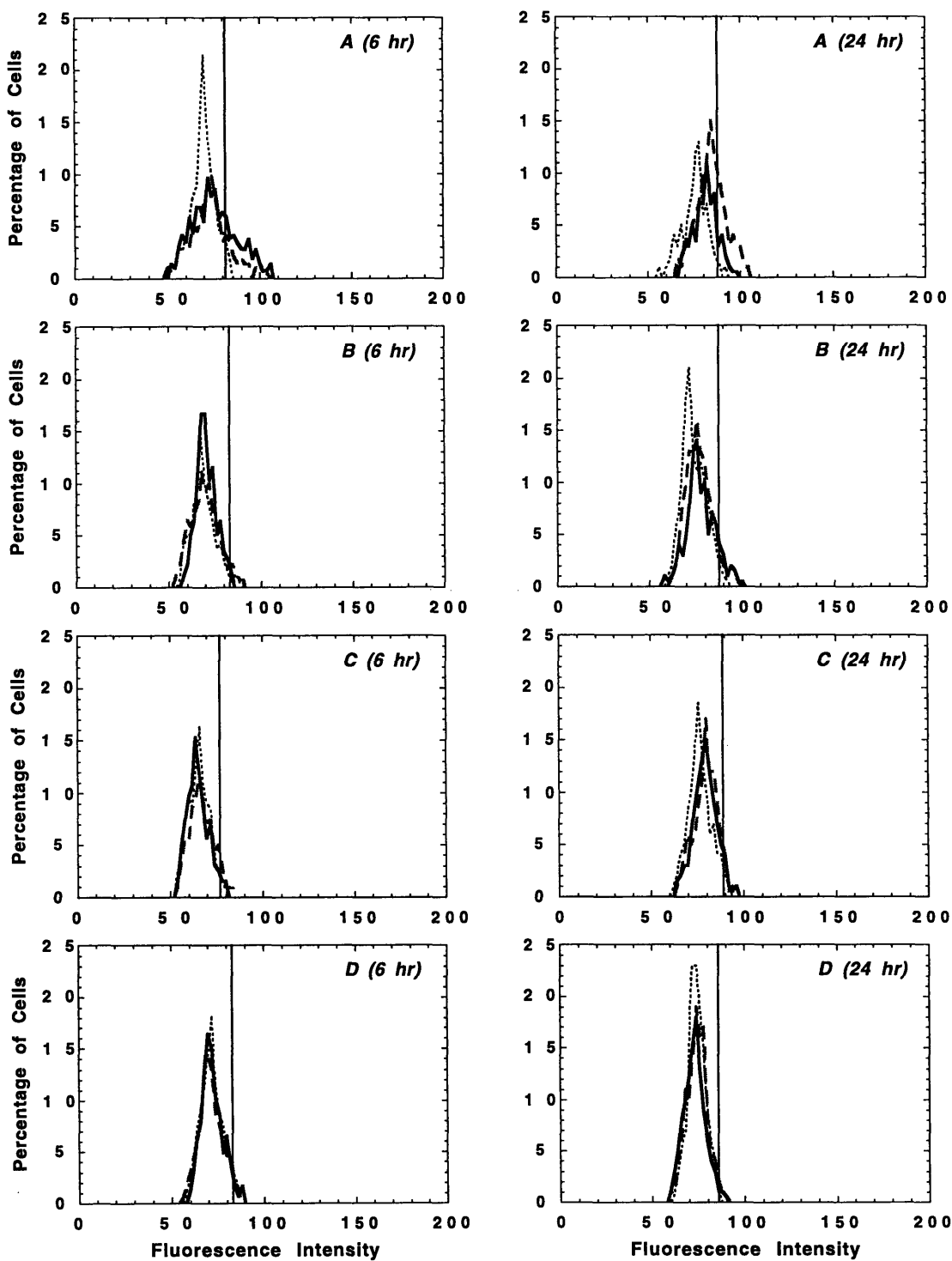
Figure B-2-4. CAM expression on HUVECs treated with bFGF for 6 and
24 hrs. Each time period shown for: a) ICAM-1, b) VCAM-1, c) E-
selectin, and d) P-selectin. —— = bFGF, - - = non, ··· = IgG control.
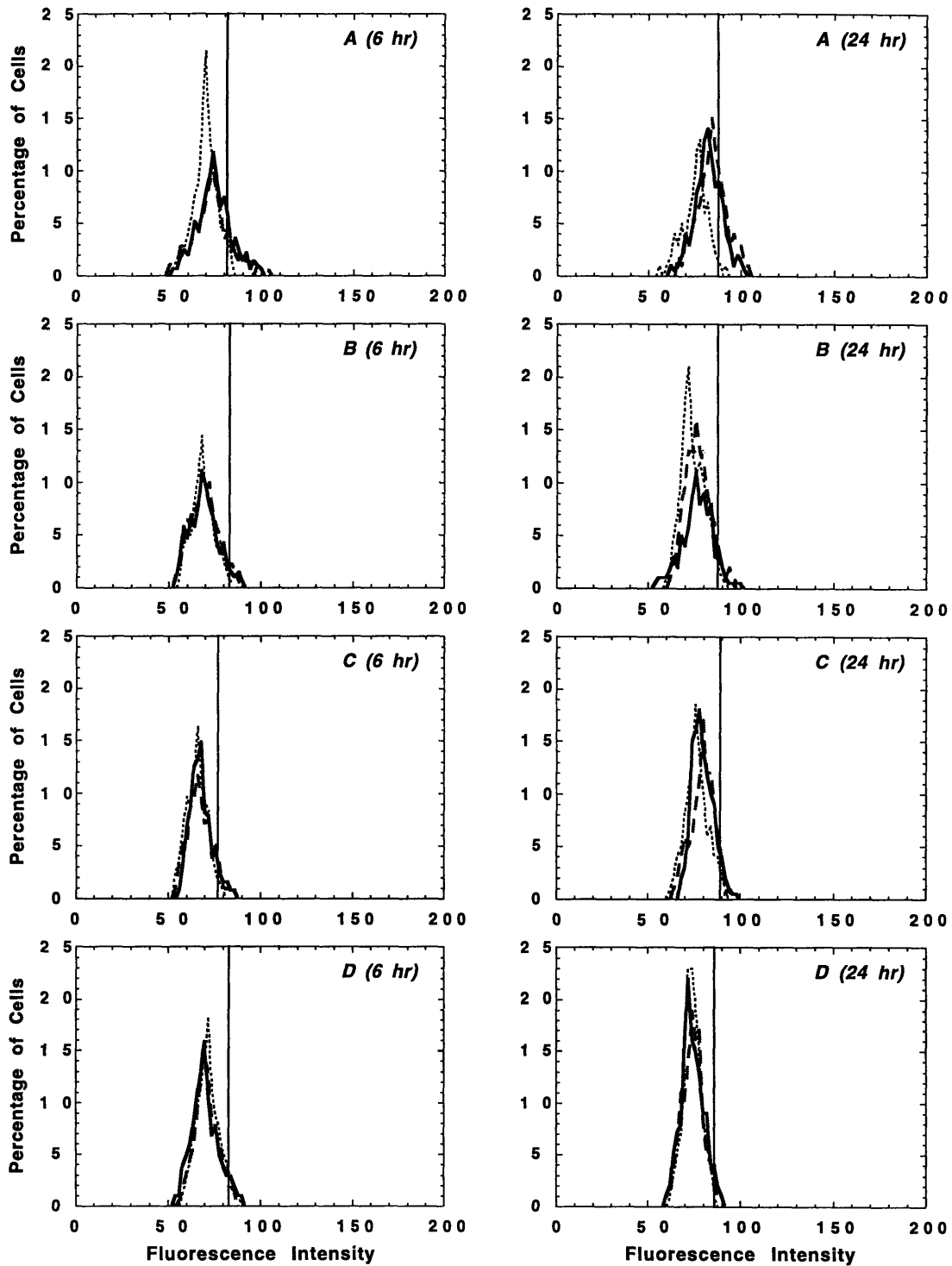
Figure B-2-5. CAM expression on HUVECs treated with TGFβ for 6 and 24 hrs. Each time period shown for: a) ICAM-1, b) VCAM-1, c) E-selectin, and d) P-selectin. — = TGFβ, - - = non, ··· = IgG control.
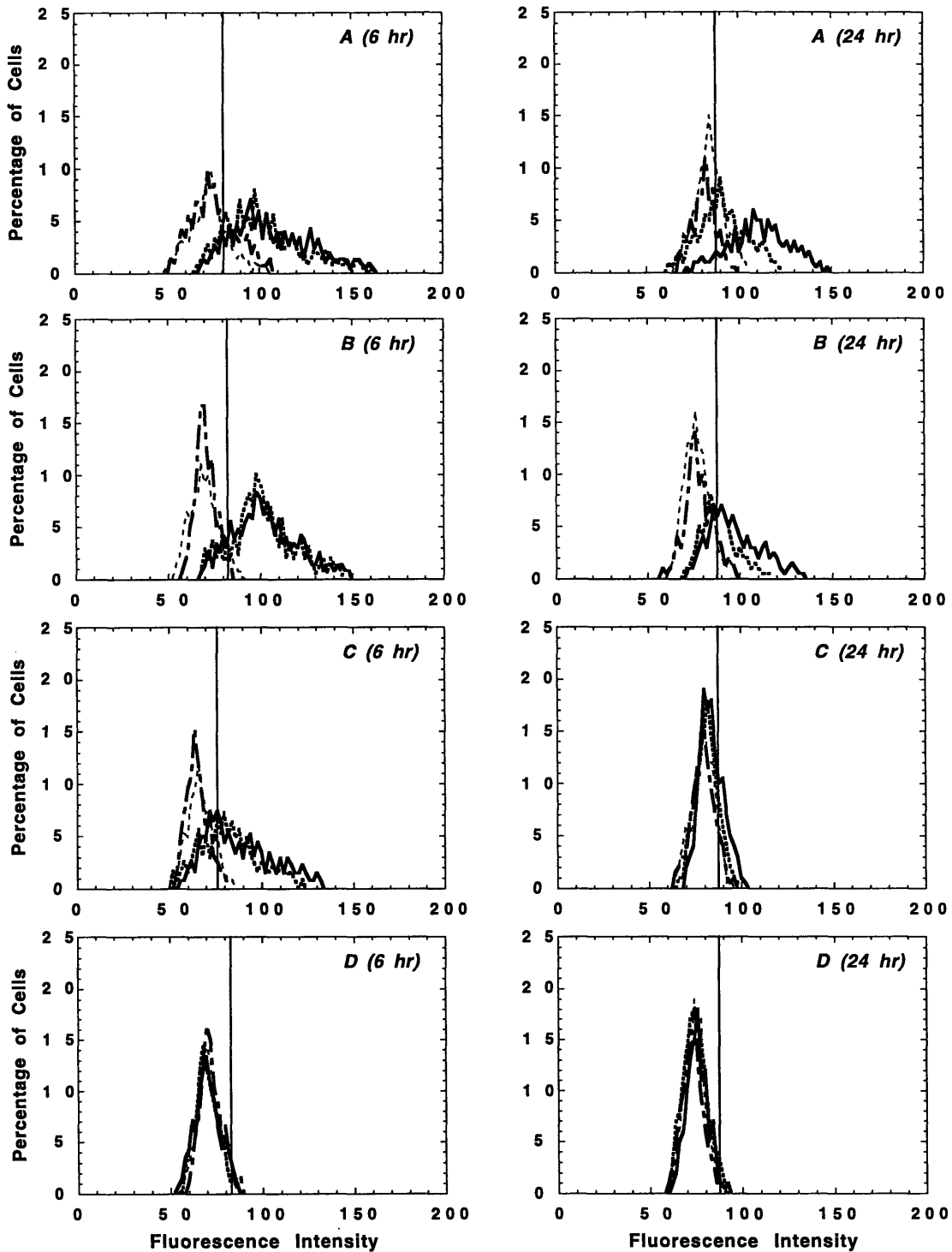
Figure B-2-6. CAM expression on HUVECs treated with TNFα+bFGF for 6 and 24 hrs. Each time period shown for: a) ICAM-1, b) VCAM-1, c) E-selectin, and d) P-selectin. —— = TNFα, ··· = TNFα+bFGF, ———— = bFGF, - - = non.
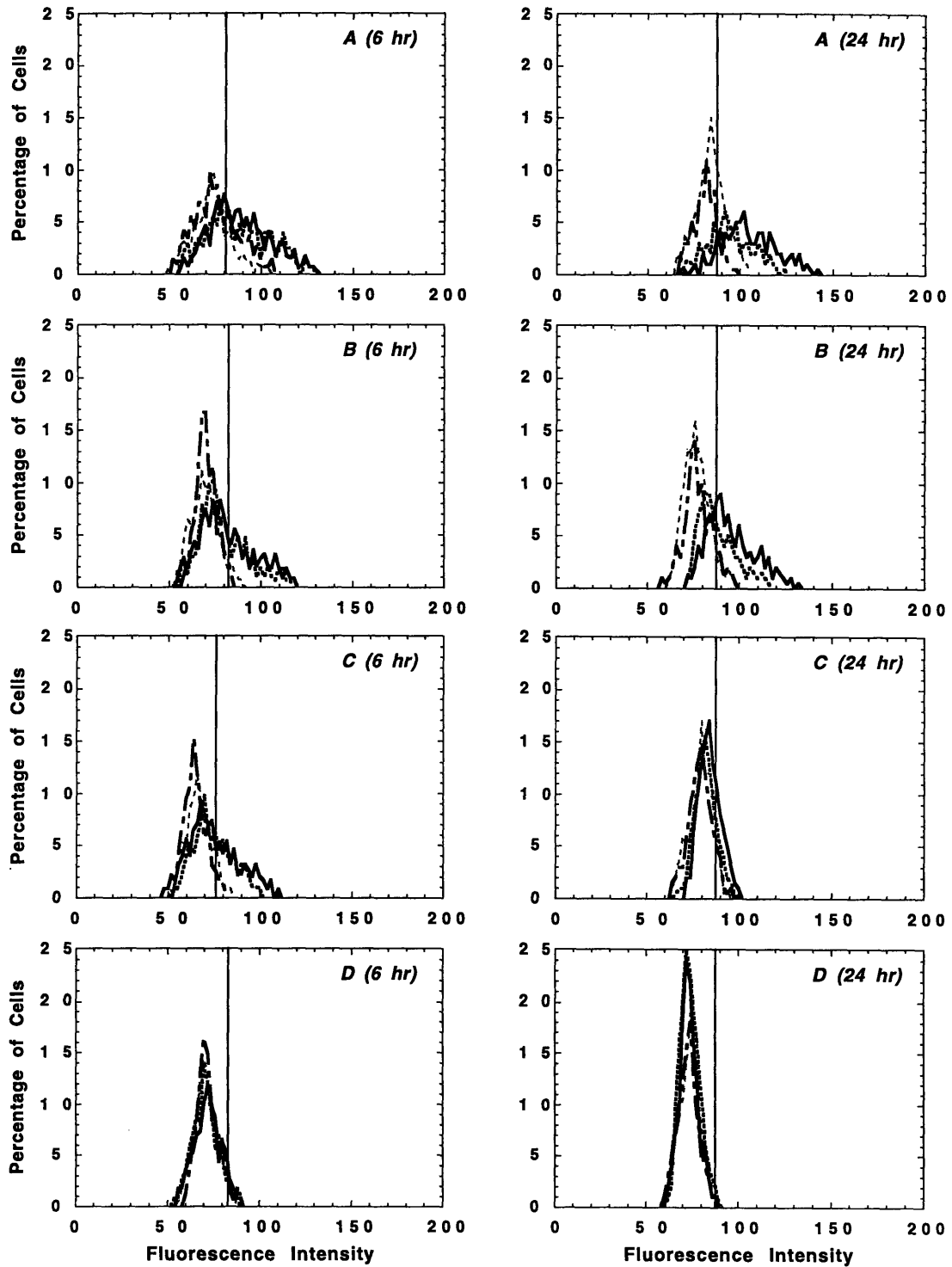
Figure B-2-7. CAM expression on HUVECs treated with VEGF+bFGF for 6 and 24 hrs. Each time period shown for: a) ICAM-1, b) VCAM-1, c) E-selectin, and d) P-selectin. — = VEGF, ⋯ = VEGF+bFGF, ——— = bFGF, - - = non.

186
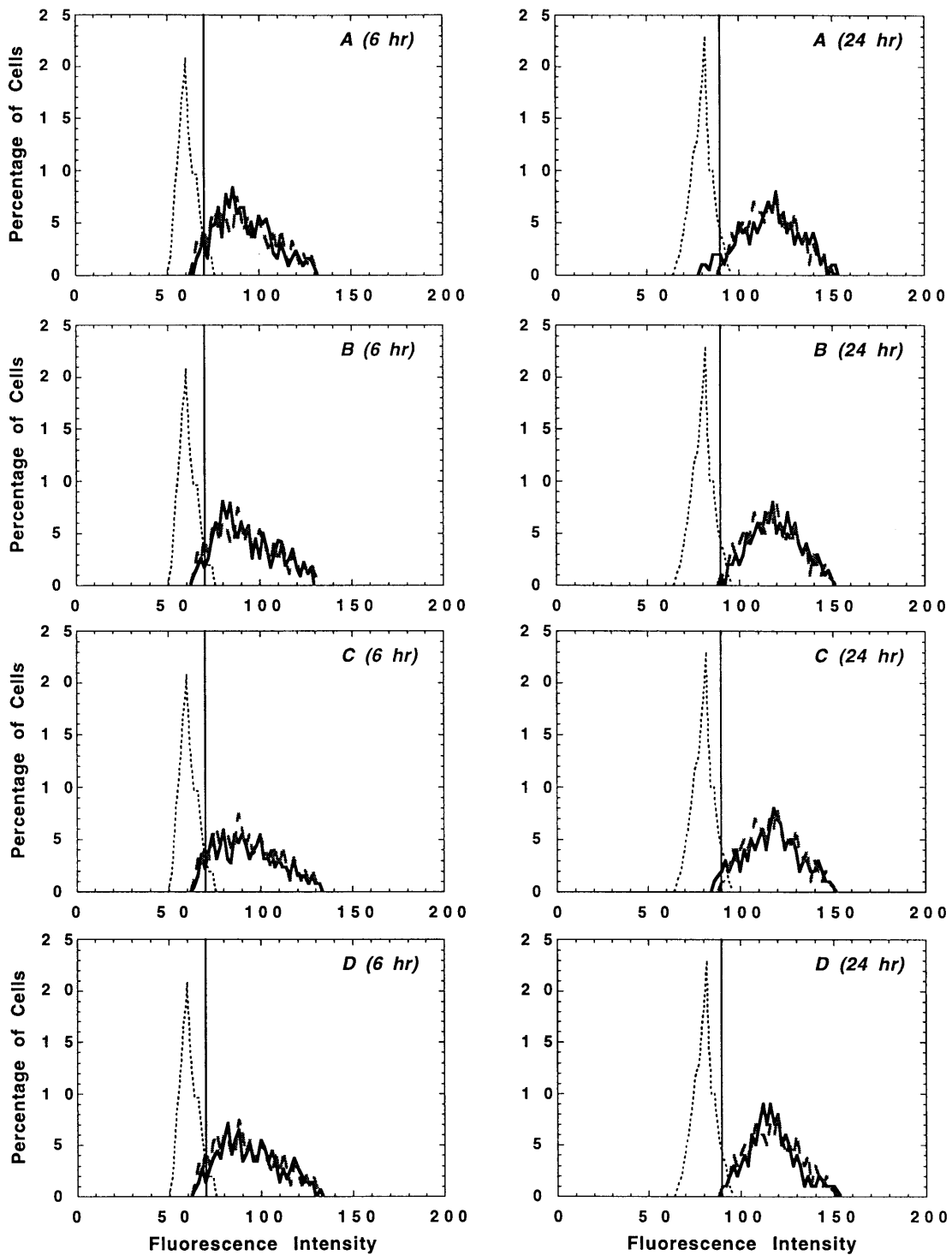
Figure B-2-8. Effect of angiogenic factors on ICAM-2 expression in HUVECs treated for 6 and 24 hrs. Factors presented are: a) TNFα, b) VEGF, c) bFGF, and d) TGFβ. — = angiogenic factor, - - = non, ⋯ = IgG control.

187
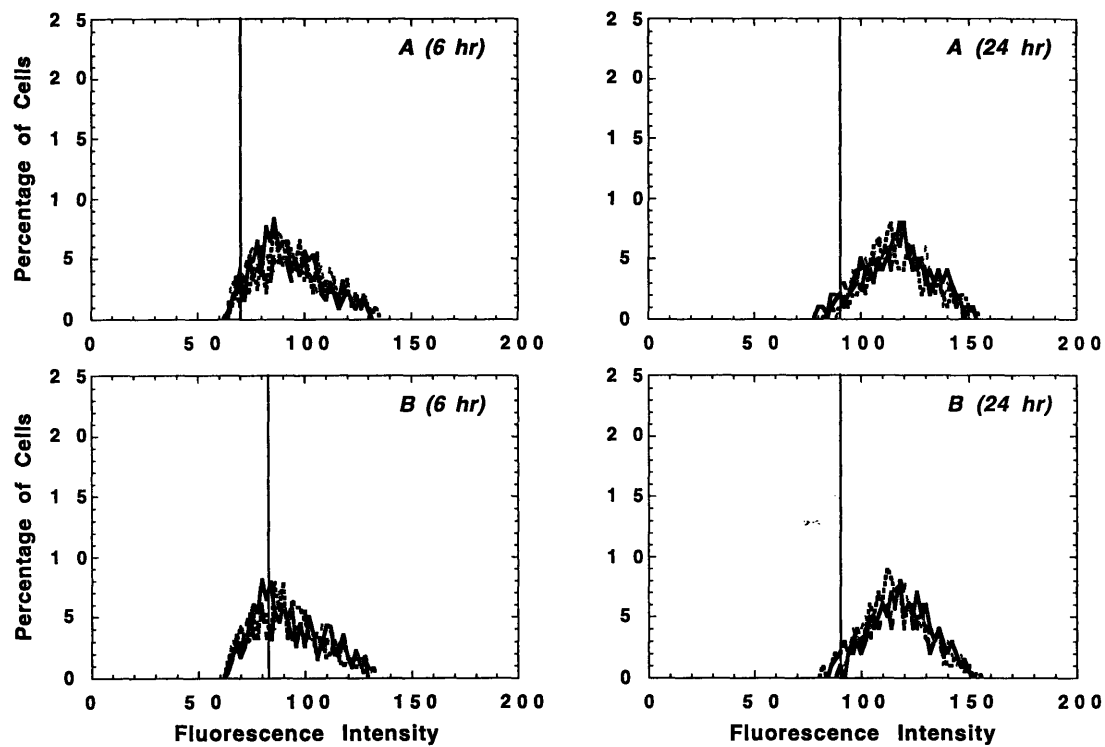
Figure B-2-9. Combined effect of angiogenic factors on ICAM-2 expression in HUVECs treated for 6 and 24 hrs. Factors presented are: a) TNFα+bFGF, and b) VEGF+bFGF. — = TNFα/VEGF, ··· = TNFα/VEGF+bFGF, ——— = bFGF, - - = non.

B.3   Functional Kinetics of Angiogenic Factors
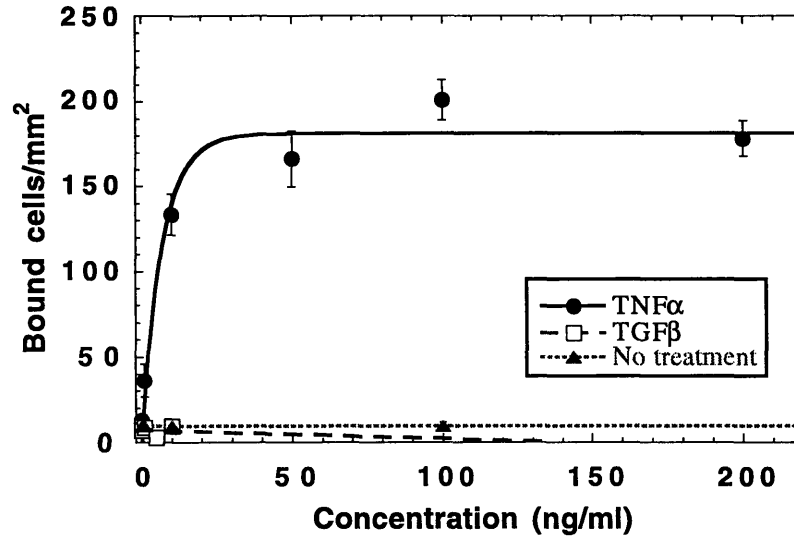
Figure B-3-1. Dose response curve of A-NK cell binding to HUVEC monolayers treated with VEGF or bFGF. A flow rate corresponding to 1 dyn/cm^2 wall shear stress was imposed. Mean numbers ± SD of bound cells for eight adjacent fields are shown for two sets of experiments.
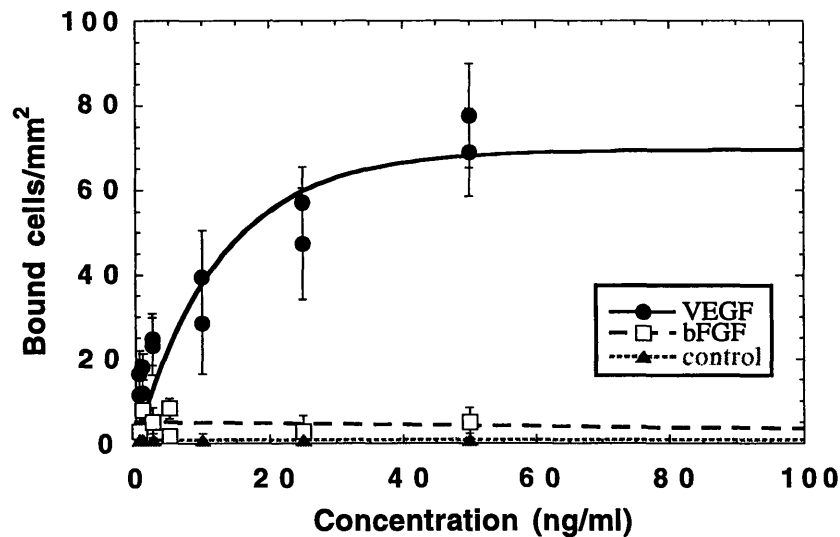
Figure B-3-2. Dose response curve of A-NK cell binding to HUVEC monolayers treated with VEGF or bFGF. A flow rate corresponding to 1 dyn/cm^2 wall shear stress was imposed. Mean numbers ± SD of bound cells for eight adjacent fields are shown for two sets of experiments.

189
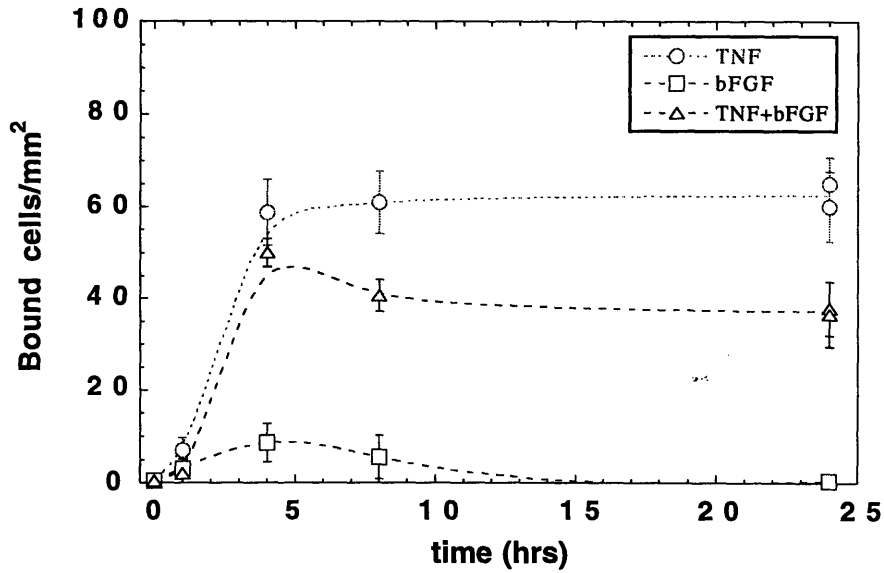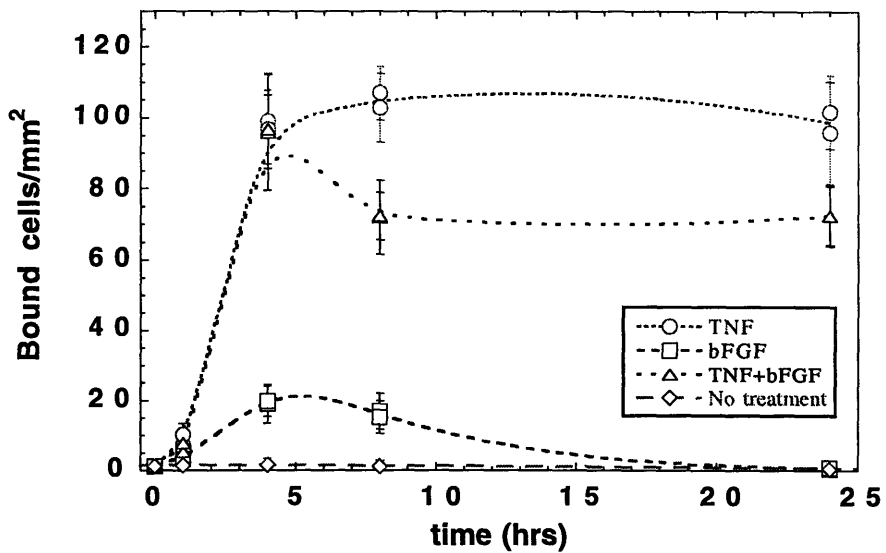
Figure B-3-3. Temporal kinetics of TNFα and bFGF treatment on A-NK cell binding. A flow rate corresponding to 1 dyn/cm² wall shear stress was imposed. Mean numbers ± SD of bound cells for eight adjacent fields are shown for two sets, (a) and (b), of two separate experiments.
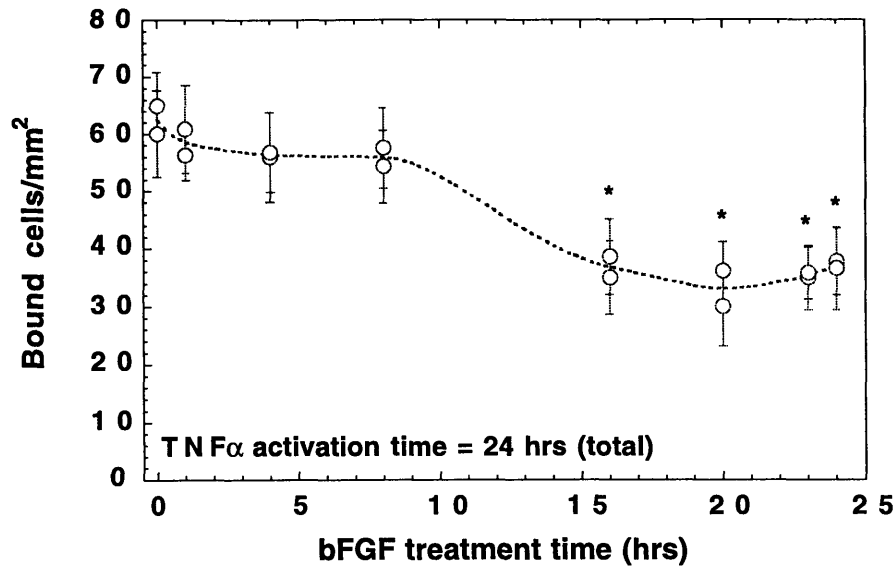
Figure B-3-4. Inhibition kinetics of A-NK cell binding to HUVEC monolayers treated with TNFα (total exposure time of 24 hr) and bFGF (time shown). A flow rate corresponding to 1 dyn/cm^2 wall shear stress was imposed. Mean numbers $\pm$ SD of bound cells for eight adjacent fields are shown for two separate experiments. * $p < 0.05$.
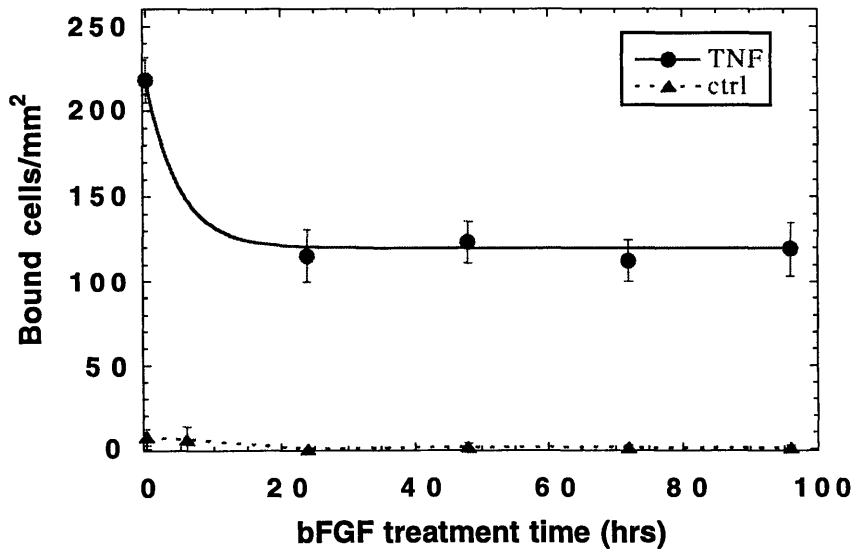
Figure B-3-5. Extended inhibition kinetics of A-NK cell binding to HUVEC monolayers treated with TNFα (total exposure time of 24 hr) and bFGF (time shown). A flow rate corresponding to 1 dyn/cm^2 wall shear stress was imposed. Mean numbers $\pm$ SD of bound cells for eight adjacent fields are shown.

191

Appendix C

Northern Blot and Signal
Transduction Analyses

The following sections provide additional information on the experiments pertaining to: a) the kinetics of CAM mRNA regulation by bFGF on TNFα-activated HUVEC monolayers (Northern blot analysis), b) the effect of bFGF on CAM mRNA stability (Northern blot analysis), c) the dose response curves and adhesion assays for A-NK binding to HUVECs treated independently with the various signal blocking agents, and d) the FIA analysis on CAM expression following addition of the blocking agents.

C.1 Kinetics of CAM mRNA Expression
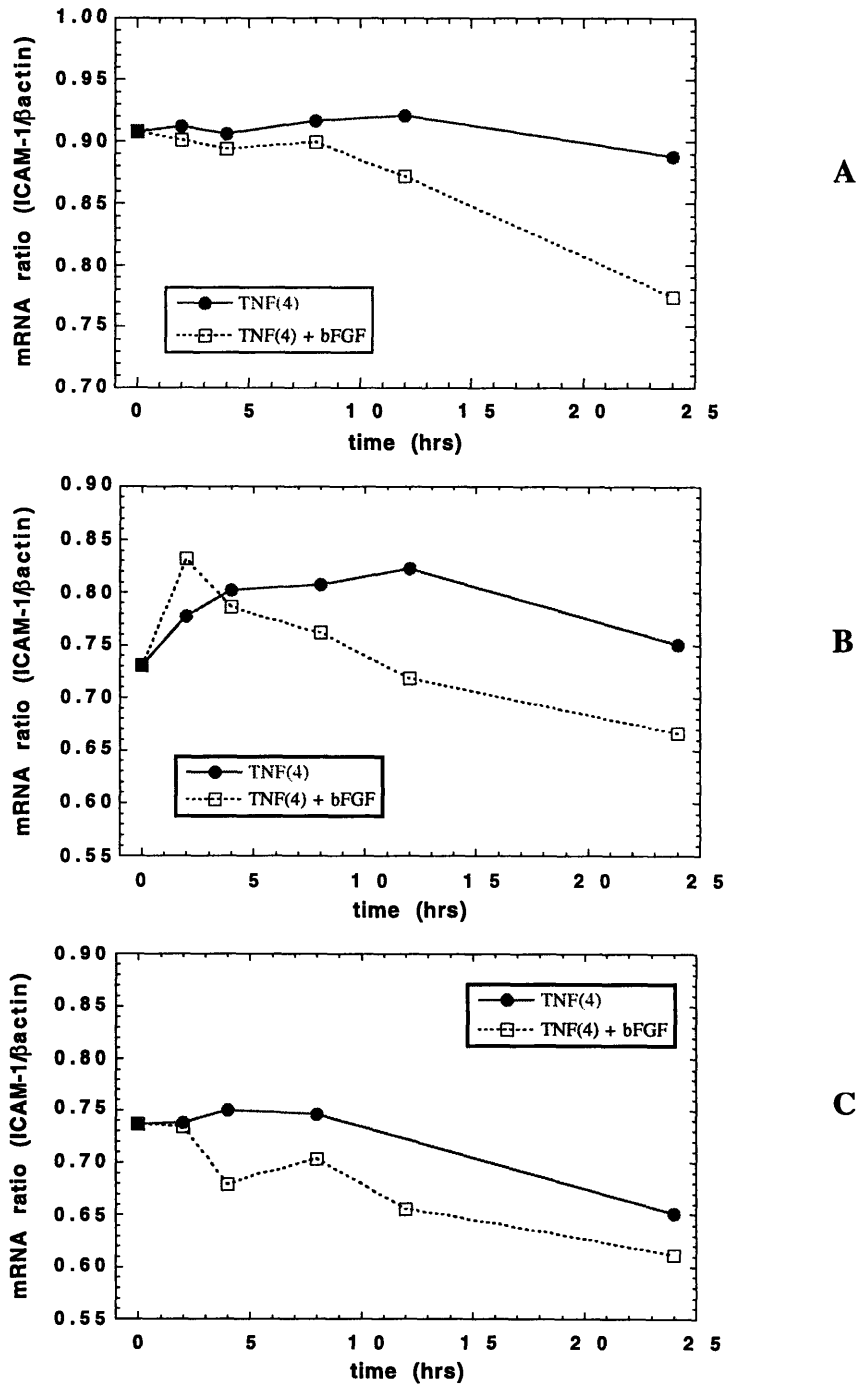
Figure C-1-1. Graphic representation of ICAM-1 mRNA kinetics of expression following 4 hr treatment with TNFα.
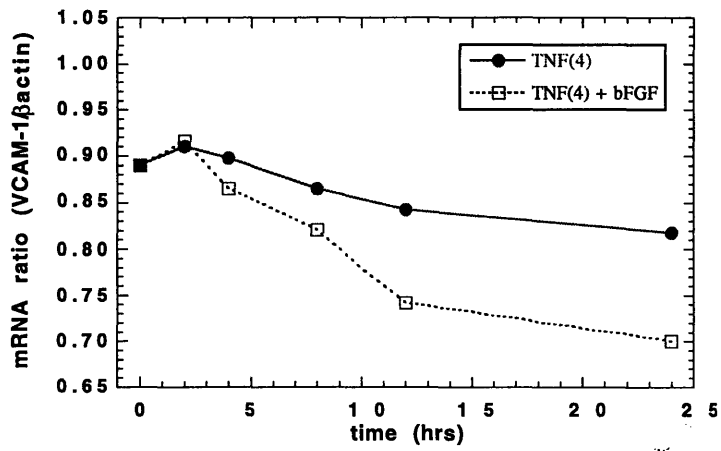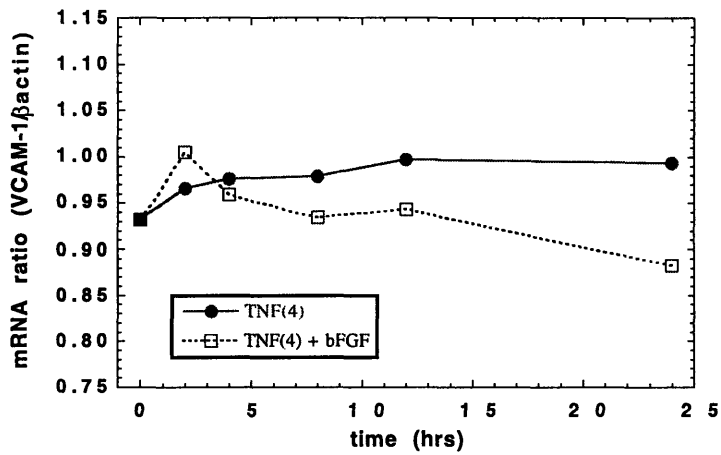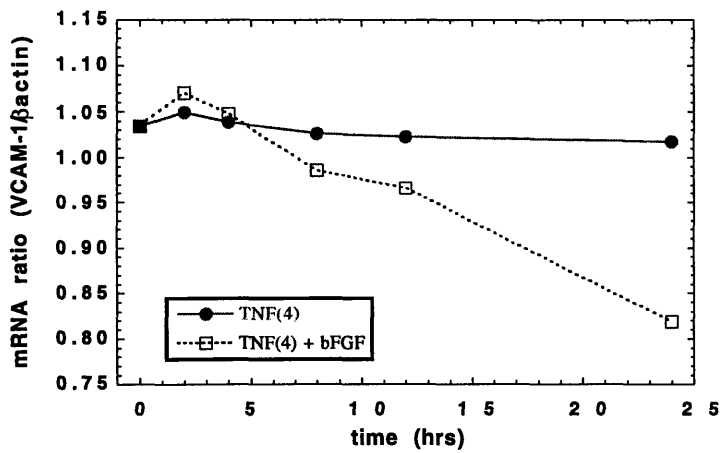
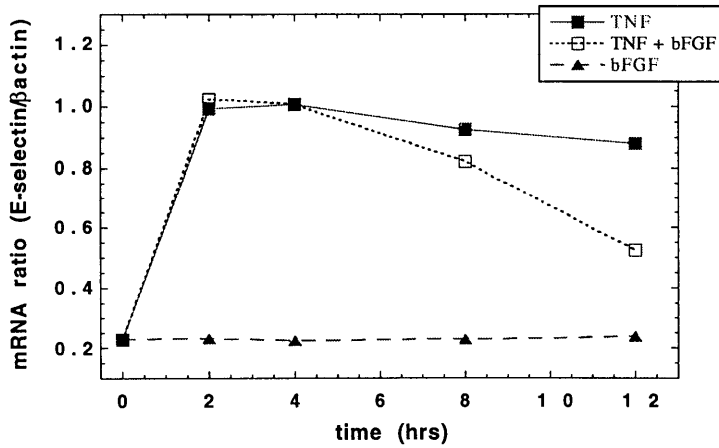Figure C-1-2. Graphic representation of VCAM-1 mRNA kinetics of expression following 4 hr treatment with TNFα.
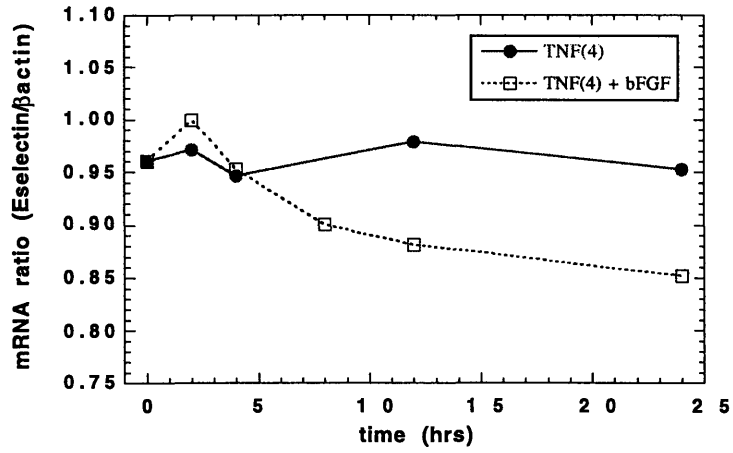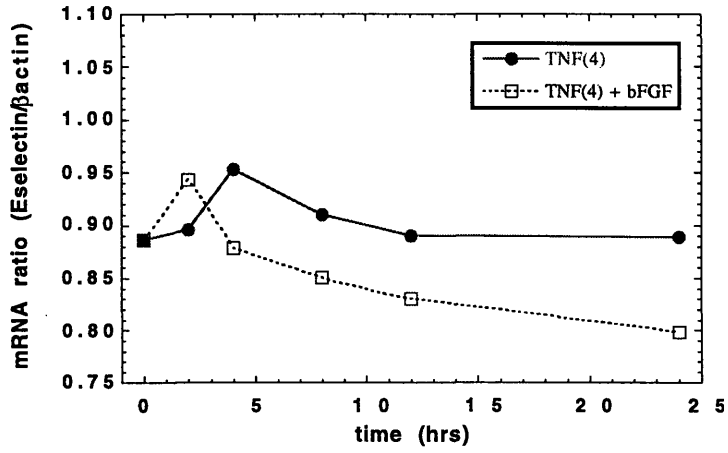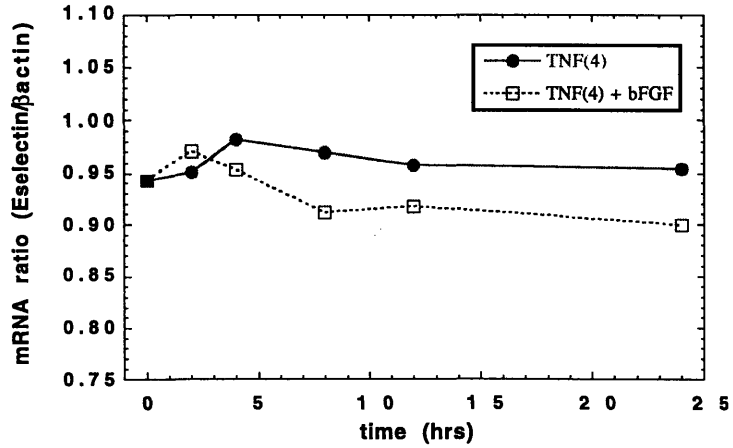
Figure C-1-3. Graphic representation of E-selectin mRNA kinetics of expression following 4 hr treatment with TNFα.
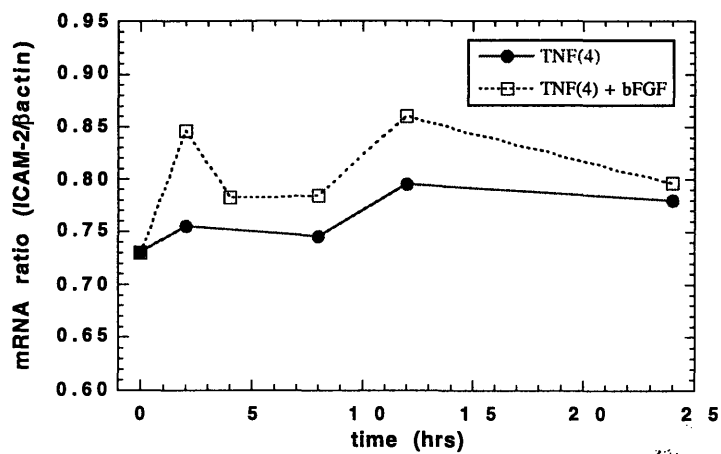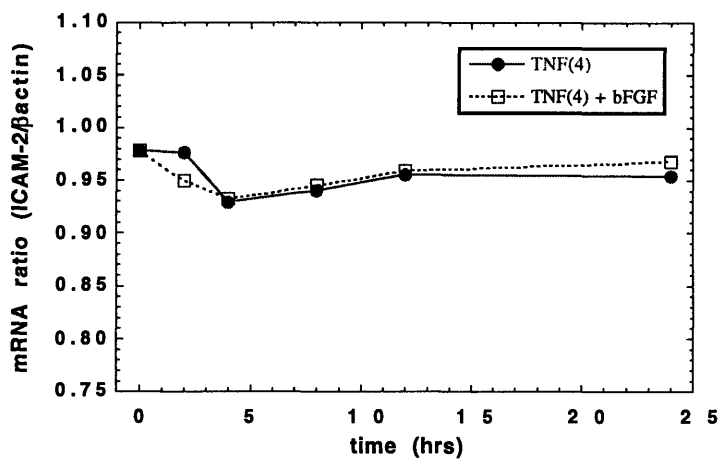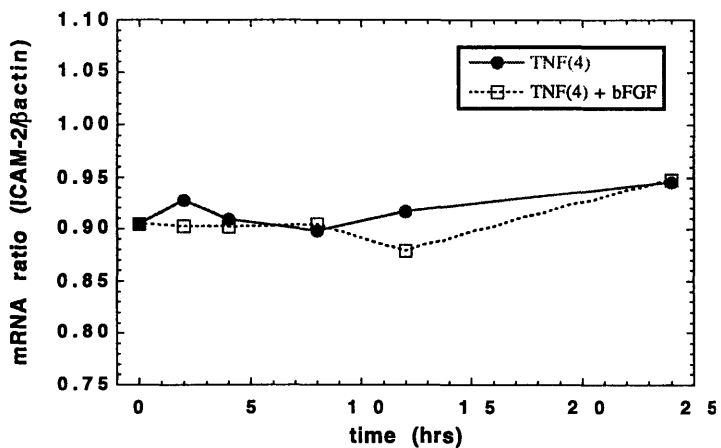
Figure C-1-4. Graphic representation of ICAM-2 mRNA kinetics of expression following 4 hr treatment with TNFα.

196

TNF (4hr)　　　　TNF(4hr) + bFGF
0　2　4　8　12　24　　　2　4　8　12　24

ICAM-1

VCAM-1

E-selectin　　　　　　　　　　　　　　　　　A

ICAM-2

β-actin

TNF (4hr)　　　　TNF(4hr) + bFGF
0　2　4　8　12　24　　　2　4　8　12　24

ICAM-1

VCAM-1

E-selectin　　　　　　　　　　　　　　　　　B

ICAM-2

β-actin

TNF (4hr)　　　　TNF(4hr) + bFGF
0　2　4　8　12　24　　　2　4　8　12　24

ICAM-1

VCAM-1

E-selectin　　　　　　　　　　　　　　　　　C

ICAM-2

β-actin
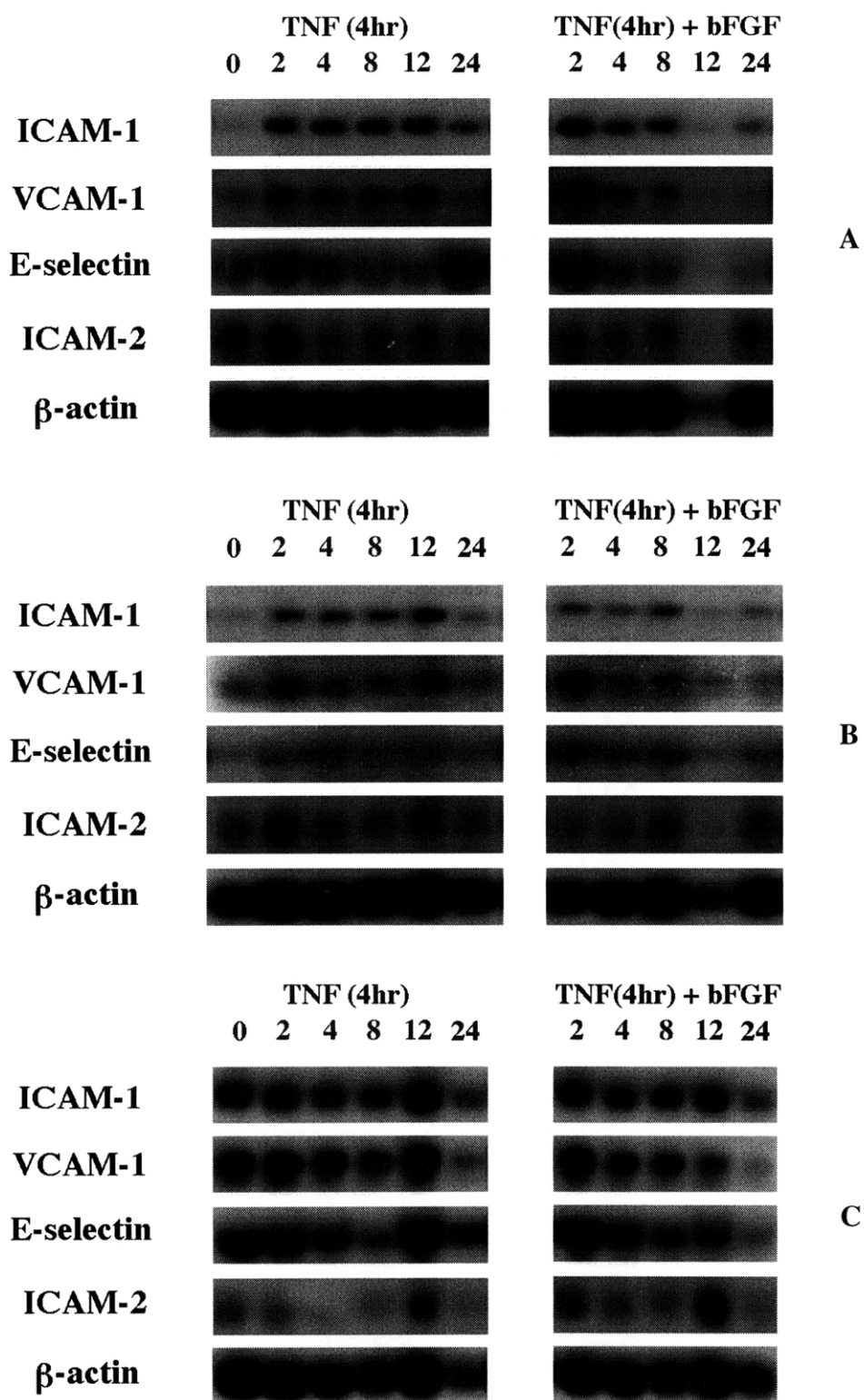
Figure C-1-5. Northern blots of mRNA kinetics of expression following 4 hr treatment with TNFα. Blots shown are from three separate experiments.

197
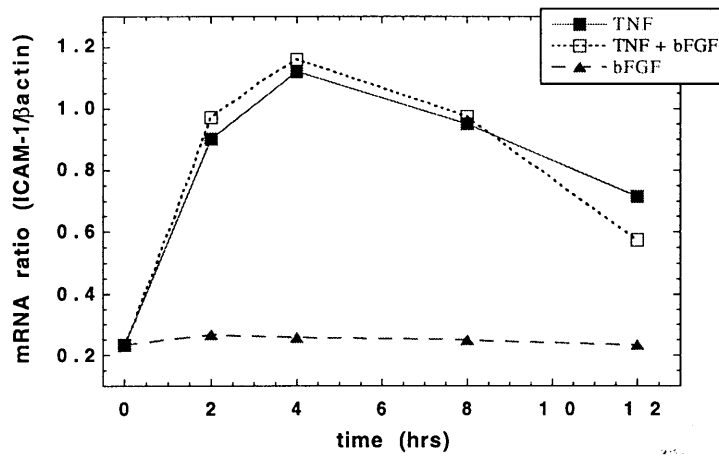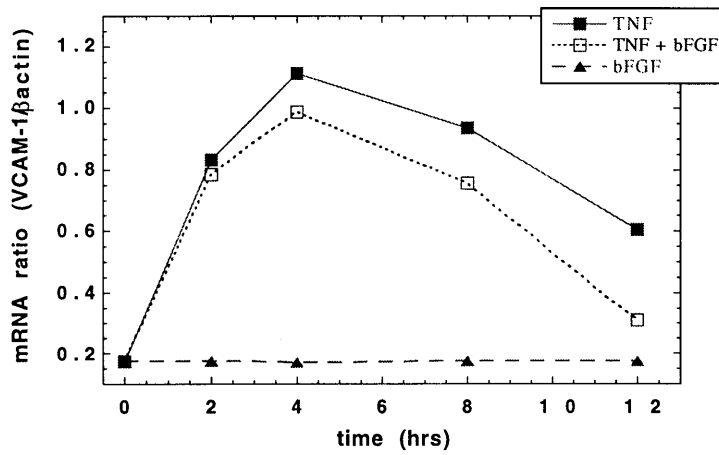
Figure C-1-6. Graphic representation of CAM mRNA kinetics of expression following simultaneous addition of TNFα and bFGF. Plots shown are: a) ICAM-1, b) VCAM-1, and c) E-selectin expression from 0 to 12 hrs of activation.
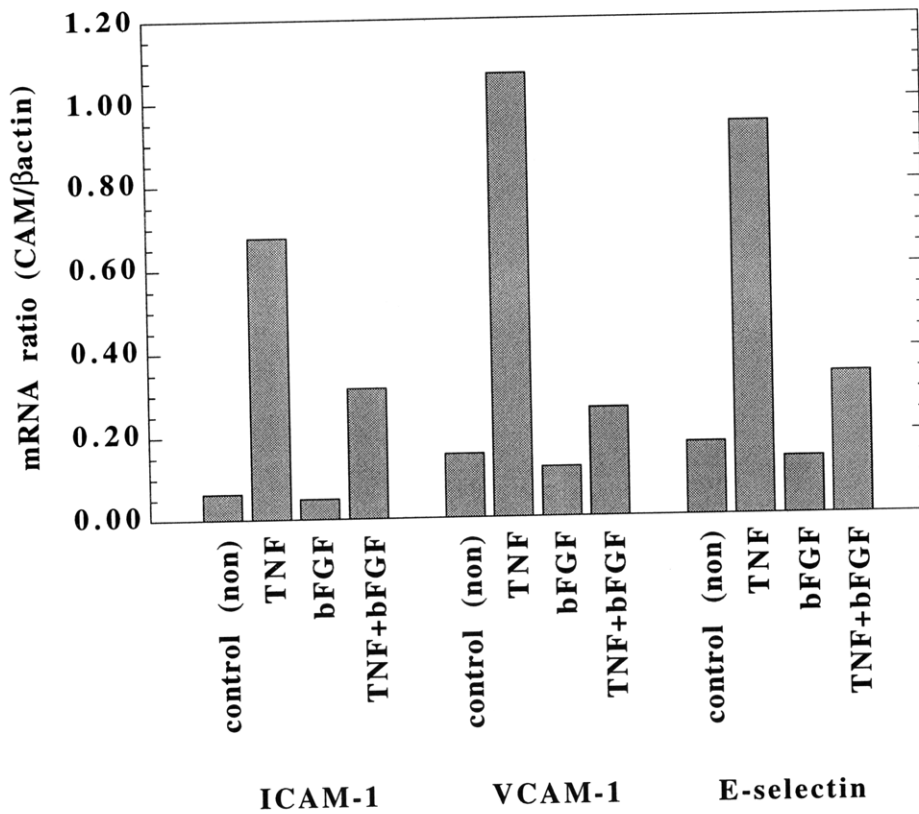
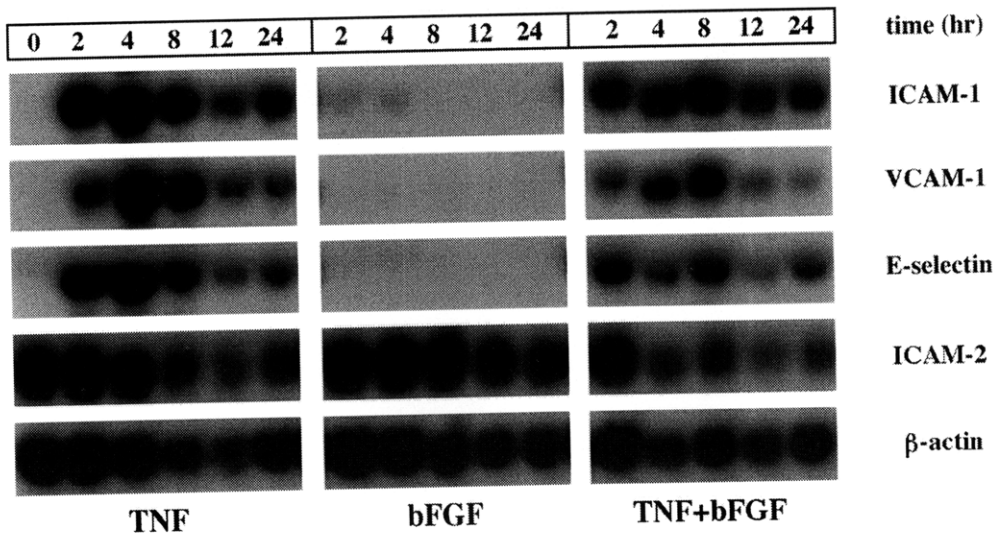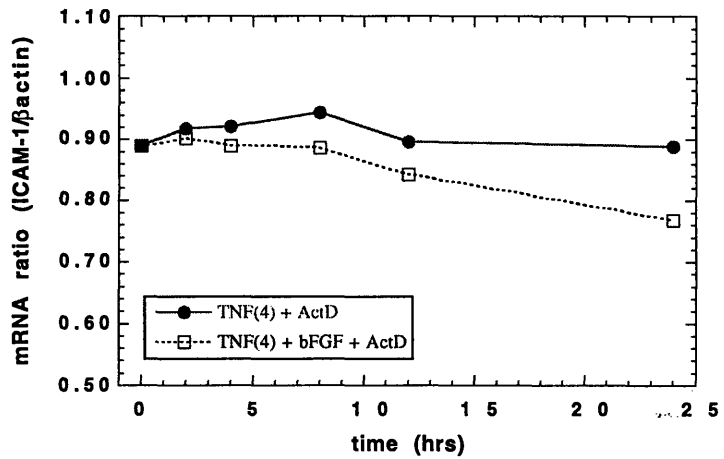Figure C-1-7. Graphic representation of CAM mRNA levels following 24 hr co-incubation of TNFα and bFGF.
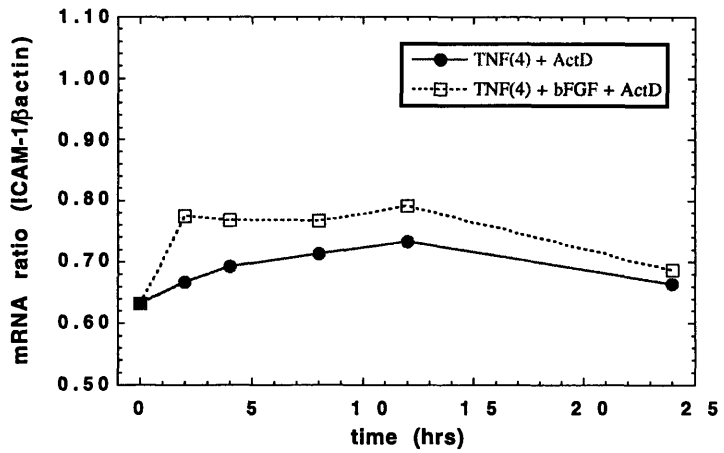

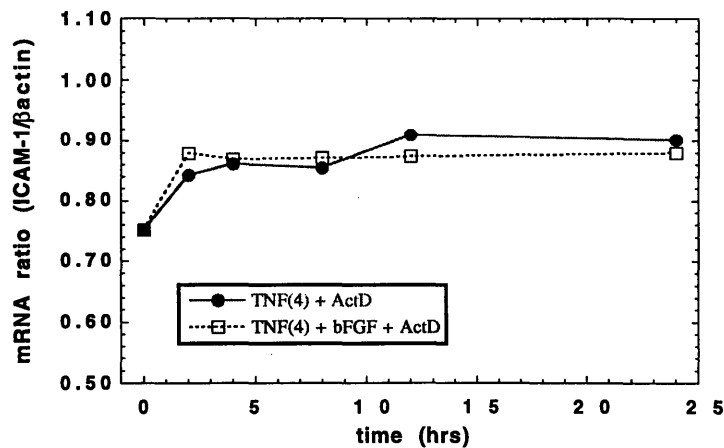Figure C-1-8. Northern blots of CAM mRNA levels following co-activation with TNFα and bFGF from 0 to 24 hrs.
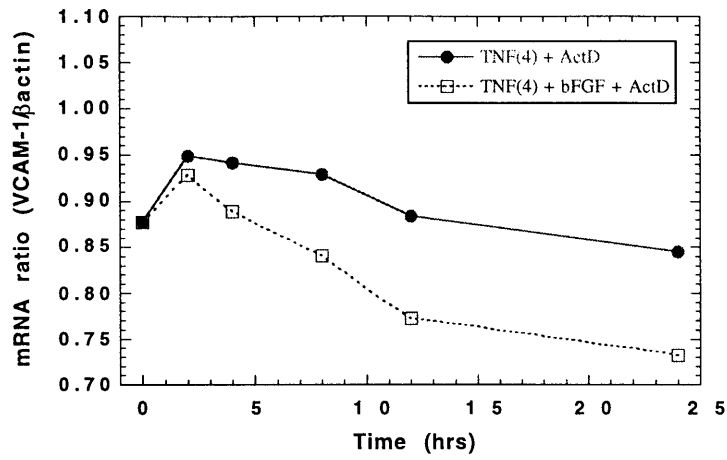
C.2 Level of mRNA Regulation

A

B
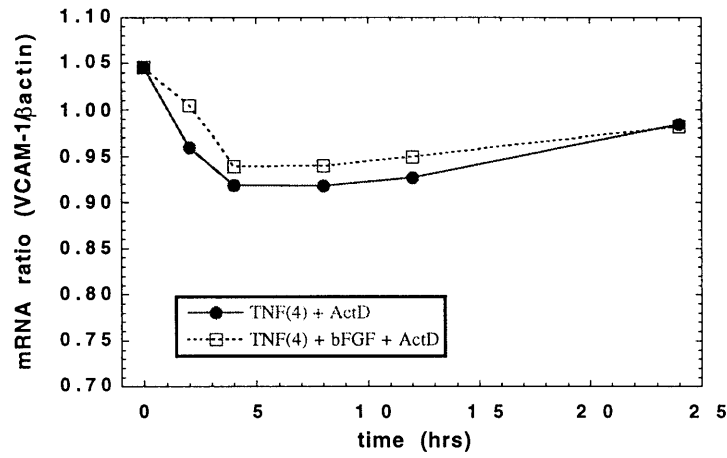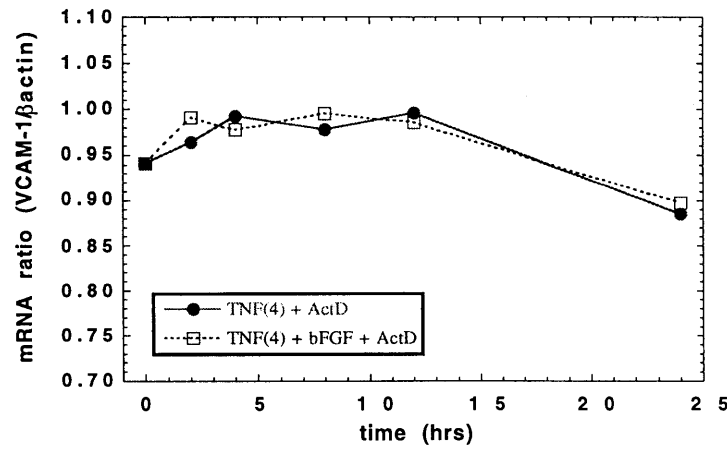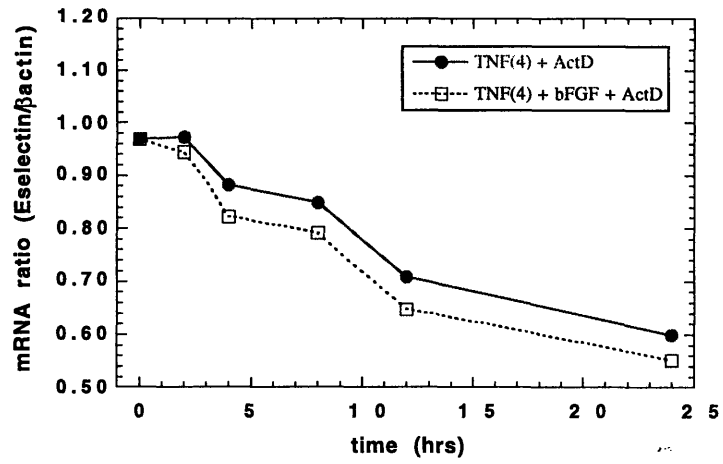

C

Figure C-2-1. Graphic representation of ICAM-1 mRNA stability analysis following 4 hr treatment with TNFα.

Figure C-2-2. Graphic representation of VCAM-1 mRNA stability analysis following 4 hr treatment with TNFα.

Figure C-2-3. Graphic representation of E-selectin mRNA stability analysis following 4 hr treatment with TNFα.

A

mRNA ratio (ICAM-2/βactin)

1.20
1.10
1.00
0.90
0.80
0.70
0.60

— ● — TNF(4) + ActD
---□--- TNF(4) + bFGF + ActD

time (hrs)
0   5   1 0   1 5   2 0   2 5

B

mRNA ratio (ICAM-2/βactin)

1.20
1.10
1.00
0.90
0.80
0.70
0.60

— ● — TNF(4) + ActD
---□--- TNF(4) + bFGF + ActD

time (hrs)
0   5   1 0   1 5   2 0   2 5

C

mRNA ratio (ICAM-2/βactin)

1.20
1.10
1.00
0.90
0.80
0.70
0.60

— ● — TNF(4) + ActD
---□--- TNF(4) + bFGF + ActD

time (hrs)
0   5   1 0   1 5   2 0   2 5
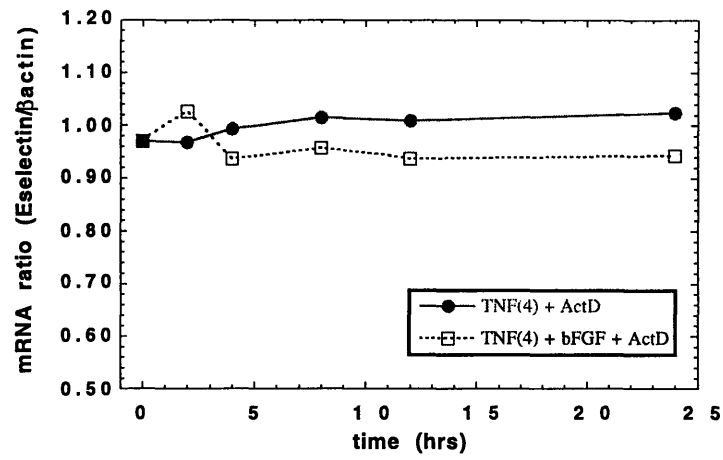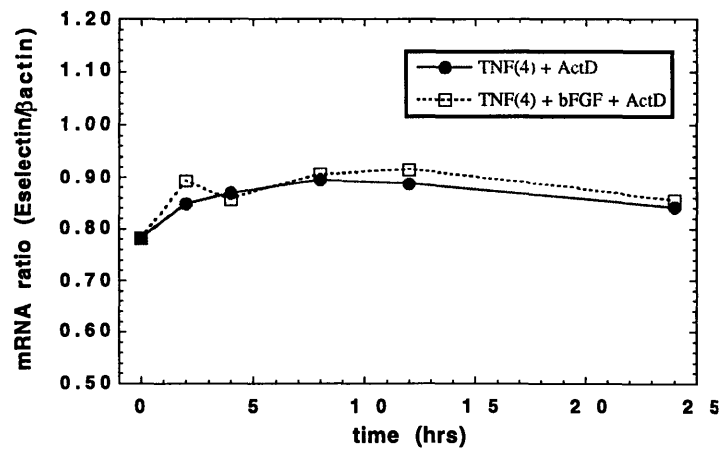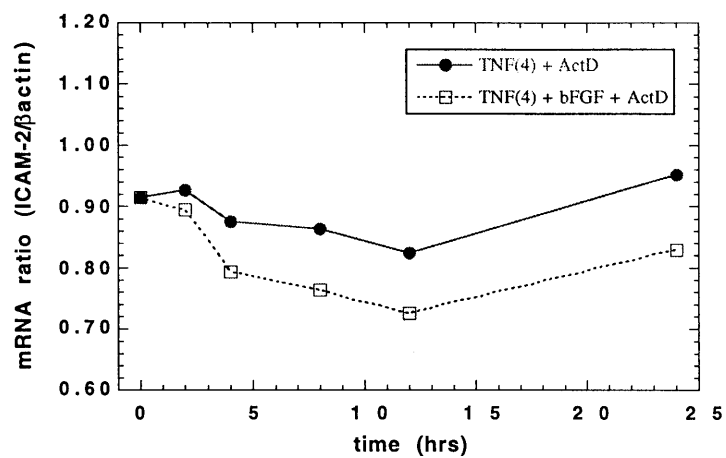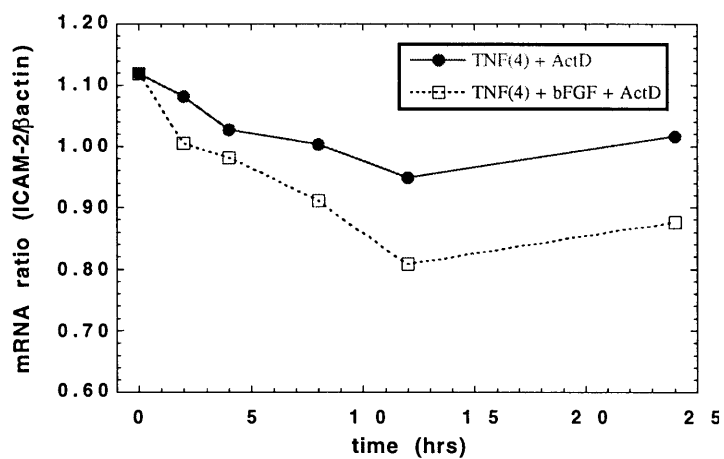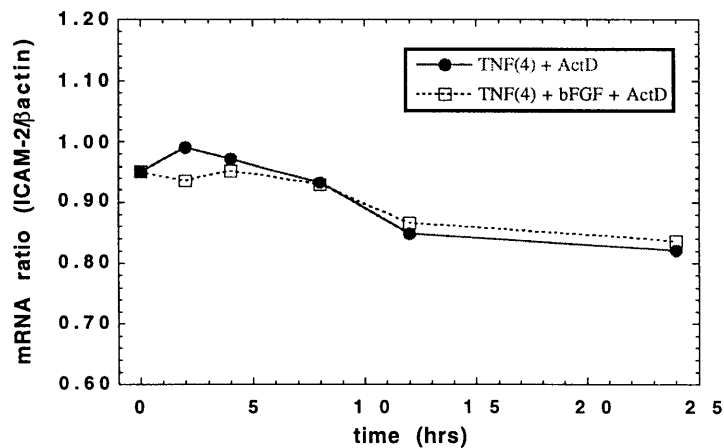
Figure C-2-4. Graphic representation of ICAM-2 mRNA stability analysis following 4 hr treatment with TNFα.

203
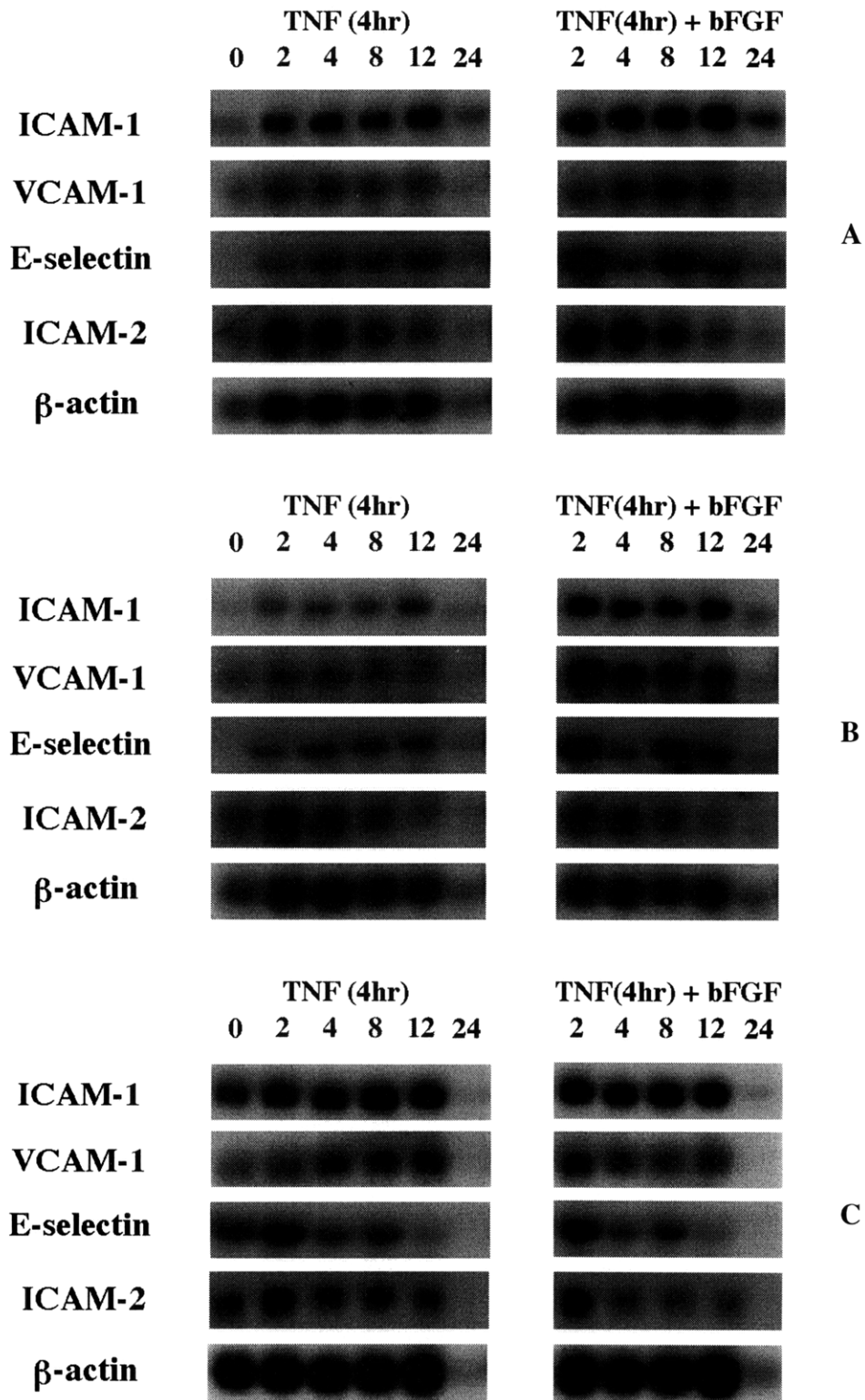
Figure C-2-5. Northern blots of mRNA stability analysis following 4 hr treatment with TNFα. Blots shown are from three separate experiments.

C.3 Signaling Inhibition Data

C.3.1 Dose Response Curves

Figure C-3-1. Heparin dose response curve on A-NK cell binding. Heparin applied on monolayer for 24 hrs. Flow rate of 0.085 mlm was utilized.

Figure C-3-2. MDHC dose response curve on A-NK cell binding. MDHC applied on monolayer for 24 hrs. Flow rate of 0.085 mlm was utilized.
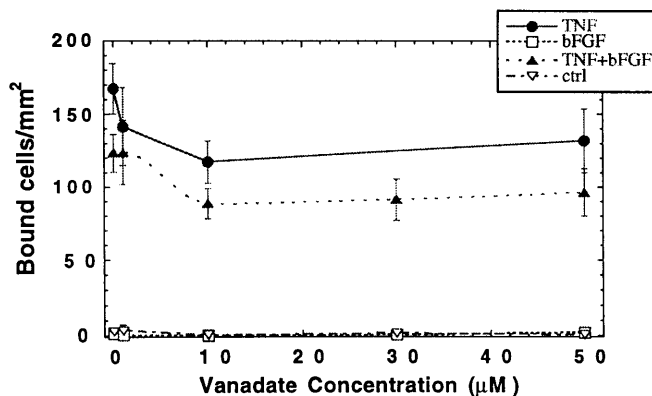
Figure C-3-3. Sodium orthovanadate dose response curve on A-NK cell binding. Vanadate applied on monolayer for 24 hrs. Flow rate of 0.085 mlm was utilized.
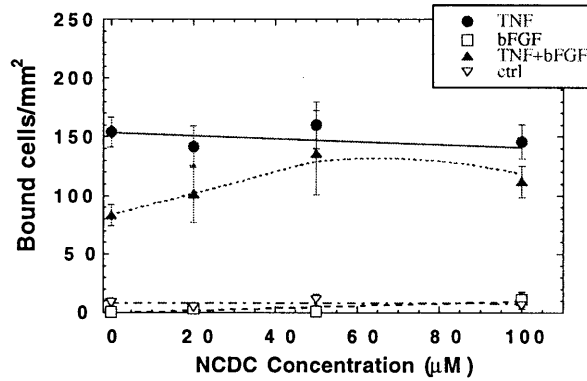
Figure C-3-4. NCDC dose response curve on A-NK cell binding. NCDC applied on monolayer for 24 hrs. Flow rate of 0.085 mlm was utilized.
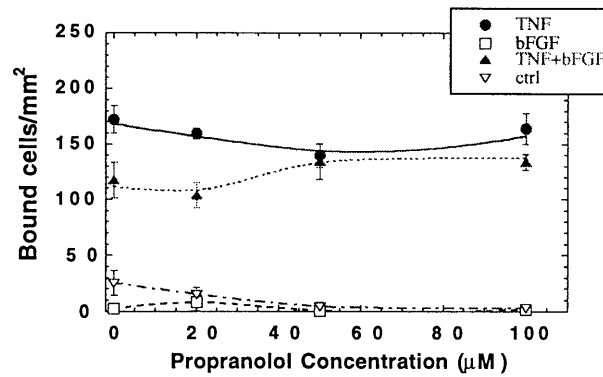
Figure C-3-5. Propranolol dose response curve on A-NK cell binding. Propranolol applied on monolayer for 24 hrs. Flow rate of 0.085 mlm was utilized.
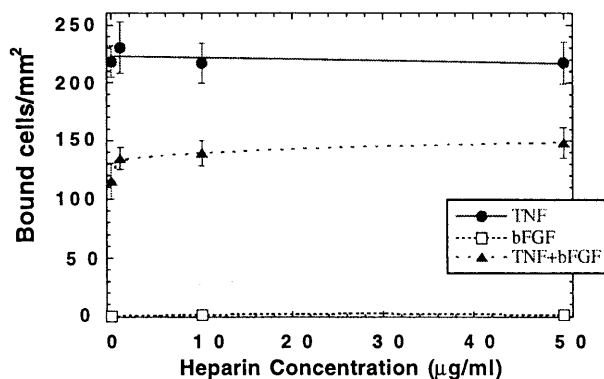

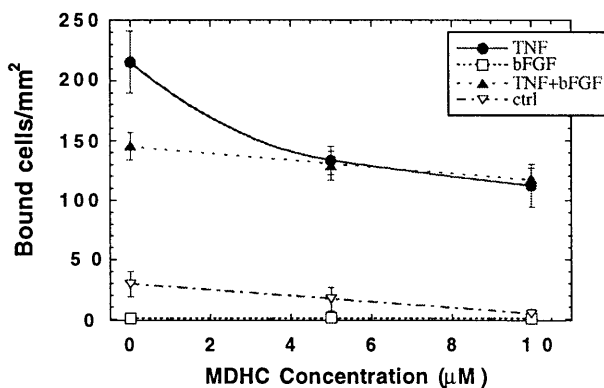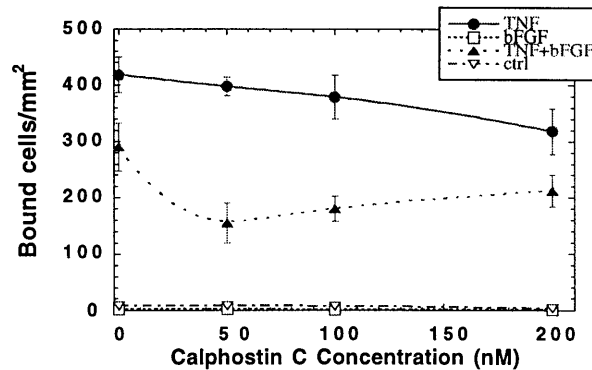Figure C-3-6. Calphostin C dose response curve on A-NK cell binding. Calphostin C applied on monolayer for 24 hrs. Flow rate of 0.085 mlm was utilized.

C.3.2 Adhesion Assay
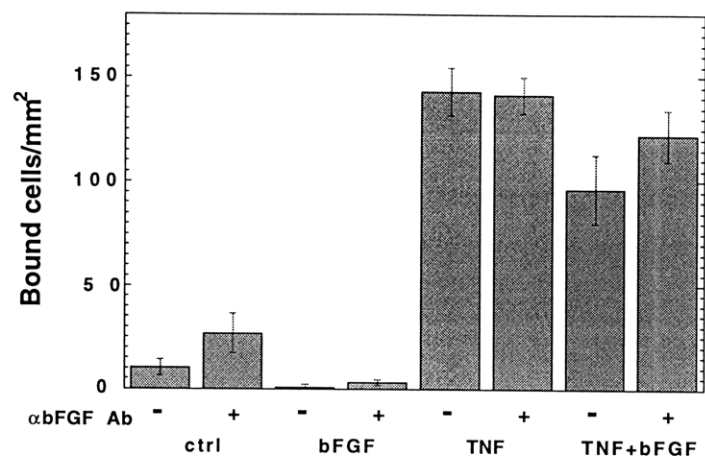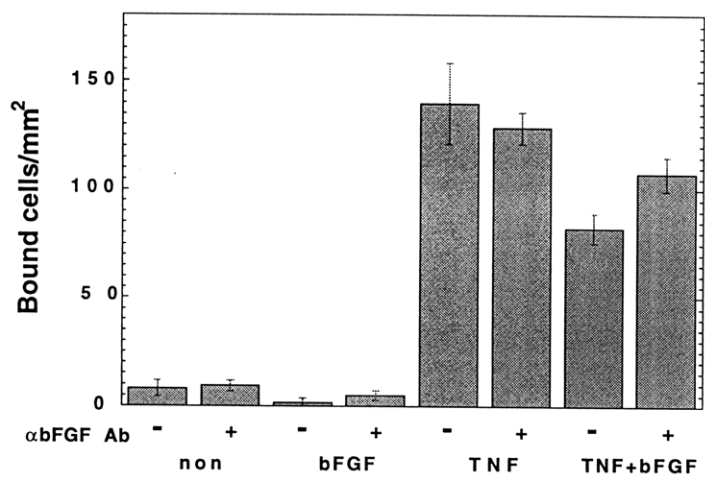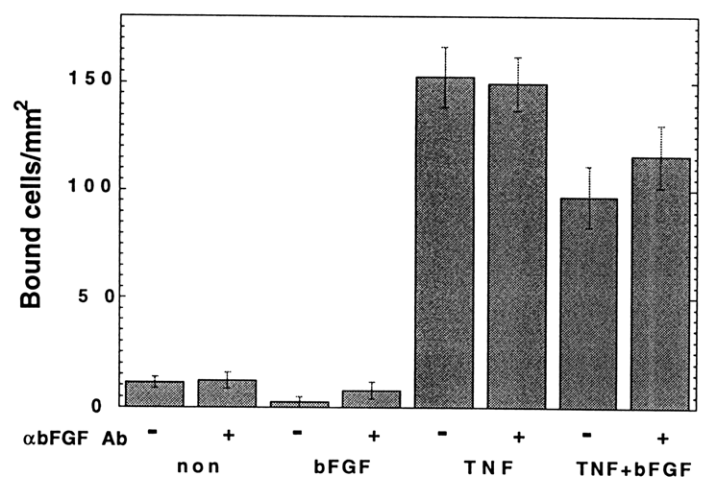
Figure C-3-7. Effect of neutralizing mAb for bFGF on A-NK cell binding to HUVEC monolayers treated with TNFα and bFGF.
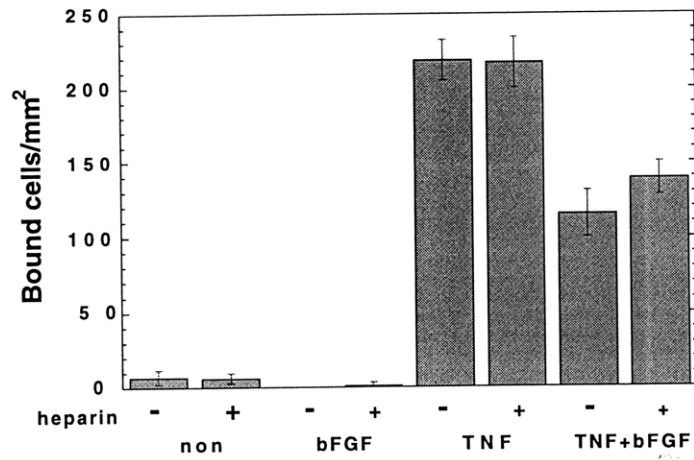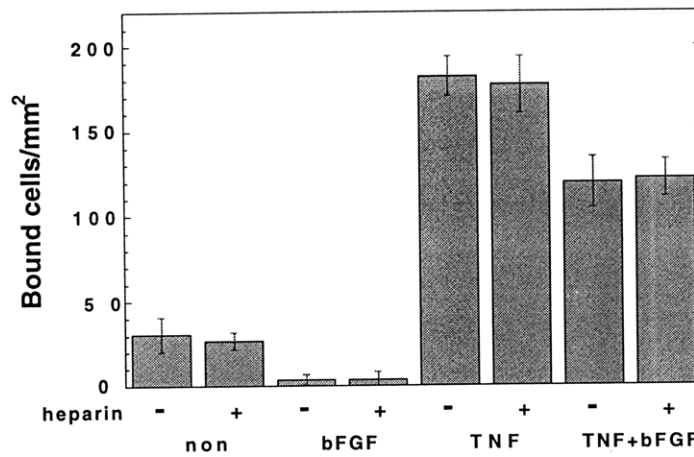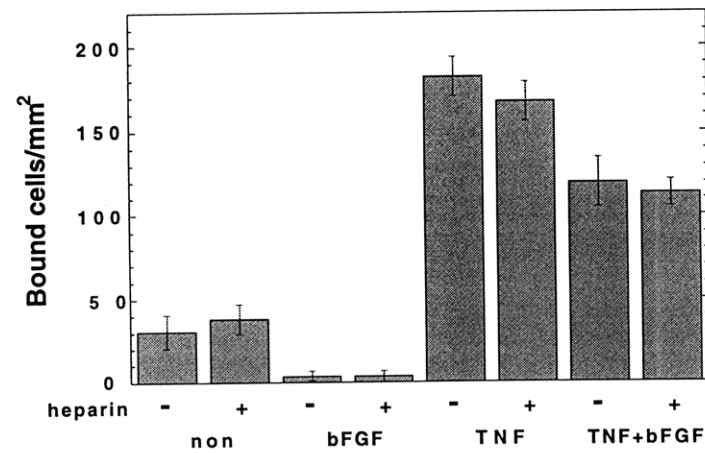
Figure C-3-8. Effect of heparin (10 µg/ml) on A-NK cell binding to HUVEC monolayers treated with TNFα and bFGF.
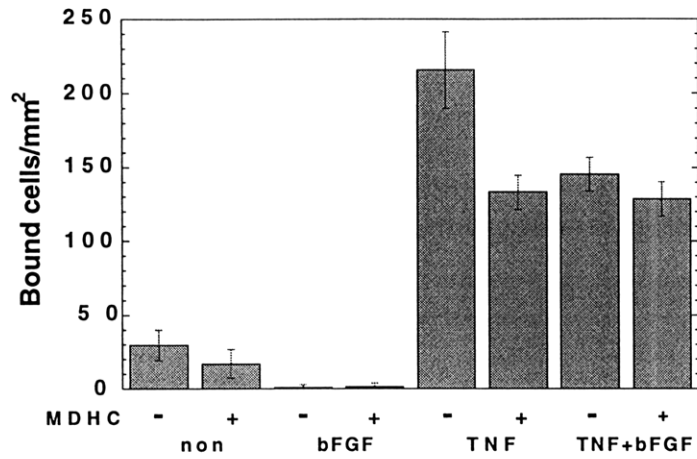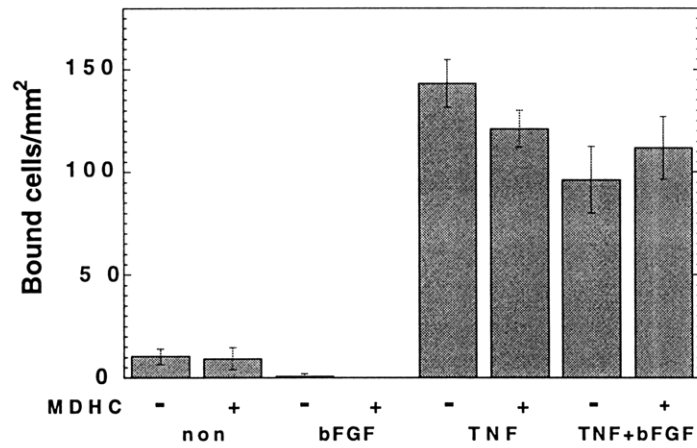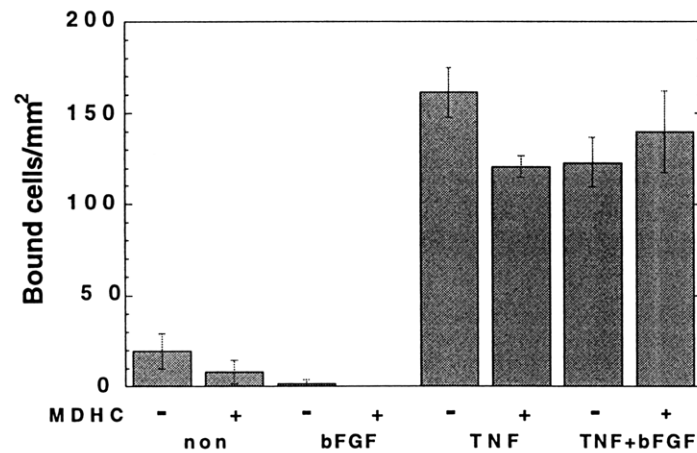
Figure C-3-9. Effect of MDHC (5 μM) on A-NK cell binding to HUVEC monolayers treated with TNFα and bFGF.
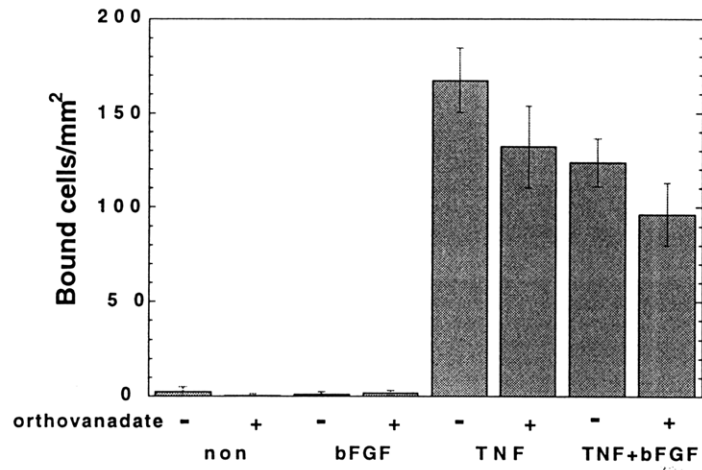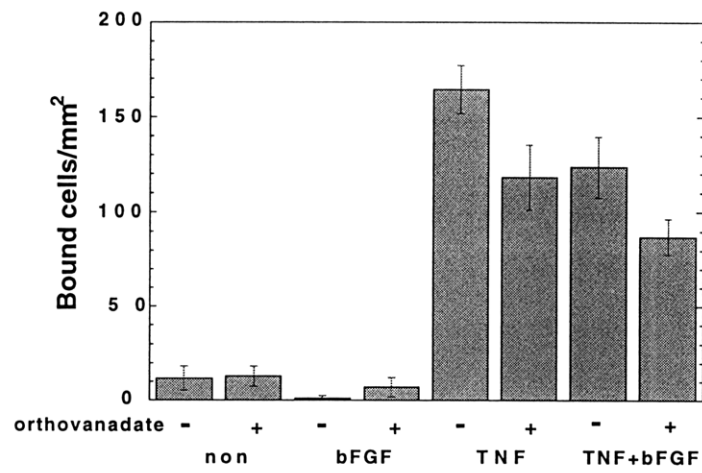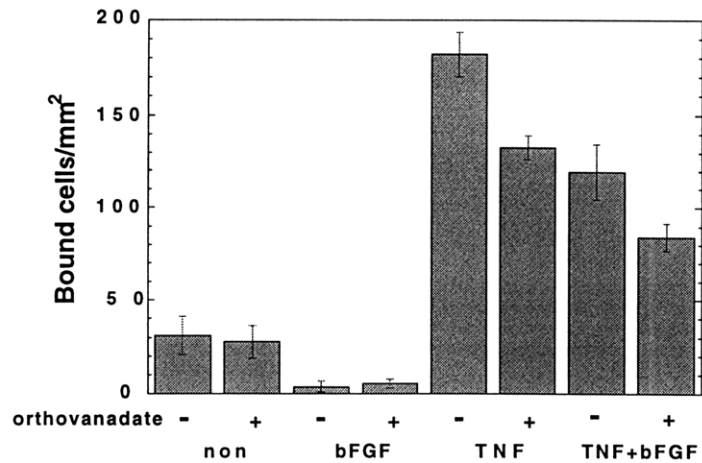
Figure C-3-10. Effect of sodium orthovanadate (30 μM) on A-NK cell binding to HUVEC monolayers treated with TNFα and bFGF.
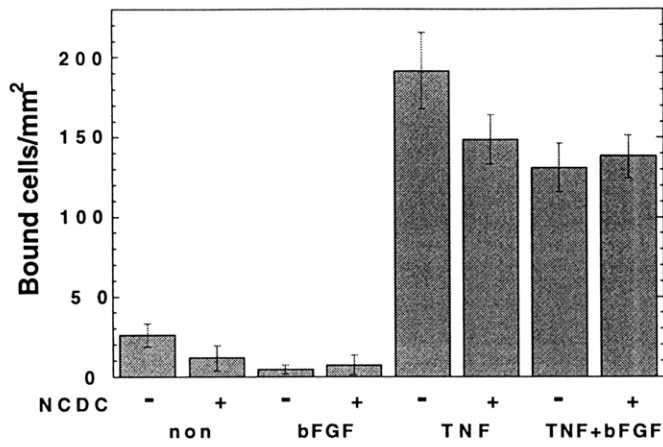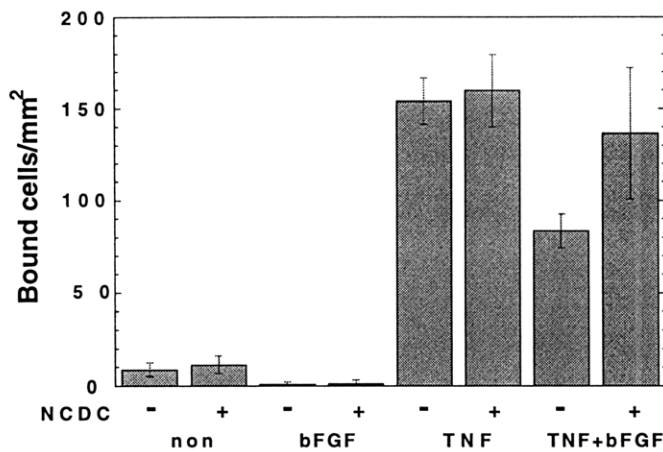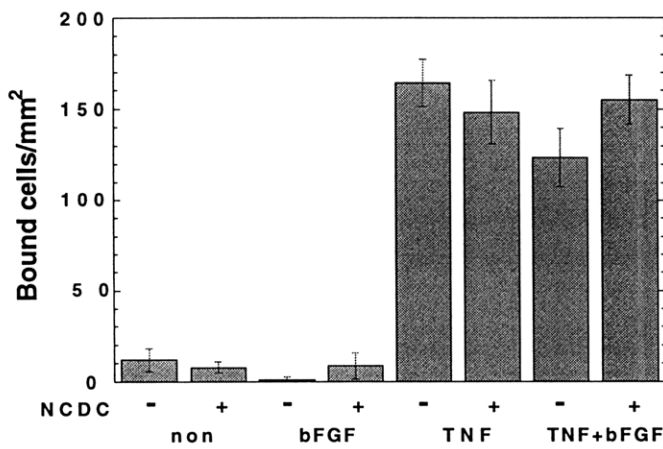
Figure C-3-11. Effect of NCDC (50 μM) on A-NK cell binding to HUVEC monolayers treated with TNFα and bFGF.
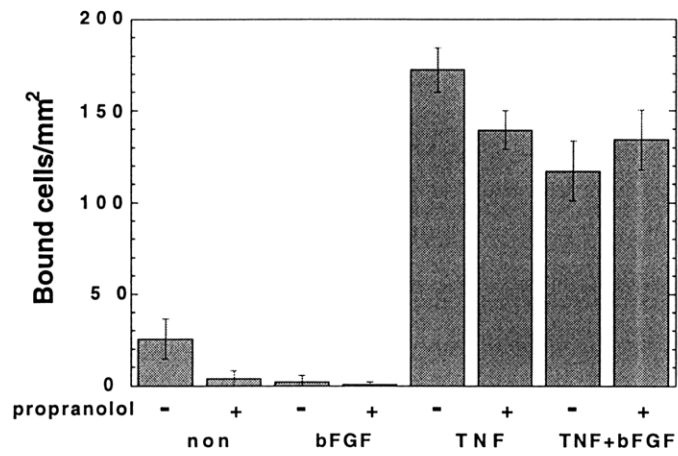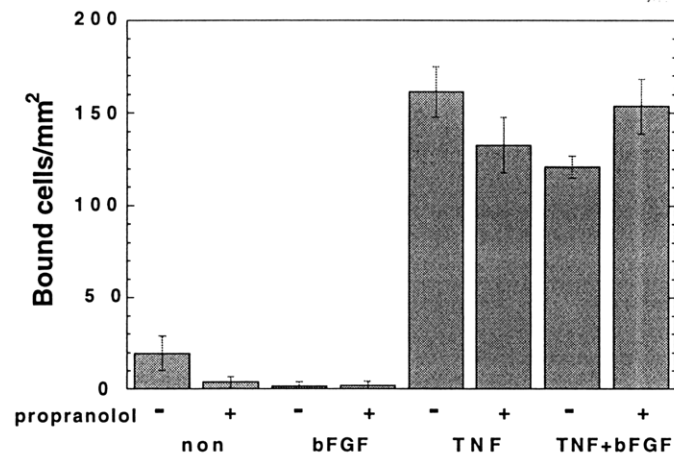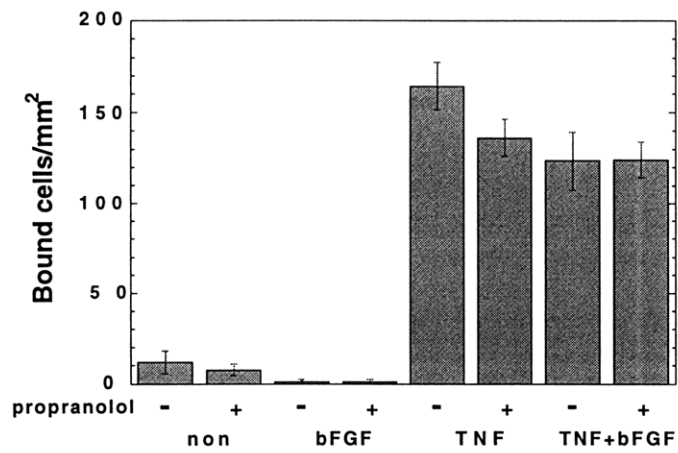
Figure C-3-12. Effect of propranolol (50 μM) on A-NK cell binding to HUVEC monolayers treated with TNFα and bFGF.
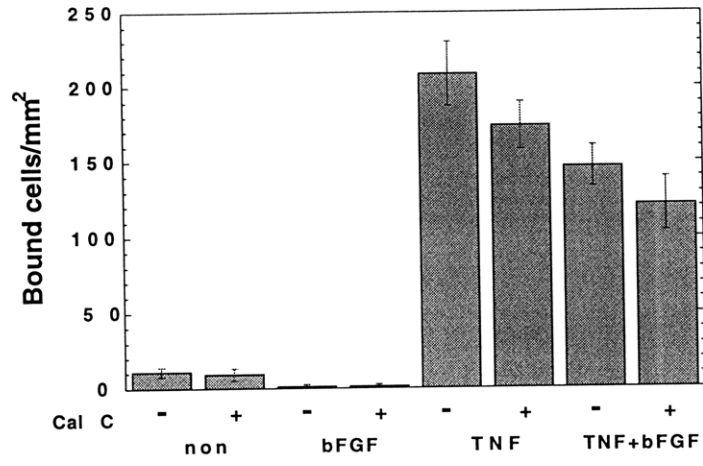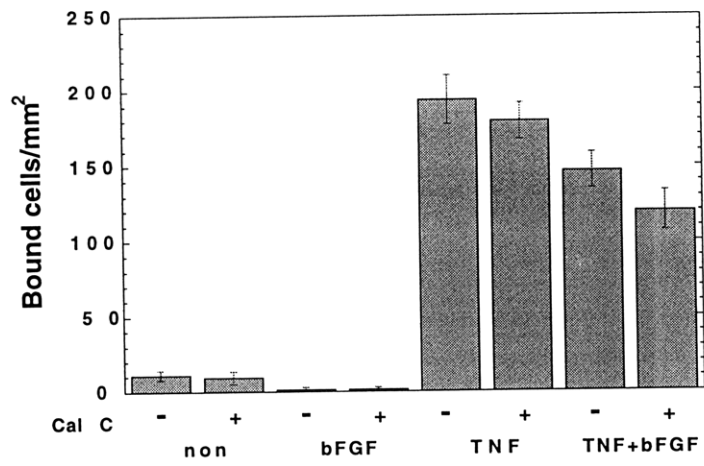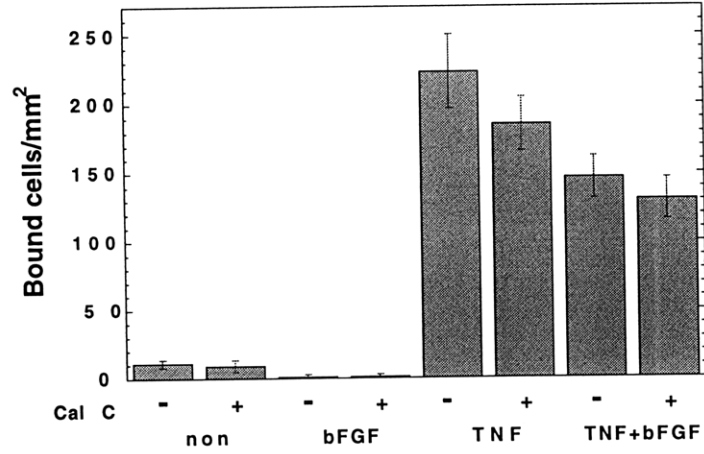
Figure C-3-13. Effect of calphostin C (50 nM) on A-NK cell binding to HUVEC monolayers treated with TNFα and bFGF.
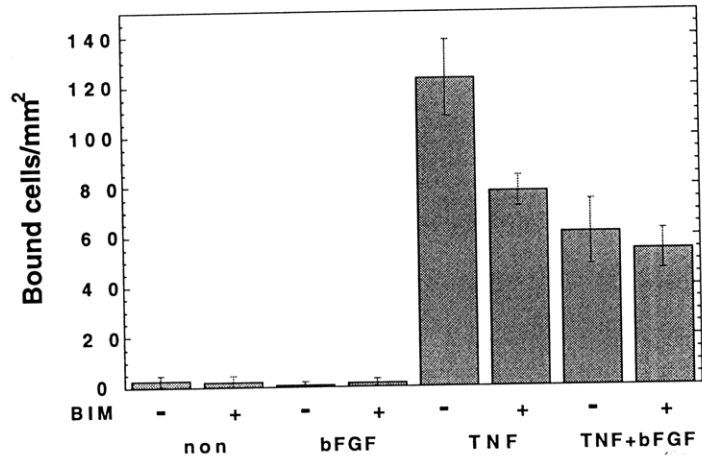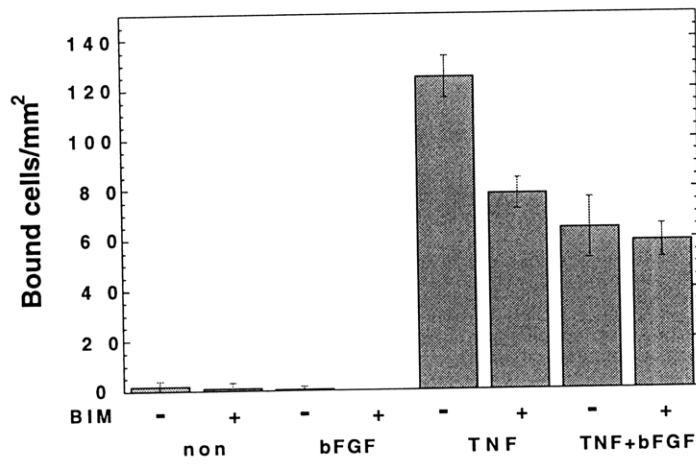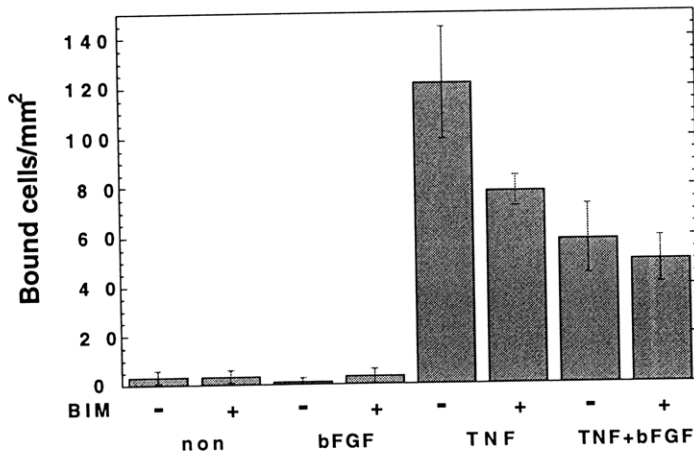
Figure C-3-14. Effect of bisindolylmaleimide (50 nM) on A-NK cell binding to HUVEC monolayers treated with TNFα and bFGF.
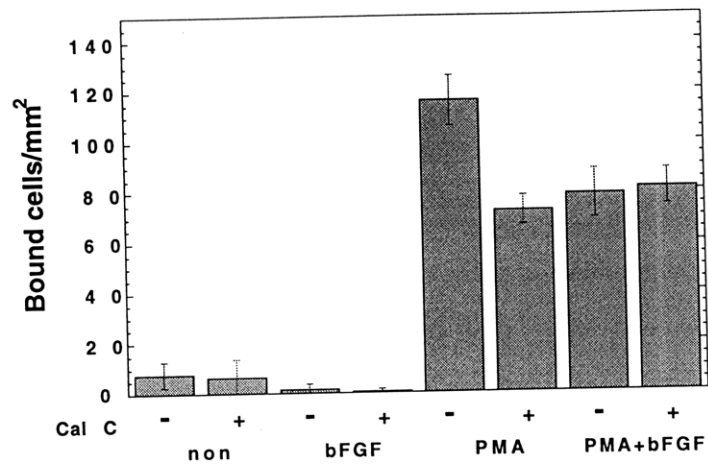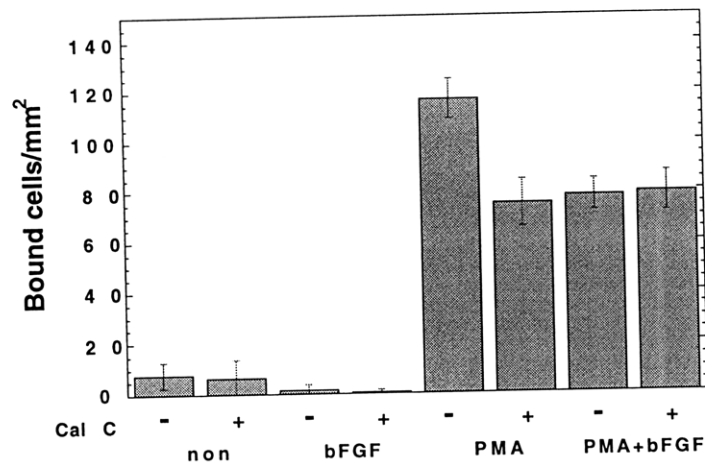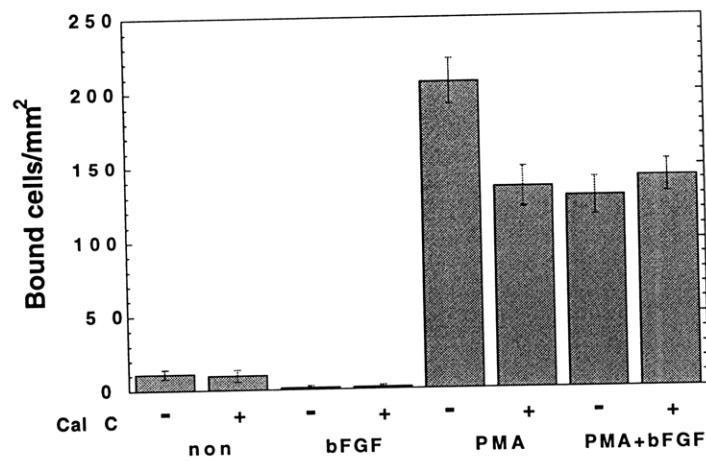
Figure C-3-15. Effect of calphostin C (50 nM) on A-NK cell binding to HUVEC monolayers treated with PMA and bFGF.

C.3.3 FIA Analysis

Table C-1. Surface CAM expression following treatment with MDHC, an inhibitor of receptor tyrosine kinases (RTK-i), and NCDC, an inhibitor of phospholipase C (PLC-i).

	IgG	ICAM-1	VCAM-1	E-selectin
1. control				
non	16.927 ± 15.930	77.593 ± 22.981	28.593 ± 10.477	10.927 ± 12.468
TNF	1.593 ± 6.173	648.590 ± 59.600	152.930 ± 30.234	112.930 ± 19.675
bFGF	5.927 ± 9.208	43.260 ± 16.442	8.593 ± 3.844	7.593 ± 6.741
TNF+bFGF	22.593 ± 11.921	397.590 ± 39.014	87.593 ± 23.730	51.593 ± 19.599
2. RTK-i				
non	15.593 ± 12.601	24.593 ± 6.984	13.927 ± 15.015	10.927 ± 12.548
TNF	10.260 ± 16.371	304.930 ± 37.905	92.260 ± 30.790	65.927 ± 13.569
bFGF	18.593 ± 7.219	26.927 ± 3.480	19.927 ± 7.055	12.593 ± 8.090
TNF+bFGF	17.927 ± 8.762	331.590 ± 54.192	83.927 ± 18.206	69.927 ± 15.026
3. PLC-i				
non	13.593 ± 9.387	29.260 ± 6.807	17.927 ± 1.856	8.593 ± 14.903
TNF	9.593 ± 6.360	471.260 ± 29.513	132.590 ± 17.458	71.260 ± 16.197
bFGF	7.593 ± 6.489	37.593 ± 6.489	19.260 ± 9.238	9.260 ± 6.245
TNF+bFGF	7.593 ± 8.413	453.930 ± 21.987	128.930 ± 22.578	61.260 ± 22.502

Table C-2. Surface CAM expression following treatment with sodium orthovanadate, an inhibitor of phosphotyrosine phosphatase (PTP-i), and propranolol, an inhibitor of phospholipase D (PLD-i).

	IgG	ICAM-1	VCAM-1	E-selectin
1. control				
non	6.877 ± 5.239	34.877 ± 13.220	11.877 ± 4.410	6.880 ± 2.906
TNF	13.210 ± 6.658	612.880 ± 29.475	216.880 ± 35.834	108.880 ± 34.187
bFGF	3.210 ± 6.083	20.210 ± 15.144	4.877 ± 8.951	3.210 ± 4.619
TNF+bFGF	8.877 ± 16.045	381.210 ± 45.654	83.877 ± 43.191	58.877 ± 14.438
2. PTP-i				
non	6.543 ± 14.530	40.540 ± 10.414	24.880 ± 7.881	14.210 ± 4.509
TNF	7.210 ± 13.503	546.880 ± 57.074	119.210 ± 17.578	104.210 ± 9.238
bFGF	5.877 ± 13.776	16.877 ± 7.753	12.540 ± 6.692	6.543 ± 6.489
TNF+bFGF	7.210 ± 9.452	327.540 ± 26.872	79.543 ± 23.596	36.543 ± 9.262
3. PLD-i				
non	1.543 ± 7.881	9.210 ± 14.503	5.877 ± 5.608	2.877 ± 4.978
TNF	8.543 ± 6.119	521.540 ± 67.432	167.880 ± 27.847	94.877 ± 11.260
bFGF	4.210 ± 4.583	11.877 ± 8.192	6.543 ± 4.978	2.543 ± 4.807
TNF+bFGF	4.543 ± 4.978	492.880 ± 65.170	163.540 ± 45.042	88.543 ± 11.260

Table C-3. Surface CAM expression following treatment with a neutralizing monoclonal antibody selective for bFGF, and heparin, a low affinity, bFGF binding molecule.

	IgG	ICAM-1	VCAM-1	E-selectin
1. control				
non	12.377 ± 4.485	36.377 ± 9.333	19.710 ± 7.371	8.710 ± 6.028
TNF	10.043 ± 4.485	994.380 ± 114.920	355.380 ± 65.547	145.380 ± 14.252
bFGF	12.043 ± 8.413	30.043 ± 6.360	13.377 ± 6.489	8.710 ± 4.726
TNF+bFGF	13.377 ± 6.065	530.040 ± 68.921	161.380 ± 35.983	87.710 ± 23.116
2. bFGFAb				
non	10.710 ± 8.622	34.043 ± 11.865	10.377 ± 4.631	8.377 ± 9.838
TNF	12.043 ± 8.007	895.710 ± 89.716	330.710 ± 67.801	125.380 ± 22.452
bFGF	8.043 ± 7.265	28.043 ± 11.624	18.710 ± 6.807	16.377 ± 8.007
TNF+bFGF	12.043 ± 8.686	755.710 ± 83.608	314.040 ± 40.916	120.040 ± 32.916
3. heparin				
non	10.710 ± 6.557	25.043 ± 4.978	18.710 ± 6.083	7.377 ± 4.807
TNF	12.377 ± 4.667	1054.00 ± 116.280	356.040 ± 49.184	124.710 ± 32.005
bFGF	12.043 ± 4.410	13.043 ± 4.333	9.043 ± 7.356	7.377 ± 9.387
TNF+bFGF	8.710 ± 4.583	560.040 ± 87.052	146.380 ± 49.157	86.043 ± 21.481

Table C-4. Surface CAM expression following treatment with the protein kinase C inhibitors (PKC-i), calphostin C and bisindolylmaleimide (BIM).

	IgG	ICAM-1	VCAM-1	E-selectin
1. control				
non	6.933 ± 9.405	50.933 ± 8.951	15.933 ± 10.745	10.267 ± 2.404
TNF	21.600 ± 7.000	564.600 ± 86.170	261.270 ± 78.257	94.600 ± 13.454
bFGF	12.933 ± 7.860	27.933 ± 5.044	19.600 ± 7.550	16.933 ± 9.280
TNF+bFGF	18.933 ± 9.528	360.930 ± 40.275	135.600 ± 31.193	59.267 ± 17.629
2. PKC-i (calphostin C)				
non	12.933 ± 5.608	43.267 ± 9.208	14.267 ± 13.618	13.933 ± 6.333
TNF	19.600 ± 10.504	549.930 ± 65.859	161.270 ± 36.112	89.267 ± 14.970
bFGF	20.933 ± 13.776	8.933 ± 5.548	19.933 ± 11.200	15.933 ± 3.180
TNF+bFGF	21.267 ± 11.289	348.270 ± 81.538	113.930 ± 37.560	49.933 ± 17.704
3. PKC-i (BIM)				
non	1.600 ± 13.614	41.600 ± 8.505	4.267 ± 6.173	13.267 ± 7.535
TNF	14.267 ± 10.088	527.600 ± 45.299	96.267 ± 40.193	83.267 ± 17.420
bFGF	12.933 ± 9.244	18.933 ± 9.262	17.600 ± 15.885	13.933 ± 9.563
TNF+bFGF	21.933 ± 7.881	334.930 ± 68.494	86.933 ± 24.781	46.933 ± 6.839

Table C-5. Surface CAM expression following treatment with the protein kinase C inhibitor calphostin C on PMA-activated monolayers.

	IgG	ICAM-1	VCAM-1	E-selectin
1. control				
non	29.567 ± 6.359	43.233 ± 14.655	33.233 ± 3.712	27.233 ± 4.978
PMA	27.233 ± 8.647	892.900 ± 119.620	528.570 ± 79.434	111.570 ± 8.413
bFGF	38.567 ± 3.383	24.233 ± 5.897	31.233 ± 5.175	26.233 ± 6.333
PMA+bFGF	34.900 ± 2.082	591.230 ± 66.996	352.570 ± 38.490	73.233 ± 26.359
2. PKC-i (calphostin C)				
non	28.900 ± 3.786	38.233 ± 10.914	27.233 ± 5.841	27.233 ± 7.965
PMA	29.567 ± 4.333	610.570 ± 82.321	341.900 ± 62.746	83.233 ± 11.215
bFGF	27.567 ± 6.333	33.567 ± 9.135	32.233 ± 5.812	25.233 ± 6.489
PMA+bFGF	26.900 ± 8.888	601.230 ± 74.414	324.900 ± 62.429	75.567 ± 20.301

Bibliography

Abassi, O., Kishimoto, T. K., McIntire, L. V., Anderson, D. C., and Smith, C. W. E-selectin supports neutrophil rolling in vitro under conditions of flow. *Journal of Clinical Investigations*, **92**: 2719-2730, 1993.

Ahmed, A., Plevin, R., Shoaibi, M. A., Fountain, S. A., Ferriani, R. A., and Smith, S. K. Basic FGF activates phospholipase D in endothelial cells in the absence of inositol-lipid hydrolysis. *American Journal of Physiology*, **266**: C206-C212, 1994.

Allavena, P., Paganin, C., Martin-Padura, I., Peri, G., Gaboli, M., Dejana, E., Marchisio, P. C., and Mantovani, A. Molecules and structures involved in the adhesion of natural killer cells to vascular endothelium. *Journal of Experimental Medicine*, **173**: 439-448, 1991.

Aronson, F. R., Libby, P., Brandon, E. P., Janicka, M. W., and Mier, J. W. IL-2 rapidly induces natural killer cell adhesion to human endothelial cells. A potential mechanism for endothelial injury. *Journal of Immunology*, **141**: 158-163, 1988.

Asaoka, Y., Nakamura, S., Yoshida, K., and Nishizuka, Y. Protein kinase C, calcium and phospholipid degradation. *Trends in Biochemical Sciences*, **17**: 414-417, 1992.

Baldin, V., Roman, A. M., Bosc, B. I., Amalric, F., and Bouche, G. Translocation of bFGF to the nucleus is G1 phase cell cycle specific in bovine aortic endothelial cells. *EMBO Journal*, **9**: 1511-1517, 1990.

Basse, P. H., Nannmark, U., Johansson, B. R., Herberman, R. B., and Goldfarb, R. H. Establishment of cell-to-cell contact by adoptively transferred adherent lymphokine-activated killer cells with metastatic murine melanoma cells. *Journal of the National Cancer Institute*, **83**: 944-950, 1991.

Bebok, Z., Markus, B., and Nemeth, P. Prognostic relevance of transforming growth factor alpha (TGF-alpha) and tumor necrosis factor alpha (TNF-alpha) detected in breast cancer tissues by immunohistochemistry. *Breast Cancer Research and Treatment*, **29**: 229-235, 1994.

Bevilacqua, M. P., Pober, J. S., Wheeler, M. E., Cotran, R. S., and Gimbrone Jr., M. A. Interleukin-1 acts on cultured human vascular endothelium to increase the adhesion of

polymorphonuclear leukocytes, monocytes, and related leukocytic cell lines. *Journal of Clinical Investigation,* **76**: 1160-1165, 1985.

Bevilacqua, M. P., Stengelin, S., Gimbrone Jr., M. A., and Seed, B. Endothelial leukocyte molecule 1: an inducible receptor for neutrophils related to complement regulatory proteins and lectins. *Science,* **243**: 1160-1164, 1989.

Bierer, B. E. and Burakoff, S. J. T cell adhesion molecules. *FASEB Journal,* **2**: 2584-2590, 1988.

Billah, M. M. and Anthes, J. C. The regulation and cellular functions of phosphatidylcholine hydrolysis. *Biochemical Journal,* **269**: 281-291, 1990.

Biselli, R., Matricardi, P. M., D'Amelio, R., and Fattorossi, A. Multiparametric flow cytometric analysis of the kinetics of surface molecule expression after polyclonal activation of human peripheral blood T lymphocytes. *Scandinavian Journal of Immunology,* **35**: 439-447, 1992.

Blood, C. H. and Zetter, B. R. Tumor interactions with the vasculature: angiogenesis and tumor metastasis. *Biochimica et Biophysica Acta,* **1032**: 89-118, 1990.

Boehm, T., Folkman, J., Browder, T., and O'Reilly, M. S. Antiangiogenic therapy of experimental cancer does not induce acquired drug resistance. *Nature,* **390**: 404-407, 1997.

Broudy, V. C., Kaushansky, K., Segal, G. M., Harlan, J. M., and Adamson, J. W. Tumor necrosis factor type α stimulates human endothelial cells to produce granulocyte/macrophage colony-stimulating factor. *Proceedings of the National Academy of Sciences,* **83**: 7467-7472, 1986.

Burgess, W. H., Dionne, C. A., Kaplow, J., Mudd, R., Friesel, R., Zilberstein, A., Schlessinger, J., and Jaye, M. Characterization and cDNA cloning of phospholipase C-γ, a major substrate for heparin-binding growth factor 1 (acidic fibroblast growth factor)-activated tyrosine kinase. *Molecular and Cellular Biology,* **10**: 4770-4777, 1990.

Burridge, K., Fath, K., Kelly, T., Nuckolls, G., and Turner, C. Focal adhesions: transmembrane junctions between the extracellular matrix and cytoskeleton. *Annual Reviews of Cellular Biology,* **4**: 487-495, 1988.

Bussolari, S. R., Dewey, C. F., Jr., and Gimbrone, M. A., Jr. Apparatus for subjecting living cells in fluid shear stress. *Reviews of Scientific Instrumentation,* **53**: 1851-1854, 1982.

Butcher, E. C. Leukocyte-endothelial cell recognition: three (or more) steps to specificity and diversity. *Cell,* **67**: 1033-1036, 1991.

Cadena, D. L. and Gill, G. N. Receptor tyrosine kinases. *FASEB Journal,* **6**: 2332-2337, 1992.

Carcamo, J., Zentella, A., and Massague, J. Type I receptors specify growth-inhibitory and transcriptional responses to transforming growth factor beta and activin. *Molecular and Cellular Biology,* **15**: 1573-1581, 1994.

Carlos, T. M., Schwartz, B. R., Kovach, N. L., Yee, E., Rosso, M., Osborn, L., Chi-Rosso, G., Newman, B., Lobb, R., and Harlan, J. M. Vascular cell adhesion molecule-1 mediates lymphocyte adherence to cytokine-activated cultured human endothelial cells. *Blood*, **76**: 965-70, 1990.

Carpenter, G. Receptors for epidermal growth factor and other polypeptide mitogens. *Annual Review of Biochemistry*, **56**: 881-914, 1987.

Cavender, D., Saegusa, Y., and Ziff, M. Stimulation of endothelial cell binding of lymphocytes by tumor necrosis factor. *Journal of Immunology*, **139**: 1855-1860, 1987.

Christofori, G. The role of fibroblast growth factors in tumour progression and angiogenesis. *In:* R. Bicknell, C. E. Lewis, and N. Ferrara (eds.), Tumour angiogenesis, pp. 201-238. Oxford: Oxford University Press, 1997.

Clark, M. A., Chen, M. J., Crooke, S. T., and Bomalaski, J. S. Tumor necrosis factor (cachectin) induces phospholipase A_2 activity and synthesis of a phospholipase A_2 activating protein in endothelial cells. *Biochemical Journal*, **250**: 125-132, 1988.

Clauss, M., Weich, H., Breier, G., Knies, U., Rockl, W., Waltenberger, J., and Risau, W. The vascular endothelial growth factor receptor Flt-1 mediates biological activities. Implications for a functional role of placenta growth factor in monocyte activation and chemotaxis. *Journal of Biological Chemistry*, **271**: 17629-17634, 1996.

Collins, T. Adhesion molecules in leukocyte emigration. *Scientific American: Science & Medicine*, **2**: 28-37, 1995.

Collins, T., Read, M. A., Neish, A. S., Whitley, M. Z., Thanos, D., and Maniatis, T. Transcriptional regulation of endothelial cell adhesion molecules: NF-κB and cytokine-inducible enhancers. *FASEB Journal*, **9**: 899-909, 1995.

Cotran, R. S. and Pober, J. S. Cytokine-endothelial interactions in inflammation, immunity, and vascular injury. *Journal of the American Society of Nephrology*, **1**: 225-235, 1990.

Coughlin, S. R., Barr, P. J., Cousens, L. S., Fretto, L. J., and Williams, L. T. Acidic and basic fibroblast growth factors stimulate tyrosine kinases activity in vivo. *Journal of Biological Chemistry*, **263**: 988-993, 1988.

Dalal, B. I., Keown, P. A., and Greenberg, A. H. Immunocytochemical localization of secreted transforming growth factor-beta 1 to the advancing edges of primary tumors and to lymph node metastases of human mammary carcinoma. *American Journal of Pathology*, **143**: 381-389, 1993.

Deisher, T. A., Haddix, T. L., Montgomery, K. F., Pohlman, T. H., Kaushansky, K., and Harlan, J. M. The role of protein kinase C in the induction of VCAM-1 expression on human umbilical vein endothelial cells. *FEBS Letters*, **331**: 285-290, 1993.

Detmar, M., Brown, L. F., Schon, M. P., Elicker, B. M., Velasco, P., Richard, L., Fukumura, D., Monsky, W., Claffey, K. P., and Jain, R. K. Increased microvascular density and enhanced leukocyte rolling and adhesion in the skin of VEGF transgenic mice. *Journal of Investigative Dermatology*, **111**: 1-6, 1998.

DeVries, C., Escobedo, J. A., Ueno, H., Houck, K., Ferrara, N., and Williams, L. T. The fms-like tyrosine kinase, a receptor for vascular endothelial cell growth factor. *Science*, **255**: 989-991, 1992.

Doctrow, S. R. and Folkman, J. Protein kinase C activators suppress stimulation of capillary endothelial cell growth by angiogenic endothelial mitogens. *Journal of Cell Biology*, **104**: 679-687, 1987.

Doroszewski, J., Golab-Meyer, Z., and Guryn, W. Adhesion of cells in flowing suspensions: effects of shearing force and cell kinetic energy. *Microvascular Research*, **18**: 421-433, 1979.

Dustin, M. L. and Springer, T. A. Lymphocyte function-associated antigen-1 (LFA-1) interaction with intercellular adhesion molecule-1 (ICAM-1) is one of at least three mechanisms for lymphocyte adhesions to cultured endothelial cells. *Journal of Cell Biology*, **107**: 321-331, 1988.

Elices, M. J., Osborn, L., Takada, Y., Crouse, C., Luhowskyj, S., Hemler, M. E., and Lobb, R. VCAM-1 on activated endothelium interacts with the leukocyte integrin VLA-4 at a site distinct from the VLA-4/fibronectin binding site. *Cell*, **60**: 577-584, 1990.

Exton, J. H. Signaling through phosphatidylcholine breakdown. *Journal of Biological Chemistry*, **265**: 1-4, 1990.

Fafeur, V., Terman, B. I., Blum, J., and Bohlen, P. Basic FGF treatment of endothelial cells down-regulates the 85-kDa TGF beta receptor subtype and decreases the growth inhibitory response to TGF-beta 1. *Growth Factors*, **3**: 237-245, 1990.

Fajardo L.-G., L. F. and Allison, A. C. Tumour necrosis factor alpha and angiogenesis. *In:* R. Bicknell, C. E. Lewis, and N. Ferrara (eds.), Tumour angiogenesis, pp. 261-271. Oxford: Oxford University Press, 1997.

Ferrara, N., Houck, K., Jakeman, L., and Leung, D. W. Molecular and biological properties of the vascular endothelial growth factor family of proteins. *Endocrinology Review*, **13**: 18-32, 1992.

Fidler, I. J. and Ellis, L. M. The implications of angiogenesis for biology and therapy of cancer metastasis. *Cell*, **79**: 185-188, 1994.

Folkman, J. What is the evidence that tumours are angiogenesis dependent? *Journal of the National Cancer Institute*, **82**: 4-6, 1990.

Folkman, J. Clinical applications of research on angiogenesis. *New England Journal of Medicine*, **333**: 1757-1763, 1995.

Folkman, J. Tumor angiogenesis. *In:* P. M. Mendelsohn, M. A. P. Howley, and L. A. Liotta (eds.), The molecular basis of cancer, pp. 206-232. Philadelphia: W.B. Saunders, 1995.

Frater-Schroder, M., Risau, W., Hallman, P., Gautschi, R., and Bohlen, P. Tumor-necrosis factor type-a, a potent inhibitor of endothelial cell growth in vitro, is angiogenic in vivo. *Proceedings of the National Academy of Sciences*, **84**: 5277-5281, 1987.

Freeman, M. R., Schneck, F. X., Gagnon, M. L., Corless, C., Soker, S., Niknejad, K., Peoples, G. E., and Klagsbrun, M. Peripheral blood T lymphocytes and lymphocytes infiltrating human cancers express vascular endothelial growth factor: a potential role for T cells in angiogenesis. *Cancer Rsearch*, **55**: 4140-4145, 1995.

Friesel, R. E. and Maciag, T. Molecular mechanisms of angiogenesis: fibroblast growth factor signal transduction. *FASEB Journal*, **9**: 919-925, 1995.

Fuortes, M., Jin, W. W., and Nathan, C. Adhesion-dependent protein tyrosine phosphorylation in neutrophils treated with tumor necrosis factor. *Journal of Cellular Biology*, **120**: 777-783, 1993.

Gamble, J. R. and Vadas, M. A. Endothelial adhesiveness for blood neutrophils is inhibited by transforming growth factor-beta. *Science*, **242**: 97-99, 1988.

Gamble, J. R. and Vadas, M. A. Endothelial cell adhesiveness for human T lymphocytes is inhibited by transforming growth factor-beta. *Journal of Immunology*, **146**: 1149-1154, 1991.

Gamble, J. R. and Khew-Goodall, Y. Transforming growth factor-beta inhibits E-selectin expression on human endothelial cells. *Journal of Immunology*, **150**: 4494-4503, 1993.

Gerszten, R. E., Luscinskas, F. W., Ding, H. T., Dichek, D. A., Stoolman, L. M., Gimbrone, M. A., and Rosenzweig, A. Adhesion of memory lymphocytes to vascular cell adhesion molecule-1-transduced human vascular endothelial cells under stimulated physiological flow conditions in vitro. *Circulation Research*, **79**: 1205-1215, 1996.

Gimbrone, M. A. J., Cotran, R. S., and Folkman, J. Human vascular endothelial cells in culture. Growth and DNA synthesis. *Journal of Cell Biology*, **60**: 673-684, 1974.

Goldspiel, B. R., Green, L., and Calis, K. A. Human gene therapy. *Clinical Pharmocology*, **12**: 488-505, 1993.

Goto, F., Goto, K., Weidel, K., and Folkman, J. Synergistic effects of vascular endothelial growth factor and basic fibroblast growth factor on the proliferation and cord formation of bovine capillary endothelial cells within collagen gels. *Journal of Laboratory Investigation*, **69**: 508-517, 1993.

Griffioen, A. W., Damen, C. A., Blijham, G. H., and Groenewegen, G. Tumor angiogenesis is accompanied by a decreased inflammatory response of tumor-associated endothelium. *Blood*, **88**: 667-673, 1996.

Griffioen, A. W., Damen, C. A., Martinotti, S., Blijham, G. H., and Groenewegen, G. Endothelial ICAM-1 expression is suppressed in human malignancies; role of angiogenic factors. *Cancer Research*, **56**: 1111-1117, 1996.

Gruppuso, P. A., Mikumo, R., Brautigan, D. L., and Braun, L. Growth arrest induced by transforming growth factor-beta 1 is accompanied by protein phosphatase activation in human keratinocytes. *Journal of Biological Chemistry*, **266**: 3444-3448, 1991.

Gualandris, A. and Presta, M. Transcriptional and post-transcriptional regulation of urokinase-type plasminogen activator expression in endothelial cells by basic fibroblast growth factor. *Journal of Cellular Physiology*, **162**: 400-409, 1995.

223

Gullino, P. M. Techniques in tumor pathophysiology. *In:* H. Busch (ed.) Methods in Cancer Research, pp. 45-92. New York: Academic Press, 1970.

Guo, D., Jia, Q., Song, H. Y., Warren, R. S., and Donner, D. B. Vascular endothelial cell growth factor promotes tyrosine phosphorylation of mediators of signal transduction that contain SH2 domains. Association with endothelial cell proliferation. *Journal of Biological Chemistry*, **270**: 6729-6733, 1995.

Haller, H., Ziegler, W., Lindschau, C., and Luft, F. C. Endothelial cell tyrosine kinase receptor and G protein-coupled receptor activation involves distinct protein kinase C isoforms. *Arteriosclerosis, Thrombosis, and Vascular Biology*, **16**: 678-686, 1996.

Halstead, J., Kemp, K., and Ignotz, R. A. Evidence for involvement of phosphatidyl-choline-phospholipase C and protein kinase C in transforming growth factor-beta signaling. *Journal of Biological Chemistry*, **270**: 13600-13603, 1995.

Hartsough, M. T. and Mulder, K. M. Transforming growth factor-beta signaling in epithelial cells. *Pharmacology and Therapeutics*, **75**: 21-41, 1997.

Hawker, J. R. and Granger, H. J. Tyrosine kinase inhibitors impair fibroblast growth factor signaling in coronary endothelial cells. *American Journal of Physiology*, **266**: H107-H120, 1994.

Heldin, C. H. Dimerization of cell surface receptors in signal transduction. *Cell*, **80**: 213-223, 1995.

Heldin, C. H., Miyazono, K., and ten Dijke, P. TGF-beta signalling from cell membrane to nucleus through SMAD proteins. *Nature*, **390**: 465-471, 1997.

Hemler, M. E. VLA proteins in the integrin family: Structures, functions, and their role on leukocytes. *Annual Review of Immunology*, **8**: 365-400, 1990.

Hohmann, H. P., Remy, R., Brockhauss, M., and van Loon, A. P. Two different cell types have different major receptors for human tumor necrosis factor (TNF-alpha). *Journal of Biological Chemistry*, **264**: 14927-14934, 1989.

Hoshikawa, M., Ohbayashi, N., Yonamine, A., Konishi, M., Ozaki, K., Fukui, S., and Itoh, N. Structure and expression of a novel fibroblast growth factor, FGF-17, preferentially expressed in the embryonic brain. *Biochemical and Biophysical Research Communications*, **244**: 187-191, 1998.

Hynes, R. O. Integrins: versatility, modulation, and signaling in cell adhesion. *Cell*, **69**: 11-25, 1992.

Imcke, E., Ruszczak, Z., Mayer-da Silva, A., Detmar, M., and Orfanos, C. E. Cultivation of human dermal microvascular endothelial cells in vitro: immunocytochemical and ultrastructural characterization and effect of treatment with three synthetic retinoids. *Archives of Dermatological Research*, **283**: 149-157, 1991.

Jain, R. K., Wei, J., and Gullino, P. M. Pharmacokinetics of methotrexate in solid tumors. *Journal of Pharmacokinetics and Biopharmaceutics*, **7**: 181-194, 1979.

Jain, R. K., Koenig, G. C., Dellian, M., Fukumura, D., Munn, L. L., and Melder, R. J. Leukocyte-endothelial adhesion and angiogenesis in tumors. *Cancer and Metastasis Reviews*, **15**: 195-204, 1996.

Jaye, M., Schlessinger, J., and Dionne, C. A. Fibroblast growth factor tyrosine kinases: molecular analysis and signal transduction. *Biochimica et Biophysica Acta*, **1135**: 185-199, 1992.

Kent, K. C., Mii, S., Harrington, E. O., Chang, J. D., Mallette, S., and Ware, J. A. Requirement for protein kinase C activation in basic fibroblast growth factor-induced human endothelial cell proliferation. *Circulation Research*, **77**: 231-238, 1995.

Kitayama, J., Nagawa, H., Yasuhara, H., Tsuno, N., Kimura, W., Shibata, Y., and Muto, T. Suppressive effect of basic fibroblast growth factor on transendothelial emigration of CD4(+) T-lymphocyte. *Cancer Research*, **54**: 4729-4733, 1994.

Klagsburn, M. The affinity of fibroblast growth factors (FGFs) for heparin; FGF-heparan sulfate interactions in cells and extracellular matrix. *Current Opinions in Cellular Biology*, **2**: 857-863, 1990.

Klein, S., Giancotti, F. G., Presta, M., Albelda, S. M., Buck, C. A., and Rifkin, D. B. Basic fibroblast growth factor modulates integrin expression in microvascular endothelial cells. *Molecular Biology of the Cell*, **4**: 973-982, 1993.

Kojima, N., Shiota, M., Sadahira, Y., Handa, K., and Hakomori, S. Cell adhesion in a dynamic flow system as compared to static system. Glycosphingolipid-glycosphingolipid interaction in the dynamic system predominates over lectin- or integrin-based mechanisms in adhesion of B16 melanoma cells to non-activated endothelial cells. *Journal of Biological Chemistry*, **267**: 17264-17270, 1992.

Kolesnick, R. N., Haimovitz-Friedman, A., and Fuks, Z. The sphingomyelin signal transduction pathway mediates apoptosis for tumor necrosis factor, Fas, and ionizing radiation. *Biochemistry of Cell Biology*, **72**: 471-474, 1994.

Kumar, R., Yoneda, J., Bucana, C. D., and Fidler, I. J. Regulation of distinct steps of angiogenesis by different angiogenic molecules. *International Journal of Oncology*, **12**: 749-757, 1998.

Kuzu, I., Bicknell, R., Fletcher, C. D., and Gatter, K. C. Expression of adhesion molecules on the endothelium of normal tissue vessels and vascular tumors. *Laboratory Investigation*, **69**: 322-328, 1993.

Landis, S. H., Murray, T., Bolden, S., and Wingo, P. A. Cancer statistics, 1998. *CA: A Cancer Journal for Clinicians*, **48**: 6-29, 1998.

Larsen, E., Celi, A., Gilbert, G. E., Furie, B. C., Erban, J. K., Bonfanti, R., Wagner, D. D., and Furie, B. PADGEM protein: a receptor that mediates the interaction of activated platelets with neutrophils and monocytes. *Cell*, **59**: 305-312, 1989.

Lawrence, M. B. and Springer, T. S. Leukocytes roll on a selectin at physiological flow rates: distinction from and prerequisite for adhesion through integrins. *Cell*, **65**: 859-873, 1991.

225

Leung, K. H. Human lymphokine-activated killer (LAK) cells I. Depletion of monocytes from peripheral blood mononuclear cells by L-phenylalanine methyl ester and optimization of LAK cell generation at high density. *Cancer Immunology Immunotherapy*, **30**: 247-254, 1989.

Levitzki, A. Tyrphostins: tyrosine kinase blockers as novel antiproliferative agents and dissectors of signal transduction. *FASEB Journal*, **6**: 3275-3282, 1992.

Levitzki, A. Signal-transduction therapy. *European Journal of Biochemistry*, **226**: 1-13, 1994.

Lo, S. K., Detmers, P. A., Levin, S. M., and Wright, S. D. Transient adhesion of neutrophils to endothelium. *Journal of Experimental Medicine*, **169**: 1779-1793, 1989.

Loetscher, H., Pan, Y. C., Lahm, H. W., Gentz, R., Brockhaus, M., Tabuchi, H., and Lesslauer, W. Molecular cloning and expression of the human 55 kD tumor necrosis factor receptor. *Cell*, **61**: 351-356, 1990.

Luscinskas, F. W. and Lawler, J. Integrins as dynamic regulators of vascular function. *FASEB Journal*, **8**: 929-938, 1994.

Luscinskas, F. W., Kansas, G. S., Ding, H., Pizcueta, P., Schleiffenbaum, B. E., Tedder, T. F., and Gimbrone, M. A., Jr. Monocyte rolling, arrest, and spreading on IL-4-activated endothelium under flow is mediated via sequential action of L-selectin, β_1-integrins and β_2-integrins. *Journal of Cell Biology*, **125**: 1417-1427, 1994.

Luscinskas, F. W., Ding, H., and Lichtman, A. H. P-selectin and vascular cell adhesion molecule-1 mediate rolling and arrest, respectively, of CD4+ T lymphocytes on tumor necrosis factor-α-activated vascular endothelium under flow. *Journal of Experimental Medicine*, **181**: 722-729, 1995.

Marchisio, P. C., Bergui, L., Corbascio, G. C., Cremona, O., D'Urso, N., Schena, M., Tesio, L., and Caligaris-Cappio, F. The localization of vinculin, talin, and integrin receptors at adhesion sites of malignant B lymphocytes. *Blood*, **72**: 8301-8312, 1988.

Marlin, S. D. and Springer, T. A. Purified intercellular adhesion molecule-1 (ICAM-1) is a ligand for lymphocyte function-associated antigen 1 (LFA-1). *Cell*, **51**: 813-816, 1987.

Marui, N., Offermann, M. K., Swerlick, R., Kunsch, C., Rosen, C. A., Ahmad, M., Alexander, R. W., and Medford, R. Vascular cell adhesion molecule-1 (VCAM-1) gene transcription and expression are regulated through an antioxidant-sensitive mechanism in human vascular endothelial cells. *Journal of Clinical Investigation*, **92**: 1866-1874, 1993.

May, M. J., Wheeler-Jones, C. P. D., and Pearson, J. D. Effects of protein tyrosine kinase inhibitors on cytokine-induced adhesion molecule expression by human umbilical vein endothelial cells. *British Journal of Pharmacology*, **118**: 1761-1771, 1996.

Melder, R. J., Walker, E. R., Herberman, R. B., and Whiteside, T. L. Surface characteristics, morphology, and ultrastructure of human adherent lymphokine-activated killer cells. *Journal of Leukocyte Biology*, **48**: 163-173, 1990.

Melder, R. J., Rosenfield, C. S., Herberman, R. B., and Whiteside, T. L. Adhesion characteristics of human interleukin-2-activated natural killer cells. *Cellular Immunology*, **132**: 177-192, 1991.

Melder, R. J. and Jain, R. K. Kinetics of interleukin-2 induced changes in rigidity of human natural killer cells. *Cell Biophysics*, **20**: 161-76, 1992.

Melder, R. J., Brownell, A. L., Shoup, T. M., Brownell, G. L., and Jain, R. K. Imaging of activated natural killer cells in mice by positron emission tomography: preferential uptake in tumors. *Cancer Research*, **53**: 5867-5871, 1993.

Melder, R. J., Salehi, H. A., and Jain, R. K. Localiztion of activated natural killer cells in MCaIV mammary carcinoma grown in cranial windows in C3H mice. *Microvascular Research*, **50**: 35-44, 1995.

Melder, R. J., Munn, L. L., Yamada, S., Ohkubo, C., and Jain, R. K. Selectin and integrin mediated T lymphocyte rolling and arrest on TNFα-activated endothelium is augmented by erythrocytes. *Biophysical Journal*, **69**: 2131-2138, 1995.

Melder, R. J., Koenig, G. C., Witwer, B., Safabakhsh, N., Munn, L. L., and Jain, R. K. During angiogenesis, vascular endothelial growth factor and basic fibroblast growth factor regulate natural killer cell adhesion to tumor endothelium. *Nature Medicine*, **2**: 11-17, 1996.

Melder, R. J., Koenig, G. C., Munn, L. L., and Jain, R. K. Adhesion of activated natural killer cells to TNFα-treated endothelium under physiological flow conditions. *Natural Immunity*, **15**: 154-163, 1996.

Miltenyi, S., Mueller, W., Weichel, W., and Radbruch, A. High gradient magnetic cell separation with MACS. *Cytometry*, **11**: 231-238, 1990.

Mohammadi, M., Dionne, C. A., Li, W., Li, N., Spivak, T., Honegger, A. M., Jaye, M., and Schlessinger, J. Point mutation in FGF receptor eliminates phosphatidylinositol hydrolysis without affecting mitogenesis. *Nature*, **358**: 681-684, 1992.

Montesano, R., Vassalli, J. D., Baird, A., Guillemin, R., and Orci, L. Basic fibroblast growth factor induces angiogenesis in vitro. *Proceedings of the National Academy of Sciences*, **83**: 7297-7301, 1986.

Moscatelli, D., Presta, M., Joseph-Silverstein, J., and Rifkin, D. B. Both normal and tumor cells produce basic fibroblast growth factor. *Journal of Cellular Physiology*, **129**: 273-276, 1986.

Moscatelli, D. Metabolism of receptor-bound and matrix-bound basic fibroblast growth factor by bovine capillary endothelial cells. *Journal of Cellular Biology*, **107**: 753-759, 1988.

Munn, L. L., Melder, R. J., and Jain, R. K. Analysis of cell flux in the parallel plate flow chamber: implications for cell capture studies. *Biophysical Journal*, **67**: 889-95, 1994.

Munn, L., Koenig, G. C., Jain, R. K., and Melder, R. J. Kinetics of adhesion molecule expression and spatial organization using targeted sampling fluorometry. *BioTechniques*, **19**: 622-631, 1995.

Neish, A. S., Williams, A. J., Palmer, H. J., Whitley, M. Z., and Collins, T. Functional analysis of the human vascular cell adhesion molecule 1 promoter. *Journal of Experimental Medicine*, **176**: 1583-1593, 1992.

Nishizuka, Y. Intracellular signaling by hydrolysis of phospholipids and activation of protein kinase C. *Science*, **258**: 607-614, 1992.

Ohkubo, C., Bigos, D., and Jain, R. K. Interleukin 2 induced leukocyte adhesion to the normal and tumor microvascular endothelium in vivo and its inhibition by dextran sulfate: implications for vascular leak syndrome. *Cancer Research*, **51**: 1561-1563, 1991.

Oppenheimer-Marks, N., Davis, L., Bogue, D., and Ramberg, J. Differential utilization of ICAM-1 and VCAM-1 during the adhesion and transendothelial migration of human T lymphocytes. *Journal of Immunology*, **147**: 2913-21, 1991.

Osborn, L. C., Hession, R., Tizzard, C., Vassalio, S., Luhowsky, G., Chi-Rosso, S., and Lobb, R. Direct expression cloning of vascular cell adhesion molecule 1, a cytokine-induced endothelial protein that binds to lymphocytes. *Cell*, **59**: 1203-1207, 1989.

Osborn, L. Leukocyte adhesion to endothelium in inflammation. *Cell*, **62**: 3-6, 1990.

Pardi, R., Bender, J. R., Dettori, C., Giannazza, E., and Engleman, E. G. Heterogenous distribution and transmembrane signaling properties of lymphocyte function-associated antigen (LFA-1) in human lymphocyte subsets. *Journal of Immunology*, **143**: 3157-3166, 1989.

Peschon, J. J., Torrances, D. S., Stocking, K. L., Glaccum, M. B., Otten, C., Willis, C. R., Charrier, K., Morrissey, P. J., Ware, C. B., and Mohler, K. M. TNF receptor-deficient mice reveal divergent roles for p55 and p75 in several models of inflammation. *Journal of Immunology*, **160**: 943-952, 1998.

Peters, K. G., Marie, J., Wilson, E., Ives, H. E., Escobedo, J., Del Rosario, M., Mirda, D., and Williams, L. T. Point mutation of an FGF receptor abolishes phosphatidylinositol turnover and Ca2+ flux but not mitogenesis. *Nature*, **358**: 678-681, 1992.

Pinckard, J. K., Sheehan, K. C., and Schreiber, R. D. Ligand-induced formation of p55 and p75 tumor necrosis factor receptor heterocomplexes on intact cells. *Journal of Biological Chemistry*, **272**: 10784-10789, 1997.

Pober, J. S., Bevilacqua, M. P., Mendrick, D. L., Lapierre, L. A., Fiers, W., and Gimbrone, M. A. Two distinct monokines, interleukin-1 and tumor necrosis factor, each independently induce biosynthesis and transient expression of the same antigen on the surface of cultured human vascular endothelial cells. *Journal of Immunology*, **136**: 1680-1684, 1986.

Pober, J. S., Lapierre, L. A., Stolpen, A. H., Brock, T. A., Springer, T. A., Fiers, W., Bevilacqua, M. P., Mendrick, D. L., and Gimbrone Jr, M. A. Activation of cultured human endothelial cells by recombinant lymphotoxin: comparison with tumor necrosis factor and interleukin-1 species. *Journal of Immunology*, **138**: 3319-3324, 1987.

Pober, J. S. and Cotran, R. S. Cytokines and endothelial cell biology. *Physiological Reviews*, **70**: 427-451, 1990.

Presta, M., Maier, J. M., and Ragnotti, G. M. The mitogenic signalling pathway but not the plasminogen activator-inducing pathway of basic fibroblast growth factor is mediated through protein kinase C in fetal bovine aortic endothelial cells. *Journal of Cell Biology*, **109**: 1877-1884, 1989.

Read, M. A., Whitley, M. Z., Williams, A. J., and Collins, T. NF-κB and IκBα: an inducible regulatory system in endothelial activation. *Journal of Experimental Medicine*, **179**: 503-512, 1994.

Read, M. A., Neish, A. S., Gerritsen, M. E., and Collins, T. Postinduction transcriptional repression of E-selectin and vascular cell adhesion molecule-1. *Journal of Immunology*, **157**: 3472-3479, 1996.

Ritchie, A. J., Johnson, D. R., Ewenstein, B. M., and Pober, J. S. Tumor necrosis factor induction of endothelial cell surface antigens is independent of protein kinase C activation or inactivation. *Journal of Immunology*, **146**: 3056-3062, 1991.

Rodeck, U., Becker, D., and Herlyn, M. Basic fibroblast growth factor in human melanoma. *Cancer Cells*, 3: 308-311, 1991.

Rosenberg, S. A. Adoptive immunotherapy for cancer. *Scientific American*, **262**: 62-69, 1990.

Roth, M. D. Interleukin 2 induces the expression of CD45RO and the memory phenotype by CD45RA+ peripheral blood lymphocytes. *Journal of Experimental Medicine*, **179**: 857-864, 1994.

Rothlein, R., Dustin, M. L., Marlin, S. D., and Springer, T. A. A human intercellular adhesion molecule (ICAM-1) distinct from LFA-1. *Journal of Immunology*, **137**: 1270-1274, 1986.

Rouslahti, E. Integrins. *Journal of Clinical Investigation*, **87**: 1-5, 1991.

Sa, G. and Fox, P. L. Basic fibroblast growth factor-stimulated endothelial cell movement is mediated by a pertussis toxin-sensitive pathway regulating phospholipase A2 activity. *Journal of Biological Chemistry*, **269**: 3219-3225, 1994.

Sasaki, A., Melder, R. J., Whiteside, T. L., Herberman, R. B., and Jain, R. K. Preferential localization of human adherent lymphokine-activated killer cells in tumor microcirculation. *Journal of the National Cancer Institute*, **83**: 433-437, 1991.

Savino, J. and Siegel, R. Laminar forced convection in rectangular channels with unequal heat addition on adjacent sides. *International Journal of Heat and Mass Transfer*, **7**: 733-741, 1964.

Schleimer, R. P. and Rutledge, B. K. Cultured human vascular endothelial cells acquire adhesiveness for neutrophils after stimulation with interleukin-1, endotoxin, and tumor-promoting phorbol diesters. *Journal of Immunology*, **136**: 649-654, 1987.

Schütze, S., Berkovic, D., Tomsing, O., Unger, C., and Krönke, M. Tumor necrosis factor induces rapid production of 1'2'diacylglycerol by a phosphatidylcholine-specific phospholipase C. *Journal of Experimental Medicine*, **174**: 975-988, 1991.

Schütze, S., Machleidt, T., and Krönke, M. Mechanisms of tumor necrosis factor action. *Seminars in Oncology*, **19**: 16-24, 1992.

Schütze, S., Potthoff, K., Machleidt, T., Berkovic, D., Wiegmann, K., and Krönke, M. TNF activates NF-κB by phosphatidlycholine-specific phospholipase C-induced "acidic" sphingomyelin breakdown. *Cell*, **71**: 765-776, 1992.

Segarini, P. R. TGF-beta receptors: a complicated system of multiple binding proteins. *Biochimica et Biophysica Acta*, **1155**: 269-275, 1993.

Senger, D. R., Van de Water, L., Brown, L. F., Nagy, J. A., Yeo, K. T., Berse, B., Jackman, R. W., Dvorak, A. M., and Dvorak, H. F. Vascular permeability factor (VPF, VEGF) in tumor biology. *Cancer and Metastasis Reviews*, **12**: 303-324, 1993.

Seymour, L. W., Shoaibi, M. A., Martin, A., Ahmed, A., Elvin, P., Kerr, D. J., and Wakelam, M. J. O. Vascular endothelial growth factor stimulates protein kinase C-dependent phospholipase D activity in endothelial cells. *Laboratory Investigation*, **75**: 427-437, 1996.

Shimizu, Y., Newman, W., Gopal, T. V., Horgan, K. J., Graber, N., Beall, L. D., van Seventer, G. A., and Shaw, S. Four molecular pathways of T cell adhesion to endothelial cells: roles of LFA-1, VCAM-1, and ELAM-1 and changes in pathway hierarchy under different activation conditions. *Journal of Cell Biology*, **113**: 1203-1212, 1991.

Sierke, S. L. and Koland, J. G. SH2 domain proteins as high-affinity receptor tyrosine kinase substrates. *Biochemistry*, **32**: 10102-10108, 1993.

Spertini, O., Kansas, G. S., Munro, J. M., Griffin, J. D., and Tedder, T. F. Regulation of leukocyte migration by activation of the leukocyte adhesion molecule (LAM-1) selectin. *Nature*, **349**: 691-694, 1991.

Spivak-Kroizman, T., Mohammadi, M., Hu, P., Jaye, M., Schlessinger, J., and Lax, I. Point mutation in the fibroblast growth factor receptor eliminates phosphatidylinositol hydrolysis without affecting neuronal differentiation of PC12 cells. *Journal of Biological Chemistry*, **269**: 14419-14423, 1994.

Springer, T. A. Traffic signals for lymphocyte recirculation and leukocyte emigration: the multistep paradigm. *Cell*, **76**: 301-314, 1994.

Springer, T. A. Traffic signals on endothelium for lymphocyte recirculation and leukocyte emigration. *Annual Review of Physiology*, **57**: 827-872, 1995.

Stauton, D. E., Dustin, M. L., and Springer, T. A. Functional cloning of ICAM-2, a cell adhesion ligand for LFA-1 homologous to ICAM-1. *Nature*, **339**: 61-64, 1989.

Sternberg, M. J. and Gullick, W. J. A sequence motif in the transmembrane region of growth factor receptors with tyrosine kinase activity mediates dimerization. *Protein Engineering*, **3**: 245-248, 1990.

Suzuki, Y., Ohtani, H., Mizoi, T., Takeha, S., Shiiba, K., Matsuno, S., and Nagura, H. Cell adhesion molecule expression by vascular endothelial cells as an immune/inflammatory reaction in human colon carcinoma. *Japanese Journal of Cancer Research*, **86**: 585-593, 1995.

230

Takagi, S., Chen, K., Schwarz, R., Iwatsuki, S., Herberman, R. B., and Whiteside, T. L. Functional and phenotypic analysis of tumor-infiltrating lymphocytes isolated from human primary and metastic liver tumors and cultured in recombinant interleukin-2. *Cancer*, **63**: 102-111, 1989.

Tisher, E., Mitchell, R., Hartman, T., Silva, M., Godspodarowicz, D., Fiddes, J. C., and Abraham, J. A. The human gene for vascular endothelial growth factor. Multiple protein forms are encoded through alternative exon splicing. *Journal of Biological Chemistry*, **266**: 26031-26037, 1991.

Ullrich, A. and Schlessinger, J. Signal-transduction by receptors with tyrosine kinase activity. *Cell*, **61**: 203-212, 1990.

van Kooten, T. G., Schakenraad, J. M., d. Mei, H. C. V., and Busscher, H. J. Development and use of a parallel-plate flow chamber for studying cellular adhesion to solid surfaces. *Journal of Biomedical Materials Research*, **26**: 725-738, 1992.

Varticovski, L., Harrison-Findik, D., Keeler, M. L., and Susa, M. Role of PI 3-kinase in mitogenesis. *Biochimica et Biophysica Acta*, **1226**: 1-11, 1994.

Vital Statistics of the United States National Center for Health Statistics. Washington, D.C. Public Health Service, 1994.

von Andrian, U. H., Chambers, J. D., McEvoy, L. M., Bargatze, R. F., Arfors, K. E., and Butcher, E. C. Two-step model of leukocyte-endothelial cell interaction in inflammation: Distinct roles for LECAM-1 and the leukocyte b2 integrins in vivo. *Proceedings of the National Academy of Sciences*, **88**: 7538-7542, 1991.

Waltenberger, J., Claesson-Welsh, L., Siegbahn, A., Shibuya, M., and Heldin, C. H. Different signal transduction properties of KDR and Flt-1, two receptors for vascular endothelial growth factor. *Journal of Biological Chemistry*, **269**: 26988-26995, 1994.

Watson, C. A., Camera-Benson, L., Palmer-Crocker, R., and Pober, J. S. Variability among human umbilical vein endothelial cultures. *Science*, **268**: 447-448, 1995.

Weber, C., Negrescu, E., Erl, W., Pietsch, A., Frankenberger, M., Löms Ziegler-Heitbrock, H. W., Siess, W., and Weber, P. C. Inhibitors of protein tyrosine kinase suppress TNF-stimulated induction of endothelial cell adhesion molecules. *Journal of Immunology*, **155**: 445-451, 1995.

Weston, S. A. and Parish, C. R. New fluorescent dyes for lymphocyte migration studies: analysis by flow cytometry and fluorescence microscopy. *Journal of Immunology Methods*, **133**: 87-97, 1990.

Wiegmann, K., Schutze, S., Kampen, E., Himmler, A., Machleidt, T., and Kronke, M. Human 55-kDa receptor for tumor necrosis factor coupled to signal transduction cascades. *Journal of Biological Chemistry*, **267**: 17997-18001, 1992.

Xia, P., Aiello, L. P., Ishii, H., Jiang, Z. Y., Park, D. J., Robinson, G. S., Takagi, H., Newsome, W. P., Jirousek, M. R., and King, G. L. Characterization of vascular endothelial growth factor's effect on the activation of protein kinase C, its isoforms, and endothelial cell growth. *Journal of Clinical Investigation*, **98**: 2018-2026, 1996.

Yago, T., Tsukuda, M., Yamazaki, H., Nishi, T., Amano, T., and Minami, M. Analysis of an initial step of T cell adhesion to endothelial monolayers under flow conditions. *Journal of Immunology*, **154**: 1216-1222, 1995.

Yamashita, H., Ichijo, H., Grimsby, S., Moren, A., ten Dijke, P., and Miyazono, K. Endoglin forms a heteromeric complex with the signaling receptors for transforming growth factor-beta. *Journal of Biological Chemistry*, **269**: 1995-2001, 1994.

Yayon, A., Klagsburn, M., Esko, J. D., Leder, P., and Ornitz, D. M. Cell surface, heparin-like molecules are required for binding of basic fibroblast growth factor to its high affinity receptor. *Cell*, **64**: 841-848, 1991.

Yoo, Y., Heo, D. S., Hata, K., Van Thiel, D. H., and Whiteside, T. L. Tumor infiltrating lymphocytes from human colon carcinomas: functional and phenotypic characteristics after long-term culture in recombinant interleukin-2. *Gastroenterology*, **98**: 259-268, 1990.

Yu, K. T., Pessin, J. E., and Czech, M. P. Regulation of insulin receptor kinase by multisite phosphorylation. *Biochimie*, **67**: 1081-1093, 1985.

Zhan, X., Plourde, C., Hu, X., Friesel, R., and Maciag, T. Association of fibroblast growth factor receptor-1 with c-Src correlates with association between c-Src and cortactin. *Journal of Biological Chemistry*, **269**: 20221-20224, 1994.

Zhu, H., Melder, R., Baxter, L., and Jain, R. K. Physiologically based kinetic model of effector cell biodistibution in mammals: Implications for adoptive immunotherapy. *Cancer Research*, **56**: 3771-3781, 1996.